In Situ Polymerization via an Environmentally-borne Initiation Stimulus

by

Scott Ryan Zavada

A dissertation submitted in partial fulfillment
of the requirements for the degree of
Doctor of Philosophy
(Macromolecular Science and Engineering)
in the University of Michigan
2016

Doctoral Committee:

Assistant Professor Timothy F. Scott, Chair
Associate Professor Kenichi Kuroda
Professor Brian J. Love
Professor Andrew J. Putnam

2016

Dedication

This dissertation is dedicated my wife, Lynn Zavada. Out of everything that happened to me while I was student at the University of Michigan, meeting you was the most amazing and wonderful.

Acknowledgements

I want to thank my PhD advisor Prof. Timothy F. Scott for all of his guidance and encouragement during my five years at the University of Michigan. I would also like to thank the members of my dissertation committee for all of their advice and feedback

I am forever grateful and honored to have received a NASA Space Technology Research Fellowship. This was amazing experience that undoubtedly transformed my graduate education experience. I specifically want to thank Dr. Keith Gordon, my mentor and collaborator within the NSTRF program, for all of his advice and assistance throughout the entire fellowship and especially for the time I was at the NASA Langley Research Center. I would also like to thank Dr. Mike Pereira and Charles Ruggeri at NASA for all of their help and extraordinary efforts when I was at the NASA Glenn Research Center.

I was repeatedly told how the University of Michigan, and particularly the Macro program, strongly emphasized having a family-type atmosphere and everything I experienced here confirmed that sentiment. I would like to thank Prof. Rick Laine, Prof. Mark Banaszak Holl, Nonna Hamilton, and Adam Mael for making major contributions in building the family atmosphere of Macro as well as all the help and assistance I received from them. My friends and colleagues within Macro were a constant source of motivation and support and I am very gratefully and humbled to have met so many outstanding people.

I was fortunate to have such extraordinary lab mate and I thank Tao Wei, Dowon Ahn, Megan Dunn, Sameer Sathe, Dan Li, Max Ma, Harry van der Laan, Samuel Leguizamon, Dr. Junting Li, Dr. Jae Hwan Jung, and Dr. Joseph Furgal for all of their help, encouragement, and assistance throughout. I especially want to mention Tao, Dowon, and Megan for their help in building the lab during the early years.

I was extraordinarily lucky to have three outstanding undergraduate students, Nick McHardy, Tsatsa Battsengel, and Nathan Wood, work with me on these research projects. I would also like to mention several other outstanding undergraduate students, Mara Clark, Carolyn Zhao, Marcus Deloney, and Joseph Poznanski, that were such a major part of the early years of our lab.

I must mention and thank Dr. Norman Sweet, Prof. John Texter, and Prof. Vijay Mannari both for writing recommendations letters for me and for the encouragement they gave me to purse a doctoral degree. I also want to thank everyone from Adrian College, Eastern Michigan University, and Precision Coatings who helped me during the time before I started at Michigan.

I am eternally thankful for the love and support of my parents, brothers, sister, sisters-in-law, and the rest of my family. I especially want to mention my sister, Aesha, for being a constant source of inspiration and support and my parents, Raymond and Cynthia Zavada, for all of their help moving me from Wixom to Ann Arbor, Ann Arbor to Ypsilanti, and Ypsilanti to Virginia.

Go Blue!

Table of Contents

List of Figures

List of Tables

List of Schemes

Abstract

The utilization of an environmentally-borne stimulus, atmospheric oxygen, has been convincingly demonstrated as a useful means for initiating in situ polymerization. As molecular oxygen is both ubiquitous and capable of participating in reduction-oxidation reactions, it particularly well-suited for affording radicals capable of initiating radical-mediated polymerization. The thiol–ene reaction is extraordinarily resistant to oxygen inhibition and thus useful as an oxygen-mediated polymerization reaction. In order to utilize oxygen as a polymerization stimulus, three initiating systems were developed, including those based on alkylboranes, oxidoreductase enzymes, and thiones. These systems are capable of solidifying thiol–ene monomer formulations within seconds, minutes, or hours, respectively, upon oxygen exposure. The interest in in situ oxygen-mediated polymerization is largely driven by two emerging applications. The first of these, self-healing materials suitable for space exploration applications, requires a reactive liquid, sandwiched between a solid support structure, that is able to flow and polymerize immediately after being punctured by space debris, thus sealing the resultant hole. To demonstrate the suitability of oxygen-mediated polymerization for self-healing materials, high-velocity ballistics testing, monitored by videography and thermal imaging, was performed and established that a reactive liquid monomer formulation can polymerize within seconds of oxygen exposure to afford a solid polymeric material capable of sealing the projectile-induced puncture. The second application is for next-generation surgical adhesives and sealants that would be suitable as emergency hemostats

and other medical procedures. As a demonstration that oxygen-mediated polymerization is a useful mechanism for producing these materials, formulations based on chitosan, a polysaccharide known for its biocompatibility and bioadhesion, were produced that afford solid hydrogels within a minute of oxygen exposure. In addition to the alkylborane- and oxidoreductase-based systems, thiones were employed to initiate bulk thiol–ene polymerization. Although thiones were shown to be capable of generating radicals in the presence of atmospheric oxygen and thiol groups, the reaction extents achievable were lower than desired owing to unwanted side reactions quenching radical production and, subsequently, suppressing polymerization. Despite this limitation, the development of approaches to suppress the quenching reaction will afford a rapid and efficient method of utilizing oxygen as an environmentally-borne polymerization initiation stimulus.

Chapter 1

Introduction

1.1 In Situ Polymerization

Polymers are large molecules produced by reactions that connect small molecule precursors, known as monomers, into much larger macromolecules with molecular weights ranging from thousands to millions and beyond.[1] The shear size of these molecules affords polymers many useful properties and, accordingly, are utilized in a bewildering array of applications. To give a few examples, polymers are utilized as the primary components in most coatings[2-4] and adhesives,[5-7] can be fabricated into plastic sheets[8, 9] or spun into fibers,[10] serve as components for energy application (e.g., batteries[11, 12] or solar cells[13]), perform as in vivo drug-carry delivery devices,[14] or function as scaffolds for tissue engineering.[15] Such an incredible range of applications requires a multitude of synthetic methods capable of yielding polymers, in the form of powders, beads, solutions and dispersions, that can further processed, through extrusion, molding or a variety of other methods, into their final, usable form. For many applications, the polymer film or mass must be formed in situ – that is, in the location where it will be used; this is how numerous types of paints, coatings, adhesives, or sealants function. A liquid is applied to surface and through a physical change (e.g., solvent evaporation or particle coalescence) or a chemical reaction, a solid polymer is formed. While many paints and adhesives for home do-it-yourself projects (e.g.,

furniture lacquer, wall paint, or wood glue) contain a volatile component, thus requiring time to dry after application, the presence of a volatile components may not always be desirable or possible. For example, in an adhesive intended to glue two pieces of paper together, the use of water is permissible as the water can evaporate through the porous paper, allowing for the solid polymer film to form and adhere the paper sheets together. Conversely, an adhesive intended to glue together two impermeable substrates (e.g., glass or metal) can not rely upon the evaporation of volatile components. For these situations, the transformation from a liquid to a solid must be driven by an in situ polymerization reaction.

Typically, in order to effect in situ polymerization, a reactive liquid must be exposed to a specific stimulus, commonly elevated temperatures, light, or chemical; exposure to the stimulus initiates polymerization, converting the liquid into a solid. Not surprisingly, different applications require different stimuli. To illustrate, it is wholly appropriate to utilize elevated temperature to bake a factory applied automotive coating – the metal car body can easily withstand the high temperatures. The elevated temperature may simply speed up a reaction, activate a catalyst or cross-linker, or drive the evaporation of a byproduct from a crosslinking reaction. In contrast, a temperature sensitive substrate like, say, low density polyethylene can not withstand overly elevated temperatures and it may be more feasible to utilize a photocurable material, where exposing the liquid reactive formulation to ultraviolet light triggers the liquid-to-solid transformation; moreover, photopolymerization also offers excellent spatial and temporal control of cross-linking. Of course, for many applications it may not be realistic to subject the material to either elevated temperature or ultraviolet light, in which case a

chemical stimulus may be more appropriate. Such materials are quite common in commercial available adhesives suitable for do-it-yourself (DIY) home projects, notably in two-component (frequent called '2K', where the 'K' stands for 'komponent', the German word for, not surprisingly, 'component') epoxy adhesives. One component of the 2K epoxy is an epoxy resin, typically an epoxy (e.g., oxirane ring)-terminated oligomer made from bisphenol A and epichlorohydrin, while the other is a multi-functional amine referred to a 'cross-linker', 'curing agent', or 'hardener'.[5, 16] Both the epoxy resin and the amine cross-liner are stable liquids that will remain liquids for years; it is only when the two components are mixed, ideally at a one-to-one stoichiometric ratio between epoxy groups and amine hydrogens, will a reaction proceed that leads to the generation of a solid, cross-linked polymer network (see Scheme 1).[5, 16] In general, for a 2K system, the two components are packaged separately and combined immediately before applications. While this strategy removes the requirement for elevated temperature or ultraviolet, there are several inherent drawbacks, including sensitivity to mixing ratios (deviating from a one-to-one stoichiometry will hinder mechanical property development) and limited time before the polymerization-induced viscosity increase leads to the material becoming unworkable. In a strategy that can address some of these limitations, the packaged chemical stimulus can be replaced with one that is environmentally-borne; that is, a compound reliably present in the location where the material will be applied is utilized as the trigger that converts a liquid monomer into a solid polymer. One of the best known examples are commercial superglues, composed mostly of alkyl cyanoacrylates,[6] that will solidify once they come in contact with atmospheric moisture, which serves as the initiation stimulus. While there are several

such systems that utilize atmospheric moisture or other atmospheric components as initiation stimuli, and these will be discussed in detail throughout this introduction, there are applications for which currently available technology proves insufficient. Herein lies my primary research interests: I am motivated to explore in situ polymerization effected by an environmentally-borne initiation stimulus as there are several burgeoning applications that would benefit greatly from this technology.

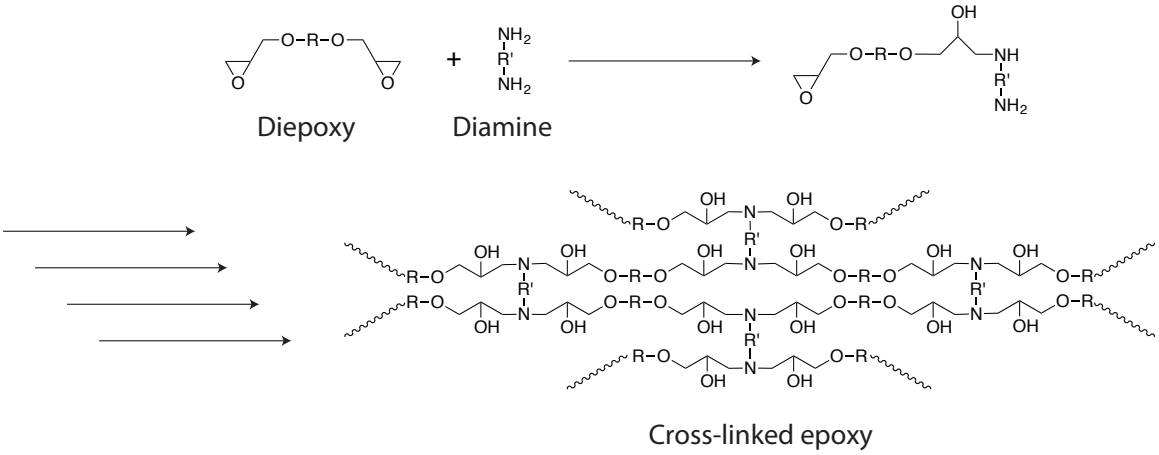

Scheme 1: Epoxy cross-linking reaction. Multifunctional epoxies and amines react together, via a step-growth polymerization mechanism, to afford a cross-linked epoxy resin.

The first of these applications is for surgical adhesive and sealants as these materials, which are applied as a liquid and, upon exposure to some stimulus, polymerize and transform into a solid in situ, are increasingly used in numerous medical and dental procedures. These biocompatible adhesives have emerged as elegant alternatives to replace surgical sutures, staples, bandages, or plates. Indeed, they have been employed to improve upon contemporary techniques in a diverse range of surgeries from the correction of cleft lips [17-19] and other reconstructive surgeries[20-24] to the fixation of fractured bones.[25-28] The most commonly used, medically-relevant adhesives and

sealants are based on the polymerization of either cyanoacrylates or fibrin;[29-31] unfortunately, the severely deleterious attributes exhibited by these existing materials limit their efficacy and broader adoption in medicine.

Cyanoacrylate adhesives consist of liquid monomer that undergoes a rapid, anion-mediated polymerization when exposed to a weak nucleophile, even upon contact with atmospheric moisture or hydroxyl and amine functional groups on skin, yielding a solid polymer.[6] Owing to their rapid reaction kinetics, capacity for environmentally-triggered cure, and high strength and excellent tissue adhesion typically exhibited by the generated polymers,[6] cyanoacrylates have found widespread use as a suture replacement for incision closure. Additionally, the application of a cyanoacrylate to an incision site is far simpler and faster than suture placement and a subsequent clinician visit by the patient for suture removal is avoided. Nevertheless, serious cytotoxicity concerns persist over the hydrolytic degradation products of cyanoacrylates (e.g., formaldehyde),[6, 32] limiting their clinical utilization exclusively to external applications. Moreover, the measures required to reduce the chronic exposure to toxic cyanoacrylate vapor experienced by health professionals can be burdensome.[33] Finally, cyanoacrylates are not amenable to chemical modifications owing to the extreme sensitivity of the cyanoacrylate functional group; this lack of extensibility severely curtails attainable property range.

Fibrin sealants mimic the final stages of blood clot formation, a process known as the coagulation cascade,[34] resulting in a cross-linked fibrin network and are commonly used as hemostats and surgical sealants to stop blood flow.[30, 31, 35] A typical fibrin sealant is packaged as a two-component system. For example, one package contains the fibrinogen and factor XIII, a transglutaminase, in its inactive form; the other package

contains thrombin, a serine protease, and a solution of $CaCl_2$. Immediately prior to use, the two packages are mixed and applied to where it is needed. After mixing, thrombin proteolytically cleaves fibrinogen into fibrin monomers and, with the aid of Ca^{2+} ions, converts the serine protease Factor XIII into its active form, Factor XIIIa. Then, by the action of thrombin and $CaCl_2$, the fibrin is cross-linked into an insoluble mass. The fibrin monomers self-assemble into fibrils that are cross-linked through a transamination reaction action catalyze do by the now activated Factor XIIIa. Thus, a solid, cross-linked mass is quickly produced by a reaction pathway that matches the final stages of the coagulation cascade. It is this solid mass that functions as the sealant or adhesive.[34]

Although these materials are derived from biological sources, they present several concerning attributes that limit their use. Although fibrin sealants are generally considered safer than cyanoacrylates owing to their identical components as those generated in a natural blood clot, these materials are derived from blood products, thus potentially acting as a transmission vector for blood-borne disease. Analogous to the aforementioned two-component epoxy adhesives (Scheme 1), typical fibrin sealant formulations consist of a two-package system that react upon combination. An over-riding drawback of such an approach is the inherent sensitivity of the system to mixing; inadequate combination of the two components will generate an adhesive with sub-optimal properties. Moreover, the cross-linked fibrin generated upon thrombin-induced fibrinogen cleavage is relatively weak and adhesion failure is a known problem.[35, 36] Thus, the development of new materials for surgical adhesives will be required to overcome these problems.

With the inherent drawbacks of both cyanoacrylate and fibrin-based materials, new materials suitable for utilization as medical-grade adhesive need to be developed. The utilization of an environmentally-borne initiation stimulus, paired with suitable polymerization chemistry, could result in the development of materials that overcome the deficiencies of presently-available materials.

A second area where he development of materials that polymerize upon contact with an environmentally-borne initiation stimulus would be of greatly utility is for the creation of autonomously-healing structures for space exploration. For example, the National Aeronautics and Space Administration (NASA) is considering manned missions to Mars. Such a mission will require the development of strong, lightweight, and durable habitats where the astronauts are able to live, work, and sleep safely on the surface of Mars.[37] NASA is especially concerned with the walls of the habitat being punctured by micrometeoroids. As the atmosphere of Mars is much thinner than that of Earth, there is a much greater chance that a micrometeoroid could reach the surface and puncture the walls of a habitat; the formation of 1-2 millimeter hole could cause the atmosphere inside to rapidly rush out, endangering the lives of the astronauts. Therefore, NASA is interested in materials capable of autonomously healing themselves upon puncture by a high velocity projectile. This is difficult as most plastics will not self-heal when punctured by a projectile; this action will irreversibly break chemical bonds and prevent the material from being able to reform. Quite impressively, there are several materials which do exhibit self-healing characteristics.[37-42] A partially neutralized ionomeric copolymer of ethylene and methacrylic acid (EMAA, commercially sold by DuPont as Surlyn), well known for its use as the outer layer of golf balls, has shown tremendous

capacity for self-healing: shooting a 5 mm thick panel of EMAA with a rifle leaves no hole. While this self-healing behavior is extraordinarily impressive, EMAA is otherwise ill-suited for utilization as a structural material as its modulus, a physical property roughly corresponding to 'stiffness', is far too low – in other words, walls made from Surlyn would be flimsy. Furthermore, EMAA is known to not self-heal when penetrated with a high velocity projectile[43] or when the film is heated to above 60°C.[40] A second material with impressive self-healing properties is poly(butadiene)-graft-poly(methyl acrylate-co-acrylonitrile) (PBG).[38] PBG has a modulus much greater than Surlyn and could be used to construct a sturdy habitat. Unfortunately, the self-healing characteristics of PBG are only evident when heated to greater than 50°C, which far exceeds the maximum surface temperature of Mars (~ 20°C).

With the limitations of currently available self-healing structures, these materials would greatly benefit from an alternative or auxiliary autonomic-healing system that retains its healing capabilities at lower temperatures. One potential approach would be to incorporate a reactive liquid layer within the walls of the structure. Indeed, there is a significant body of work that demonstrates he use of liquid filled microcapsules to heal polymeric materials when cracked. In one of the field's seminal papers, White, Sottos, Moore, and coworkers devised a composite where dicyclopentadiene (DCPD)-filled capsules are dispersed within an epoxy resin that also contained an embedded ruthenium-based Grubbs' catalyst.[44] Upon the formation of microcracks, the capsules rupture and release the contained DCPD, allowing it to freely flow into the crack. Once it to comes in in contact with Grubbs' catalyst, the DCPD undergoes ring opening meta thesis polymerization, yielding solid poly(dicyclopentadiene) that heals the crack and aids in

restoring some of the strength of the original composite.(Scheme 2) Such a material may be useful for autonomously-healing damage not readily observed, including the slow formation of fatigue-induced micro cracks. In addition the DCPG/Grubbs' catalyst system, others chemistries have been utilized for similar purposes, notably cyanoacrylates.[45]

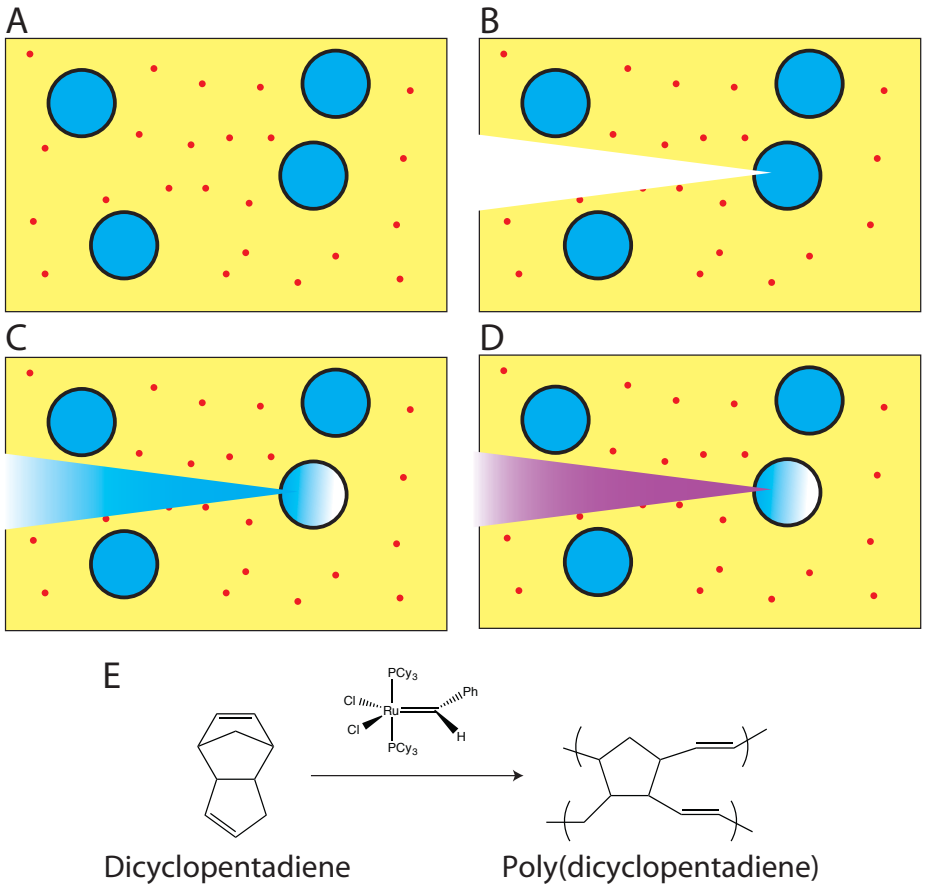

Scheme 2: Healing of microcracks in an epoxy composite by using reactive monomer-filled microcapsules. A) DCPD-filled microcapsules, in blue, are embedded within an epoxy composite along with a ruthenium-based Grubbs' catalyst, in red. B) Stress on the epoxy block causes a crack to form, rupturing a DCPD-containing microcapsule. C) The DCPD from the ruptured microcapsule contacts the catalyst, initiating ring-opening metathesis polymerization. D) The solid poly(dicylcopentadiene), shown in purple, has healed the crack. E) Ring-opening metathesis polymerization of dicylcopentadiene, catalyzed by a ruthenium-based Grubbs' catalyst. Adapted from source.[44]

A commonly utilized analogy compares the reactive liquid to blood and the polymerization reaction to the formation of a blood clot after a cut in the skin.[46-48] White, Sottos, Moore, and coworkers developed the blood analogy even further by constructing composite with a network of hollow tubes, analogous to vasculature, capable of carrying fresh healing agent to a damaged site.[48] This approach is amenable to several types of polymerization chemistries and has been demonstrated not only with the DCPD/Grubb's system, but also with two-part epoxies where portion of the vascular urge contains an epoxy-functional resin, while a second, separate network holds the amine cross-linker.

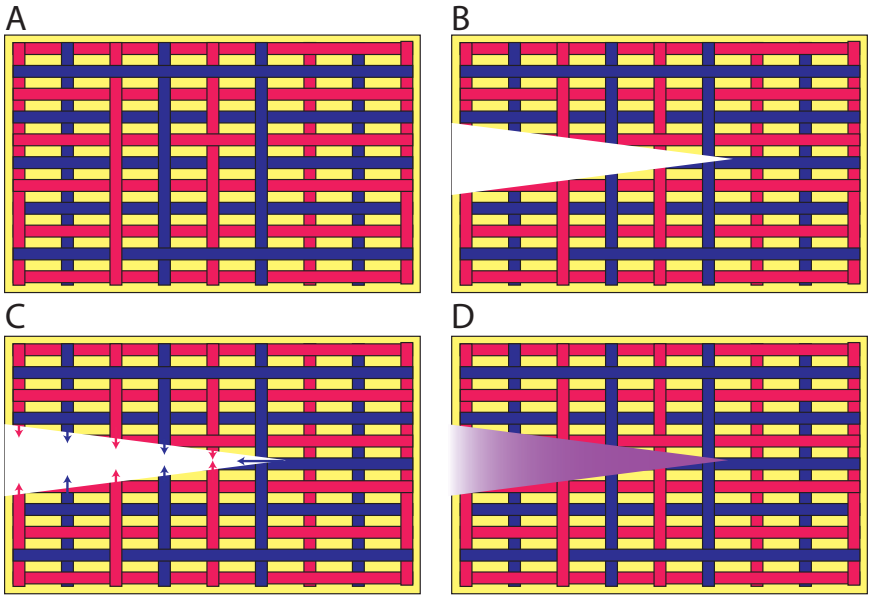

Scheme 3: Healing of microcracks in a composite by using reactive monomer-filled tubes. A) Microtubules, filled either with an epoxy resin, in blue, or an amine-cross-linker, in red, are embedded within a composite. B) Stress on the material causes a crack to form, the microtubules. C) The epoxy and amine flow out of the microtubules and are able to mix. D) The crack is filled and healed by the resulting solid, cross-linked epoxy resin, shown in purple.

Rupturing these networks allows both the epoxy resin and the amine cross-linker to contact one another and, as they mix together, polymerize and solidify via a step-growth

mechanism.(Scheme 3) This group has continued to develop even more complex vascular networks that aim to mimic vasculature found in nature.

These systems provide us with inspiration but exhibit limitations that hinder their applicability to micrometeoroid damage mitigation. Namely, the reaction rates are too slow to seal the breech in approximately a second or, ideally, less. Insufficient rapid solidification times could result in the liquid being ejected out into the vacuum of space or the near vacuum conditions of Mars.

The use of an environmentally-borne polymerization stimulus could lead to the development of materials that address these issues. This approach would be to utilize a multi-layer structure with a viscous, reactive liquid layer sandwiched in between to rigid polymer supports. This reactive liquid layer would remain a liquid under air-free conditions and would only polymerize upon exposure to air; that is, one of the atmosphere's components (e.g., one of the atmospheric gases). This multi-layer structure could conceivably used to build space exploration habitats on Mars. When this construction is punctured (by, for example, a micrometeoroid), the reactive liquid layer will begin to flow toward the vacuum. Concurrently, the exposure to the interior atmosphere as it rushes out through the hole will initiate polymerization causing the viscosity of the reactive liquid layer to rise and eventually solidify, forming a seal that prevents further atmospheric loss. Thus, the development of a suitable in situ polymerizable system may lead to the advancement of this very desirable technology.

1.2 Environmentally-borne Stimuli

To advance the development of the biomedical and self-healing materials discussed above, a suitable environmentally-borne initiation stimulus needs to be identified. Of the compounds reliably present throughout all human-habitable environments, the obvious choices to investigate are the atmospheric components, including nitrogen, oxygen, argon, carbon dioxide, and water. As the cyanoacrylate chemistry was briefly described above, our discussion will start with the utilization of atmospheric humidity as a means to initiate polymerization reactions.

1.2.1 Water

The utilization of water present as atmospheric humidity has been extensively utilized as an environmentally-borne reagent capable of effecting polymerization through a variety of chemical reaction and these materials are well known for their use as coatings, adhesives and sealants.[49-53] Typically, these materials are stable liquids, existing either as neat precursors, dissolved in solution, or dispersed in a liquid continuous phase, that will only solidify via in situ polymerization after they are exposed to the environment in the location where they will are to be used.

A well-known commercial example is moisture-cured isocyanate-based coatings. Indeed, isocyanate chemistry is extensively utilized for numerous commercial and industrial coatings, elastomers, fibers, foams, and other polymeric materials. Isocyanate chemistry is particularly rich and varied and is especially well-known for the production of urethane and urea linkages through reactions with hydroxyl or amines groups, respectively; these reactions follow an step-growth mechanism and are notable in that no byproduct is produced in the reaction.[2, 54] (Scheme 4) For example, automotive paints

may be formulated as a two-component urethane system, where one component is made of a polyol, often an acrylic or polyester, while the second component contains a multi-functional isocyanate prepolymer. When the two components are combined, often in the presence of tin or tertiary amine catalyst, urethane cross-links form between the polyol and isocyanate via a step-growth polymerization reaction. Similarly, replacing the polyol with a polyamine will result, in a reaction that is typically quite brisk, in the formation of urea linkages. In addition to these well-known reactions, isocyanates are capable of reacting with carboxylic acid groups to yield, after evolution of carbon dioxide, an amide linkage, while the reaction between an isocyanate and a thiol forms a thiocarbamate.[55] Furthermore, isocyanates are reactive with water, yielding an unstable carbamic acid group that evolves carbon dioxide to form a primary amine.[50-53, 56] This amine will then rapidly react with a second isocyanate group to complete the formation of a urea linkage. Thus, a moisture-cured isocyanate-based coating can be formulated from multi-functional isocyanate pre-polymers; after application, as atmospheric humidity permeates into the coatings, urea cross-links will form.

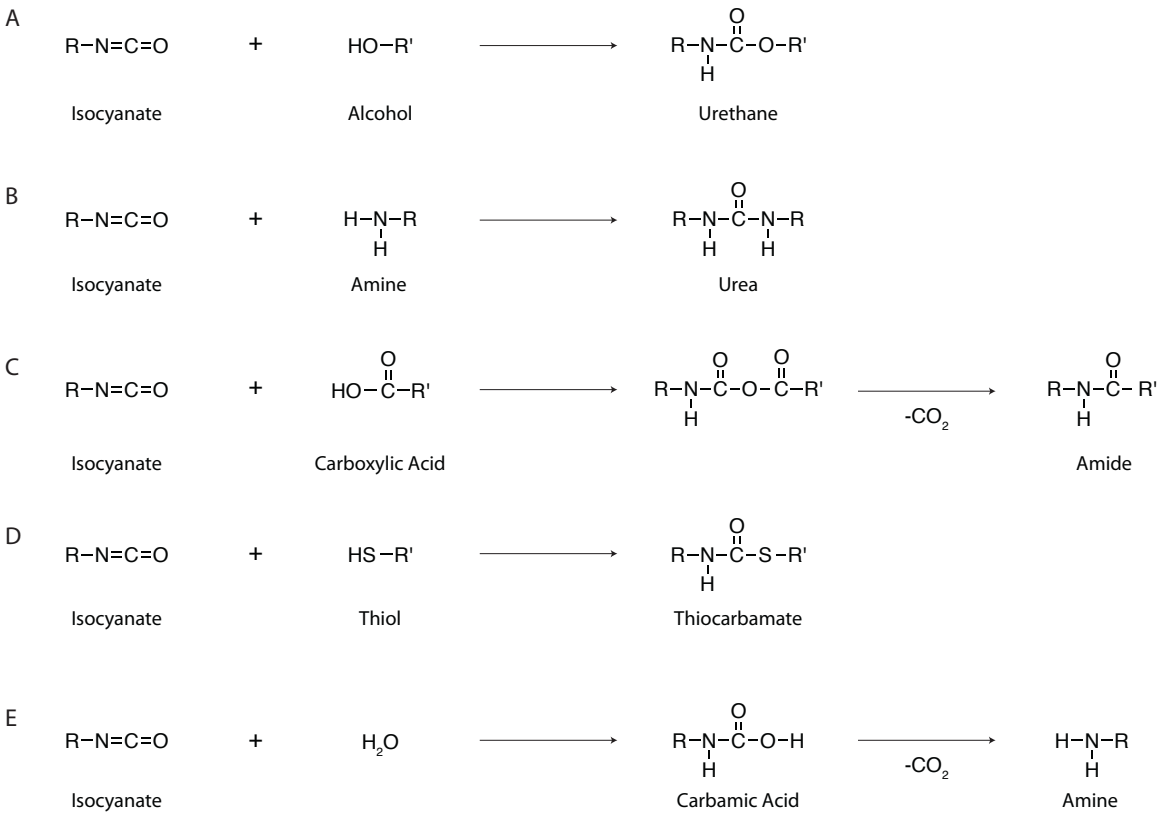

Scheme 4: Isocyanate reactions.

While other isocyanate-based coatings utilize the reaction between polyols or polyamine (to form, respectively, urethanes or urea linkages) in a step-growth addition reaction, the isocyanate-water reaction produces carbon dioxide as a byproduct. So this reaction depends upon not only the diffusion of water into the coating to bring about cure, but also upon the evolved carbon dioxide successfully diffusing out of the coating. The evolved carbon dioxide can lead bubble formation, useful for a foam but not so desirable for a protective coating that must function as a barrier. Another drawback of moisture-cured isocyanate-based systems is that there cannot be hydroxyl, carboxylic acid, amines, or thiols present as any of these are capable of reacting with the isocyanate group, severely limiting the types of precursors suitable for use with this method.

Another class of recognizable moisture-cured commercial product are silicone sealants. These consist of poly(dimethylsiloxane) that has been modified to have diacetoxy end groups. Exposure of this polymer to atmospheric moisture results in hydrolysis of the acetoxy group, liberating acetic acid and yielding a hydroxyl group.[49, 57] Cross-links between PDMS chain result from the condensation reaction between hydroxyl and acetoxy groups. Conceptually, this is nearly identical to moisture-cured isocyanate chemistry in that both polymerize via step-growth, condensation mechanisms. As was the case for isocyanates, cross-linking acetoxy-functional siloxane resins relies both on the diffusion of atmospheric humidity into the materials as well as diffusion outward of the acetic acid byproduct.

Silane-based sol-gel chemistry is another well-known water-mediated polymerization method where alkoxysilane moieties undergo successive hydrolysis and condensation reactions to form Si-O-Si inorganic networks.[58] To give a simple example,(Scheme 5a-c) an acid catalyst is added to an ethanolic aqueous solution of tetraethoxysilane (TEOS), causing some of the ethoxy groups to hydrolyze to silanols – complete hydrolysis is prevented by the presence of large amounts of water. This partially hydrolyzed solution can then be applied to a substrate via dip coating and permitted to dry. As the water and ethanol evaporate, the ethoxy and silanol groups undergo hydrolysis and condensation reaction and driving these reactions to completion results in an inorganic SiO_2 network. Alternatively, trialkoxysilane moieties on the ends of a linear organic molecule can undergo similar hydrolysis and condensation reactions to form an organic-inorganic hybrid – such an approach has been utilized for PDMS-based silicone sealants as an alternative to the acetic acid-evolving acetoxy-functional

materials.[57] The water-mediated hydrolysis step of this reaction sequence can be exploited to develop formulations that rely on atmospheric humidity as the water source. One such approach involves the photo-mediated generation of an acid catalyst. For example, Kowalewska combined a trimethoxysilyl precursor with a diphenyliodonium salt photoinitiator (e.g., a photoacid generator); upon irradiation in an environment with 50% humidity, the photoinitiator forms a superacid capable of rapidly catalyzing hydrolysis of the trimethoxysilane moieties into silanols; subsequent condensation reaction leads to the formation of Si-O-SI crosslinks (Scheme 5d).[59] This concept was further developed by Croutxé-Barghorn and coworkers where monomers containing both trimethoxysilane groups and aliphatic epoxides were combined with Irgacure-250, an iodonium salt that forms superacids upon exposure to UV light.[60] Upon UV irradiation, the liberated superacid initiates both the hydrolysis/condensation sequence, forming inorganic Si-O-Si linkages, and the cationic polymerization of the epoxide rings. This results in an in situ-generated polymer with inorganic cross-links. While these techniques are certainly strong examples of water-mediated polymerization, their requirement for UV light strongly limits their more widespread utility. Moreover, it also suffers many of the same drawback as the silicone sealants in that a condensation reaction byproduct must diffuse out in order to drive the reaction to completion.

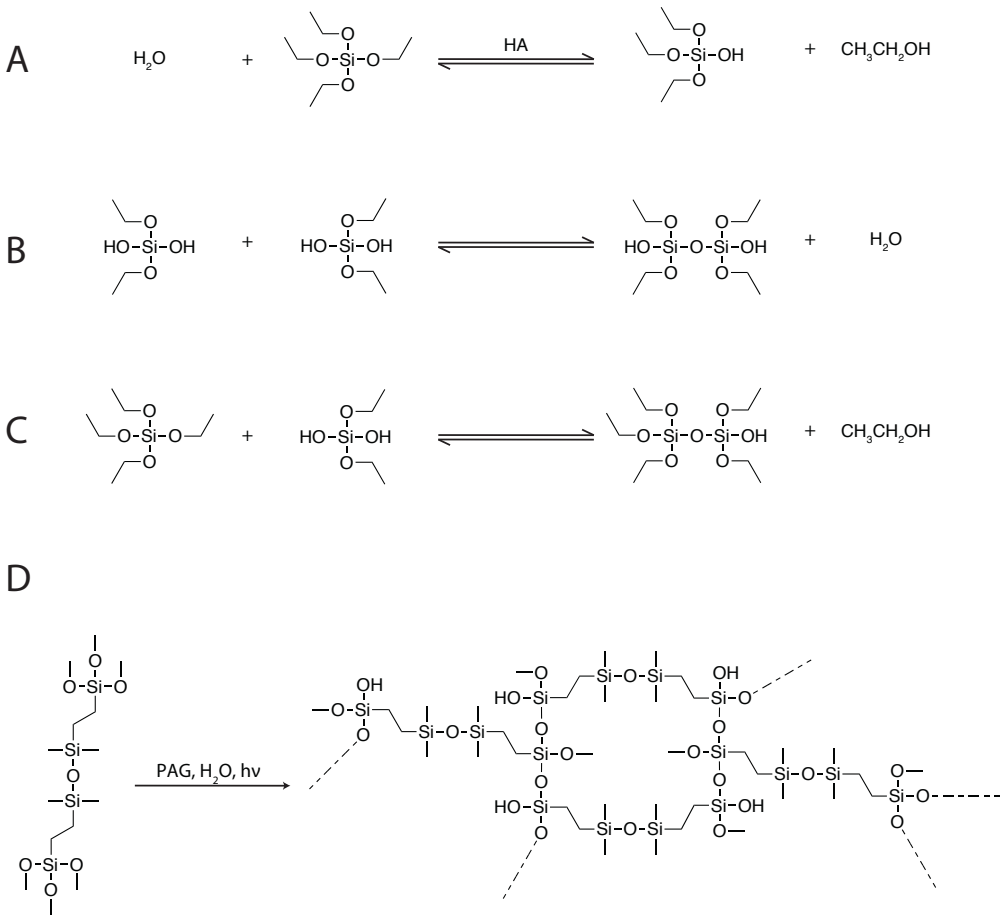

Scheme 5: Sol-gel chemistry. A) Tetraethoxysilane (TEOS) is partially hydrolyzed via an acid catalyzed reaction. B) Partially-hydrolyzed TEOS undergoes a condensation reaction to yield Si-O-Si linkage and water as a byproduct. C) Alternatively, partially hydrolyzed TEOS can undergo a condensation reaction that yields alcohol as a byproduct. D) In the presence of a photoacid generator (PAG) and atmospheric moisture, a bis(trimethoxysilane) oligomer undergoes, after exposure to UV light, hydrolysis and condensation reactions to form a cross-linked network with Si-O-Si linkages.[58, 59]

A limitation of these water-mediated polymerization methods (e.g., isocyanates, acetoxy-functional silicones, and alkoxysilanes) is that they all rely on step-growth condensation reactions and require one water molecule per cross-link. Rather than relying on systems where water is a stoichiometric reactant it may be more efficient to use water as an initiator, where each molecule of water leads to the formation of many links. In what may be one of the best examples of a polymerization reaction initiated by

an environmentally-borne compound, alkyl cyanoacrylates use water, or any weak nucleophile, as an initiator for an anionic polymerization reaction. This is unusual as the presence of water tends to terminate most anionic polymerizations; it is the extreme reactivity of the cyanoacrylate monomer, which results from the strong electron-withdrawing nature of both the cyano and ester groups, that causes the polymerization reaction to occur.[61] Cyanoacrylates have long been used for adhesives with ethyl cyanoacrylate commonly used in commercial superglues, while n-butyl cyanoacrylate and 2-octyl cyanoacrylate are used in medical applications owing to their increased biocompatibility.[6] The cyanoacrylates adhesives are formulated to be stable, and remain liquid, while kept in their original container and it is only after they are released into the environment will anionic polymerization proceed. While the use of monofunctional alkyl cyanoacrylate monomers dominate commercial applications, leading to the formation of linear polymers, cross-linked networks can be formed by utilizing multi-functional monomers.

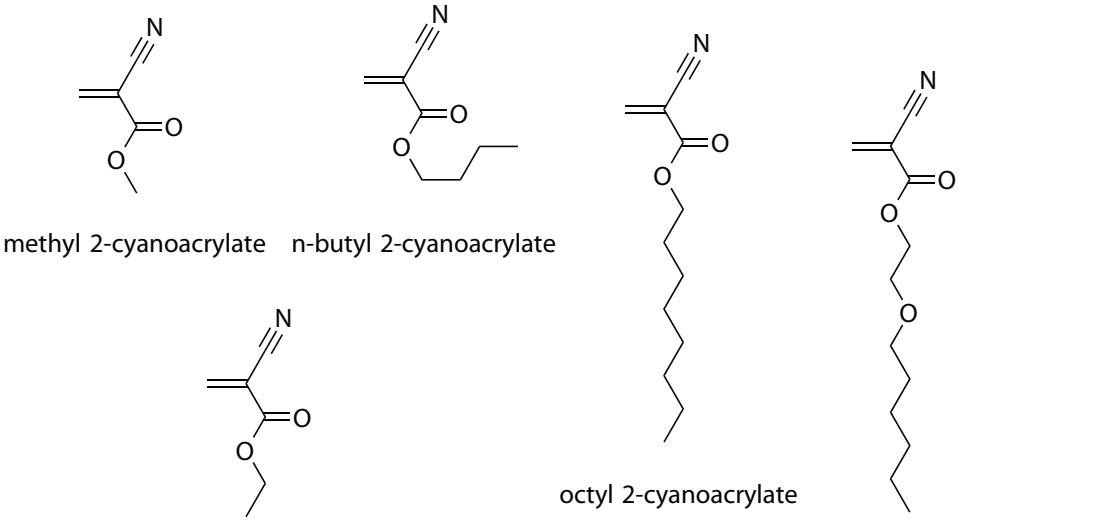

Scheme 6: Common cyanoacrylate monomers.

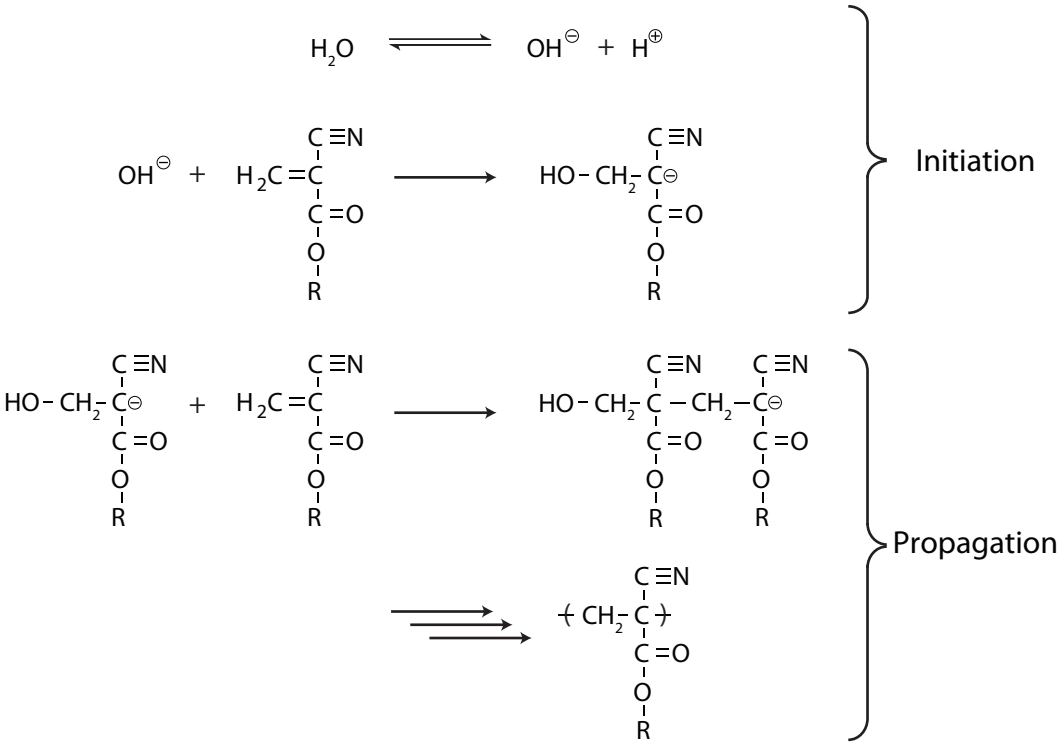

Scheme 7: Anionic polymerization of alkyl cyanoacrylates.

After their accidental discovery in the early 1950s, poly(alkyl cyanoacrylates) were first utilized as industrial adhesives in the 1958, investigated as medical adhesives in the 1960s and 1970s, introduced as commercially-available consumer products in the 1970s and are currently being investigated for a variety of new applications. Their widespread acceptance into such a broad range of fields has been driven by numerous positive attributes. They are especially known for their excellent adhesion to numerous substrates and can be formulated to bond with such disparate materials as plastics, metals, wood, rubber, and skin. Indeed, it is their outstanding adhesion to skin that had led cyanoacrylates to become one of the most widely utilized adhesives for surgical procedures and are especially well-known for these use a replacement for sutures to heal cuts in the skin. They are additionally valued for their brisk reaction rates: with careful formulation, the cure time can be adjusted from seconds to minutes.

With their widespread adoption, at first glance it may seem that the water-mediated polymerization of cyanoacrylates represents the ideal capable of in situ polymerization initiated via an environmentally-borne initiator. Indeed, owing to their extensive utilization, they are reasonably viewed as the gold standard by which all other systems must be judged. Nonetheless, there are serious concerns and drawbacks over cyanoacrylate chemistry that, as will be discussed throughout this dissertation, drive the search for other in situ polymerizable systems.

While cyanoacrylates undoubtedly serve a vital role in medical care as suture replacements, their further widespread utilization is hindered by serious concerns over toxicity. While cyanoacrylates are generally seen as safe for external use, though there are reports of skin necrosis caused by the polymerization exotherm,[62] their suitability for internal surgeries is less assured. The primary issue here are the cytotoxic byproducts that are capable of forming as the poly(alkyl cyanoacrylates) degrades, most notably formaldehyde but also a host of others including cyanoacetates, aliphatic alcohols, and poly(cyanoacrylic acids).[63] Moreover, while the unreacted monomers are not typically a problem for the patients, they do represent a potential occupational hazard for the doctors, nurse, dentists, technicians, and other health care workers who are exposed to these materials regularly over many years; repeated exposure to cyanoacrylates monomers can lead to asthma or dermatitis.[33, 64] Toxicity can be mitigated by modifying the moiety adjacent to the ester linkage; longer alkyl chains have been shown to have reduced toxicity[65] and replacing the alkyl chain with an ether may allow for further improvements.[63] Nonetheless, these types of restrictions severely limit the range of attainable properties.

Certainly, not all of the potential applications for cyanoacrylates are medically-relevant and for these, the health-related concerns will be less applicable. Nevertheless, there are additional problems with cyanoacrylate chemistry that must be addressed. One inherent drawback in relying on atmospheric moisture for initiation is that relative humidity can vary wildly depending on location, season, and time of day, leading to unpredictable reaction rates. For example, Lewis et al, in investigating the use of ethyl 2-cyanoacrylate as a means to develop latent fingerprints, found that no polymer would form when the relative humidity was less than 7%.[66] Even more concerning, Foley et al reported that when attempting to polymerize ethyl 2-cyanaoacrylate when the RH was less than 30%, frequently no polymer would form.[67] While this reaction rate dependence can be acceptable for an environment where the humidity an always be tightly regulated, for many applications, this is simply not possible.

A second, more subtle, issue with reaction rates is the extremely fast gel times reported by for cyanoacrylate a may require a means of initiation other than that of atmospheric moisture. For example, the commercially-available product Dermabond, a 2-octyl cyanoacrylate commonly used for surgical procedures, is packaged in an applicator device that delivers the liquid monomer through a proprietary initiator-laden sponge, effectively treating this a two-component system.[68] When Dermabond is delivered through the sponge, as it would be used when as a wound closure adhesive, the 'set time' required is approximately 50 seconds; conversely, when the liquid monomer formulation is exposed to the atmosphere without allowing it to contact the initiator, set time increased to over 8 minutes. Kennedy and coworkers explored several initiators of 2-octyl cyanoacrylate and were able to create formulations that could set within tens of

seconds.[68] As impressive as this is, upon closer examination, this is not a water-mediated polymerization – It is the action of the amine initiator that is initiating polymerization and allowing for such brisk reaction rates. While this is less of a concern when designing a medical-device intended for use by a trained health care worker in a controlled environment, it is our explicit goal to find a system capable of polymerizing upon contact with an environmentally-borne initiator.

Finally, perhaps the biggest issue with cyanoacrylate chemistry is the inherent limitations of the types of functional groups that may be present on the monomer. The most commercially important monomers, as has been discussed above, are all monofunctional alkyl cyanoacrylates. Modifications to the cyanoacrylate monomers are mainly limited to replacing the alkyl chain with one containing ether linkages or terminal allyl groups. Incorporation of other functional groups is inherently limited as any moiety remotely nucleophilic will initiate polymerization, thus precluding the use of hydroxyl, carboxylate acids, amines, and thiols. Indeed, we have similar limitations for any system capable of water-mediated polymerization (e.g., an isocyanate-based formulation) and such reactivity could lead to premature gelation, rendering the product completely unusable.

Therefore, despite the many positive attributes of alkyl cyanoacrylates and their long, history of commercial success in a variety of fields, their numerous drawbacks force us to continue our search for a system capable of in situ polymerization initiated by an environmentally-borne initiation stimulus. Nonetheless, by examining the beneficial characteristics of cyanoacrylate chemistry, we have a model for our desired system that strongly suggests we focus our search on polymerization reactions where the

environmentally-borne reagent serves as a catalyst or an initiator, rather than as a stoichiometric reagent. In other words, the polymerization mechanism should utilize an active site, points in the chain or networks where further additions may occur. This requirement is strongly suggestive of a chain-growth mechanism, where a radical, cation, or anion (as with alkyl cyanoacrylates) serves as the active site. However, these are not the only polymerization mechanisms that utilize an active site – an important point that will be revisited shortly.

1.2.2 Atmospheric Gases

Having exhausted the range of possibilities where atmospheric moisture is utilized as a polymerization stimulus and finding these options unsatisfactory, we must now examine other chemical compounds that are reliably present in human-habitable environments. The most obvious choice are the atmospheric gases, the four most common being nitrogen, oxygen, argon, and carbon dioxide. Of these, we can safely disregard the noble gas argon owing to its extremely stability; it participates in very few reactions and a list of compounds it readily forms is amusingly short.[69]

Consider the utilization of atmospheric nitrogen as an environmentally-borne polymerization reagent. Nitrogen is certainly plentiful in human-habitable environments, making up approximately 79% of our atmosphere. Unfortunately, molecular nitrogen, made of two nitrogen atoms bound by a triple bond, it notoriously stable. While molecular nitrogen can be converted into ammonia via the Haber-Bosch process, this requires very high temperatures and this process is not adaptable to ambient conditions. Indeed, molecular nitrogen participates in few reactions at ambient temperatures. For this reason alone, it seems that the idea of using atmospheric molecular nitrogen as an

environmentally-borne reagent should be rapidly dismissed and our attention turned elsewhere. However, on reflection, perhaps nitrogen should not be ignored so easily. After all, nitrogenase enzymes present in cyanobacteria convert molecular nitrogen into ammonia,[70] which can then undergo a complex series of reactions where it can be converted to and from nitrates and eventually, through assimilation reactions, is converted into nitrogen-containing biomacromolecules (e.g., proteins and nucleic acids).[71] Unfortunately, this process is extraordinarily complicated and, at present, the development of synthetic means to mimic the action of nitrogenases is still an active area of research.[72] Beyond this issue, there are a host of other problems that would also need to be dealt, including that nitrogenases are quite sensitive to the presence of oxygen – a major hindrance in performing in situ polymerization in a human habitable environment.[70] As a result, there is currently no clear path to using atmospheric nitrogen as a reagent for in situ polymerization and we must return to our original conclusion that nitrogen is a poor choice for an environmentally-borne polymerization reagent.

As nitrogen is a poor choice for an environmentally-borne polymerization initiator, let us consider another atmospheric gas, carbon dioxide (CO_2). At first glance, CO_2 is also a poor initiator choice as its atmospheric concentration is only 0.039% – about 1/2000 of atmospheric nitrogen. Moreover, CO_2 is also quite unreactive. In fact, because of its chemical inertness, supercritical CO_2 is utilized as a reaction medium for variety of polymerization reactions, including free radical, cationic, and oxidative coupling polymerizations, for which it has been shown not to participate in initiation, propagation, chain-transfer or termination reactions.[73] Such limited reactivity at supercritical conditions strongly suggests that most polymerization reactions would not

be affected by the much lower CO_2 concentration present in the atmosphere. Conversely, CO_2 certainly participates in reactions under ambient conditions as it is necessary for the survival of most plant life; it is utilized as an environmentally-borne reagent in the photosynthetic processes plants use to generate sugars – including polymeric ones like cellulose. Indeed, CO_2 has been used as a reagent in synthetic polymer chemistry. As a chemical reagent, it has numerous desirable attributes – mainly that it is cheap, non-flammable, and readily available – and it has been utilized as a reagent in countless reactions. It is especially well known for its use in a reaction with cycloaliphatic epoxides to form polycarbonates.[74-77] To give a recent example, limonene epoxide and carbon dioxide, at a pressure of 100 PSI, has been used with a zinc-based catalyst to yield an alternating copolymer with excellent stereo- and regioregularity.(Scheme 8)[78]

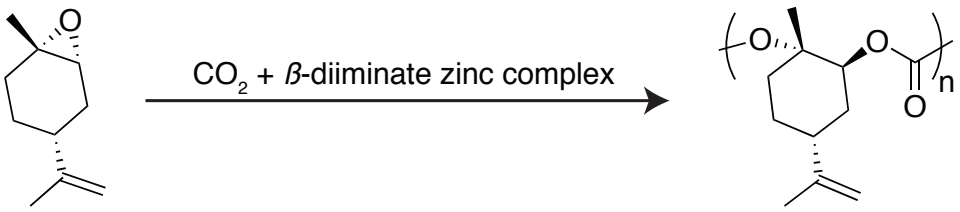

R-trans-limonene oxide Poly(R-limonene carbonate)

Scheme 8: Utilizing carbon dioxide as a reagent in making polycarbonate.

Despite this demonstrated utility in polymer chemistry, none of the examples utilize carbon dioxide at atmospheric concentrations nor are they, given their low yields and/or the requirement for non-ambient conditions (e.g., elevated temperature), readily adaptable to in situ processes. Indeed, there appear to be few opportunities for utilization of CO_2 as an environmentally-borne reagent no it is somewhat surprising that, given the aforementioned limits to carbon dioxide's reactivity, there have been instances were CO_2 has been utilized as an environmentally-borne reagent. Urban and co-workers devised a

polyurethane, using a tin-catalyst, that contained sugar moieties.[79] This sugar-modified polyurethane exhibited self-repair properties in the presence of carbon dioxide and water at atmospheric concentrations. When a 100 μm scratch is induced on a sheet of these sugar-modified polyurethanes, the scratch will heal itself in approximately 30 minutes whereas a control experiment using a polyurethane without the sugar moieties did not heal. The healing mechanism itself is quite complicated and it involves the tin catalysts reacting with the sugar moieties and the resulting tin complex, in reactions involving CO_2 and water, can react to form carbonates, urethane, or urea linkages.

Yet even with this quite interesting example, with the low reaction rates its appears it would be quite difficult and rather impractical to utilize this method for in situ polymerization. Moreover, none of the reactions discussed here utilize carbon dioxide as an initiator or catalyst; rather, carbon dioxide is utilized exclusively as a stoichiometric "reagent. Thus, with its low atmospheric concentration and limited reactivity, carbon dioxide does not seem to be a good candidate as an environmentally-borne initiation stimulus.

Having dismissed argon, nitrogen, and carbon dioxide as poor choices for an environmentally-borne initiator, we are left with oxygen. While oxygen has a lower atmospheric concentration than nitrogen (21% vs. 79%), its concentration is still relatively high compared with all other options (e.g., argon, carbon dioxide, and water). Furthermore, it is considerably more reactive than nitrogen, carbon dioxide, or argon and it is especially well-known for its ability to participate in redox reactions.[80] With these promising characteristics, oxygen is clearly an excellent candidate for use as an environmentally-borne initiator. Indeed, oxygen has been widely utilized as an initiating

system component for several types of polymerization reactions, some of which may be useful for our purposes, and these systems will be investigated in the next section.

1.3 Strategies for Oxygen-mediated Polymerization

1.3.1 Oxidative Cross-linking of Drying Oils

One of the most commercially important oxygen-mediated polymerization mechanisms is the oxidative cross-linking of oil-based coatings, used for centuries for both artistic and protective paints.[81] These materials all contain unsaturated fatty acids, commonly linolenic acid or linoleic acid, and, when formulated as paints, undergo a complex process of solvent evaporation and chemical reactions that drives the transformation from a liquid into a solid, cross-linked film.[54] The materials are in the form of either triglycerides, made from glycerol and fatty acids, or so-called alkyds, oil-modified polyester resins made from polyols, polyacids, and fatty acids. The ability of the unsaturated oil to undergo oxygen-mediated cross-linking largely depends on the presence of doubly allylic moieties, as the bis-allylic hydrogen is readily abstractable. As the paint film is applied to surface, atmospheric oxygen begins to permeate into the paint film, inducing the formation of hydroperoxides; subsequent hydroperoxide decomposition reaction yields alkyl and alkoxy radicals that terminate via combination to form C-C, C-O-C, and C-O-O-C linkages. The film is cross-linked through these radical termination reactions rather than propagation reaction with the internal alkenes.[82] Included within the paint formulations are metal soaps, called ‘driers’, that catalyze multiple reactions. Moreover, real paint formulations almost always include multiple driers, with some that aid surface cure and others that promote through cure. Among the most important and commonly utilized driers are those containing cobalt. Unfortunately,

there are serious concerns over their toxicity and while the search for replacements continues, no superior replacement has been identified yet.

Oil-based paints typically are viewed as slowly reacting systems as they tend to cross-link over days, weeks, and months. While an initial "dry-to-the-touch" state may be achievable in 8-24 hours, a completely cross-linked film takes much longer. Furthermore, as cross-linking continues over time, the film may actually become overly cross-linked, leading to embrittlement. Conversely, there may also be chain scissioning reactions that lead to a weakening of the paint film.[54, 81]

While these oil-based systems have proven to be well-suited for paints and coatings, and with the development of water-borne versions continue to be utilized, their utility beyond coatings is questionable, given their slow reaction rates and toxicity issues over the metal driers. Thus, while drying oils and alkyds provide a wonderful demonstration of the utility of oxygen-mediated polymerization, systems that are more generally applicable need to be investigated.

1.3.2 Enzymes

Enzymes are proteins that catalyze biochemical reactions. By binding a substrate to the active site of an enzyme, the activation energy of the reaction can be decreased, resulting in a substantial reaction rate increase. For example, the enzyme orotidine 5'-phosphate decarboxylase accelerates the orotidine 5'-monophosphate decarboxylation rate by 1017 times the uncatalyzed reaction rate.[83] Whereas enzymes are responsible for all naturally synthesized biomacromolecules, they are also capable of retaining catalytic properties outside of biological systems and thus have been employed for in vitro polymer synthesis. The first enzymatic polymerization was reported in 1951 by Parravano who

demonstrated an oxidase-mediated polymerization of methyl methacrylate.[84] Since then, many enzymes have been investigated as a means to initiate or control polymerization reactions in order to take advantage of their strengths, including high catalytic turnover, environmentally-friendliness (e.g., production from renewable resources), facile control of polymer architecture, and easy separation from products. Many, though certainly not all,[85-91] enzyme-mediated polymerization reactions involve free radicals; these free radical species are generated either directly by the enzyme or via a secondary reaction involving an enzyme-derived product, methods that eliminate the requirement for the thermal energy or irradiation used to initiate conventional free radical polymerization. These enzymatic, radical-generating reactions all utilize reduction and oxidation steps and, accordingly, most of the enzymes used in these processes are termed oxidoreductases. Commonly, these enzymes utilize either oxygen or hydrogen peroxide as a substrate and are generally known as oxidases or peroxidases, respectively. Among the radical-generating oxidases and peroxidases, the most commonly utilized enzymes for radical-mediated polymerization reactions include horseradish peroxidase, glucose oxidase, and laccase. Through different reactions mechanisms, these three enzymes, as well as several others with similar behavior, are able to initiate, catalyze, or otherwise influence several polymerization reactions, most commonly the chain-growth polymerization of vinyl monomers and polymerization via the oxidative coupling of phenolic monomers. As our interest here is in oxygen-mediated polymerization, oxidoreductase-based initiating systems that afford radicals as a result of oxygen exposure are of great interest. As will be discussed at length in the following sections,

oxidoreductases can either afford radicals directly or generate a product that will, in a subsequent reaction, yield initiating radicals.

1.3.2.1 Chain-growth Polymerization of Vinyl Monomers

The chain-growth free radical polymerization of vinyl monomers (e.g., acrylates, methacrylates, acrylamides, and styrenics) is utilized in a broad array of applications, including plastics, coatings, adhesives, and sealants. Polymerization commences upon an initiation step where a radical, generated by exposing a thermal, photo, or redox initiator to its associated stimulus (heat, light, or chemical, respectively), adds across the carbon-carbon double bond of a vinyl monomer, generating a carbon-centered radical.[92, 93] This radical, in turn, reacts with another vinyl monomer, increasing the size of the molecule and again regenerating a carbon-centered radical; these propagation reactions rapidly repeat and the polymer chain grows quickly. Polymerization ceases through one of several termination reactions, including combination and disproportionation, that eliminate the radical, or through chain transfer, a side reaction where the radical on the growing chain abstracts a labile hydrogen, stopping propagation on the original chain and leading to the initiation of a second growing chain. Another common side reaction occurs when an active radical on the growing chain propagates to molecular oxygen to yield a peroxy radical (Scheme 9). Unlike carbon-centered radicals, the peroxy radical reacts sluggishly with monomers, drastically reducing the reaction rates, and causing polymerization to nearly cease.[94] Consequently, the radical-mediated chain-growth polymerization of vinyl monomers is typically very susceptible to oxygen inhibition.

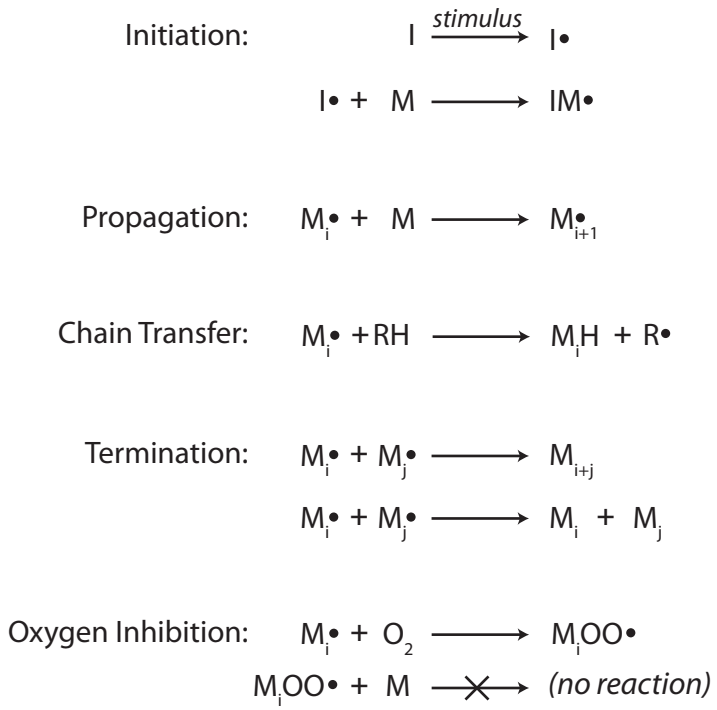

Scheme 9: Chain-growth polymerization reactions.[92, 93] I = an initiator, M = vinyl monomer, M_i or M_j = polymer with,* i *or* j *repeat units, respectively, O = oxygen, H = hydrogen, RH = a compound with a readily abstractable hydrogen, R = RH after hydrogen abstraction.

In addition to thermal-, photo-, and organometallic redox-initiators, enzymes have been used to generate the radicals necessary for the initiation of chain-growth polymerization. An early report by Derango and coworkers demonstrated that several enzymes (horseradish peroxidase, xanthine oxidase, chloroperoxidase, and alcohol oxidase) would, in the presence of suitable substrates, polymerize aqueous solutions of acrylamide and hydroxyethylmethacrylate (HEMA);[95] as the polymerization proceeded, the polymer would either precipitate out of solution or would form a hydrogel. The enzymes used by the Derango group are all oxidoreductases—enzymes that concurrently reduce one substrate while oxidizing another. Commonly employed oxidoreductases include peroxidases, which reduce hydrogen peroxide, and oxidases, which reduce molecular oxygen; the substrate that is being oxidized depends upon the particular

enzyme, but may be one of the monomers themselves or an additional compound known as a mediator. Three oxidoreductase enzymes, horseradish peroxidase, glucose oxidase, and laccase, dominate the discussion here.

1.3.2.1.1 Horseradish peroxidase

One of the most commonly used enzymes for polymerization reactions is horseradish peroxidase (HRP), a heme-containing enzyme with a molar mass of approximately 40 kDa[96] that is capable of generating radicals by reducing hydrogen peroxide to water while oxidizing two equivalents of a hydrogen-donating mediator (Scheme 10);[97-99] the oxidation of the mediator affords radicals capable of initiating polymerization. HRP, derived from the horseradish root, contains several different isoenzymes of which the C isoenzyme (HRP C) is the most commonly used.[100] HRP has been utilized in many applications, including waste treatment, where it has been utilized in the removal of phenolic compounds from wastewater,[101-103] and immunoassay-type biochemical testing.[104-106]

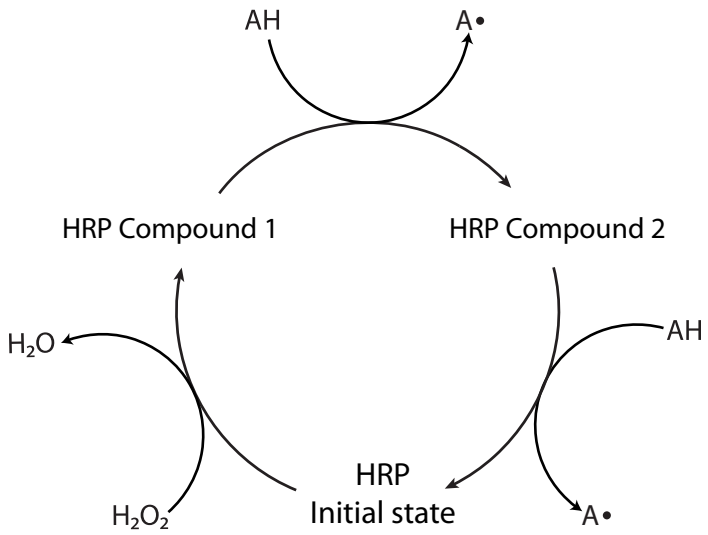

Scheme 10: Horseradish peroxidase (HRP) catalyzes the reduction of hydrogen peroxide to water by oxidizing two equivalents of a hydrogen-donating mediator AH. HRP compounds 1 and 2 are oxidized forms of HRP that are each capable of oxidizing the mediator AH, yielding radicals that may be utilized for the initiation of radical-mediated polymerization]. [97-99] ***Arrows show reaction direction.***

Amongst its many roles in catalyzing polymerization reactions, HRP has been utilized extensively for the solution polymerization of vinyl monomers. Expanding on the early work described by Derango and coworkers,[95] Lalot and coworkers demonstrated that acrylamide is readily polymerized into poly(acrylamide) by utilizing HRP, hydrogen peroxide, and a diketone mediator, commonly acetylacetone, as a ternary initiating system (Scheme 11); the reaction proceeds at room temperature upon combining the aqueous solution of acrylamide with all three components of the initiating system.[97, 107-109] A recurring theme of enzymatic polymerization is that, for many systems, no reaction proceeds until all necessary components are present, opening up the possibility that such initiating systems may be suitable for in situ polymerization. For the system described by Lalot and coworkers, if only two of the three initiating components were added, no reaction proceeded until the addition of the third.[107] In the presence of all three (utilizing

1.8 g/L HRP, 0.01 M H_2O_2, and 0.017 M acetylacetone), polymerization proceeded over several hours, leading to the formation of atactic poly(acrylamide) with a number-average molecular weight (M_n) of between 150 and 460 kg/mol and reaction conversions of 70%–90%. One significant reason for this extended reaction period was an approximately one hour induction period where no polymerization occurred, likely attributable to oxygen-induced inhibition. Notably, a decrease in reaction yield, from 92% to 72%, was observed as the acrylamide concentration was raised from 1 to 5 M; although the authors attributed this reduced yield to an increase in viscosity, enzyme deactivation via denaturation would yield similar results.

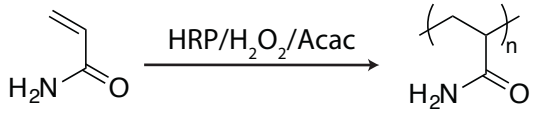

Scheme 11: Acrylamide is polymerized into poly(acrylamide) in the presence of HRP, hydrogen peroxide, and acetylacetone (Acac).[97, 107-109]

It is interesting to note that, whereas Lalot reported no polymerization in the absence of acetylacetone,[107] Derango and coworkers reported the utilization of HRP without the addition of any mediator.[95] This apparent discrepancy is readily explained in that the Derango group used significantly more hydrogen peroxide; thus, the addition of a mediator permits substantially lower hydrogen peroxide concentrations. This is tremendously useful as hydrogen peroxide can deactivate HRP, a problem that is particularly severe at high hydrogen peroxide concentrations.[97] As a demonstration, in the results provided by Lalot, no polymerization proceeded in the absence of the mediator and would, as noted above, start immediately upon its addition;[107] however, delaying the addition of the mediator permitted the hydrogen peroxide to degrade HRP, leading to a

significant decrease in yield. For example, in the polymerization of an aqueous solution of acrylamide monomer, when all three components (e.g., HRP, acetylacetone, and hydrogen peroxide) were present together, the reaction yield was 87%. Similar results were obtained when either HRP or acetylacetone were initially omitted from the formulation and subsequently added one hour later. In contrast, if the acetylacetone was initially omitted and then added later, no polymerization was observed; thus, the hydrogen peroxide necessary for initiation also participated in a deactivation reaction that irreversibly yielded an inactive, non-catalytic form of HRP.

An in-depth exploration of the polymerization of acrylamide by HRP, hydrogen peroxide, and acetylacetone was performed by Wen and coworkers to provide insight into some of the questions raised by earlier work.[110] Regarding the lengthy inhibition periods observed by Lalot,[107] Wen found that the inhibition period prior to polymerization was caused by oxygen inhibition. This inhibition time could be reduced or eliminated by increasing the concentration of acetylacetone, to as high as 0.13 M, as this led to an increase in the radical generation rate; as these radicals reacted with and consumed oxygen, propagation reactions successfully competed with the inhibition reactions allowing the polymerization to proceed once the oxygen concentration was sufficiently low. Owing to the reduced inhibitory period, reactions times were significantly shorter than those observed by Lalot; however, the synthesized poly(acrylamide) batches were similar to those described by Lalot, having M_ns of 200 to 630 kg/mol and dispersities ($Đ$), a measure of the molecular weight distribution width, of 2.0 to 3.0, with yields of 72% to 97%.[110]

In addition to generating soluble polymers in solution, HRP/hydrogen peroxide/acetylacetone ternary initiating systems have been used to generate cross-linked hydrogels by utilizing aqueous solutions of multi-functional vinyl monomers. In work by Wang and coworkers, this method was used to copolymerize acrylated human serum albumin and *N*,*N*-dimethylacrylamide; upon addition of the initiating system component, gels formed within 1 min.[111] These experiments again confirmed the inhibitory influence of hydrogen peroxide, as no gelation was observed when it was used in excess. Interestingly, the residual HRP, effectively immobilized after gelation, retained much of its activity in the hydrogel matrix.

HRP-mediated polymerization has also been utilized to generate polymers on surfaces.[112] Here, poly(acrylamide)-grafted particles were formed by polymerizing acrylamide in the presence of HRP, hydrogen peroxide, and β-diketone-functionalized silica particles. As polymerization was initiated at the β-diketone moiety located on the surface of the silica particles, this process resulted in a core-shell morphology, yielding poly(acrylamide) layers with thicknesses of 15–192 nm; the poly(acrylamide) itself had M_n ranging from 63 to 273 kg/mol, with $Đ$ values from 1.5 to 3.0. Once again, both the initiating and inhibitory roles of hydrogen peroxide were confirmed in these experiments as no poly(acrylamide) shell was formed either in its absence or its presence in excess.

Whereas enzyme-mediated polymerization is naturally suited for use with aqueous monomers, given that many enzymes naturally prefer an aqueous and pH-controlled milieu, HRP is sufficiently tolerant of some organic solvents that it may be utilized with monomers that require the addition of non-trivial amounts of solvent for dissolution. For example, methyl methacrylate, a monomer commonly polymerized via a

free-radical mechanism, has poor solubility in water but does dissolve in aqueous solutions of either tetrahydrofuran (THF) or dioxane. By again utilizing the HRP, hydrogen peroxide, and acetylacetone ternary initiating system in a 25% THF aqueous solution, poly(methyl methacrylate) (PMMA) was readily generated with a M_n of 72 kg/mol and a $Đ$ of 3.1 at 85% yield, and was > 80% syndiotactic.[113] In an example that used even more hydrophobic monomers, styrene, 4-methylstyrene, and 2-vinylnaphthalene were all readily polymerized by HRP when dissolved in a suitable solvent system and in the presence of hydrogen peroxide and a mediator.[98] The authors of this study investigated solvent and mediator effects and found that both significantly influenced yield and molecular weight. Dimethylformamide (DMF), methanol, or dioxane as solvent resulted in particularly low yields, while the best solvent system was found to be THF:H_2O in a 4:1 volumetric ratio. When styrene was dissolved in this solvent system and polymerized in the presence of acetylacetone, the M_n was nearly 32 kg/mol with a yield of 21.2%, while replacing acetylacetone with cyclopentadiene increased the M_n and yield to 68 kg/mol and 59.4%, respectively, affording a poly(styrene) that was nearly completely atactic. Interestingly, the authors reported that the mediator was incorporated into the generated polymer, introducing the potential for post-polymerization modification. Interestingly, the authors reported < 5% yields during control experiments where iron(II) salts were used in place of HRP, although hydroxyl radicals, generated as a result of the Fenton reaction,[114-116] would be anticipated to effect polymerization. This is perhaps unexpected as the utilization of the non-enzymatic Fenton reaction in combination with the enzymatic production of hydrogen peroxide has been previously reported.[117] The lack of iron-mediated polymerization here was likely

owing to high (e.g., 0.16 M) Fe^{2+} concentrations leading to polymerization-suppressing inhibitory and terminating reactions.[118]

As an alternative to solution polymerization in non-aqueous systems, HRP-mediated emulsion polymerization has also been utilized with monomers having limited water solubility. To illustrate, an emulsion of styrene in water, stabilized by the surfactant sodium dodecyl sulfate (SDS), was polymerized under anaerobic conditions by the familiar HRP, hydrogen peroxide, and acetylacetone ternary initiating system.[119] As the components of the initiating system are all water soluble, polymerization proceeded through an emulsion polymerization mechanism, where polymers growing within surfactant-stabilized micelles yielded stable particles. This resulted in the formation of stable poly(styrene) particles, with diameters of 30–50 nm and yields typically between 40% and 60%; the polymer had M_n ranging from 173 to 516 kg/mol with $Đ$ of between 3 and 8, with both being influenced by hydrogen peroxide concentration. Another approach to enzyme-mediated emulsion polymerization was demonstrated by utilizing HRP immobilized on a silicon wafer.[120] The immobilization of HRP to a solid substrate conceivably simplifies its removal from the reaction mixture and allows its reuse. Emulsions of ethylene glycol dimethacrylate, stabilized by cetyltrimethylammonium bromide, were polymerized with the immobilized HRP, hydrogen peroxide, and acetylacetone. Although conversions were low—less than 5%—control experiments using free HRP yielded similar results. While the polymerization results described here were somewhat disappointing, given the very low yields, the procedure did successfully demonstrate the reusability of immobilized HRP.

1.3.2.1.2 Glucose Oxidase

Another oxidoreductase, glucose oxidase (GOx), has also been utilized to initiate vinyl polymerization. GOx is a dimeric glycoprotein obtained from various sources and has been extracted from several fungi including Aspergillus[121, 122] and Penicillium.[122, 123] This enzyme is composed of two identical polypeptide chain subunits connected by a disulfide bond,[122, 123] with a total molar mass that varies from 130 to 175 kDa,[122] and relies on a tightly bound cofactor, flavin adenine dinucleotide (FAD), for its catalytic activity. GOx utilizes molecular oxygen as an electron acceptor to catalyze the oxidation of β-d-glucose to d-glucono-δ-lactone and hydrogen peroxide.[121, 124] This reaction initially proceeds by the enzymatic oxidation of glucose to d-glucono-δ-lactone, which is then non-enzymatically hydrolyzed to gluconic acid and is generally of little importance to subsequent reactions, while the cofactor FAD is reduced to $FADH_2$. Subsequently, the reduced cofactor is reoxidized by molecular oxygen to yield hydrogen peroxide (Scheme 12a).[125] The in situ generated hydrogen peroxide can then be converted into initiating radicals through several strategies. An early example, by Iwata and coworkers[117] utilized Fenton chemistry (Scheme 12b)[114-116] whereby the oxidization of Fe^{2+} to Fe^{3+} concomitantly reduced hydrogen peroxide to a hydroxyl anion and a hydroxyl radical – the polymerization initiating species. Here, aqueous solutions of 2-hydroxyethyl methacrylate (HEMA), dissolved in a 0.1 M acetate buffer solution, were polymerized by the addition of GOx, glucose, and ammonium ferrous sulfate ($(NH_4)_2Fe(SO_4)_2$) (Scheme 13). The authors confirmed that no polymerization proceeded in the absence of oxygen or Fe^{2+}, but formulations lacking either of these components would begin to polymerize once the missing components was added. This concept was explored in depth in a series

of papers by Bowman and coworkers where hydrogels were formed from aqueous solutions of acrylate monomers.[118, 126-129] In their earliest paper,[118] hydrogels were formed from poly(ethylene glycol) diacrylate (PEGDA) and 2-hydroxyethyl acrylate within minutes of adding the initiating system components. The oxygen required for the reaction as supplied simply by the dissolved gases normally present (about 10^{-3} M) in the monomers. While oxygen is known to inhibit the chain-growth polymerization of acrylates, the GOx-mediated reaction consumed the oxygen sufficiently quickly to enable polymerization to proceed without significant oxygen inhibition. Regarding control over reaction rates, both Fe^{2+} and glucose played significant roles. Increasing the glucose concentration increased the polymerization rate until a point is reached where the system is saturated; as GOx is limited in how fast it can process glucose, excess glucose (greater than 1.0×10^{-3} M glucose with 6.25×10^{-7} GOx) did not increase reaction rates further once this point was reached. In contrast, whereas polymerization rates increase with raised Fe^{2+} at low Fe^{2+} concentrations, rates began to decrease at high Fe^{2+} concentrations (approximately 3×10^{-4} M). This iron-mediated inhibition was attributable to radical-consuming side reactions involving either Fe^{2+} or Fe^{3+} ions. Despite these minor limitations, this initiating system was used to generate cell-encapsulating hydrogels, where the high resultant cell viability demonstrated the cytocompatibility of the initiating system components, including the residual GOx. [118] Thus, the hydrogels generated by this method could be suitable for utilization in biomedical applications.

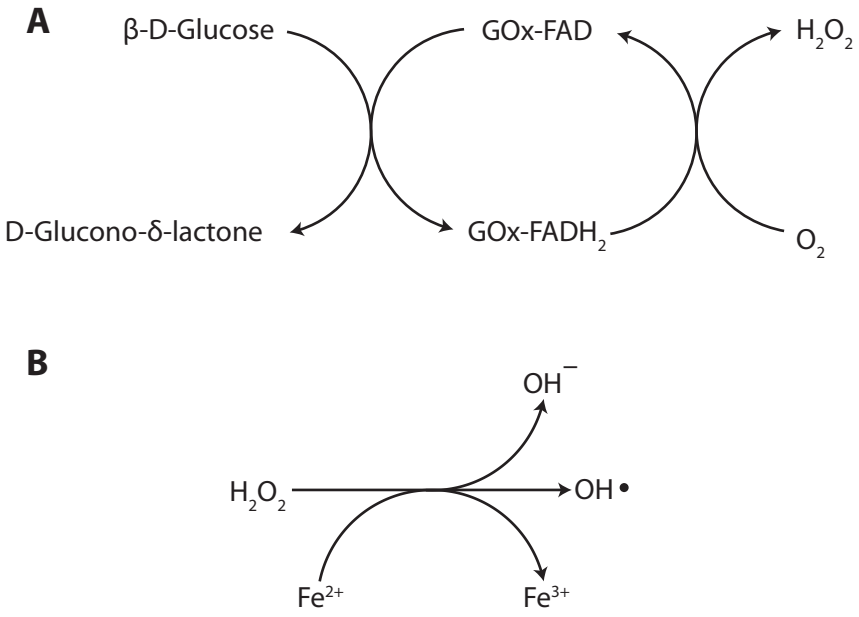

Scheme 12: (A) Glucose oxidase catalyzes the reduction of oxygen and oxidation of glucose into hydrogen peroxide and gluconolactone, respectively. (B) Hydrogen peroxide is readily converted to hydroxyl radicals via the Fenton Reaction with Fe^{2+} ions.[114-116] Arrows show reaction direction.

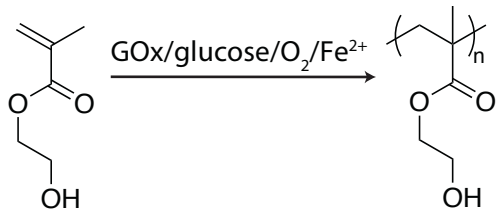

Scheme 13: 2-Hydroxyethyl methacrylate (HEMA) is polymerized into poly(HEMA) in the presence of glucose oxidase (GOx), glucose, oxygen, and Fe^{2+}. [117]

As noted above, a peculiarity of HRP-mediated polymerization is the rapid enzyme degradation by hydrogen peroxide.[97, 98] This represents a serious challenge as hydrogen peroxide is the most common oxidant in the redox reaction catalyzed by HRP. While it is possible to circumvent HRP deactivation by simply adding the hydrogen peroxide slowly, limiting the concentration present at any given time, this manual and tedious solution is not always applicable, notably during in situ polymerizations. Instead of manually controlling the concentration, hydrogen peroxide can be generated in situ by utilizing

GOx, an approach that minimizes the hydrogen peroxide concentration present at any time as the GOx-generated hydrogen peroxide is quickly consumed by HRP. Such a bienzymatic system has been utilized both for thiol–ene reactions and for the oxidative coupling of phenols (both of which are discussed at length below), and has also been used for vinyl polymerization. For example, the GOx/HRP system was utilized to form bioinorganic hybrid hydrogels by polymerizing poly(ethylene glycol) methacrylate (PEGMA) in the presence of calcium niobate (CNO) nanosheets.[130] Self-assembled sandwich structures, generated by combining HRP and CNO, were dispersed in an aqueous solution and polymerization would proceed after PEGMA, GOx, and glucose were added in the presence of molecular oxygen. During polymerization, the assembled HRP/CNO structures would exfoliate, leading to the formation of a composite structure. As the enzymes were generally left unaffected by the polymerization, they were still able to function as catalysts even after hydrogel formation. To evaluate the reusability of the immobilized enzymes, pyrogallol and glucose were added to the hydrogels; an enzymatic cascade, similar to the polymerization reaction, would proceed and the hydrogen peroxide, generated by GOx, would induce HRP-mediated oxidation of pyrogallol into purpurogallin. Even after five cycles, the enzymes retained over 80% of their activity. Furthermore, the authors also found that the presence of the CNO nanosheets aided in preventing enzyme thermal deactivation, permitting these materials to be used under a broader range of conditions and suggesting their utility in a variety of sensor and purification applications.

Bienzymatic systems have also been employed to solve other problems, notably circumventing oxygen inhibition. As discussed above, the radical-mediated

polymerization of vinyl monomers is particularly susceptible to oxygen inhibition. The presence of GOx in a bienzymatic initiating system thus functions not only in its aforementioned role for the in situ production of hydrogen peroxide but also as an oxygen scavenger, deceasing the oxygen concentration such that propagation is no longer inhibited. In one example, the enzyme-mediated polymerization of 3-aminopropyl methacrylamide (APMA) was utilized to effect gold nanoparticle aggregation; once a sufficient degree of polymerization was reached, the resultant aggregation of the gold nanoparticles afforded a color shift readily monitored by changes in the visible spectrum.[131] In this system, both GOx and HRP were utilized and it was the presence of GOx that permitted the polymerization reaction to proceed without inhibition under atmospheric conditions.

Not all GOx-mediated reactions utilize molecular oxygen as the oxidant. Polymerization of PEGDA has been initiated by GOx (4×10^{-6} M), in the presence of glucose, catalyzing the reduction of *N*-hydroxy-5-norbornene-2,3-dicarboximide (HNDC) into a carbon-centered radical species.[132] Moreover, this reaction still proceeded in the presence of HNDC-conjugated heparin, resulting in a hybrid PEGDA/HNDC-conjugated heparin hydrogel. Unlike the examples of GOx-mediated polymerization described above, molecular oxygen seemingly played no initiating role—all materials were thoroughly degassed prior to use. Such heparin-based hydrogels may be suited for drug delivery as the heparin-degrading enzyme heparanase is frequently overexpressed by some forms of cancer.[133]

1.3.2.1.3 Laccase

Laccases, copper-containing oxidoreductases that are obtained from a variety of organisms, commonly fungi, including *Pycnoporus coccineus*,[134] *Myceliophthora thermophile*,[135] *Trametes trogii*,[136] and *Trametes versicolor*,[137-139] catalyze the reduction of molecular oxygen while concurrently oxidizing a hydrogen-donating substrate (Scheme 14).[135] These reactions result in the formation of radical-bearing species and have been utilized in pulp/paper,[140] food/beverage, and waste treatment applications.[141, 142] Laccase is of growing interest for polymerization reactions as it is able to directly generate radicals by oxidation of a mediator, commonly acetylacetone, unlike GOx which usually requires a second reaction to afford initiating radicals from the generated hydrogen peroxide. By utilizing a ternary initiating system similar to ones with HRP discussed above, Kobayashi and coworkers demonstrated the polymerization of acrylamide in the presence of oxygen, 0.016 M acetylacetone, and 7.8 g/L laccase (Scheme 15), affording polymer with a M_n of 23 kg/mol and a $Đ$ of 2.0 at 97% yield.[134] The presence of acetylacetone was necessary to perform the polymerization at room temperature, which otherwise required elevated temperatures to generate polymer. In a study expanding upon this work, Hollmann and coworkers confirmed the lack of polymer formation in the absence of any component of the ternary initiating system (*i.e.,* oxygen, acetylacetone, or laccase) when performing the reaction at room temperature, as well the inhibitory role adopted by oxygen—a problem they termed the "oxygen dilemma".[135] Furthermore, they explored the limitations of laccase-mediated vinyl polymerization, notably the low activity of the enzyme and its poor stability. As a result of these issues, laccase is far less common than HRP to effect radical-mediated polymerizations;

nevertheless, vinyl polymerizations mediated by laccase continue to be explored. To address the dual initiating/inhibiting roles oxygen plays, del Monte and coworkers utilized GOx as an oxygen scavenger.[143] They found that a quaternary initiating system composed of laccase, a mediator, GOx, and glucose would readily induce the polymerization of PEGDA monomers in aqueous solution at 37 °C, leading to the formation of a cross-linked hydrogel. Interestingly, oxygen-mediated inhibitory reactions completely prevented polymerization the absence of GOx and glucose, perhaps surprising as both laccase and GOx utilize oxygen as oxidant and thus each should be capable of removing oxygen from the solution. Also of note is that the hydrogen peroxide generated by GOx did not play any obvious role in the reaction mechanism, as the addition of catalase (an enzyme that removes hydrogen peroxide, converting it into oxygen and water) had minimal influence on the reaction conversion. Notably, instead of using a more typical diketone (e.g., acetylacetone), polyethylene glycol-polypropylene glycol-polyethylene glycol (PEG-PPG-PEG) block copolymers were utilized as macro-mediators; as initiation proceeded from a PEG-PPG-PEG-centered radical, the mediators were incorporated into the polymer network. While the utilization of macro-mediators led to lower conversions than when acetylacetone was utilized, the temperatures required were still sufficiently low to prevent enzyme deactivation. Moreover, the laccase encapsulated within the hydrogel retained 90% of its activity after polymerization, rendering it suitable for pollutant degradation applications.

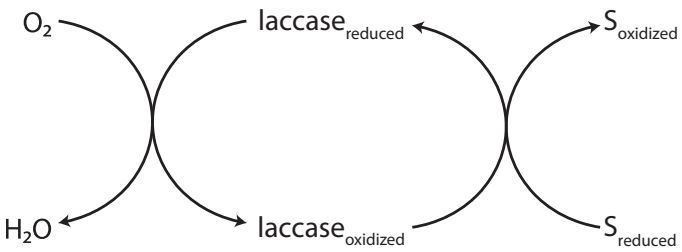

Scheme 14: Laccase catalyzes the reduction of oxygen to water by oxidizing an appropriate substrate.[135] Arrows shown reaction direction.

In an exploration of the pollutant removal ability of a laccase-bearing polymer matrix, Zhang and coworkers first grafted poly(acrylamide) to chitosan in a laccase-mediated polymerization;[138] once again, the necessity of a mediator, acetylacetone, was confirmed as no polymer formed in its absence. The resulting combination of the chitosan-poly(acrylamide) graft copolymer, laccase, and acetylacetone were then successfully used to decolorize a model organic pollutant, malachite green, confirming that laccase was not deactivated during the formation of the chitosan-poly(acrylamide) graft copolymer.

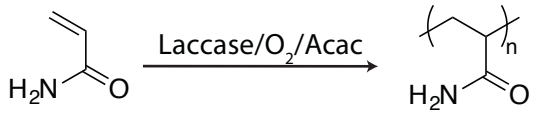

Scheme 15: Acrylamide is polymerized into poly(acrylamide) in the presence of laccase, oxygen, and acetylacetone (Acac).[134]

In one particularly sophisticated application, laccase was used in the fabrication of composite nano-gel particles, generated from *N*,*N*'-bis(acryloyl)cystamine and loaded with two enzymes, catalase and superoxide dismutase, for utilization in ultrasound imaging.[144] The formulation contained clusters made from supermagnetic iron oxide and an acrylate- and biotin-functionalized chitosan, as well as the laccase and *N*,*N*′-bis(acryloyl)cystamine needed to form a nano-gel layer around the clusters, and polymerization at 25 °C resulted in the formation of 13 nm diameter particles.

While the laccase examples described thus far have utilized oxygen as a necessary component for initiation, results reported by di Lena and coworkers described the laccase-mediated polymerization of methacrylates via an anaerobic mechanism.[145] They found that an aqueous solution of poly(ethylene glycol) methacrylate could be anaerobically polymerized in the presence of laccase, ascorbic acid, and ethyl 2-bromoisobutyrate; all three components of this ternary initiating system were required to achieve significant reaction conversion, as no reaction occurred in the absence of laccase or ascorbic acid, while reaction conversions of only 2% were attained in the absence of ethyl 2-bromoisobutyrate. This initiating system is notable as it resembles those utilized for atom transfer radical polymerization (ATRP), a living polymerization method used to generate polymers with narrow dispersities (*i.e.,* the breadth of a polymer's molecular weight distribution).[146] Unfortunately, despite the superficial similarity to ATRP, the laccase/ascorbic acid/bromo-compound ternary initiating system led to the formation of polymers with a $Đ$ of greater than 1.94, much higher than those readily attainable through ATRP (often less than 1.1). Moreover, there was no correlation between molecular weight and reaction conversion—another trait of living radical polymerization. Even though the dispersities were disappointingly high, they found that it was possible to narrow the molecular weight distribution, achieving a $Đ$ of 1.35, by utilizing a different living polymerization method, reversible addition fragmentation chain transfer (RAFT).[146] In subsequent research, by this group and others, there have been many additional reports on enzyme-mediated living radical polymerization;[147-152] however, as it is not closely related to oxygen-mediated polymerization, any further discussion is beyond our scope.

1.3.2.2 Oxidative Coupling

Phenol and related compounds will polymerize via an oxidative coupling mechanism in the presence of oxygen and a suitable catalyst (often copper salts and amines) (Scheme 16). This process is best known for the commercial manufacture of poly(phenylene oxide) (PPO) from 2,6-substituted phenols via a polycondensation reaction, generating water as a byproduct, with a complex reaction mechanism that exhibits characteristics of both chain- and step-growth polymerization.[153, 154] While the details of the reaction mechanisms are quite different from both vinyl chain-growth and thiol–ene step-growth polymerization, the utilization of oxidases and peroxidases to effect polymerization via oxidative coupling shares many characteristics with the other enzyme-mediated polymerization mechanisms.

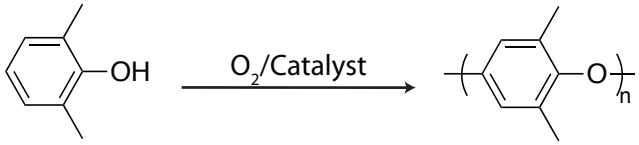

Scheme 16: The polymerization of 2,6-dimethylphenol into a poly(phenylene oxide) via oxidative coupling.

1.3.2.2.1 Horseradish Peroxidase

In many early examples, HRP was used to remove phenols from water by initiating oxidative coupling reactions that yielded dimeric, oligomeric and polymeric products.[101, 102] The intention here was not to produce polymers for use, but rather to aid in the removal of toxic pollutants; these products tend to be insoluble and readily precipitate, allowing for their facile removal by filtration. To illustrate, HRP and hydrogen peroxide were added to aqueous solutions of phenols to generate the readily separable higher molecular weight products.[101] In contrast to the behavior observed with vinyl

polymerization, phenol reacted directly with HRP and thus no additional mediator (e.g., acetylacetone) was required. Other than this difference, the utilization of HRP for either vinyl polymerization or oxidative coupling has many similarities, including a tendency for HRP to be deactivated by excess hydrogen peroxide; one strategy to inhibit HRP-deactivation was to add poly(ethylene glycol) as it seemed to offer some protection to the enzyme and extended its useful lifetime.[101] Beyond this early work, the pollution removal capabilities of HRP continue to be developed. Tang and coworkers combined the HRP/hydrogen peroxide system with a composite made of graphene oxide and nano-Fe_3O_4 (GO/Fe_3O_4) and explored the capabilities of these materials for removing 2,4,-dichlorophenol (DCP).[103] The HRP/hydrogen peroxide system was shown to remove 35% DCP within 2 h, while the GO/Fe_3O_4 composite on its own would only remove 9%. Combining the two systems demonstrated a synergistic effect where 93% of the DCP was removed, most of which occurred in the first 30 min. Other research has explored methods for preventing the deactivation of HRP by hydrogen peroxide. In efforts by Lopez-Gallego and coworkers,[155] hydrogen peroxide was generated in situ by the action of two enzymes. This trienzymatic system, reminiscent of the GOx/HRP bienzymatic cascade discussed previously, used formate dehydrogenase, nicotinamide adenine dinucleotide (NADH) oxidase, and HRP, along with two redox cofactors, oxidized nicotinamide adenine dinucleotide (NAD^+) and flavin mononucleotide (FMN). First, by the action of formate dehydrogenase, formic acid was oxidized to carbon dioxide while NAD^+ was converted to its reduced form (NADH). The reduced NADH underwent a redox reaction with FMN, regenerating the oxidized NAD^+ concomitantly with the reduced $FMNH_2$ which, by the action of NADH-oxidase, was oxidized back to FMN as

molecular oxygen was reduced to hydrogen peroxide. Finally, by the familiar behavior of HRP, phenolic contaminants were polymerized. Interestingly, this enzymatic cascade did not function when all the enzymes were solubilized; while this inhibitory mechanism was not elucidated, it appears likely that one of the enzymes may have been deactivated by the presence of hydrogen peroxide. Nevertheless, when the formate dehydrogenase and NADH-oxidase were immobilized on glyoxal-functional agarose beads and HRP on boronate-functional agarose beads, this trienzymatic system functioned well and proved capable of removing phenolic contaminants.

In addition to its role in phenolic contaminant removal, HRP has also been explored as a means to generate useful polymeric materials. As many phenolic compounds, as well as their potential polymeric forms, have limited solubility in water, these reactions are often performed in mixed solutions of water and organic solvents. In an early example by Dordick and coworkers,[156] the polymerization of 4-phenylphenol and other substituted phenols in water/dioxane solutions was demonstrated. While the activity of HRP decreased as the dioxane concentration was increased, it still remained quite active at dioxane concentrations as high as 80% or 90%. This is important as substituted phenols have low solubility in water and their oligomeric derivatives even less so, thus the production of higher MW products necessitated the utilization of solvent blends with significant dioxane concentrations. For example, a solution of 4-phenylphenol in 10% dioxane and water, with the addition of HRP and hydrogen peroxide, formed oligomeric products of only 0.5 kg/mol, whereas increasing the concentrations of dioxane to 85% led to products with M_n of 26 kg/mol. This effect was

largely attributable to the increased solubility of the products in the water/dioxane solvent blends.

In a demonstration of how enzymatic polymerization leads to the facile synthesis of functional macromolecules, Cui and coworkers polymerized pyrogallic acid to generate moderately-high molecular weight polymers.[157] Adding HRP and hydrogen peroxide to pyrogallic acid solutions in water/solvent blends, again necessary to solubilize both the monomers and generated polymer, resulted in poly(pyrogallic acid) polymers with M_n as high as 39 kg/mol; these materials were found to have excellent antioxidant properties, exceeding those of commonly-used commercial materials.

Difficulties with solubility can be avoided by utilizing water-soluble, phenol-functionalized materials. This approach has been utilized to produce cross-linked hydrogels, where phenol-functionalized polysaccharides have been regularly polymerized by the HRP/hydrogen peroxide initiating system. To give two examples by different groups, both phenol-functional alginate, examined by Sakai and coworkers,[158] and dextran, explored by Feijen and coworkers,[159] rapidly polymerize after exposure to HRP and hydrogen peroxide, with both systems achieving gel times of less than 10 s. Both groups also noted that gelation times increased at high hydrogen peroxide concentrations, attributable to HRP deactivation. As mentioned previously, a bienzymatic system where GOx generates hydrogen peroxide in situ can be utilized to circumvent the HRP deactivation, an approach that has been explored at length.[160-166]

Lignin, a complex aromatic macromolecule found in cell walls that is present as a waste product in paper pulping processing, is currently under-utilized as a natural resource. By having facile methods available for modifying lignin, this waste material

could be readily incorporated into polymeric industrial products (e.g., paint, coatings, and adhesives). It has been found that sulfonated lignin can be utilized as an industrial dispersant, with tremendous improvement in properties observed at higher molecular weights. Qiu and coworkers were able to increase the molecular weight of sulfonated lignin six-fold via polymerization initiated by HRP and hydrogen peroxide.[167]

In addition to phenolic monomers, other monomers have been polymerized by HRP-mediated oxidative reactions, including those used to make conductive polymers.[168, 169] Samuelson and coworkers utilized the HRP/hydrogen peroxide initiating systems to generate polyaniline (PANI).[168] A major challenge in the enzyme-mediated polymerization of aniline is its lack of water-solubility. While there have been many reports on methods to circumvent its poor water solubility (e.g., using solvent blends, or by emulsion polymerization), the resulting product is typically not the desired benzenoid-quinoid form of the polymer, instead forming a branched structure that limits conjugation length and the resulting conductivity. The approach by Samuelson involved polymerizing aniline in the presence of a polyelectrolyte template, sulfonated polystyrene, that both aided polymer solubility and promoted monomer alignment. The resulting PANI demonstrated conductivity that was readily controlled by changing process conditions. Similarly, this approach of using sulfonated polystyrene as template was also utilized in the formation of another conductive polymer, poly(3,4-ethylenedioxythiophene) (PEDOT), where the monomer, 3,4-ethylenedioxythiophene, was polymerized in the presence of the template and HRP/hydrogen peroxide as the initiating system.[169]

1.3.2.2.2 Glucose Oxidase

For HRP-mediated polymerization reactions performed in a reactor and intended for subsequent utilization, hydrogen peroxide can be added at any arbitrary rate, minimizing the concentration at any time, and mitigating deactivation of the enzyme. This approach, however, is not possible for any type of in situ polymerization. Thus, it is useful to be able to generate the necessary hydrogen peroxide only as it is needed; this approach has been employed, as has been already seen in several examples discussed above, for vinyl and thiol–ene reactions, where GOx generates hydrogen peroxide in situ, which can then be used by further reaction with a peroxidase to initiate polymerization.[162-166]

The apparent earliest utilization of this bienzymatic system, by Kobayahsi and coworkers, was for the polymerization of substituted phenols. [163] Phenol and several 4-alkylphenols, which the alkyl groups ranging from methyl to pentyl, were polymerized using the GOx/glucose/oxygen/HRP quaternary initiating system (with both enzymes at a concentration of 2 g/L) with no external mediator required (Scheme 17). The polymers generated had M_n as high as 13 kg/mol, with the solubility of the polymer likely the limiting factor for molecular weight. This method was readily adapted for the production of hydrogels by using water-soluble, phenol-functionalized polymers, including hyperbranched polyglycerols,[162] alginates,[165] and poly(vinyl alcohol).[166] As this technique has been utilized with biocompatible polymers, it holds promise for the development of scaffolds for living cells and biomedical adhesives, suitable for hemostats and wound closures, as has been demonstrated on rat models.[166]

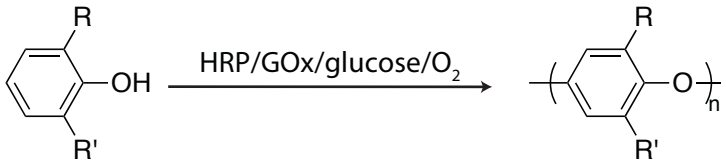

Scheme 17: Utilizing horseradish peroxidase (HRP), glucose oxidase (GOx), glucose, and oxygen as a quaternary initiating system for polymerizing substituted phenols.[163]

1.3.2.2.3 Laccase

As was the case for vinyl polymerization, laccase has also been utilized for initiating polymerization by oxidative coupling. The reaction proceeds readily in the presence of molecular oxygen and phenolic compounds, without requiring an additional mediator. The laccase-mediated oxidative coupling of phenols bears a strong resemblance to the HRP-mediated reaction – many of the applications are quite similar—though, since laccase utilizes oxygen as an oxidant, one crucial difference is the lack of enzyme deactivation upon hydrogen peroxide exposure. In a fairly simple example, laccase has been investigated as a method for generating polymers from phenolic compounds and related materials.[170] The molecular weights of polymers made from phenol or 4-*tert*-butyl phenol were typically in the 1–2 kg/mol range. Other monomers resulted in polymers of higher molecular weight, with polymers made from *m*-cresol having M_n approximately 15 kg/mol and those from bisphenol A over 21 kg/mol. As the reactions were performed in aqueous solutions of solvents, molecular weight was likely influenced by the solubility of the generated polymer.

Laccase-mediated reactions were also investigated as a means to generate small molecule products from phenolic precursors.[171] This reaction was performed in ethanol/water solutions and, unlike with vinyl polymerizations, no external mediator (e.g., acetylacetone) was required. While some small molecule products were produced,

there was also significant amounts of undesirable oligo- and polymeric products formed. In utilization similar to that of HRP, this ability to generate insoluble products from phenolic compounds has been utilized for the removal of contaminants from waste streams, including bisphenol A[142, 172, 173] or 1-naphthol.[137] There is particular interest in developing methods for the facile removal of bisphenol A, as this compound is used in the production of many commercial polymeric products and has numerous deleterious medical attributes associated with it.

In an application similar to an HRP-mediated one described above, laccase has been utilized to modifying lignin, a phenolic waste product obtained from paper mills.[136] In efforts to find facile methods for making use of this common waste product, a laccase-mediated reaction was utilized to increase the molecular weight of lignin six-fold; their were also extensive modifications to the functional groups present, with carbonyl and aliphatic hydroxyl groups becoming more prevalent as the concentration of methoxyl and aromatic hydroxyl groups decreasing. As noted previously,[167] increasing the molecular weight of lignin tends to improve its performance as an industrial dispersant and it seems likely that both laccase and HRP are capable of modifying lignin for this purpose.

As is the case for HRP, laccase is also capable of polymerizing non-phenolic monomers via oxidative coupling, often for the production of conductive polymers.[139, 174] As the monomers, including pyrrole[139] and 4-aminodiphenylamine,[174] and resultant polymers are sparingly water soluble, alternative methods are required to prevent precursors and products from precipitating. Thus, enzymatic polymerization reactions using these monomers have been performed in the presence of vesicles formed by sodium bis-(2-ethylhexyl)sulfosuccinate, a common industrial surfactant widely known as AOT.

While the AOT vesicles assisted in keeping the generated polymer dispersed they also acted as templates for polymerization, decreasing the number of defects in the polymer and helping improve the electrical properties by increasing conjugation length.[139, 174] This vesicle template utilization was similar to that of the sulfonated polystyrene discussed above in HRP-mediated reactions.[168, 169]

1.3.2.3 Applicability of Enzyme-mediated Reactions Towards In Situ Polymerization

As seen throughout this detailed discussion on enzyme-mediated polymerization, oxidoreductases, including HRP, GOx, and laccase, have been deployed, in variety of roles (e.g., initiator, catalyst, oxygen scavenger), to perform radical-mediated polymerization reactions in an extraordinarily wide range of environments, from in vitro solution and emulsion polymerization, to the in situ generation of cross-linked hydrogels, to the formation of polymers on a surface or inside hollow particles. With this demonstrated versatility, it seems quite reasonable that oxidoreductases will be useful in initiating oxygen-mediated polymerization. Oxidases, in the presence of atmospheric oxygen and a suitable substrate, will readily either generate radicals directly or afford hydrogen peroxide that can then be converted to radicals either by the action of a peroxidase or through a non-enzymatic route (e.g., Fenton reaction). As enzymes can be quite stable in pH controlled aqueous environments, oxidoreductase-based initiating system seems especially well-suited for in situ hydrogel formation and may be particularly relevant for the medical adhesive and sealant applications discussed above. Conversely, with the possibility of stability issues in a non-aqueous environment, they may not be the best choice for, say, bulk polymerization – a likely requirement for the

self-healing applications that are also of interest. Thus, additional initiating systems suitable for oxygen-mediated bulk polymerization will be investigated.

1.3.3 Alkylboranes

1.3.3.1 Alkylboranes as Initiators for Vinyl Polymerization

Alkylboranes have long been utilized for the chain-growth polymerization initiation, with reports going back to at least the late 1950s, though it took several years for even the most basic details of the reaction mechanism to be properly elucidated. Furukawa and coworkers, in 1957,[175] demonstrated the polymerization of vinyl monomers (including vinyl chloride, vinyl acetate, vinylidene chloride and acrylonitrile) using triethylborane as the initiator; the same year, Kolesnikov and Federova reported similar findings, utilizing tributylborane to polymerize acrylonitrile.[176] While Furukawa initially identified the polymerization mechanism as anionic, in 1958, Fordham and Sturm correctly asserted that the mechanism must be radical-mediated.[177] To establish this, they polymerized monomer pairs that were known to form copolymers of differing monomer ratio depending on the polymerization mechanism (anionic, cationic, or radical); they found that when methyl methacrylate (MMA) was polymerized with either acrylonitrile or styrene, the concentration of MMA present in resulting copolymers closely agreed with previous concentrations reported for radical-mediated processes. Numerous reports followed that strongly supported the radical-mediated nature of the alkylborane-initiated polymerization reaction.[178-184]

In the early confusion of the alkylborane-mediated polymerization mechanism, it was not immediately apparent that oxygen was required to generate initiating radicals – there was no mention in the initial papers of either Furukawa[175] or Fordham.[177] A brief

paper by Kolesnikov and Federova pointed out that the alkylborane-mediated polymerization of acrylonitrile would only show significant yield in the presence of atmospheric oxygen (Scheme 18)[185] and a report from Ashkiri indicated that the trace amounts of oxygen present in imperfectly degassed reagents seems to be sufficient for polymerization initiation.[186] Quite quickly thereafter, more evidence rapidly accumulated that initiating radicals would only form when alkylboranes were exposed to molecular oxygen.[178-180, 183]

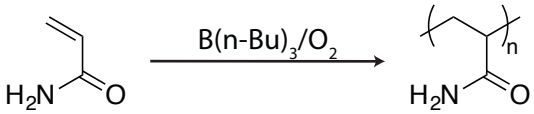

Scheme 18: Chain-growth polymerization of acrylonitrile initiated by tributylborane and molecular oxygen. [185]

Thus, by the late 1960s, it was well established that radicals capable of initiating free polymerization reactions were readily generated by the reaction of molecular oxygen and alkylboranes. Interestingly, there have been numerous contradicting reports as to whether the initiating radials formed are either alkyl or alkoxy radicals and there were disagreements as to how these radicals could form.[182] For example, two mechanisms have been proposed as the radical generating reactions, with the first of these predicting the formation of alkyl radicals (see Equations 1–3)

$$R_3B + O_2 \longrightarrow R_2BOO\bullet + R\bullet \quad (1)$$

$$R\bullet + O_2 \longrightarrow ROO\bullet \quad (2)$$

$$RO_2\bullet + R_3B \longrightarrow R_2BOOR + R\bullet \quad (3)$$

and the second predicting alkoxy radicals (4).

$$R_3B + O_2 \longrightarrow R_2BOOR \longrightarrow R_2BO\bullet + RO\bullet \quad (4)$$

While Sonnenschein and coworkers showed that the second of these was thermodynamically favored, they also demonstrated the complexity of the reaction by showing other mechanistic routes that could lead to the formation of alkyl radicals as well as alkoxy radicals. Additional insight into the mechanism was established by Chung and Zhang, where they utilized a triethylborane/O_2 initiating system to polymerize vinylidene fluoride into poly(vinylidene fluoride) (PVDF).[187] They performed a series of experiments where the oxygen-to-triethylborane ratio was varied and, to establish the identity of the initiating radical, end group analysis was performed using NMR. For low oxygen-to-triethylborane ratio, the initiating radical was exclusively an ethyl radical, as no ethoxy end groups were detected, and it was only when the concentration of oxygen begins to exceed that of triethylborane were ethoxy end groups detected. Thus, if an experiment where to be performed in a milieu with an abundance of oxygen, it is likely that both alkyl and alkoxy radicals would be formed.

Finally, additional mechanistic studies where performed by Zheng and coworkers where they used mass spectroscopy to examine the variety of products formed by the reaction between oxygen and tributylborane.[181] Confirming the results of Chang and Sonnenschein,[182, 187] both butoxy and butyl radicals were formed, the latter through several pathways. A summary of the main radical-affording reactions is given in Equations 5–7:

(5)

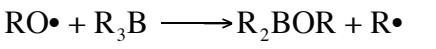

(6)

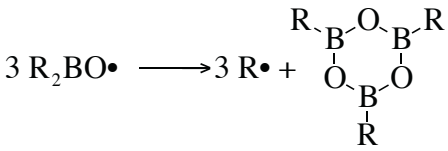

(7)

Thus, the reaction between trialkylboranes and molecular oxygen affords several products and it is the alkyl and alkoxy radicals that are of greatest interest as these species are those likely to initiate polymerization.

It should be apparent from the above discussion that oxygen plays a critical role in the radical-yielding reactions with alkylboranes: as has been convincingly demonstrated, alkylboranes will only initiate radical-mediated chain-growth polymerization of vinyl monomers in the presence of oxygen. Unfortunately, the utilization of oxygen in a radical-mediated chain-growth polymerization method can be problematic as this reaction is extraordinarily sensitive to oxygen. As discussed above (Scheme 9), oxygen is capable of reacting with the propagating carbon-centered radical, forming a peroxy radical that does not propagate at an appreciable rate. This creates a dilemma: oxygen is not only necessary for initiation, but it also plays an inhibitory role where excessive oxygen concentrations retard polymerization rates. A paper from 1962 by Welch and coworkers asserted that maximal reaction rates and extents were demonstrated when the concentrations of oxygen and triethylborane were at roughly the same concentrations.[178] This phenomenon was quite clearly shown in work by 2006 Chung,[187] where the alkylborane/oxygen initiating systems were utilized to polymerize vinylidene fluoride. Varying the oxygen-to-triethylborane ratio influenced the reaction conversion with lower

conversions observed at either low or high oxygen concentrations. Above a ratio of 5.2 mmol O_2 to 2.4 mmol triethylborane, no polymerization was observed, with the lack of polymerization almost certainly caused by oxygen inhibition. The oxygen inhibition problem strongly suggests that, while alkylboranes are quite useful for performing radical-mediated vinyl polymerization in an environment with facile control of oxygen concentration, it seems less useful for in situ polymerization, where the oxygen concentration is not readily controlled.

While the oxygen-mediated radical-generation of alkylboranes may not be useful for in situ polymerization of vinyl monomers via a chain-growth mechanism owing to its sensitivity to the presence of oxygen, it may be of use for initiating the thiol–ene reaction, the radical-mediated step-growth polymerization reaction that, as discussed in the following section, displays extraordinary resistance to oxygen-inhibition.

1.3.3.2 Alkylboranes as Thiol–ene Initiators

The thiol–ene reaction, an anti-Markovnikov addition between a thiol and an electron-rich carbon-carbon double bond (e.g., vinyl ether or allyl ether), is a radical-mediated reaction that, unlike the chain-growth vinyl polymerization described above, proceeds through a step-growth mechanism.[55, 188] Initiation of the thiol–ene reaction commences upon the generation of radicals which can either add across a carbon-carbon double bond, affording a carbon-centered radical, or abstract a hydrogen from a thiol monomer, yielding a sulfur-centered thiyl radical. Subsequently, the reaction proceeds via alternating propagation and chain transfer events where a thiyl radical initially adds across a double bond to afford a carbon-centered radical. Owing to the use of electron-rich carbon-carbon double bonds, this carbon-centered radical is unable to propagate;

however, it is able to participate in a chain transfer reaction with the ubiquitous thiol, abstracting a thiol hydrogen and yielding the final product, a thioether linkage, and regenerating a thiyl radical (Scheme 19A). As this is a step-growth mechanism, the thiol and carbon-carbon double bonds are consumed in a 1:1 stoichiometric ratio. Whereas monofunctional reactants will only coupling together and not polymerize, difunctional reactants will form linear polymers and multi-functional monomers are necessary to form cross-linked polymer networks. A distinguishing characteristic of the thiol–ene polymerizations is that, unlike radical-mediated vinyl polymerizations, they are extraordinarily resistant to oxygen inhibition;[55, 188, 189] the peroxy radical generated by the addition of the carbon-centered radical to oxygen is able to abstract a thiol hydrogen, permitting the cycle of alternating propagation and chain transfer reactions to continue (Scheme 19B). This inherent tolerance to oxygen permits thiol–ene polymerization to proceed under atmospheric conditions and suggests that it is well-suited for oxygen-mediated initiation.

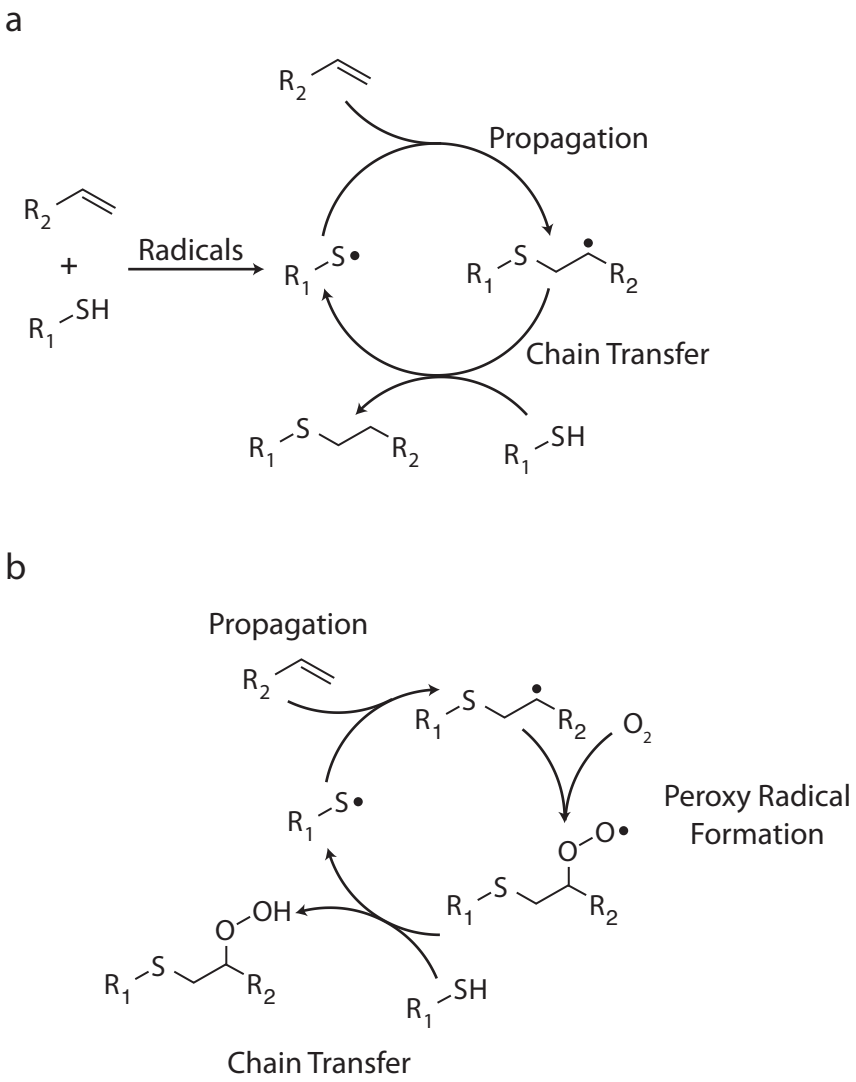

Scheme 19: Radical-mediated thiol–ene reaction. A) Thiols and electron-rich carbon-carbon double bonds form thioether linkages via radical-mediated, alternating propagation and chain transfer reactions.[55, 188] B) The thiol–ene reaction is resistant to oxygen inhibition as any peroxy radicals formed are still capable of abstracting thiol hydrogens.[55, 188, 189]

To my knowledge, there has been no prior intentional utilization of alkylborane/O_2 as a thiol–ene polymerization initiating system. However, there are many examples of the alkylborane/O_2 initiating system used to perform small molecule thiol–ene chemistry, where thiols have been added to vinyl- and alkynyl-bearing compounds. (The reaction between thiols and alkynyl compounds is known as the thiol–yne reaction as is the carbon-carbon triple bond analogue of the thiol–ene reaction.[190-192]) A

particularly early example, by Davies and Roberts,[193] demonstrates that thiyl radicals can be generated from 1-butylthiol and tributylborane in the presence of atmospheric oxygen and that the thiyl radical is capable of adding across the carbon-carbon double bond of 1-octene. After this, there have been many other reports. For example, Oshima and coworkers demonstrated the addition of thiols to either alkenes or alkynes using triethylborane and as the initiator.[194] Interestingly, the role of oxygen is not made explicit and is only mentioned obliquely in a footnote. Despite this, there can be doubt that molecular oxygen is required in this system as there is no mention of monomer degassing and thus, with the low concentrations of oxygen utilized in the chain-growth vinyl polymerizations discussed above, there is certainly sufficient oxygen present to effect radical formation from triethylborane. The triethylborane/O_2 initiating system was utilized to couple a variety of aromatic and aliphatic acetylenes or alkenes with either aliphatic or aromatic thiols, with conversion varying from 53 to 95%. For a thiol–ene example, 1-dodecene and 1-butylthiol formed 1-butylthiododecane (Scheme 20a). To give a few thiol-yne examples, 1-dodecyne and benzenethiol were coupled, by addition of triethylborane, to form 1-phenylthio-1-dodecene (Scheme 20b); replacing the benzenethiol with the aliphatic 1-butylthiol yielded 1-butylthio-1-dodecene, though the yields were typically lower with aliphatic reactants. As this is a thiol–yne reaction, the alkenyl sulfides formed from the thiol–acetylene reaction are also capable of addition by the thiol–ene mechanism and thus compete with acetylenes. Given that the yields of some of the reported reactions were somewhat modest, with some as low as 50 or 60%, it is likely the presence of the diaddition products(Scheme 20c), where the alkenyl sulfide

reacts with another thiol via the thiol–ene mechanism, partially accounts for the low conversions seen in some of the thiol–acetylene experiments.

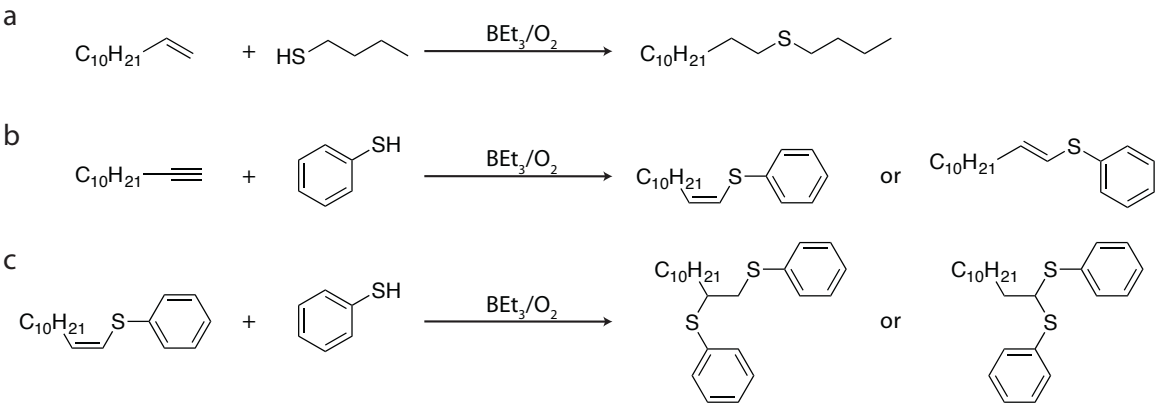

Scheme 20: Thiol–ene and thiol–yne reactions initiated by triethylborane and oxygen. A) 1-dodecene and butylthiol react to form a thioether. B) 1-dodecyne and benzenethiol react to form an alkenyl sulfide, with two stereoisomers possible. C) The alkenyl sulfide can react with a second thiol to form diaddition products. [194]

Also of interest is that reactants with multiple unsaturations were utilized to form, per the authors' claims, ring-containing products. Additional research into forming ring-containing structure via thiol-yne chemistry and alkylborane initiators was performed by Demchuk and coworkers,[195] where they demonstrated the formation of dithiacycloalkanes from a variety of dithiols and a monofunctional acetylenes with a tripropylborane/O_2 initiating system. The role of oxygen is acknowledged here as being necessary to form the propyl radicals from tripropylborane. Once radicals are generated, the production of the dithiacycloalkanes results from, in the first step, the reaction of a thiol and the acetylene to yield an alkenylsulfide which, in a second step, then reacts with the second thiol. These reactions were performed in moderately dilute solutions (starting material concentrations were approximately 0.1 M) and the yields were between 39 and 71%. This work is especially interesting as there is a possibility of linear oligo- or polymeric material forming during this reaction as the alkenyl sulfide is capable of reacting with a

thiol on a second dithiol. In other words, cyclization only occurs when the acetylene reacts with the two thiols on a single dithiol molecule and linear products will formed with the thiols are from different dithiol molecules. It is unfortunate that the authors seem only interested in the cyclization reaction as they completely ignore the possibility of linear products forming, even though this would partially explain the modest yields reported. Had these systems been investigated more thoroughly, this would have possibly been the first report of thiol–yne polymerization initiated by an alkylborane/O_2 initiating system.

As further demonstration of the versatility in using alkylboranes and oxygen as initiators for thiol–ene or –yne chemistry, work by Sato and coworkers demonstrated the addition of a thiol to an ynamide group,[196] an N-alkynylamide with an internal carbon-carbon triple bond adjacent to a nitrogen with an electron withdrawing group, proceeding through the same alternating propagation and chain-transfer steps of the thiol–ene and –yne reactions. Similar to the work by Oshima,[194] triethylborane is utilized as the initiator, though here the necessity of molecular oxygen is made explicit, and the triethylborane/O_2 initiating system was utilized, with the initial temperature at -30ºC, to successfully couple arenethiols to the ynamide-functional N-benzyl-N-(1-octynyl)-p-toluenesulfonamide (Scheme 21). When the arenethiol was benzenethiol or one with an electron withdrawing group, the reaction product displayed surprising good regioselectivity, with Z/E ratio > 99/1. This extraordinary control over regioselectivity was later exploited by Reddy and coworkers.[197] In this fairly recent example, triethylborane/O_2 initiating system was used to initiate the coupling of small, monofunctional aromatic thiols with acetylenes as a step in synthesis of Rigosertib, an anti-cancer agent that is only active in its E isomeric form.

They found that changing the reaction conditions, including reaction temperature and solvent, had significant influence on the Z/E ratio, which was readily varied from 100:0, favored at low temperatures, to 0:100, which was only observed when small amounts of methanol were added to the reactor. The authors explained that the presence of a polar solvent slows down hydrogen abstraction from the thiol, permitting the Z-isomer of the carbon-centered radical to isomerize into the more stable E-isomer.

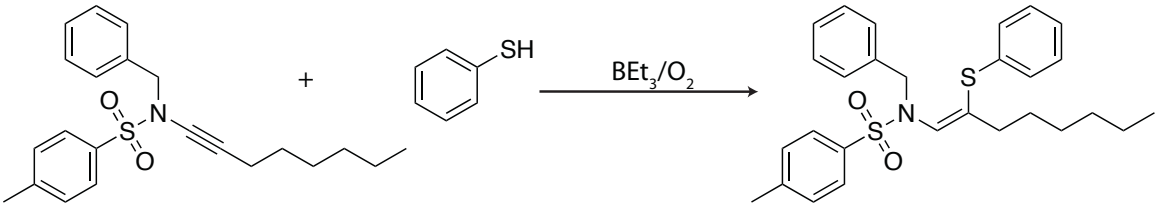

Scheme 21: Thiol-ynamide reaction initiated by triethylborane and oxygen. N-benzyl-N-(1-octynyl)-p-toluenesulfonamide and benzenethiol couple together, the presence of triethylborane and oxygen, to from N-benzyl-N-[(Z)-2-(phenylsulfanyl)-1- octenyl]-p-toluenesulfonamide.[196]

Thus, with the high conversions reported in the alkylborane-mediated thiol-ene reactions of small molecules, the alkylborane/O_2 initiating system seems particularly well-suited for thiol–ene chemistry and it seems quite reasonable that, if multifunctional thiols and ene monomers are utilized, this initiating system could be readily adapted for polymerization reactions. Moreover, given that the thiol–ene reaction is extraordinarily resistant to oxygen inhibition, it seemed likely that the alkylborane/O_2 system will be especially useful for initiating oxygen-mediated thiol–ene polymerization.

1.3.4 Polymerization Chemistry

In the above discussion, two outstanding oxygen-mediated initiating system candidates were discussed: oxidoreductase enzymes and alkylboranes. Both systems, after exposure to molecular oxygen, generate radicals capable of initiating polymerization reactions; the

enzyme-based systems are particularly well-suited for use in an aqueous milieu, and thus are a good match for biomedical applications that require in situ hydrogel formation, while the alkylboranes seem potentially quite useful for polymerization in a non-aqueous environment, suggesting their capacity for initiating bulk polymerization reactions, and seems quite suitable for self-healing applications.

Having established viable means for generating radicals in response to oxygen exposure, we must now decide on what to do with we these radicals – that is, which of the many radical-mediated polymerization chemistries is the best match for the requirements of both the biomedical and self-healing applications. In the course of the discussion on enzyme- and alkylborane-mediated reactions, three radical-mediated chemistries have been discussed: the polymerization of vinyl monomers via a chain-growth mechanism, the oxidative coupling reactions of phenolic monomers, and the step-growth thiol–ene reaction between thiols and allyl rich carbon-carbon double bonds. Of these three, the chain-growth polymerization of vinyl monomers is the most familiar as it has numerous industrial applications in inks, coatings, and adhesives and it has certainly been utilized in performing both bulk and aqueous solution polymerization. Because of its familiarity, its strengths and weaknesses are quite well documented and this reaction has one deleterious attribute that must be addressed: oxygen inhibition. As shown above (Scheme 9), the presence of molecular oxygen severely retards polymerization rates owing to the formation of peroxy radicals. Indeed, in one of the alkylborane examples, no polymerization of vinylidene fluoride was observed at modest oxygen concentrations.[187] Moreover, oxygen inhibition was noted throughout the discussion on enzyme-mediated reactions and is responsible for some of the long induction times

witnessed – that is, oxygen must be consumed before substantial polymerization will proceed.[107, 131] Despite this, there are means to successfully deal with oxygen inhibition. Using an example for the enzyme discussion above, glucose oxidase has been utilized as an oxygen scavenger,[143] allowing for oxygen concentrations to sufficiently decrease to levels that permit polymerization to proceed. This idea places glucose oxidase in a dual role, playing both initiator and scavenger, and has allowed for the successful polymerization of aqueous solution of acrylate monomers.[118] So clearly, in many applications, the issue of oxygen inhibition can be dealt with if necessary. Unfortunately, for the biomedical and self-healing applications that are of interest here, presently available strategies are likely insufficient. To give an example, in the autonomous healing of a micrometeoroid-induced puncture,[37, 38], the unrelenting flow of oxygen-containing air flowing through the puncture would likely overwhelm any oxygen scavenging system, rendering it useless and preventing the polymerization necessary to seal the plug. Thus, while oxygen inhibition can be mitigated and accounted for, the innate oxygen sensitivity of chain-growth vinyl polymerization renders it a poor first choice for oxygen-mediated polymerization.

Conversely, the radical-mediated step-growth thiol–ene reaction is extraordinarily resistant to oxygen inhibition. As discussed above (Scheme 19B), the peroxy radicals that can form in the presence of oxygen are still capable of abstracting thiol hydrogens, permitting the thiol–ene cycle to continue.[55, 188, 189] This tolerance to the presence of oxygen makes thiol–ene chemistry an ideal candidate for performing oxygen-mediated polymerization. Furthermore, there is vast body of literature on the thiol–ene reaction that describes the incredibly broad range of mechanical properties that can be attained by

changing monomer structure and functionality. The thiol–ene reaction is also quite tolerant of other functional groups, permitting a wider array of monomers to be utilized than, say, cyanoacrylate chemistry where many functional groups (e.g., amines) would prematurely initiate polymerization. Another advantage of thiol-ene chemistry is that its step-growth mechanism forms a more homogenous cross-linked networked than one formed through a chain-growth network[198] and, in addition, the delayed onset of gelation tends to generate less shrinkage stress;[199] both of these result in improved mechanical properties.

Incidentally, this preference for step-growth over chain-growth mechanisms also suggests that thiol–ene chemistry is a better first choice than the oxidative coupling (e.g., the third of the three radical-mediated polymerization chemistries discussed above). While the oxidative coupling of phenolic monomers does not appear to be oxygen inhibited, its polymerization mechanism is complex and has characteristics of both step and chain growth. Moreover, while the in situ formation of hydrogels via oxidative coupling has been thoroughly investigated, its utilization for in situ bulk polymerization doesn't seem to be described, whereas the thiol–ene reaction has been extensively used in both hydrogel[198, 200, 201] and bulk polymerization reactions.[199, 202-205]

Thus, the research presented in this dissertation will focus on the utilization of oxygen to initiate radical-mediated thiol–ene polymerization. As our interests here are in developing materials suitable for either self-healing and biomedical applications, both bulk and aqueous solution polymerization will be investigated. Based on the discussions above, alkylboranes will be investigated as initiators for bulk polymerization and

oxidoreductases will be used for aqueous solution polymerization leading to the formation of hydrogels.

1.4 Overview of Subsequent Chapters

Chapter Two examines, through the use of ballistics testing, the self-healing properties of thiol–ene monomer formulation that utilize trialkylboranes as oxygen-mediated initiator. Chapter Three extends this discussion by utilizing a much more stringent ballistics test protocol – one that better mimics lunar or Martian conditions. Chapter Four explores the potential for enzyme-based initiating systems to form thiol–ene-based hydrogels through an oxygen-mediated process. Chapter Five further examines the enzyme-based initiating system and describes their role in fabricating chitosan-based hydrogels. Chapter Six discusses a novel approach to oxygen-mediated polymerization that looks beyond that alkylborane and enzyme chemistries by examining a derivative of oltipraz, a compound explored as a chemopreventive, as a method for affording radicals in the presence of oxygen. The dissertation is concluded in Chapter Seven with a discussion on the major results described here as well as comments on the potential for future research.

1.5 References:

1. Carothers, W. H., Polymerization. *Chem. Rev.* **1931,** *8* (3), 353-426.
2. Chattopadhyay, D. K.; Raju, K. V. S. N., Structural engineering of polyurethane coatings for high performance applications. *Prog. Polym. Sci.* **2007,** *32* (3), 352-418.
3. Sørensen, P. A.; Kiil, S.; Dam-Johansen, K.; Weinell, C. E., Anticorrosive coatings: a review. *J. Coat. Technol. Res.* **2009,** *6* (2), 135-176.
4. Gray, J. E.; Luan, B., Protective coatings on magnesium and its alloys — a critical review. *J. Alloys. Compounds* **2002,** *336* (1–2), 88-113.
5. Deng, Y.; Martin, G. C., Diffusion and Diffusion-Controlled Kinetics during Epoxy-Amine Cure. *Macromolecules* **1994,** *27* (18), 5147-5153.
6. Thennarasu, S.; Krishnamurti, N.; Shantha, K. L., Developments and applications of cyanoacrylate adhesives. *J. Adhes. Sci. Technol.* **1989,** *3* (4), 237-260.
7. Bartlett, M. D.; Croll, A. B.; Crosby, A. J., Designing Bio-Inspired Adhesives for Shear Loading: From Simple Structures to Complex Patterns. *Adv. Funct. Mater.* **2012,** *22* (23), 4985-4992.

8. Incarnato, L.; Scarfato, P.; Di Maio, L.; Acierno, D., Structure and rheology of recycled PET modified by reactive extrusion. *Polymer* **2000,** *41* (18), 6825-6831.
9. Seppala, J.; Heino, M.; Kapanen, C., Injection-Molded Blends of a Thermotropic Liquid-Crystalline Polymer with Polyethylene Terephthalate, Polypropylene, and Polyphenylene Sulfide. *J. Appl. Polym. Sci.* **1992,** *44* (6), 1051-1060.
10. Babaarslan, O., Method of Producing a Polyester/Viscose Core-Spun Yarn Containing Spandex Using a Modified Ring Spinning Frame. *Textile Res. J.* **2001,** *71* (4), 367-371.
11. Scrosati, B.; Garche, J., Lithium batteries: Status, prospects and future. *J. Power Sources* **2010,** *195* (9), 2419-2430.
12. Brabec, C. J.; Sariciftci, N. S.; Hummelen, J. C., Plastic solar cells. *Adv. Funct. Mater.* **2001,** *11* (1), 15-26.
13. Li, G.; Zhu, R.; Yang, Y., Polymer solar cells. *Nat. Photonics* **2012,** *6* (3), 153-161.
14. Peppas, N. A.; Bures, P.; Leobandung, W.; Ichikawa, H., Hydrogels in pharmaceutical formulations. *Euro. J. Pharm. Biopharm.* **2000,** *50* (1), 27-46.
15. Hutmacher, D. W., Scaffolds in tissue engineering bone and cartilage. *Biomaterials* **2000,** *21* (24), 2529-2543.
16. Grave, C.; McEwan, I.; Pethrick, R. A., Influence of stoichiometric ratio on water absorption in epoxy resins. *J. Appl. Polym. Sci.* **1998,** *69* (12), 2369-2376.
17. Collin, T. W.; Blyth, K.; Hodgkinson, P. D., Cleft lip repair without suture removal. *J. Plast. Reconstr. Aesthet. Surg.* **2009,** *62* (9), 1161-5.
18. Wilson, A. D. H.; Mercer, N., Dermabond, Tissue Adhesive Versus Steri-Strips, in Unilateral Cleft Lip Repair: An Audit of Infection and Hypertrophic Scar Rates. *Cleft Palate Cran. J.* **2008,** *45* (6), 614-619.
19. Spauwen, P. H.; de Laat, W. A.; Hartman, E. H., Octyl-2-cyanoacrylate tissue glue (Dermabond) versus Monocryl 6 x 0 Sutures in lip closure. *Cleft Palate Craniofac J* **2006,** *43* (5), 625-7.
20. Lustgarten, L.; Abadi, J. R.; Sancevic, R.; Meneses, P.; Perez Morrel, A.; Lugo, J., Use of a protein-based tissue adhesive as an aid for the surgical reconstruction of advanced and recurrent skin cancer tumors to the head and neck region: a technical report. *Surg. Neurol.* **2007,** *68* (1), 53-9; discussion 59.
21. Singh, K.; Moyer, H.; Williams, J. K.; Schwartz, Z.; Boyan, B. D., Fibrin glue: a scaffold for cellular-based therapy in a critical-sized defect. *Ann. Plast. Surg.* **2011,** *66* (3), 301-5.
22. Kotlarchyk, M. A.; Shreim, S. G.; Alvarez-Elizondo, M. B.; Estrada, L. C.; Singh, R.; Valdevit, L.; Kniazeva, E.; Gratton, E.; Putnam, A. J.; Botvinick, E. L., Concentration independent modulation of local micromechanics in a fibrin gel. *PLoS One* **2011,** *6* (5), e20201.
23. Imola, M. J.; Sciarretta, V.; Schramm, V. L., Skull base reconstruction. *Curr. Opin. Otolaryngol. Head Neck Surg.* **2003,** *11* (4), 282-90.
24. Marchac, D.; Greensmith, A., Long-term experience with methylmethacrylate cranioplasty in craniofacial surgery. *J. Plast. Reconstr. Aes.* **2008,** *61* (7), 744-752.
25. Yilmaz, C.; Kuyurtar, F., Fixation of a talar osteochondral fracture with cyanoacrylate glue. *Arthroscopy* **2005,** *21* (8), 1009.
26. Ruiz, A. J. O.; Vicente, A.; Alonso, F. C.; Jornet, P. L., A new use for self-etching resin adhesives: Cementing bone fragments. *J. Dent.* **2010,** *38* (9), 750-756.
27. Endres, K.; Marx, R.; Tinschert, J.; Wirtz, D. C.; Stoll, C.; Riediger, D.; Smeets, R., A new adhesive technique for internal fixation in midfacial surgery. *Biomed. Eng. Online* **2008,** *7*, 16.
28. Dadas, B.; Alkan, S.; Cifci, M.; Basak, T., Treatment of tripod fracture of zygomatic bone by N-2-butyl cyanoacrylate glue fixation, and its effects on the tissues. *Eur. Arch. Otorhinolaryngol.* **2007,** *264* (5), 539-44.
29. Spotnitz, W. D., Fibrin sealant: Past, present, and future: A brief review. *World. J. Surg.* **2010,** *34* (4), 632-4.

30. Spotnitz, W. D.; Burks, S., State-of-the-art review: Hemostats, sealants, and adhesives II: Update as well as how and when to use the components of the surgical toolbox. *Clin. Appl. Thromb. Hemost.* **2010,** *16* (5), 497-514.
31. Wheat, J. C.; Wolf, J. S., Jr., Advances in bioadhesives, tissue sealants, and hemostatic agents. *Urol. Clin. North Am.* **2009,** *36* (2), 265-75.
32. Vote, B. J.; Elder, M. J., Cyanoacrylate glue for corneal perforations: A description of a surgical technique and a review of the literature. *Clin. Exp. Ophthalmol.* **2000,** *28* (6), 437-42.
33. Leggat, P. A.; Kedjarune, U.; Smith, D. R., Toxicity of cyanoacrylate adhesives and their occupational impacts for dental staff. *Ind. Health* **2004,** *42* (2), 207-11.
34. Sierra, D. H., Fibrin sealant adhesive systems: A review of their chemistry, material properties and clinical applications. *J. Biomater. Appl.* **1993,** *7* (4), 309-52.
35. Spotnitz, W. D.; Burks, S., Hemostats, sealants, and adhesives: Components of the surgical toolbox. *Transfusion* **2008,** *48* (7), 1502-16.
36. Eriksen, J. R.; Bech, J. I.; Linnemann, D.; Rosenberg, J., Laparoscopic intraperitoneal mesh fixation with fibrin sealant (Tisseel) vs. titanium tacks: A randomised controlled experimental study in pigs. *Hernia* **2008,** *12* (5), 483-91.
37. Brandon, E. J.; Vozoff, M.; Kolawa, E. A.; Studor, G. F.; Lyons, F.; Keller, M. W.; Beiermann, B.; White, S. R.; Sottos, N. R.; Curry, M. A.; Banks, D. L.; Brocato, R.; Zhou, L. S.; Jung, S. Y.; Jackson, T. N.; Champaigne, K., Structural health management technologies for inflatable/deployable structures: Integrating sensing and self-healing. *Acta Astronaut.* **2011,** *68* (7-8), 883-903.
38. Gordon, K.; Penner, R.; Bogert, P.; Yost, W. T.; Siochi, E., Puncture self-healing polymers for aerospace applications. *Abstr. Pap. Am. Chem. Soc.* **2011,** *242*.
39. Kalista, S. J.; Ward, T. C., Thermal characteristics of the self-healing response in poly (ethylene-co-methacrylic acid) copolymers. *J. R. Soc. Interface* **2007,** *4* (13), 405-411.
40. Kalista, S. J., Self-healing of poly(ethylene-co-methacrylic acid) copolymers following projectile puncture. *Mech. Adv. Mater. Struc.* **2007,** *14* (5), 391-397.
41. Varley, R. J.; van der Zwaag, S., Development of a quasi-static test method to investigate the origin of self-healing in ionomers under ballistic conditions. *Polym. Test.* **2008,** *27* (1), 11-19.
42. Varley, R. J.; van der Zwaag, S., Towards an understanding of thermally activated self-healing of an ionomer system during ballistic penetration. *Acta. Mater.* **2008,** *56* (19), 5737-5750.
43. Haase, T.; Rohr, I.; Thoma, K., The self-healing of an ionomer at projectile velocities from quasi-static to hypervelocity impact. *RCMA* **2012,** *22* (1), 67-76.
44. White, S. R.; Sottos, N. R.; Geubelle, P. H.; Moore, J. S.; Kessler, M. R.; Sriram, S. R.; Brown, E. N.; Viswanathan, S., Autonomic healing of polymer composites. *Nature* **2001,** *409* (6822), 794-797.
45. Brochu, A. B. W.; Matthys, O. B.; Craig, S. L.; Reichert, W. M., Extended fatigue life of a catalyst free self-healing acrylic bone cement using microencapsulated 2-octyl cyanoacrylate. *J. Biomed. Mater. Res. B* **2015,** *103* (2), 305-312.
46. Hansen, C. J.; Wu, W.; Toohey, K. S.; Sottos, N. R.; White, S. R.; Lewis, J. A., Self-Healing Materials with Interpenetrating Microvascular Networks. *Adv. Mater.* **2009,** *21* (41), 4143-+.
47. Hamilton, A. R.; Sottos, N. R.; White, S. R., Self-Healing of Internal Damage in Synthetic Vascular Materials. *Adv. Mater.* **2010,** *22* (45), 5159-+.
48. Toohey, K. S.; Sottos, N. R.; Lewis, J. A.; Moore, J. S.; White, S. R., Self-healing materials with microvascular networks. *Nat. Mater.* **2007,** *6* (8), 581-585.
49. Comyn, J., Moisture cure of adhesives and sealants. *Int. J. Adhes. Adhes.* **1998,** *18* (4), 247-253.
50. Arukula, R.; Narayan, R.; Sreedhar, B.; Rao, C. R. K., High corrosion resistant - redox active - moisture curable - conducting polyurethanes. *Prog. Org. Coat.* **2016,** *94*, 79-89.

51. Naik, R. B.; Malvankar, N. G.; Mahato, T. K.; Ratna, D.; Hastak, R. S., Novel moisture-cured hyperbranched urethane alkyd resin for coating application. *J. Coat. Technol. Res.* **2014,** *11* (4), 575-586.
52. Chattopadhyay, D. K.; Sreedhar, B.; Raju, K. V. S. N., The phase mixing studies on moisture cured polyurethane-ureas during cure. *Polymer* **2006,** *47* (11), 3814-3825.
53. Mishra, A. K.; Chattopadhyay, D. K.; Sreedhar, B.; Raju, K. V. S. N., FT-IR and XPS studies of polyurethane-urea-imide coatings. *Prog. Org. Coat.* **2006,** *55* (3), 231-243.
54. Wicks Jr, Z. W.; Jones, F. N.; Pappas, S. P.; Wicks, D. A., *Organic coatings: science and technology*. John Wiley & Sons: 2007.
55. Hoyle, C. E.; Lowe, A. B.; Bowman, C. N., Thiol-click chemistry: a multifaceted toolbox for small molecule and polymer synthesis. *Chem. Soc. Rev.* **2010,** *39* (4), 1355-1387.
56. Daniel-da-Silva, A. L.; Bordado, J. C. M.; Martín-Martínez, J. M., Moisture curing kinetics of isocyanate ended urethane quasi-prepolymers monitored by IR spectroscopy and DSC. *J. Appl. Polym. Sci.* **2008,** *107* (2), 700-709.
57. Comyn, J.; de Buyl, F.; Shephard, N. E.; Subramaniam, C., Kinetics of cure, crosslink density and adhesion of water-reactive alkoxysilicone sealants. *Int. J. Adhes. Adhes.* **2002,** *22* (5), 385-393.
58. Brinker, C. J., Hydrolysis and Condensation of Silicates - Effects on Structure. *J. Non-Cryst. Solids* **1988,** *100* (1-3), 31-50.
59. Kowalewska, A., Photoacid catalyzed sol-gel process. *J. Mater. Chem.* **2005,** *15* (47), 4997-5006.
60. Chemtob, A.; Versace, D. L.; Belon, C.; Croutxe-Barghorn, C.; Rigolet, S., Concomitant Organic-Inorganic UV-Curing Catalyzed by Photoacids. *Macromolecules* **2008,** *41* (20), 7390-7398.
61. Lee, H., *Cyanoacrylate resins, the instant adhesives : a monograph of their applications and technology*. Pasadena Technology Press: Pasadena, Calif., 1981; p viii, 241 p.
62. Wang, A. A.; Martin, C. H., Full-thickness skin necrosis of the fingertip after application of superglue. *J. Hand. Surg. Am.* **2003,** *28a* (4), 696-698.
63. Mizrahi, B.; Stefanescu, C. F.; Yang, C.; Lawlor, M. W.; Ko, D.; Langer, R.; Kohane, D. S., Elasticity and safety of alkoxyethyl cyanoacrylate tissue adhesives. *Acta Biomater.* **2011,** *7* (8), 3150-7.
64. Leggat, P. A.; Smith, D. R.; Kedjarune, U., Surgical applications of cyanoacrylate adhesives: a review of toxicity. *ANZ J. Surg.* **2007,** *77* (4), 209-13.
65. Toriumi, D. M.; Raslan, W. F.; Friedman, M.; Tardy, M. E., Histotoxicity of Cyanoacrylate Tissue Adhesives - a Comparative-Study. *Arch. Otolaryngol.* **1990,** *116* (5), 546-550.
66. Lewis, L. A.; Smithwick, R. W.; Devault, G. L.; Bolinger, B.; Lewis, S. A., Processes involved in the development of latent fingerprints using the cyanoacrylate fuming method. *J. Forensic. Sci.* **2001,** *46* (2), 241-246.
67. Mankidy, P. J.; Ramakrishnan, R. B.; Foley, H. C., Facile catalytic growth of cyanoacrylate nanofibers. *Chem. Commun.* **2006,** (10), 1139-1141.
68. Szanka, I.; Szanka, A.; Kennedy, J. P., Rubbery wound closure adhesives. II. initiators for and initiation of 2-octyl cyanoacrylate polymerization. *J. Polym. Sci. A Polym. Chem.* **2015,** *53* (14), 1652-1659.
69. Khriachtchev, L.; Pettersson, M.; Runeberg, N.; Lundell, J.; Rasanen, M., A stable argon compound. *Nature* **2000,** *406* (6798), 874-876.
70. Tsygankov, A. A., Nitrogen-fixing cyanobacteria: A review. *Appl. Biochem. Micro.* **2007,** *43* (3), 250-259.
71. Igarashi, R. Y.; Seefeldt, L. C., Nitrogen fixation: The mechanism of the Mo-dependent nitrogenase. *Crit. Rev. Biochem. Mol. Biol.* **2003,** *38* (4), 351-384.

72. Anderson, J. S.; Rittle, J.; Peters, J. C., Catalytic conversion of nitrogen to ammonia by an iron model complex. *Nature* **2013,** *501* (7465), 84-+.
73. Cooper, A. I., Polymer synthesis and processing using supercritical carbon dioxide. *J. Mater. Chem.* **2000,** *10* (2), 207-234.
74. Inoue, S.; Koinuma, H.; Tsuruta, T., Copolymerization of Carbon Dioxide and Epoxide. *J. Polym. Sci. Pol. Lett.* **1969,** *7* (4pb), 287-&.
75. Inoue, S.; Koinuma, H.; Tsuruta, T., Copolymerization of Carbon Dioxide and Epoxide with Organometallic Compounds. *Makromolekul. Chem.* **1969,** *130* (Dec), 210-&.
76. Ree, M.; Bae, J. Y.; Jung, J. H.; Shin, T. J., A new copolymerization process leading to poly(propylene carbonate) with a highly enhanced yield from carbon dioxide and propylene oxide. *J. Polym. Sci. A Polym. Chem.* **1999,** *37* (12), 1863-1876.
77. Coates, G. W.; Moore, D. R., Discrete metal-based catalysts for the copolymerization CO2 and epoxides: Discovery, reactivity, optimization, and mechanism. *Angew. Chem. Int. Ed.* **2004,** *43* (48), 6618-6639.
78. Auriemma, F.; De Rosa, C.; Di Caprio, M. R.; Di Girolamo, R.; Coates, G. W., Crystallization of Alternating Limonene Oxide/Carbon Dioxide Copolymers: Determination of the Crystal Structure of Stereocomplex Poly(limonene carbonate). *Macromolecules* **2015,** *48* (8), 2534-2550.
79. Yang, Y.; Urban, M. W., Self-Repairable Polyurethane Networks by Atmospheric Carbon Dioxide and Water. *Angew. Chem. Int. Ed.* **2014,** *53* (45), 12142-12147.
80. Wood, P. M., The Potential Diagram for Oxygen at Ph-7. *Biochem. J.* **1988,** *253* (1), 287-289.
81. van Gorkum, R.; Bouwman, E., The oxidative drying of alkyd paint catalysed by metal complexes. *Coord. Chem. Rev.* **2005,** *249* (17-18), 1709-1728.
82. Soucek, M. D.; Khattab, T.; Wu, J., Review of autoxidation and driers. *Prog. Org. Coat.* **2012,** *73* (4), 435-454.
83. Radzicka, A.; Wolfenden, R., A proficient enzyme. *Science* **1995,** *267* (5194), 90-93.
84. Parravano, G., Chain reactions induced by enzymic systems. *J. Am. Chem. Soc.* **1951,** *73* (1), 183-184.
85. Yung, C. W.; Wu, L. Q.; Tullman, J. A.; Payne, G. F.; Bentley, W. E.; Barbari, T. A., Transglutaminase crosslinked gelatin as a tissue engineering scaffold. *J. Biomed. Mater. Res. A* **2007,** *83* (4), 1039-46.
86. Liu, Y.; Kopelman, D.; Wu, L. Q.; Hijji, K.; Attar, I.; Preiss-Bloom, O.; Payne, G. F., Biomimetic sealant based on gelatin and microbial transglutaminase: An initial *in vivo* investigation. *J. Biomed. Mater. Res. B* **2009,** *91* (1), 5-16.
87. Fuchs, S.; Kutscher, M.; Hertel, T.; Winter, G.; Pietzsch, M.; Coester, C., Transglutaminase: New insights into gelatin nanoparticle cross-linking. *J. Microencapsul.* **2010,** *27* (8), 747-54.
88. Hunley, M. T.; Sari, N.; Beers, K. L., Microstructure analysis and model discrimination of enzyme-catalyzed copolyesters. *ACS Macro Lett.* **2013,** *2* (5), 375-379.
89. Jaros, D.; Schwarzenbolz, U.; Raak, N.; Lobner, J.; Henle, T.; Rohm, H., Cross-linking with microbial transglutaminase: Relationship between polymerisation degree and stiffness of acid casein gels. *Int. Dairy J.* **2014,** *38* (2), 174-178.
90. Kavitha, V.; Mandal, A. B.; Gnanamani, A., Microbial mediated dimerization of fattyacids of sunflower oil: An effective role of lipase and biosurfactant. *J. Appl. Polym. Sci.* **2014,** *131* (15), 40555.
91. Mena, M.; Shirai, K.; Tecante, A.; Barzana, E.; Gimeno, M., Enzymatic syntheses of linear and hyperbranched poly-L-lactide using compressed R134a-ionic liquid media. *J. Supercrit. Fluids* **2015,** *103*, 77-82.
92. Colombani, D., Chain-growth control in free radical polymerization. *Prog. Polym. Sci.* **1997,** *22* (8), 1649-1720.

93. Achilias, D. S., A review of modeling of diffusion controlled polymerization reactions. *Macromol. Theory Simul.* **2007,** *16* (4), 319-347.
94. O'Brien, A. K.; Bowman, C. N., Impact of oxygen on photopolymerization kinetics and polymer structure. *Macromolecules* **2006,** *39* (7), 2501-2506.
95. Derango, R. A.; Chiang, L. C.; Dowbenko, R.; Lasch, J. G., Enzyme-mediated polymerization of acrylic monomers. *Biotechnol. Tech.* **1992,** *6* (6), 523-526.
96. Lavery, C. B.; MacInnis, M. C.; MacDonald, M. J.; Williams, J. B.; Spencer, C. A.; Burke, A. A.; Irwin, D. J. G.; D'Cunha, G. B., Purification of peroxidase from horseradish (Armoracia rusticana) roots. *J. Agric. Food. Chem.* **2010,** *58* (15), 8471-8476.
97. Durand, A.; Lalot, T.; Brigodiot, M.; Marechal, E., Enzyme-mediated initiation of acrylamide polymerization: Reaction mechanism. *Polymer* **2000,** *41* (23), 8183-8192.
98. Singh, A.; Ma, D. C.; Kaplan, D. L., Enzyme-mediated free radical polymerization of styrene. *Biomacromolecules* **2000,** *1* (4), 592-596.
99. Berglund, G. I.; Carlsson, G. H.; Smith, A. T.; Szoke, H.; Henriksen, A.; Hajdu, J., The catalytic pathway of horseradish peroxidase at high resolution. *Nature* **2002,** *417* (6887), 463-468.
100. Veitch, N. C., Horseradish peroxidase: A modern view of a classic enzyme. *Phytochemistry* **2004,** *65* (3), 249-259.
101. Yu, J.; Taylor, K. E.; Zou, H. X.; Biswas, N.; Bewtra, J. K., Phenol conversion and dimeric intermediates in horseradish peroxidase-catalyzed phenol removal from water. *Environ. Sci. Technol.* **1994,** *28* (12), 2154-2160.
102. Cooper, V. A.; Nicell, J. A., Removal of phenols from a foundry wastewater using horseradish peroxidase. *Water Res.* **1996,** *30* (4), 954-964.
103. Huang, J.; Chang, Q.; Ding, Y. B.; Han, X. Y.; Tang, H. Q., Catalytic oxidative removal of 2,4-dichlorophenol by simultaneous use of horseradish peroxidase and graphene oxide/Fe_3O_4 as catalyst. *Chem. Eng. J.* **2014,** *254*, 434-442.
104. Bobrow, M. N.; Harris, T. D.; Shaughnessy, K. J.; Litt, G. J., Catalyzed reporter deposition, a novel method of signal amplification - application to immunoassays. *J. Immunol. Methods* **1989,** *125* (1-2), 279-285.
105. Yu, X.; Munge, B.; Patel, V.; Jensen, G.; Bhirde, A.; Gong, J. D.; Kim, S. N.; Gillespie, J.; Gutkind, J. S.; Papadimitrakopoulos, F.; Rusling, J. F., Carbon nanotube amplification strategies for highly sensitive immunodetection of cancer biomarkers. *J. Am. Chem. Soc.* **2006,** *128* (34), 11199-11205.
106. Tang, D. P.; Yuan, R.; Chal, Y. Q., Ultrasensitive electrochemical immunosensor for clinical immunoassay using thionine-doped magnetic gold nanospheres as labels and horseradish peroxidase as enhancer. *Anal. Chem.* **2008,** *80* (5), 1582-1588.
107. Emery, O.; Lalot, T.; Brigodiot, M.; Marechal, E., Free-radical polymerization of acrylamide by horseradish peroxidase-mediated initiation. *J. Polym. Sci. A Polym. Chem.* **1997,** *35* (15), 3331-3333.
108. Teixeira, D.; Lalot, T.; Brigodiot, M.; Marechal, E., β-diketones as key compounds in free-radical polymerization by enzyme-mediated initiation. *Macromolecules* **1999,** *32* (1), 70-72.
109. Durand, A.; Lalot, T.; Brigodiot, M.; Marechal, E., Enzyme-mediated radical initiation of acrylamide polymerization: Main characteristics of molecular weight control. *Polymer* **2001,** *42* (13), 5515-5521.
110. Cai, Z. Q.; Wang, W. C.; Ruan, G.; Wen, X. F., Kinetic study of acrylamide radical polymerization initiated by the horseradish peroxidase-mediated system. *Int. J. Chem. Kinet.* **2012,** *44* (7), 475-481.
111. Su, T.; Zhang, D.; Tang, Z.; Wu, Q.; Wang, Q. G., HRP-mediated polymerization forms tough nanocomposite hydrogels with high biocatalytic performance. *Chem. Commun.* **2013,** *49* (73), 8033-8035.

112. Fukushima, H.; Kohri, M.; Kojima, T.; Taniguchi, T.; Saito, K.; Nakahira, T., Surface-initiated enzymatic vinyl polymerization: Synthesis of polymer-grafted silica particles using horseradish peroxidase as catalyst. *Polym. Chem.* **2012,** *3* (5), 1123-1125.
113. Kalra, B.; Gross, R. A., Horseradish peroxidase mediated free radical polymerization of methyl methacrylate. *Biomacromolecules* **2000,** *1* (3), 501-505.
114. Sutton, H. C.; Winterbourn, C. C., On the Participation of Higher Oxidation-States of Iron and Copper in Fenton Reactions. *Free Radical Biol. Med.* **1989,** *6* (1), 53-60.
115. Nappi, A. J.; Vass, E., Comparative studies of enhanced iron-mediated production of hydroxyl radical by glutathione, cysteine, ascorbic acid, and selected catechols. *Biochim. Biophys. Acta, Gen. Subj.* **1997,** *1336* (2), 295-302.
116. Siedlecka, E. M.; Wieckowska, A.; Stepnowski, P., Influence of inorganic ions on MTBE degradation by Fenton's reagent. *J. Hazard. Mater.* **2007,** *147* (1-2), 497-502.
117. Iwata, H.; Hata, Y.; Matsuda, T.; Ikada, Y., Initiation of radical polymerization by glucose oxidase utilizing dissolved oxygen. *J. Polym. Sci. A Polym. Chem.* **1991,** *29* (8), 1217-1218.
118. Johnson, L. M.; Fairbanks, B. D.; Anseth, K. S.; Bowman, C. N., Enzyme-mediated redox initiation for hydrogel generation and cellular encapsulation. *Biomacromolecules* **2009,** *10* (11), 3114-21.
119. Shan, J.; Kitamura, Y.; Yoshizawa, H., Emulsion polymerization of styrene by horseradish peroxidase-mediated initiation. *Colloid Polym. Sci.* **2005,** *284* (1), 108-111.
120. Naves, A. F.; Carmona-Ribeiro, A. M.; Petri, D. F. S., Immobilized horseradish peroxidase as a reusable catalyst for emulsion polymerization. *Langmuir* **2007,** *23* (4), 1981-1987.
121. Hatzinikolaou, D. G.; Hansen, O. C.; Macris, B. J.; Tingey, A.; Kekos, D.; Goodenough, P.; Stougaard, P., A new glucose oxidase from Aspergillus niger: Characterization and regulation studies of enzyme and gene. *Appl. Microbiol. Biotechnol.* **1996,** *46* (4), 371-381.
122. Kalisz, H. M.; Hendle, J.; Schmid, R. D., Structural and biochemical properties of glycosylated and deglycosylated glucose oxidase from Penicillium amagasakiense. *Appl. Microbiol. Biotechnol.* **1997,** *47* (5), 502-507.
123. Rando, D.; Kohring, G. W.; Giffhorn, F., Production, purification and characterization of glucose oxidase from a newly isolated strain of Penicillium pinophilum. *Appl. Microbiol. Biotechnol.* **1997,** *48* (1), 34-40.
124. Pluschkell, S.; Hellmuth, K.; Rinas, U., Kinetics of glucose oxidase excretion by recombinant Aspergillus niger. *Biotechnol. Bioeng.* **1996,** *51* (2), 215-220.
125. Witt, S.; Wohlfahrt, G.; Schomburg, D.; Hecht, H. J.; Kalisz, H. M., Conserved arginine-516 of Penicillium amagasakiense glucose oxidase is essential for the efficient binding of β-D-glucose. *Biochem. J.* **2000,** *347*, 553-559.
126. Johnson, L. M.; Deforest, C. A.; Pendurti, A.; Anseth, K. S.; Bowman, C. N., Formation of three-dimensional hydrogel multilayers using enzyme-mediated redox chain initiation. *ACS Appl. Mater. Interfaces* **2010,** *2* (7), 1963-72.
127. Berron, B. J.; Johnson, L. M.; Ba, X.; McCall, J. D.; Alvey, N. J.; Anseth, K. S.; Bowman, C. N., Glucose oxidase-mediated polymerization as a platform for dual-mode signal amplification and biodetection. *Biotechnol. Bioeng.* **2011,** *108* (7), 1521-1528.
128. Shenoy, R.; Bowman, C. N., Kinetics of interfacial radical polymerization initiated by a glucose-oxidase mediated redox system. *Biomaterials* **2012,** *33* (29), 6909-6914.
129. Shenoy, R.; Tibbitt, M. W.; Anseth, K. S.; Bowman, C. N., Formation of core-shell particles by interfacial radical polymerization initiated by a glucose oxidase-mediated redox system. *Chem. Mater.* **2013,** *25* (5), 761-767.
130. Liao, C. A.; Wu, Q.; Wei, Q. C.; Wang, Q. G., Bioinorganic nanocomposite hydrogels formed by HRP-GOx-cascade-catalyzed polymerization and exfoliation of the layered composites. *Chem. Eur. J.* **2015,** *21* (36), 12620-+.

131. Gormley, A. J.; Chapman, R.; Stevens, M. M., Polymerization amplified detection for nanoparticle-based biosensing. *Nano Lett.* **2014,** *14* (11), 6368-6373.
132. Su, T.; Tang, Z.; He, H. J.; Li, W. J.; Wang, X.; Liao, C. N.; Sun, Y.; Wang, Q. G., Glucose oxidase triggers gelation of N-hydroxyimide-heparin conjugates to form enzyme-responsive hydrogels for cell-specific drug delivery. *Chem. Sci.* **2014,** *5* (11), 4204-4209.
133. Simizu, S.; Ishida, K.; Wierzba, M. K.; Sato, T. A.; Osada, H., Expression of heparanase in human tumor cell lines and human head and neck tumors. *Cancer Lett.* **2003,** *193* (1), 83-89.
134. Ikeda, R.; Tanaka, H.; Uyama, H.; Kobayashi, S., Laccase-catalyzed polymerization of acrylamide. *Macromol. Rapid Commun.* **1998,** *19* (8), 423-425.
135. Hollmann, F.; Gumulya, Y.; Tolle, C.; Liese, A.; Thum, O., Evaluation of the laccase from Myceliophthora thermophila as industrial biocatalyst for polymerization reactions. *Macromolecules* **2008,** *41* (22), 8520-8524.
136. Ai, M. Q.; Wang, F. F.; Huang, F., Purification and characterization of a thermostable laccase from Trametes trogii and its ability in modification of kraft lignin. *J. Microbiol. Biotechnol.* **2015,** *25* (8), 1361-70.
137. Aktas, N.; Cicek, H.; Unal, A. T.; Kibarer, G.; Kolankaya, N.; Tanyolac, A., Reaction kinetics for laccase-catalyzed polymerization of 1-naphthol. *Bioresour. Technol.* **2001,** *80* (1), 29-36.
138. Yang, H.; Sun, H. F.; Zhang, S. J.; Wu, B. D.; Pan, B. C., Potential of acetylacetone as a mediator for Trametes versicolor laccase in enzymatic transformation of organic pollutants. *Environ. Sci. Pollut. Res.* **2015,** *22* (14), 10882-10889.
139. Junker, K.; Zandomeneghi, G.; Schuler, L. D.; Kissner, R.; Walde, P., Enzymatic polymerization of pyrrole with Trametes versicolor laccase and dioxygen in the presence of vesicles formed from AOT (sodium bis-(2-ethylhexyl) sulfosuccinate) as templates. *Synth. Met.* **2015,** *200*, 123-134.
140. Bajpai, P., Application of enzymes in the pulp and paper industry. *Biotechnol. Progr.* **1999,** *15* (2), 147-157.
141. Kanagaraj, J.; Senthilvelan, T.; Panda, R. C., Degradation of azo dyes by laccase: Biological method to reduce pollution load in dye wastewater. *Clean Technol. Environ. Policy* **2015,** *17* (6), 1443-1456.
142. Escalona, I.; Grooth, J.; Font, J.; Nijmeijer, K., Removal of BPA by enzyme polymerization using NF membranes. *J. Membr. Sci.* **2014,** *468*, 192-201.
143. Nieto, M.; Nardecchia, S.; Peinado, C.; Catalina, F.; Abrusci, C.; Gutierrez, M. C.; Ferrer, M. L.; del Monte, F., Enzyme-induced graft polymerization for preparation of hydrogels: Synergetic effect of laccase-immobilized-cryogels for pollutants adsorption. *Soft Matter* **2010,** *6* (15), 3533-3540.
144. Wang, X.; Niu, D. C.; Li, P.; Wu, Q.; Bo, X. W.; Liu, B. J.; Bao, S.; Su, T.; Xu, H. X.; Wang, Q. G., Dual-enzyme-loaded multifunctional hybrid nanogel system for pathological responsive ultrasound imaging and T_2-weighted magnetic resonance imaging. *ACS Nano* **2015,** *9* (6), 5646-5656.
145. Ng, Y. H.; di Lena, F.; Chai, C. L. L., Metalloenzymatic radical polymerization using alkyl halides as initiators. *Polym. Chem.* **2011,** *2* (3), 589-594.
146. Matyjaszewski, K., Atom transfer radical polymerization (ATRP): Current status and future perspectives. *Macromolecules* **2012,** *45* (10), 4015-4039.
147. Ng, Y. H.; di Lena, F.; Chai, C. L. L., PolyPEGA with predetermined molecular weights from enzyme-mediated radical polymerization in water. *Chem. Commun.* **2011,** *47* (22), 6464-6466.
148. Sigg, S. J.; Seidi, F.; Renggli, K.; Silva, T. B.; Kali, G.; Bruns, N., Horseradish peroxidase as a catalyst for atom transfer radical polymerization. *Macromol. Rapid Commun.* **2011,** *32* (21), 1710-1715.

149. Silva, T. B.; Spulber, M.; Kocik, M. K.; Seidi, F.; Charan, H.; Rother, M.; Sigg, S. J.; Renggli, K.; Kali, G.; Bruns, N., Hemoglobin and red blood cells catalyze atom transfer radical polymerization. *Biomacromolecules* **2013,** *14* (8), 2703-2712.
150. Dinu, M. V.; Spulber, M.; Renggli, K.; Wu, D. L.; Monnier, C. A.; Petri-Fink, A.; Bruns, N., Filling polymersomes with polymers by peroxidase-catalyzed atom transfer radical polymerization. *Macromol. Rapid Commun.* **2015,** *36* (6), 507-514.
151. Sanchez-Sanchez, A.; Arbe, A.; Kohlbrecher, J.; Colmenero, J.; Pomposo, J. A., Efficient synthesis of single-chain globules mimicking the morphology and polymerase activity of metalloenzymes. *Macromol. Rapid Commun.* **2015,** *36* (17), 1592-1597.
152. Zhou, H.; Jiang, W.; An, N.; Zhang, Q. P.; Xiang, S. D.; Wang, L. P.; Tang, J., Enzyme mimetic-catalyzed ATRP and its application in block copolymer synthesis combined with enzymatic ring-opening polymerization. *RSC Adv.* **2015,** *5* (53), 42728-42735.
153. Hay, A. S., Polymerization by oxidative coupling: Discovery and commercialization of PPO® and Noryl® resins. *J. Polym. Sci. A Polym. Chem.* **1998,** *36* (4), 505-517.
154. Ionescu, M.; Mihis, A. B., The mechanism of chain growth in oxidative polycondensation of phenols. *Macromol. Symp.* **1997,** *122*, 249-256.
155. Rocha-Martin, J.; Velasco-Lozano, S.; Guisan, J. M.; Lopez-Gallego, F., Oxidation of phenolic compounds catalyzed by immobilized multi-enzyme systems with integrated hydrogen peroxide production. *Green Chem.* **2014,** *16* (1), 303-311.
156. Dordick, J. S.; Marletta, M. A.; Klibanov, A. M., Polymerization of phenols catalyzed by peroxidase in nonaqueous media. *Biotechnol. Bioeng.* **1987,** *30* (1), 31-36.
157. Zheng, K.; Zhang, L.; Gao, Y. H.; Wu, Y. F.; Zhao, W. S.; Cui, Y. C., Enzymatic oxidative polymerization of pyrogallic acid for preparation of hindered phenol antioxidant. *J. Appl. Polym. Sci.* **2015,** *132* (12), 41591.
158. Sakai, S.; Kawakami, K., Synthesis and characterization of both ionically and enzymatically cross-linkable alginate. *Acta Biomater.* **2007,** *3* (4), 495-501.
159. Jin, R.; Hiemstra, C.; Zhong, Z. Y.; Feijen, J., Enzyme-mediated fast in situ formation of hydrogels from dextran-tyramine conjugates. *Biomaterials* **2007,** *28* (18), 2791-2800.
160. Moriyama, K.; Wakabayashi, R.; Goto, M.; Kamiya, N., Enzyme-mediated preparation of hydrogels composed of poly(ethylene glycol) and gelatin as cell culture platforms. *RSC Adv.* **2015,** *5* (4), 3070-3073.
161. Moriyama, K.; Minamihata, K.; Wakabayashi, R.; Goto, M.; Kamiya, N., Enzymatic preparation of a redox-responsive hydrogel for encapsulating and releasing living cells. *Chem. Commun.* **2014,** *50* (44), 5895-5898.
162. Wu, C. Z.; Strehmel, C.; Achazi, K.; Chiapisi, L.; Dernedde, J.; Lensen, M. C.; Gradzielski, M.; Ansorge-Schumacher, M. B.; Haag, R., Enzymatically cross-linked hyperbranched polyglycerol hydrogels as scaffolds for living cells. *Biomacromolecules* **2014,** *15* (11), 3881-3890.
163. Uyama, H.; Kurioka, H.; Kobayashi, S., Novel bienzymatic catalysis system for oxidative polymerization of phenols. *Polym. J.* **1997,** *29* (2), 190-192.
164. Taboada-Puig, R.; Junghanns, C.; Demarche, P.; Moreira, M. T.; Feijoo, G.; Lema, J. M.; Agathos, S. N., Combined cross-linked enzyme aggregates from versatile peroxidase and glucose oxidase: Production, partial characterization and application for the elimination of endocrine disruptors. *Bioresour. Technol.* **2011,** *102* (11), 6593-6599.
165. Sakai, S.; Komatani, K.; Taya, M., Glucose-triggered co-enzymatic hydrogelation of aqueous polymer solutions. *RSC Adv.* **2012,** *2* (4), 1502-1507.
166. Sakai, S.; Tsumura, M.; Inoue, M.; Koga, Y.; Fukano, K.; Taya, M., Polyvinyl alcohol-based hydrogel dressing gellable on-wound via a co-enzymatic reaction triggered by glucose in the wound exudate. *J. Mater. Chem. B* **2013,** *1* (38), 5067-5075.

167. Zhou, H. F.; Chang, Y.; Wu, X. L.; Yang, D. J.; Qiu, X. Q., Horseradish peroxidase modification of sulfomethylated wheat straw alkali lignin to improve its dispersion performance. *ACS Sustainable Chem. Eng.* **2015,** *3* (3), 518-523.
168. Liu, W.; Kumar, J.; Tripathy, S.; Senecal, K. J.; Samuelson, L., Enzymatically synthesized conducting polyaniline. *J. Am. Chem. Soc.* **1999,** *121* (1), 71-78.
169. Duan, L. P.; Zhao, Y.; Guo, F. H.; Liu, W. C.; Hou, C. P.; Ni, Z. H., Enzymatic-catalyzed polymerization of water-soluble electrically conductive polymer PEDOT:PSS. *Polym. Adv. Technol.* **2014,** *25* (8), 896-899.
170. Mita, N.; Tawaki, S.; Uyama, H.; Kobayashi, S., Laccase-catalyzed oxidative polymerization of phenols. *Macromol. Biosci.* **2003,** *3* (5), 253-257.
171. Navarra, C.; Goodwin, C.; Burton, S.; Danieli, B.; Riva, S., Laccase-mediated oxidation of phenolic derivatives. *J. Mol. Catal. B: Enzym.* **2010,** *65* (1-4), 52-57.
172. Hou, J. W.; Dong, G. X.; Ye, Y.; Chen, V., Enzymatic degradation of bisphenol-A with immobilized laccase on TiO_2 sol-gel coated PVDF membrane. *J. Membr. Sci.* **2014,** *469*, 19-30.
173. Hautphenne, C.; Debaste, F., Harnessing laccases for the synthesis of bisphenol A biopolymers. *Chem. Eng. Technol.* **2015,** *38* (7), 1223-1228.
174. Junker, K.; Luginbuhl, S.; Schuttel, M.; Bertschi, L.; Kissner, R.; Schuler, L. D.; Rakvin, B.; Walde, P., Efficient polymerization of the aniline dimer p-aminodiphenylamine (PADPA) with Trametes versicolor laccase/O_2 as catalyst and oxidant and AOT vesicles as templates. *ACS Catal.* **2014,** *4* (10), 3421-3434.
175. Furukawa, J.; Tsuruta, T.; Inoue, S., Triethylboron as an Initiator for Vinyl Polymerization. *J. Polym. Sci.* **1957,** *26* (113), 234-236.
176. Kolesnikov, G. S.; Fedorova, I. S., Polymerization of acrylonitrile in presence of tributylborine. *Bull. Acad. Sci. USSR* **1957,** *6* (2), 251-252.
177. Fordham, J. W. L.; Sturm, C. L., Mechanism of Trialkylboron Initiated Polymerization. *J. Polym. Sci.* **1958,** *33* (126), 503-504.
178. Welch, F. J., Polymerization of Methyl Methacrylate by Triethylboron-Oxygen Mixtures. *J. Polym. Sci.* **1962,** *61* (171), 243-&.
179. Brindley, P. B.; Pearson, R. G., Free-Radical Polymerization of Methyl Methacrylate in Presence of Trialkylboranes. *J. Polym. Sci. Pol. Lett.* **1968,** *6* (12), 831-835.
180. Allies, P. G.; Brindley, P. B., Mechanism of Autoxidation of Trialkylboranes. *J Chem Soc B* **1969,** (9), 1126-&.
181. Liu, S. J.; Zheng, Z.; Li, M. R.; Wang, X. L., Study of the radical chemistry promoted by tributylborane. *Res. Chem. Intermediat.* **2012,** *38* (8), 1893-1907.
182. Sonnenschein, M. F.; Webb, S. P.; Kastl, P. E.; Arriola, D. J.; Wendt, B. L.; Harrington, D. R.; Rondan, N. G., Mechanism of trialkylborane promoted adhesion to low surface energy plastics. *Macromolecules* **2004,** *37* (21), 7974-7978.
183. Zutty, N. L.; Welch, F. J., The Mechanism of Vinyl Polymerization Initiated by Metal Alkyls - Copolymerization Studies. *J. Polym. Sci.* **1960,** *43* (142), 445-452.
184. Zaremski, M. Y.; Garina, E. S.; Gurskii, M. E.; Bubnov, Y. N., Organoboranes-atmospheric oxygen systems as unconventional initiators of radical polymerization. *Polym. Sci. Ser. B* **2013,** *55* (5-6), 304-326.
185. Kolesnikov, G. S.; Fedorova, L. S., Mechanism of the polymerization of acrylonitrile in presence of trib utylborine. *Bull. Acad. Sci. USSR* **1958,** *7* (7), 883-883.
186. Ashikari, N.; Nishimura, A., The Monomer Reactivity Ratios in the Copolymerization of Vinyl Compounds with Trialkylboron Catalysts. *J. Polym. Sci.* **1958,** *31* (122), 249-251.
187. Zhang, Z. C.; Chung, T. C. M., Reaction mechanism of borane/oxygen radical initiators during the polymerization of fluoromonomers. *Macromolecules* **2006,** *39* (16), 5187-5189.
188. Hoyle, C. E.; Bowman, C. N., Thiol-Ene Click Chemistry. *Angew. Chem. Int. Ed.* **2010,** *49* (9), 1540-1573.

189. Lowe, A. B., Thiol-ene "click" reactions and recent applications in polymer and materials synthesis. *Polym. Chem.* **2010,** *1* (1), 17-36.
190. Fairbanks, B. D.; Scott, T. F.; Kloxin, C. J.; Anseth, K. S.; Bowman, C. N., Thiol-Yne Photopolymerizations: Novel Mechanism, Kinetics, and Step-Growth Formation of Highly Cross-Linked Networks. *Macromolecules* **2009,** *42* (1), 211-217.
191. Lowe, A. B.; Hoyle, C. E.; Bowman, C. N., Thiol-yne click chemistry: A powerful and versatile methodology for materials synthesis. *J. Mater. Chem.* **2010,** *20* (23), 4745-4750.
192. Chan, J. W.; Shin, J.; Hoyle, C. E.; Bowman, C. N.; Lowe, A. B., Synthesis, Thiol-Yne "Click" Photopolymerization, and Physical Properties of Networks Derived from Novel Multifunctional Alkynes. *Macromolecules* **2010,** *43* (11), 4937-4942.
193. Davies, A. G.; Roberts, B. P., Homolytic organometallic reactions. Part IV. Homolytic alkylthiyldealkylation of organoboranes. *Journal of the Chemical Society B: Physical Organic* **1971**, 1830-1837.
194. Ichinose, Y.; Wakamatsu, K.; Nozaki, K.; Birbaum, J.-L.; Oshima, K.; Utimoto, K., Et3B induced radical addition of thiols to acetylenes. *Chem. Lett.* **1987,** (8), 1647-1650.
195. Demchuk, D. V.; Lutsenko, A. I.; Troyanskii, â. I.; Nikishin, G. I., Homolytic reactions of dithiols with alkynes: A method of synthesis of 1,3- and 1,4-dithiacycloalkanes. *Bull. Acad. Sci. USSR* **1990,** *39* (12), 2542-2550.
196. Sato, A.; Yorimitsu, H.; Oshima, K., Regio- and Stereoselective Radical Additions of Thiols to Ynamides. *Synlett* **2009,** (1), 28-31.
197. Pallela, V. R.; Mallireddigari, M. R.; Cosenza, S. C.; Akula, B.; Subbaiah, D. R. C. V.; Reddy, E. P.; Reddy, M. V. R., Hydrothiolation of benzyl mercaptan to arylacetylene: application to the synthesis of (E) and (Z)-isomers of ON 01910 center dot Na (Rigosertib (R)), a phase III clinical stage anti-cancer agent. *Org. Biomol. Chem.* **2013,** *11* (12), 1964-1977.
198. Tibbitt, M. W.; Kloxin, A. M.; Sawicki, L. A.; Anseth, K. S., Mechanical Properties and Degradation of Chain and Step-Polymerized Photodegradable Hydrogels. *Macromolecules* **2013,** *46* (7), 2785-2792.
199. Lu, H.; Carioscia, J. A.; Stansbury, J. W.; Bowman, C. N., Investigations of step-growth thiol-ene polymerizations for novel dental restoratives. *Dent. Mater.* **2005,** *21* (12), 1129-36.
200. McCall, J. D.; Anseth, K. S., Thiol-Ene Photopolymerizations Provide a Facile Method To Encapsulate Proteins and Maintain Their Bioactivity. *Biomacromolecules* **2012,** *13* (8), 2410-2417.
201. Lin, C. C.; Raza, A.; Shih, H., PEG hydrogels formed by thiol-ene photo-click chemistry and their effect on the formation and recovery of insulin-secreting cell spheroids. *Biomaterials* **2011,** *32* (36), 9685-95.
202. Carioscia, J. A.; Lu, H.; Stanbury, J. W.; Bowman, C. N., Thiol-ene oligomers as dental restorative materials. *Dent. Mater.* **2005,** *21* (12), 1137-43.
203. Cramer, N. B.; Bowman, C. N., Kinetics of thiol-ene and thiol-acrylate photopolymerizations with real-time Fourier transform infrared. *J. Polym. Sci. A Polym. Chem.* **2001,** *39* (19), 3311-3319.
204. Lee, T. Y.; Roper, T. M.; Jonsson, E. S.; Guymon, C. A.; Hoyle, C. E., Thiol-ene photopolymerization kinetics of vinyl acrylate/multifunctional thiol mixtures. *Macromolecules* **2004,** *37* (10), 3606-3613.
205. Scott, T. F.; Kloxin, C. J.; Draughon, R. B.; Bowman, C. N., Nonclassical dependence of polymerization rate on initiation rate observed in thiol-ene photopolymerizations. *Macromolecules* **2008,** *41* (9), 2987-2989.

Chapter 2

Rapid, Puncture-Initiated Healing via Oxygen-Mediated Polymerization

Abstract: Autonomously healing materials that utilize thiol−ene polymerization initiated by an environmentally borne reaction stimulus are demonstrated by puncturing tri-layered panels, fabricated by sandwiching thiol−ene−trialkylborane resin formulations between solid polymer panels, with high velocity projectiles; as the reactive liquid layer flows into the entrance hole, contact with atmospheric oxygen initiates polymerization, converting the liquid into a solid plug. Using infrared spectroscopy, we find that formulated resins polymerize rapidly, forming a solid polymer within seconds of atmospheric contact. During high-velocity ballistics experiments, additional evidence for rapid polymerization is provided by high-speed video, demonstrating the immediate viscosity increase when the thiol−ene−trialkylborane resins contact atmospheric oxygen, and thermal imaging, where surface temperature measurements reveal the thiol− ene reaction exotherm, confirming polymerization begins immediately upon oxygen exposure. While other approaches for materials self-repair have utilized similar liquid-to-solid transitions, our approach permits the development of materials capable of sealing a breach within seconds, far faster than previously described methods.

2.1 Introduction

Numerous applications, spanning the biomedical, automotive, and aerospace fields, would greatly benefit from the development of polymeric materials that undergo spontaneous self-repair when damaged, extending product lifetime or preventing catastrophic failure. To date, mechanisms for the self-repair of materials have largely utilized liquid-to-solid transitions, where the action of damage to a material initiates the polymerization of an incorporated reactive liquid monomer formulation.[1-6] This reactive liquid is stored in reservoirs, such as microcapsules or capillaries, embedded in a polymeric continuous phase; the containment of the reactive liquid prevents contact with a proximate reaction stimulus, such as an initiator, catalyst, or coreactant, that could either be stored in separate reservoirs or within the continuous phase itself. Only upon application of a sufficiently high force are the walls of the capsules or capillaries disrupted, releasing the reactive liquid within and allowing it to not only flow into the damaged region but also encounter its reaction stimulus. The subsequent polymerization reaction converts the liquid into a solid which, owing to the mechanical resilience of the generated polymer, repairs and strengthens the damaged region.[1-6] While this technique has been demonstrated as a means for repairing microcracks, expanding it to other modes of healing may be advantageous, especially for materials that will automatically seal a breach formed by a high-velocity projectile. An alternative self-healing approach utilizes a solid thermoplastic polymer that, when punctured by a high-velocity projectile, partially melts to allow the passage of the projectile while retaining sufficient melt strength to permit elastic recovery; subsequent polymer chain interfusion seals the breach. For example, partially neutralized poly(ethylene-co-methacrylic acid) (EMAA), a relatively

low modulus ionomer, undergoes puncture-induced healing at room temperature. Unfortunately, EMAA fails at temperatures greater than 60°C and its low modulus precludes its use in structural applications.[7, 8] Conversely, poly(butadiene)-graft-poly(methyl acrylate-co-acrylonitrile) (PBG), a much stiffer material at room temperature and better suited for structural utilization, only displays puncture-healing characteristics at elevated temperatures.[9]

The puncture of a thin material, millimeters or centimeters thick, by a high-velocity projectile can be devastating under certain scenarios. For example, if the material functions as a pressurized container wall, such as in a fuel tank, an airplane hull, or the walls of a space exploration vehicle,[10] any breach causes the interior contents, whether fuel or air, to be rapidly ejected. The consequences are especially severe for manned spacecraft as the rapid loss of atmosphere would immediately endanger those inside. Systems that rely upon the mixing of two reactive liquid components, capable of slowly filling and repairing a puncture site over several hours, have been developed;[11] however, for situations involving the breach of pressurized container walls, much faster healing mechanisms are required. Here, we describe a new autonomous-healing method to achieve extremely fast reaction rates by utilizing an environmentally-borne initiation stimulus that is able to rapidly contact with and diffuse into a reactive liquid monomer formulation and effect polymerization.

Among compounds reliably present in human-occupied environments, those likely to act as initiation stimuli include water vapor (present as humidity) and other atmospheric gases (e.g., nitrogen, oxygen, carbon dioxide, etc.). Water is a well known initiator of several polymerization reactions, most notably the anionic polymerization of

alkyl cyanoacrylates utilized in commercial and medical adhesives.[12] Unfortunately, deficiencies of alkyl cyanoacrylate chemistry include its susceptibility to attack from nucleophilic species, severely limiting the choice of materials acting as liquid monomer reservoirs, as well as the sensitivity of the polymerization rate on the relative environmental humidity, where low humidity environments afford reaction rates that may prove too low[13, 14] for rapid breach sealing. Of the other gases reliably present in habitable atmospheres, nitrogen and carbon dioxide exhibit very low reactivity. Conversely, oxygen is both plentiful and able to participate in radical-yielding redox reactions that are suitable for the initiation of radical-mediated polymerizations.

A notable example of oxygen's ability to rapidly yield radicals is its reaction with alkylboranes such as triethylborane and tributylborane (TBB). In the presence of oxygen, alkylboranes rapidly and exothermically produce, among other products, alkyl and alkoxy radicals (see Equation 8),[15, 16] species capable of initiating radical-mediated reactions including the chain-growth polymerization of (meth)acrylates and other vinyl monomers.[17, 18]

$$R_3B \xrightarrow{O_2} R\cdot + RO\cdot + \text{other products} \qquad (8)$$

Given the extreme reactivity of alkylboranes to oxygen, even very low oxygen concentrations, such as those present as dissolved gas in monomer, are more than sufficient to initiate the reaction. This minimal requirement for oxygen is necessary as typical radical-mediated chain-growth polymerization reactions are strongly inhibited by oxygen, where the propagating radical reacts with oxygen to yield a sluggishly reacting peroxy radical.[19] Notably, Chung *et al.* demonstrated severe polymerization inhibition

when alkylboranes were utilized in the presence of high oxygen concentrations;[17] although oxygen was required to generate the initiating species, in excess it prevented polymer growth by interfering with the propagation step, suggesting that alkylboranes are ill-suited as initiators for conventional, chain-growth radical-mediated polymerizations in environments with high oxygen concentrations.

In contrast to radical-mediated chain-growth reactions, the radical-mediated thiol–ene addition reaction between thiols and electron-rich carbon-carbon double bonds (e.g., allyl ether or vinyl ether functional groups) (Scheme 19) is extraordinarily resistant to oxygen inhibition, a consequence of hydrogen abstraction by the peroxy radical from the ubiquitous thiol,[20] and thus is more appropriate for oxygen-mediated polymerizations.[21] Alkylboranes have previously been used to initiate coupling reactions, likely via the radical-generating alkylborane-oxygen reaction, between monofunctional thiol- and both vinyl- and alkynyl-bearing compounds;[22-25] however, initiation of thiol–ene polymerizations by alkylboranes has not been reported. Given the oxygen tolerance of the thiol–ene reaction, this polymerization mechanism is particularly amenable to the utilization of oxygen as an environmentally-borne reactant with alkylboranes. Here, we demonstrate the ability of thiol–ene-alkylborane formulations to rapidly polymerize after oxygen exposure and the self-healing capability of these formulations when subjected to ballistics testing.

2.2 Experimental

2.2.1 Materials

Ethylene glycol dimercaptopropionate (EGDMP) was donated by Evans Chemetics. Trimethylolpropane diallyl ether (TMPDAE) and tributylborane (TBB) were purchased

from Sigma-Aldrich; TMPDAE and EGDMP were vacuum distilled prior to use and TBB was used as received. *N*-Nitrosophenylhydroxylamine aluminum salt, a radical inhibitor, was purchased from Wako Chemicals and used as received. The 1 mm poly(butadiene)-graft-poly(methyl acrylate-co-acrylonitrile) (PBG – Barex 210 IG from Ineos) and partially neutralized poly(ethylene-co-methacrylic acid) (EMAA – Surlyn 8940 from DuPont) panels were provided by the NASA Langley Research Center.

2.2.2 Synthesis

Trimethylolpropane triallyl ether (TMPTAE) was formed, using a method from the literature,[26] by reacting TMPDAE in toluene solution overnight at 70°C with excess sodium hydride and allyl bromide.

2.2.3 Monomer Degassing

Prior to all experiments (both real-time FTIR and ballistics), all liquid monomers were degassed by at least 12 freeze-pump-thaw cycles: 10-20 mL of monomer, in a glass vacuum flask, was frozen in liquid nitrogen; the headspace above the frozen monomer was evacuated by applying a vacuum of less than 0.5 torr; and, after sealing the flask, the frozen monomer was allowed to melt at room temperature. These steps were repeated until no gas bubbles evolved during the thaw step.

2.2.4 Dynamic Mechanical Analysis

Performed using a DMA Q 800 from TA instruments. Temperature was ramped from -60°C to 40°C while under tension with a 0.1% strain and frequency of 1 Hz.

2.2.5 Real-time FTIR Kinetics

Under oxygen-free conditions achieved in an anaerobic glovebox, rigorously degassed TMPDAE and EGDMP in a 1:1 stoichiometric functional group ratio, TBB at varying concentrations, and 0.1 wt% inhibitor (*N*-nitrosophenylhydroxylamine aluminum salt) were combined and a 19±2 μm thick layer of the formulated resin (Figure 1) was deposited on a glass slide in a sealed sample cell. (Figure 2 and Figure 3)

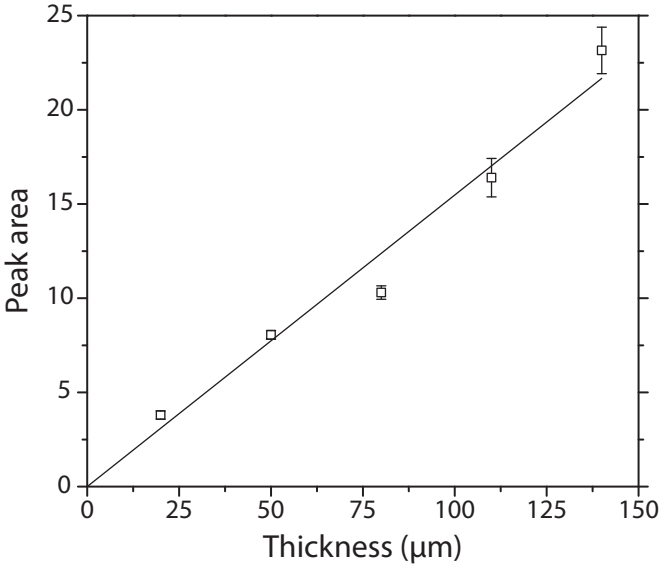

Figure 1: Measuring monomer formulation thickness. A standard curve was created by measuring the area underneath the thiol peak (2572 cm^{-1}) of the EGDMP-TMPDAE monomer formulation at various thicknesses. The thickness was controlled by infusing the monomer formulation between two glass slides separated by shims of known dimensions. A plot of area versus thickness gives a regression line of Area = Thickness (μm) × 0.1548. Using the spectra taken from the IR kinetics experiments, the average area was 2.71±0.24, corresponding to a thickness of 18.7±1.6 μm.

Infrared spectra of the formulations were monitored remotely and in transmission using a Nicolet 6700 FT-IR spectrometer equipped with a fiber optic coupling accessory via chalcogenide optical fiber patch cables (Newport Corporation catalog number 76906) fitted with silver reflective collimators (Thorlabs catalog number RC04SMA-P01); these

optical fibers and collimators were employed as they permit transmission to ~2200 cm^{-1}. The polymerization reaction proceeded only after the introduction of air (~21% O_2) or other oxygen/nitrogen gas mixtures into the sample chamber via ports on either side,(Figure 2 and Figure 3) and the reaction was monitored by observing the disappearance of the allyl ether (3100 cm^{-1}) and thiol (2570 cm^{-1}) absorbance peaks,[26] using the methyl peak at 4370 cm^{-1} as an internal standard.[27, 28] Spectra were collected at a rate of two per second; whereas averaging was not required for resins formulated with 1 and 2 wt% TBB, spectra for resins formulated with 0 and 0.5 wt% TBB were averaged over four scans.

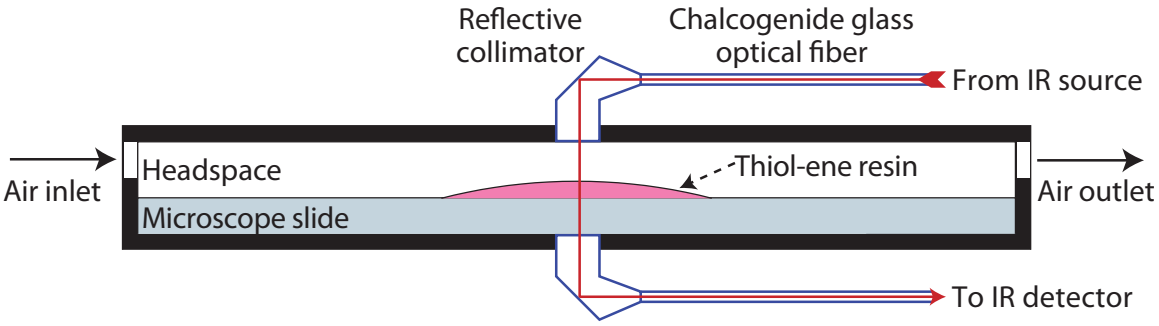

Figure 2: Model thiol–ene-alkylborane formulations, spread as thin films on glass microscope slides, were placed inside a sample cell under anaerobic conditions. Chalcogenide fiber optic cables were used to send and receive an IR beam through the sample, allowing for the reaction conversion measurement of both thiol and allyl ether functional groups. The polymerization reaction started only after air (~21% oxygen) was allowed to flow through the chamber via inlet and outlet ports.

2.2.6 Assembly of Tri-layered Sample Panels

Sample panels (75 mm × 75 mm × 3 mm) were assembled by sandwiching a 1 mm thick spacer between the edges of two 1 mm thick sheets of PBG and EMAA. The edges of the sandwich structure were then sealed using a two-component epoxy adhesive, leaving a small hole for the injection of liquid resins. In an anaerobic glove box (<10 ppm O_2), the reactive monomer formulations consisting of comonomers in a 1:1 thiol:ene

stoichiometric ratio, TBB, and 0.1 wt% inhibitor, were mixed and injected to fill the gap between the two solid panels, after which the small injection hole was sealed using additional epoxy adhesive. The panels were stored at -20°C during transport to the testing facility and were allowed to equilibrate for five minutes at ambient conditions prior to ballistics testing.

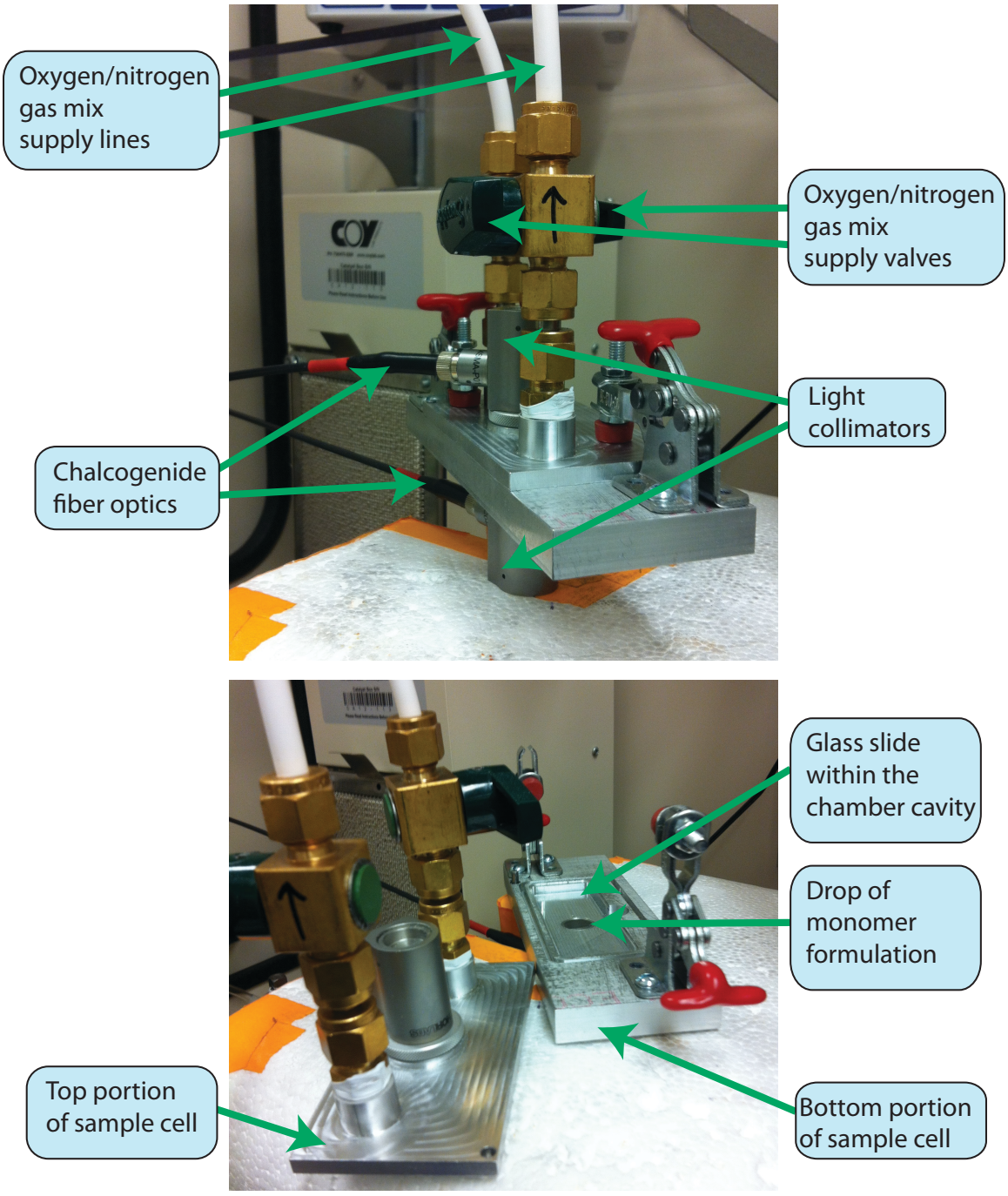

Figure 3: Photographs of sealed sample cell utilized in IR kinetics experiments. Top photograph: closed sample cell, sitting within an anaerobic chamber, showing the chalcogenide fiber optic cable and reflective light collimators that carry the infrared beam to and from the sample cell, as well as the gas lines that deliver the oxygen/nitrogen gas mixtures. Bottom photograph: open cell showing the glass slide upon which the thiol–ene monomer formulation is placed.

2.2.7 Ballistics

Test panels were affixed in a sample holder that clamped the panel on all edges. Bullets (0.223″ caliber full metal jacket, 3.57 g) were fired at the panels using a bolt-action rifle from 11 meters away. Phantom 12 high speed video cameras, recording at frame rates of 85,800 or 100,000 frames/second, were positioned at 45° to the entrance and exit surfaces at both the front and back of the sample. Videography analysis determined the entrance and exit bullet velocities to be 1.01±0.01 $km \cdot s^{-1}$ and 0.97±0.02 $km \cdot s^{-1}$, respectively. A FLIR ThermaCam SC 600 Thermal IR camera, recording over a temperature range of 30-155°C at 500 frames per second for 24 seconds, was used to measure the surface temperature evolution after bullet penetration. To estimate temperatures above 155°C, Gaussian fitting was performed on four slices of data (horizontal, vertical, and both diagonals) through the center of the thermal hot spots and the average was reported.

2.3 Results and Discussion

2.3.1 Polymerization Kinetics

To demonstrate their potential for rapid reaction rates, the kinetics of alkylborane/oxygen-initiated thiol–ene polymerizations were examined with model thiol–ene resins, produced from difunctional thiol and allyl ether monomers (Scheme 22) such that the resultant polymers were not cross-linked, using real-time FTIR spectroscopy by following the disappearance of the thiol and allyl ether absorbance peaks.[26] These model resins, mixed at 1:1 thiol:ene stoichiometric ratios, were formulated under anaerobic conditions with varying concentrations of TBB, spread as thin films on microscope slides, and placed in a gas-tight sample cell (Figure 2 and Figure 3). As anticipated, whereas the TBB-containing formulations were stable under anaerobic conditions (Figure

4), polymerizations proceeded in TBB-containing formulations immediately when air (i.e., 21% oxygen) was introduced into the sample cell (Figure 5 and Figure 6); reactions rates remained rapid even at diminished oxygen concentrations (Figure 7). In the absence of TBB, contact with oxygen did not induce thiol–ene polymerization whereas increasing the TBB concentration raised both the polymerization rates and extents, an effect most evident at TBB concentrations of 1 wt% and higher. Thiol–ene polymerizations using multifunctional monomers formulated with TBB and contacted with oxygen lead to rapid gelation and formation of a polymer network. Notably, attempts to examine the polymerization reactions of cross-linking thiol–ene resins using IR spectroscopy were unsuccessful as the reaction itself rapidly yielded a thin, buckled skin that scattered the IR beam and resulted in poor signal-to-noise ratios; the utilization of the non-cross-linking, difunctional monomer system described above prevented the buckled surface formation. As the radical-mediated thiol–ene polymerization proceeds via step-growth, the gel point can be readily predicted from the monomer functionality;[29] for example, a 3-2 monomer system (e.g., a trithiol with a diallyl ether) will gel at approximately 71% reaction conversion, a 6-2 system at approximately 45% conversion, and a 40-6 system at approximately 7% conversion. Assuming the monomer functionality does not greatly influence the pre-gelation polymerization rate, for the reaction conversion trajectories reported here, a thiol–ene formulation with 2 wt% TBB would gel in less than 24 seconds, 8 seconds, or 2 seconds by using monomer functionalities of a 3-2, 6-2, or 40-6, respectively. As evidence that the polymerization mechanism proceeds via the radical-mediated thiol–ene reaction, the thiol and allyl ether functional groups are consumed at nearly the same rate, with the thiol group consumption proceeding slightly faster than that

of the vinyl groups, potentially attributable to a side reaction between thiyl radicals and butylboranes.[16]

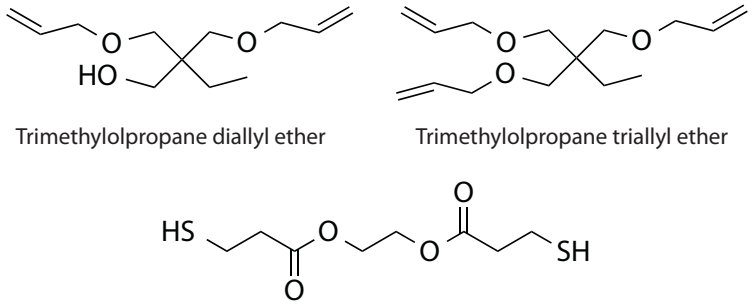

Scheme 22: Allyl ether and thiol monomers utilized in kinetics and ballistics experiments.

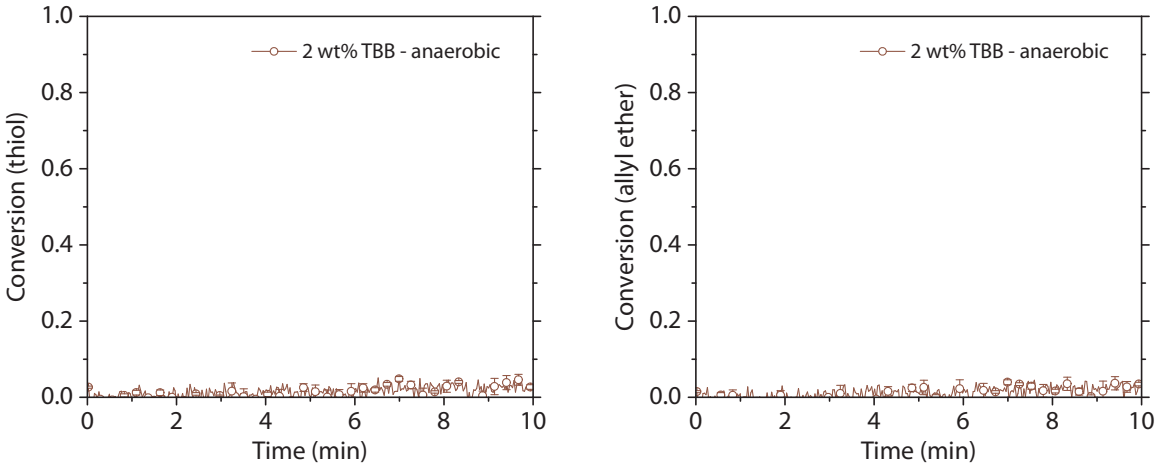

Figure 4: Model thiol–ene-TBB resin reaction kinetics under anaerobic conditions. A model thiol–ene resin, formulated with 2 wt% TBB, was monitored with FTIR spectroscopy in the absence of oxygen.

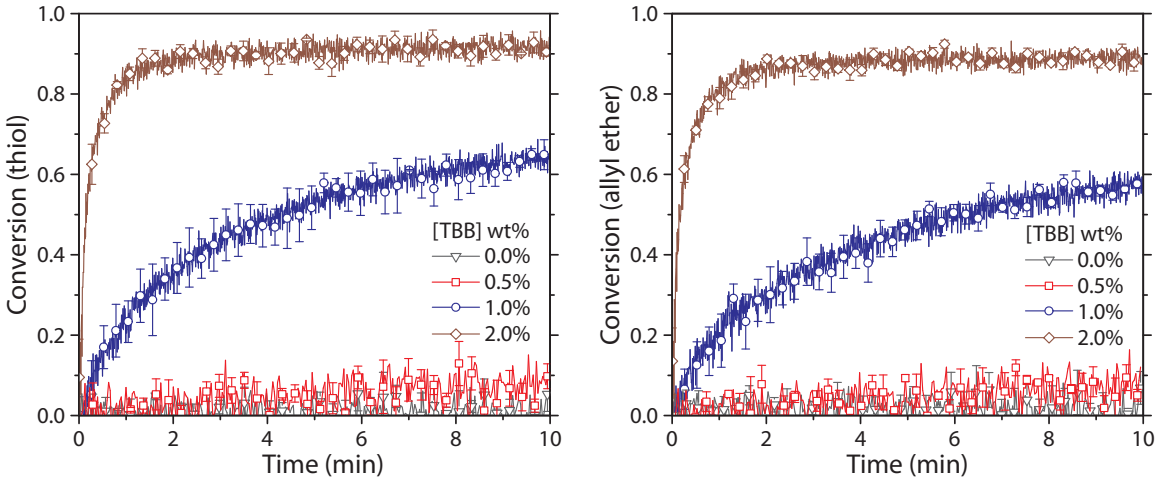

Figure 5: Reaction kinetics of oxygen-mediated thiol–ene polymerization. Conversion versus time for thiol (left) and allyl ether (right) functional groups in EGDMP/TMPDAE resins formulated with TBB at varying concentrations upon exposure to air.

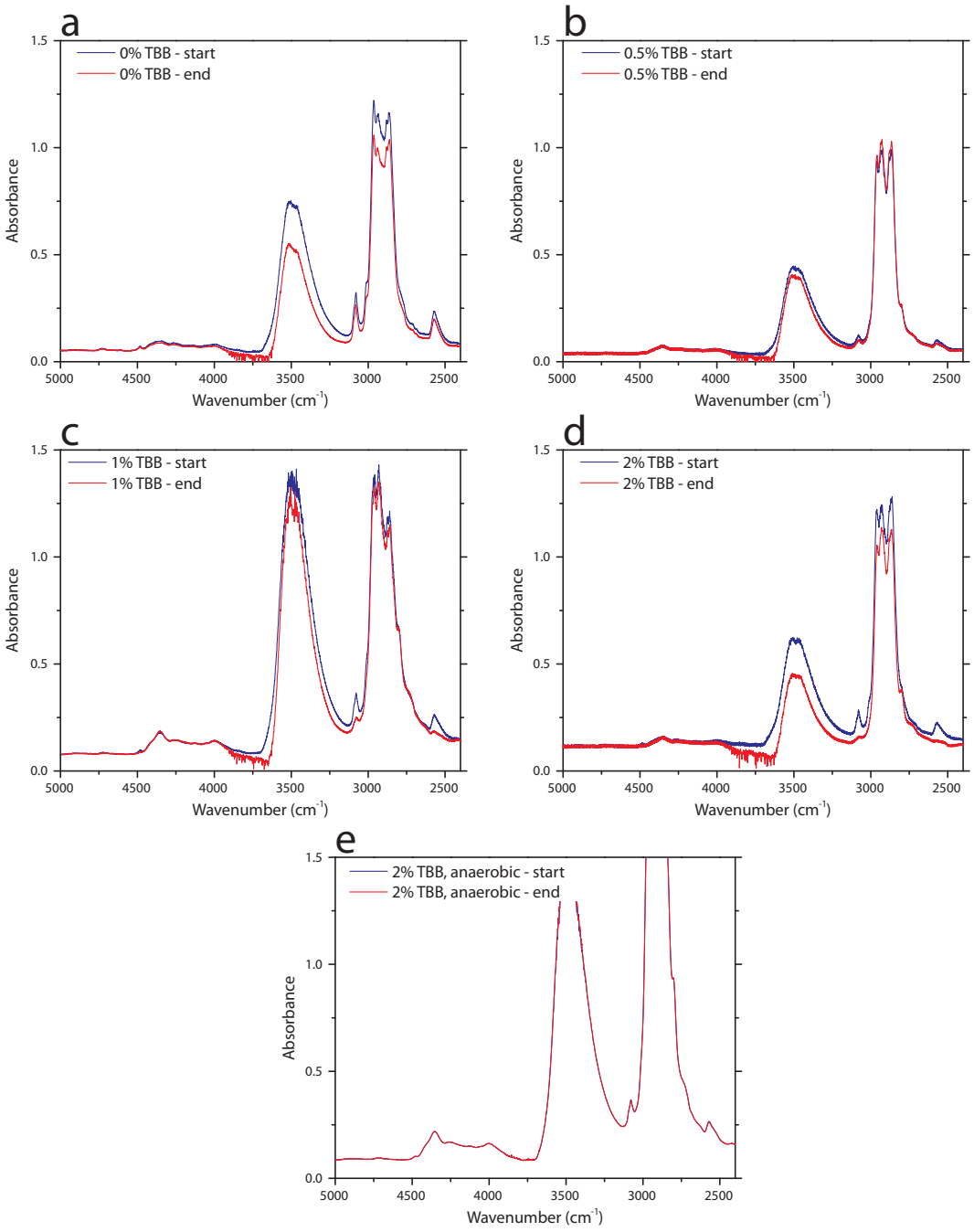

Figure 6: FTIR spectra of thiol–ene formulations prior to and after polymerization kinetics experiments. a-d) Spectra, with varying TBB concentrations, prior to oxygen exposure and after 10 minutes exposure are shown with blue and red lines, respectively. e) Two spectra of a formulation containing 2% TBB measured 10 minutes apart while kept under anaerobic conditions. Reactions were monitored by observing the disappearance of the allyl ether (3100 cm^{-1}) and thiol (2570 cm^{-1}) absorbance peaks, using the methyl absorbance peak at 4370 cm^{-1} as an internal standard.

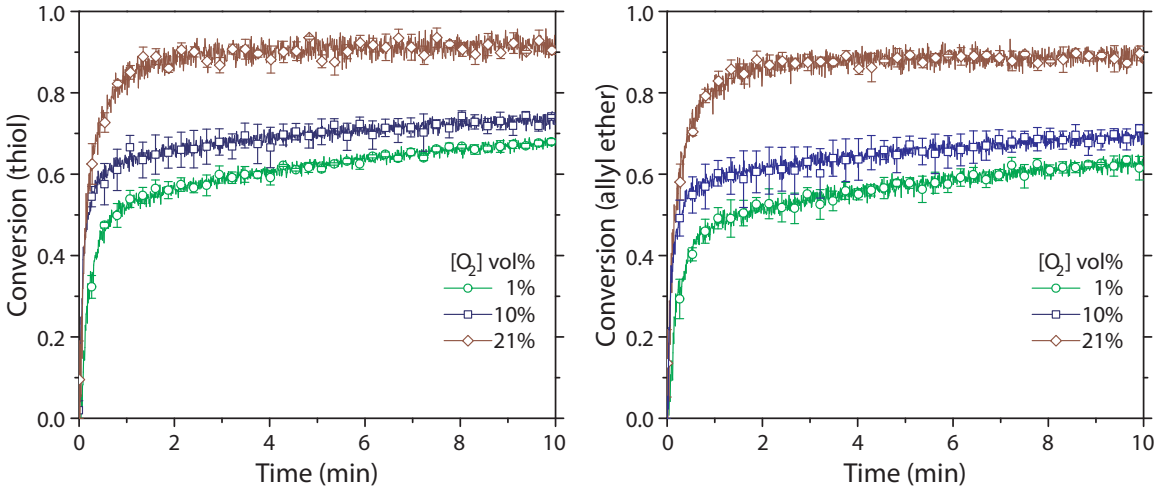

Figure 7: Reaction kinetics of oxygen-mediated thiol–ene polymerization. Conversion versus time for thiol (left) and allyl ether (right) functional groups in EGDMP/TMPDAE resins formulated with 2% TBB when exposed to 1%, 10%, and 21% oxygen-in-nitrogen gas mixtures.

2.3.2 Ballistics Testing

Having demonstrated that thiol–ene-TBB formulations rapidly polymerize upon oxygen exposure, these formulations were incorporated into tri-layered structures and subjected to ballistics testing to simulate micrometeoroid puncture of a spacecraft wall. The tri-layered structures were constructed by sandwiching a 1 mm thick reactive liquid monomer formulation layer between two 1 mm thick solid support panels (Scheme 23). The front, solid support panel was composed of PBG, chosen to ensure the formation of an approximately 1 mm diameter entrance hole upon projectile puncture, whereas the rear panel was composed of EMAA, a softer material that fully reseals upon ballistics puncture; this configuration permitted ready observation of the middle layer polymerization upon oxygen contact at the front entrance hole (Scheme 23). The results of firing a projectile from a rifle at the tri-layered panels were recorded with high-speed

video (placed in front of and behind the sample), high-speed infrared (IR) thermal cameras to record surface temperature, or both.

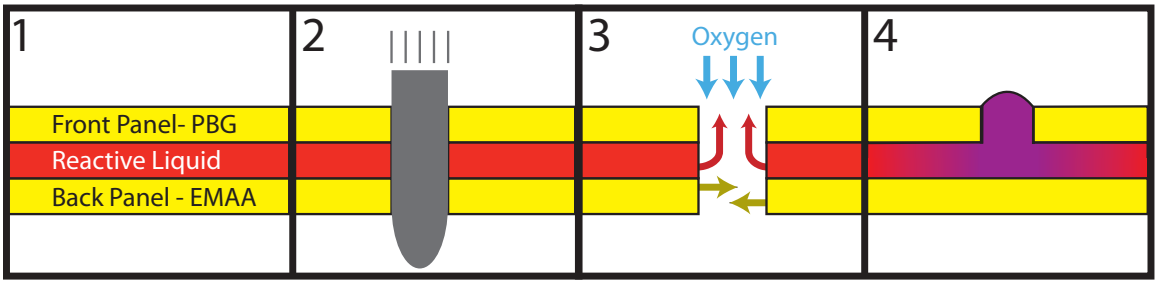

Scheme 23: Ballistics testing of resin-filled panels. a) (1) Tri-layered panels, fabricated by sandwiching thiol–ene-borane resin formulations between solid polymer panels (PBG in front, EMAA at back, see text for panel and sample clamp dimensions) were (2) subjected to ballistics testing where penetration by 5.68 mm diameter bullets resulted in 1-2 mm diameter entrance holes with no exit holes; (3) as the reactive liquid layered flowed into the entrance hole, contact with atmospheric oxygen initiated polymerization, (4) converting the liquid into a solid.

The influence of varying TBB concentration (from 0 to 2 wt%), in a resin formulation utilizing EGDMP and trimethylolpropane triallyl ether (TMPTAE, Scheme 24), on panel response upon puncture by a rifle-fired bullet and subsequent contact with atmospheric oxygen were initially examined using high-speed videography (Table 1).

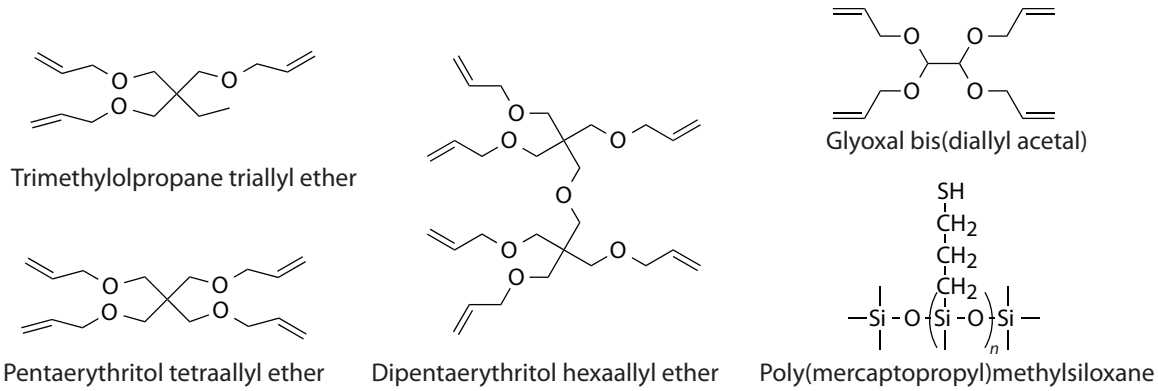

Scheme 24: Additional monomers utilized in ballistics experiments.

A comparison of the formulations with and without TBB (Table 1) revealed a striking difference in the amount of material ejected from the entrance hole (Figure 8). For formulations omitting TBB, a plume of monomer sprayed from the entrance hole approximately 1 ms after penetration for 2.3±0.8 ms. In contrast, for TBB-containing formulations, irrespective of the TBB concentration, bullet penetration yielded little to no liquid monomer ejection.[30] Whereas TBB-free monomer formulations did not polymerize upon oxygen exposure, resulting in ready ejection of the low viscosity liquid resin, the rapid, radical-generating oxygen-borane reaction in TBB-containing formulations proceeds immediately upon oxygen exposure such that the resultant polymerization reactions and concomitant increases in viscosity[31] curtail material ejection. Post-ballistic inspection and videography, performed within minutes of ballistic penetration, revealed that the formulations lacking TBB remained low viscosity liquids that could be readily squeezed out the projectile entrance hole, whereas those formulated with TBB ranged from a gel (0.5 wt% TBB) to a solid, entrance hole-filling plug (2 wt% TBB) surrounded by an approximately 1 cm diameter region of polymerized material (Figure 9). Moreover, the thermomechanical properties of polymer generated from the oxygen-mediated polymerization were found to closely resemble those of a conventionally-photopolymerized resin (Figure 10).

Table 1: Summary of all the reactive liquid monomer formulations subjected to ballistics testing. Abbreviations: ethylene glycol dimercaptopropionate (EGDMP) and trimethylolpropane triallyl ether (TMPTAE).

Experiment number	Thiol monomer	Allyl ether monomer	Tributylborane (wt%)
1	EGDMP	TMPTAE	0%
2	EGDMP	TMPTAE	0.5%
3	EGDMP	TMPTAE	1.0%
4	EGDMP	TMPTAE	2.0%
5		Air gap	

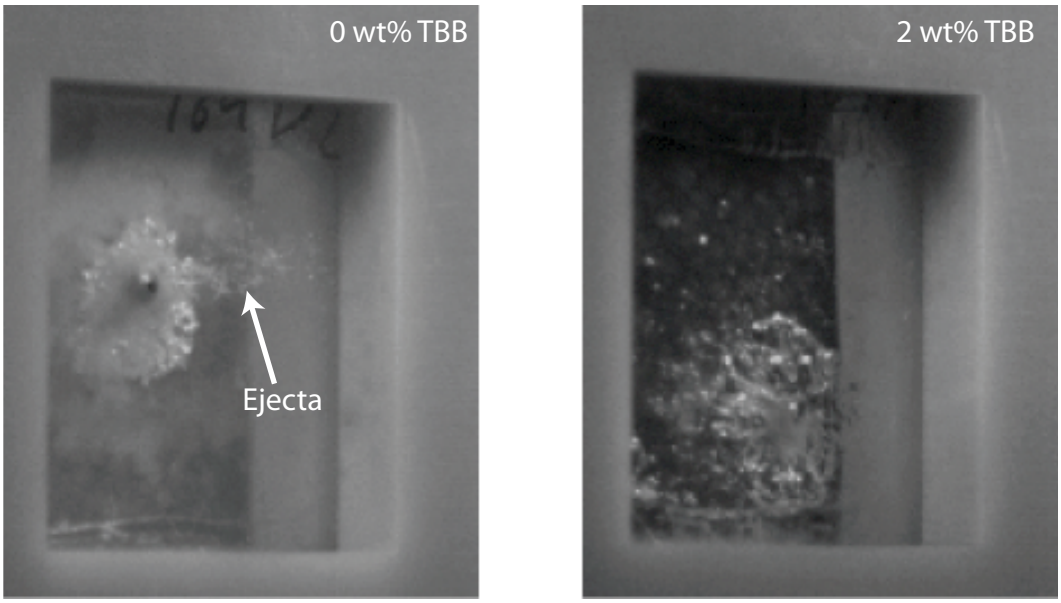

Figure 8: Still images of panels and resin ejection during testing, taken from high-speed videography footage 2.5 ms after bullet impact.

Figure 9: Photographs of a healed panel. a) Entrance- and b) exit-side photographs of a healed puncture site with the rear EMAA layer removed. c) Vacuum applied to entrance-side puncture site of this test panel with the EMAA layer removed. Note the vacuum gauge shows a vacuum of 2.3 x 10^{-1} Torr, corresponding to a ΔP across the polymerized thiol–ene plug of ~0.999 atm.

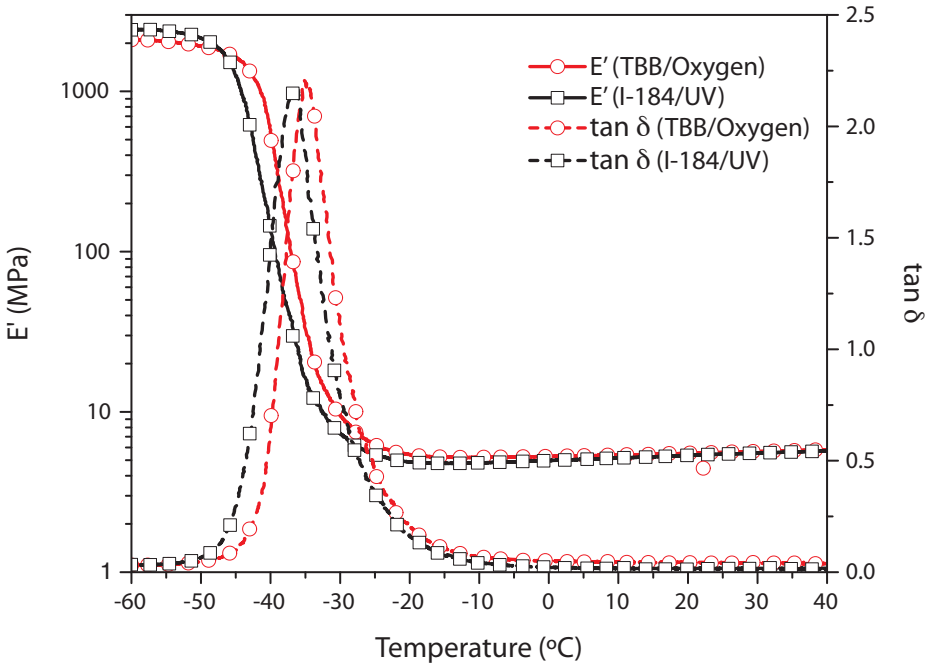

Figure 10: Storage modulus and tan δ of EGDMP/TMPTAE monomer formulations polymerized either by an oxygen-mediated process (i.e., exposing a TBB-containing formulation to the atmosphere) or photopolymerization (i.e., irradiating a photoinitiator (Irgacure 184)-containing formulation with 365 nm light at 10 mW/cm^2 for one hour).

Owing to the challenging experimental setup, in situ spectroscopic polymerization monitoring during ballistic testing proved infeasible as bullet penetration site variability risked damaging any integrated sensor necessary for measurement and potentially leading to hazardous bullet ricochet. Gordon *et al.* recently reported that the ballistic puncture of a PBG panel caused the surface temperature to increase by approximately 235 K,[9] attributable to projectile kinetic energy deposition into the stationary panel, and the anticipated thiol–ene polymerization employed here is exothermic.[21] Thus, panel surface temperatures were monitored remotely during ballistics experiments using high-speed thermography, providing a convoluted measurement of the exothermic reaction in TBB-containing resins that proceeds upon ballistic penetration and oxygen contact. Tri-layered panels were constructed with reactive liquid monomer resins formulated with

TMPTAE, EGDMP, and from 0 to 2 wt% TBB concentrations (Table 1), as well as additional panels with the liquid resin omitted entirely, leaving a 1 mm air-filled gap. The temperature range employed to monitor the sample thermal evolution upon bullet penetration was 30 to 155°C, an instrument-limited range that allowed observation of most of the temperature decay but was insufficient to capture the temperature peak immediately upon projectile impact. Consequently, the peak temperatures were established by fitting Gaussian temperature profiles across slices centered at the thermal hot spot (Figure 11), such that the thermal evolution could be determined throughout the experiment, the duration of which was again instrument limited to 24 seconds. Using these fitted values, for the samples that contained the liquid middle layer, the maximum temperature achieved was 262±6°C, an increase of 239±6 K above ambient temperature and in good agreement with the previously reported value,[9] and was not significantly influenced by the TBB concentration in samples incorporating the formulated resins. However, despite the consistency of the attained peak temperatures, direct observation of the thermal images demonstrates that the temperature decay for samples incorporating TBB-containing resins was significantly slower than the initiator-free formulation (Figure 12). This variation in temperature decay rates is highlighted in Figure 13 and Table 2, where the rate at which the penetration site temperature after bullet impact returns to ambient is markedly slower as the TBB concentration is raised. These results are readily explained by considering the oxygen-mediated, thiol–ene exothermic polymerization; upon contact with air, the TBB initiator immediately reacts with atmospheric oxygen to generate radical species that initiate the thiol–ene polymerization, releasing heat and causing the temperature to remain higher for longer when compared with TBB-free and

air-gap control panels. In the absence of TBB, no polymerization reaction, and thus no exotherm, occurred upon bullet penetration, confirming that the kinetic energy deposited by the bullet in the sample was insufficient to induce polymerization and that the presence of both oxygen and TBB are necessary to initiate the reaction. Interestingly, the air-gap samples cooled more slowly than the TBB-free, resin-filled samples; this may be attributable to the lower thermal conductivity of air compared with the liquid resin, such that the air-filled samples are more thermally insulated than those filled with liquid.

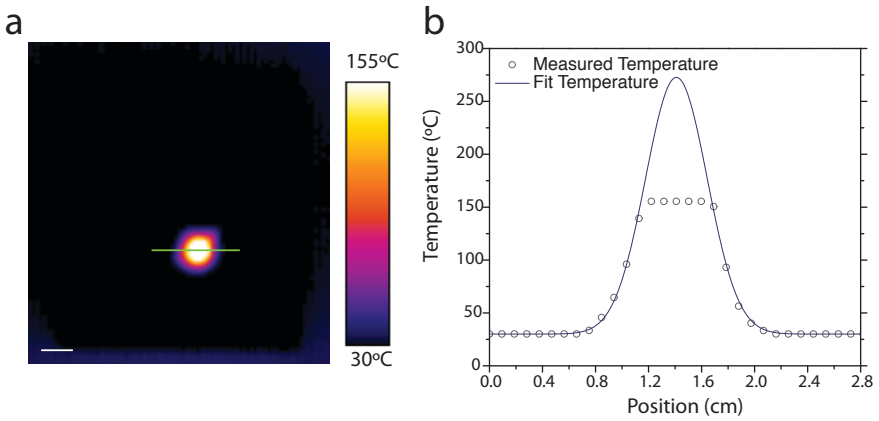

Figure 11: Estimating maximum temperature of hot spot by using Gaussian fitting of thermal IR data. a) As the thermal IR camera exclusively measures over a pre-determined temperature range (30 – 155°C, scale = 1 cm), Gaussian data fitting is used to estimate the actual maximum temperature across a slice, shown as a green line, centered on the hot spot. b) The measured temperatures are shown as circles and the fitted Gaussian as a line.

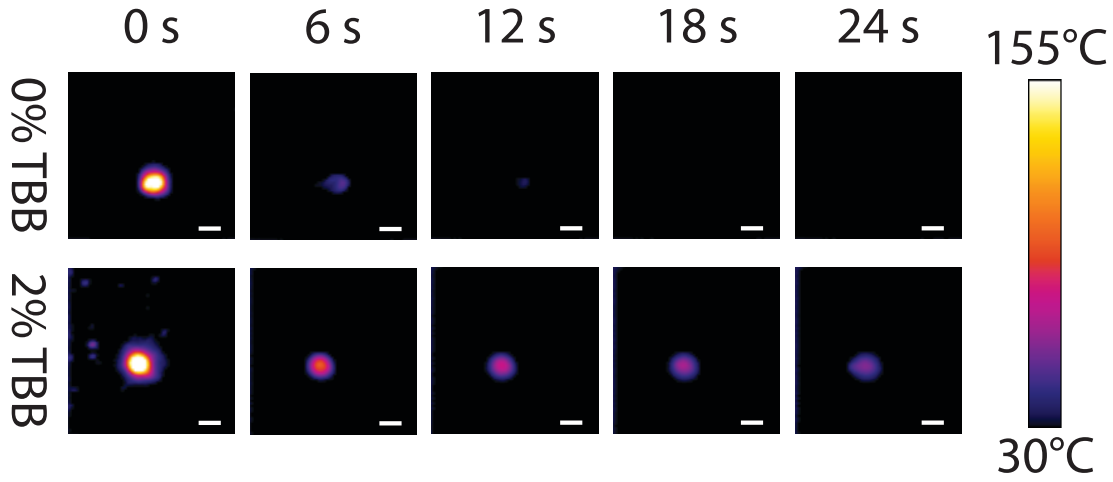

Figure 12: Thermographic image series for EGDMP-TMPTAE resin-filled test panels containing 0 (top) and 2 wt% (bottom) TBB after bullet puncture at t = 0 s (scale = 1 cm).

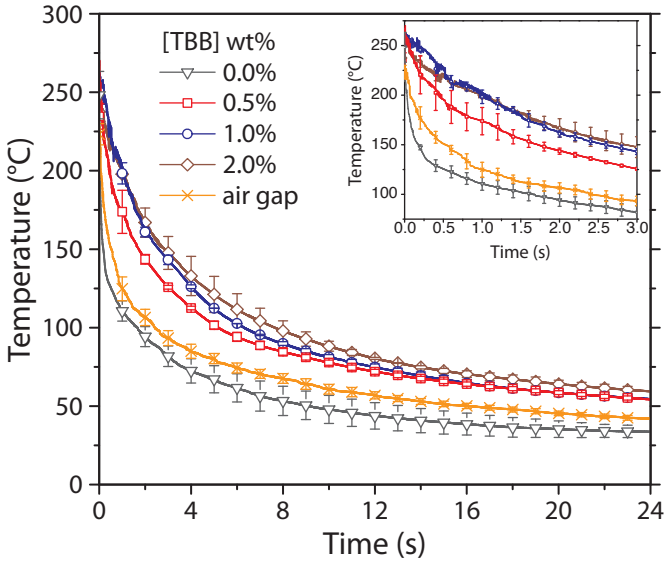

Figure 13: Maximum temperature at puncture site versus time for EGDMP-TMPTAE resin-filled test panels containing varying TBB concentrations and an unfilled test panel. Temperatures above 155°C, outside the range of the thermal IR camera, were estimated by Gaussian fits to the temperature profiles within the camera temperature range.

Table 2: Time for temperature decay to 75°C and 125°C after ballistics puncture, determined using the data reported in Figure 13.

Experiment number	Tributylborane (wt%)	$t_{125°C}$ (s)	$t_{75°C}$ (s)
1	0%	0.5	3.6
2	0.5%	3.1	10.8
3	1.0%	4.1	11.9
4	2.0%	4.7	13.9
5	Air gap	1.0	5.9

2.4 Conclusion

The rapid reaction rates achievable by thiol–ene-alkylborane formulations, as evidenced by FTIR spectroscopy, high-speed videography, and thermography, demonstrate the potential for an environmentally-borne reaction initiation stimulus to be utilized for self-healing applications. Although the model system described here was constructed from both structural (PBG) and non-structural (EMAA and the resin itself) components, further application-oriented development of this concept would afford load-bearing walls capable of autonomous healing after multiple projectile penetration events, preserving the atmosphere inside pressurized vessels such as manned spacecraft.

2.5 References:

1. White, S. R.; Sottos, N. R.; Geubelle, P. H.; Moore, J. S.; Kessler, M. R.; Sriram, S. R.; Brown, E. N.; Viswanathan, S., Autonomic healing of polymer composites. *Nature* **2001,** *409* (6822), 794-797.
2. Wool, R. P., Self-healing materials: a review. *Soft Matter* **2008,** *4* (3), 400-418.
3. Toohey, K. S.; Sottos, N. R.; Lewis, J. A.; Moore, J. S.; White, S. R., Self-healing materials with microvascular networks. *Nat. Mater.* **2007,** *6* (8), 581-585.
4. Dry, C., Procedures developed for self-repair of polymer matrix composite materials. *Compos. Struct.* **1996,** *35* (3), 263-269.
5. Pang, J. W. C.; Bond, I. P., A hollow fibre reinforced polymer composite encompassing self-healing and enhanced damage visibility. *Compos. Sci. Technol.* **2005,** *65* (11-12), 1791-1799.
6. Pang, J. W. C.; Bond, I. P., 'Bleeding composites' - damage detection and self-repair using a biomimetic approach. *Compos. Part a-Appl. S.* **2005,** *36* (2), 183-188.
7. Kalista, S. J., Self-healing of poly(ethylene-co-methacrylic acid) copolymers following projectile puncture. *Mech. Adv. Mater. Struc.* **2007,** *14* (5), 391-397.

8. Varley, R. J.; van der Zwaag, S., Towards an understanding of thermally activated self-healing of an ionomer system during ballistic penetration. *Acta. Mater.* **2008,** *56* (19), 5737-5750.
9. Gordon, K.; Penner, R.; Bogert, P.; Yost, W. T.; Siochi, E., Puncture self-healing polymers for aerospace applications. *Abstr. Pap. Am. Chem. Soc.* **2011,** *242*.
10. Brandon, E. J.; Vozoff, M.; Kolawa, E. A.; Studor, G. F.; Lyons, F.; Keller, M. W.; Beiermann, B.; White, S. R.; Sottos, N. R.; Curry, M. A.; Banks, D. L.; Brocato, R.; Zhou, L. S.; Jung, S. Y.; Jackson, T. N.; Champaigne, K., Structural health management technologies for inflatable/deployable structures: Integrating sensing and self-healing. *Acta Astronaut.* **2011,** *68* (7-8), 883-903.
11. White, S. R.; Moore, J. S.; Sottos, N. R.; Krull, B. P.; Cruz, W. A. S.; Gergely, R. C. R., Restoration of Large Damage Volumes in Polymers. *Science* **2014,** *344* (6184), 620-623.
12. Vauthier, C.; Dubernet, C.; Fattal, E.; Pinto-Alphandary, H.; Couvreur, P., Poly(alkylcyanoacrylates) as biodegradable materials for biomedical applications. *Adv. Drug Deliv. Rev.* **2003,** *55* (4), 519-548.
13. Mankidy, P. J.; Ramakrishnan, R. B.; Foley, H. C., Facile catalytic growth of cyanoacrylate nanofibers. *Chem. Commun.* **2006,** (10), 1139-1141.
14. Lewis, L. A.; Smithwick, R. W.; Devault, G. L.; Bolinger, B.; Lewis, S. A., Processes involved in the development of latent fingerprints using the cyanoacrylate fuming method. *J. Forensic. Sci.* **2001,** *46* (2), 241-246.
15. Liu, S. J.; Zheng, Z.; Li, M. R.; Wang, X. L., Study of the radical chemistry promoted by tributylborane. *Res. Chem. Intermediat.* **2012,** *38* (8), 1893-1907.
16. Ollivier, C.; Renaud, P., Organoboranes as a source of radicals. *Chem. Rev.* **2001,** *101* (11), 3415-3434.
17. Zhang, Z. C.; Chung, T. C. M., Reaction mechanism of borane/oxygen radical initiators during the polymerization of fluoromonomers. *Macromolecules* **2006,** *39* (16), 5187-5189.
18. Brindley, P. B.; Pearson, R. G., Free-Radical Polymerization of Methyl Methacrylate in Presence of Trialkylboranes. *J. Polym. Sci. Pol. Lett.* **1968,** *6* (12), 831-835.
19. O'Brien, A. K.; Bowman, C. N., Impact of oxygen on photopolymerization kinetics and polymer structure. *Macromolecules* **2006,** *39* (7), 2501-2506.
20. Cramer, N. B.; Scott, J. P.; Bowman, C. N., Photopolymerizations of thiol-ene polymers without photoinitiators. *Macromolecules* **2002,** *35* (14), 5361-5365.
21. Hoyle, C. E.; Bowman, C. N., Thiol-Ene Click Chemistry. *Angew. Chem. Int. Ed.* **2010,** *49* (9), 1540-1573.
22. Ichinose, Y.; Wakamatsu, K.; Nozaki, K.; Birbaum, J.-L.; Oshima, K.; Utimoto, K., Et3B induced radical addition of thiols to acetylenes. *Chem. Lett.* **1987,** (8), 1647-1650.
23. Masuda, Y.; Hoshi, M.; Nunokawa, Y.; Arase, A., A Remarkably Efficient Initiation by 9-Bbn in the Radical-Addition Reactions of Alkanethiols to Alk-1-Enes. *J. Chem. Soc. Chem. Comm.* **1991,** (20), 1444-1445.
24. Pallela, V. R.; Mallireddigari, M. R.; Cosenza, S. C.; Akula, B.; Subbaiah, D. R. C. V.; Reddy, E. P.; Reddy, M. V. R., Hydrothiolation of benzyl mercaptan to arylacetylene: application to the synthesis of (E) and (Z)-isomers of ON 01910 center dot Na (Rigosertib (R)), a phase III clinical stage anti-cancer agent. *Org. Biomol. Chem.* **2013,** *11* (12), 1964-1977.
25. Sato, A.; Yorimitsu, H.; Oshima, K., Regio- and Stereoselective Radical Additions of Thiols to Ynamides. *Synlett* **2009,** (1), 28-31.
26. Scott, T. F.; Kloxin, C. J.; Draughon, R. B.; Bowman, C. N., Nonclassical dependence of polymerization rate on initiation rate observed in thiol-ene photopolymerizations. *Macromolecules* **2008,** *41* (9), 2987-2989.
27. Westad, F.; Schmidt, A.; Kermit, M., Incorporating chemical band-assignment in near infrared spectroscopy regression models. *J. Near Infrared Spectrosc.* **2008,** *16* (3), 265-273.

28. Hourant, P.; Baeten, V.; Morales, M. T.; Meurens, M.; Aparicio, R., Oil and fat classification by selected bands of near-infrared spectroscopy. *Appl. Spectrosc.* **2000,** *54* (8), 1168-1174.
29. Miller, D. R.; Macosko, C. W., New Derivation of Post Gel Properties of Network Polymers. *Macromolecules* **1976,** *9* (2), 206-211.
30. Zavada, S. R.; McHardy, N. R.; Gordon, K. L.; Scott, T. F., Rapid, Puncture-Initiated Healing via Oxygen-Mediated Polymerization. *ACS Macro Lett.* **2015,** *4* (8), 819-824.
31. Chiou, B. S.; Khan, S. A., Real-time FTIR and in situ rheological studies on the UV curing kinetics of thiol-ene polymers. *Macromolecules* **1997,** *30* (23), 7322-7328.

Chapter 3

Pressure Gradient Ballistics Test Method for Evaluating Puncture-Initiated Healing

Abstract: In order to develop self-healing materials suitable for micrometeoroid-puncture mitigation in lunar or Martian environments, ballistic test methods are required that simulate vacuum or near-vacuum environments. Here, a ballistics test method that applies a pressure differential between the front and back of a test panel has been developed and was demonstrated to be a much more stringent puncture-healing test than previously-utilized methods that kept both sides of a test panel at atmospheric pressure. This new pressure gradient ballistics test method convincingly demonstrated the reactive monomer formulations, based on thiol–ene chemistry, containing both the alkylborane initiator and glass fiber performed significantly better than those without either; this is especially important as the previously-utilized atmospheric pressure ballistics test did not distinguish between reactive formulations that either contained or omitted glass fiber. While the thiol–ene/alkylborane/glass fiber formulation performed significantly better than those without either the alkylborane initiator or glass fiber, it only partially-sealed the puncture-induced hole owing to excessive loss of resin before it became sufficiently cross-linked to resist extrusion out toward the vacuum. Nonetheless, despite the lack of complete puncture sealing, the results here are highly encouraging and provide further evidence that oxygen-mediated polymerization is a feasible self-healing mechanism.

3.1 Introduction

As previously demonstrated (see Chapter 2), reactive liquid formulations made of thiol and allyl ether monomers with the initiator tributylborane were shown to exhibit extraordinarily fast reaction rates immediately on exposure to atmospheric oxygen, forming solid polymer within seconds. While these results are encouraging and represent an important step in developing multilayered structures capable of autonomously-healing high velocity projectile-induced punctures, a tremendous amount of work remains before such a material could be incorporated with the walls of a space exploration habitat, spacecraft, or spacesuit. The requirements for a self-healing structure capable of being incorporated into the walls of a habitat are extraordinarily demanding as they must properly function when punctured under incredibly broad range of projectile types, sizes, velocities, or impact angles. (In addition to other requirements like long-term stability.) The composition of these reactive liquids will likely need to be far more sophisticated than the thiol/allyl ether/alkylborane formulations previously utilized and may need to contain fillers to both modify the properties of either the liquid and the resulting polymer. Furthermore, any material proposed as a viable self healing-structure must be subjected to thorough and intense testing that mimics as closely as possible the conditions present in space travel. Indeed, while ballistics testing has been commonly used to evaluate self-healing capabilities in response to sudden puncture, all of the testing on polymeric materials has been performed at atmospheric pressure with no gradient across the test panel.

Most of the ballistics testing on self-healing materials has investigated the healing properties of EMAA. The earliest work on EMAA as a self-healing materials appears in a Master's Thesis by Fall utilized a handgun to fire 9 mm bullets, with a velocity of 360 m/s, at test panels at ambient pressure and temperature.[1] Later work by Kalista followed a similar procedure with projectile fired from a pellet gun at 200 m/s.[2, 3] By using ovens or refrigeration units, Kalista able to evaluate healing at temperatures ranging from -30°C to 90 °C. While the test samples are subjected to a pressure differential after ballistics impact, to demonstrate that the material has completely sealed, the ballistics test themselves are performed with the test panel at ambient pressure. Nearly all of the ballistics testing on EMAA has utilized similar protocols: while the bullet type/shape and the velocity was varied, all have been performed at ambient pressure and most used ambient temperature. (see Table 3 for a summary).

Table 3: Summary of literature describing ballistics test methods for self-healing materials.

Year and Author	Velocity	*Projectile*	*Temperature*	*Material Tested*
2001 Fall[1]	370 m/s	RT	Ambient	EMAA
2007 Kalista[2]	200 m/s	4.5 mm pellet	-30,-10,10, RT, 60, 70, 80, 90 C	EMAA
2008 Varley[4]	340 m/s or 790 m/s	5 or 9 mm round nose; 7.62 mm pointed	RT	EMAA
2011 Siochi[5]	1000 m/s	5.56 mm pointed bullet	15 and 50 C	EMAA,PBG
2011 Penco and di Landro[6]	370 m/s or 700 m/s	4.65 mm bullets	RT	EMAA + epoxidized rubber
2012 Penco and di Landro[7]	700 m/s	4.65 mm bullets	RT	EMAA + epoxidized rubber
2012 Haase[8]	420, 630, 690, or 6000 m/s	3 or 5 mm steel sphere	RT	EMAA
2013 Sundaresan[9]	220 m/s	4.5 mm pellet	RT	EMAA

As should be obvious from Table 3, and also pointed out by Brandon and Coworkers,[10] most self-healing has been performed under ambient temperature and pressure – that is, "terrestrial conditions". While performing ballistics experiments at these conditions is convenient, it is not representative of lunar or Martian conditions. For example, the velocity of micrometeoroids is far greater than those listed in Table 3 with the exception of work by Haase and coworkers,[8] all ballistics experiments used velocities of less than 1000 m/s. The work by Hasse, using a two-stage gun, did perform ballistic experiments on EMAA panels at approximately 6000 m/s, significantly higher than all other reports, though still less than micrometeoroid velocity (approximately 30,000 to 70,000 m/s).[11] Haase found that EMAA, which exhibits startlingly good self-healing behavior at lower velocities, completely fails to heal at 6000 m/s, casting doubt on its suitability as a lone self-healing mechanism. Such results clearly demonstrate the importance of utilizing test methods that mimic the actual conditions encountered in space exploration. Of course, it is easy to comprehend why such unrealistic test methods have been so commonly utilized; the lower velocities are commonly utilized as access to pellet guns or even rifles is far easier than access to sophisticated, and expensive, ballistics facilities. While the ballistic testing procedure, utilized to stimulate MMOD puncture, described in the previous chapter was of great utility in demonstrating the rapid reaction times of the reactive formulations, the conditions used in this test do not represent those that would be experienced during a lunar or Martian mission. The most serious limitation was the lack of a pressure differential between the front and back side of the test panel; everything was run under atmospheric pressure. Obviously, such

conditions are not representative of surface conditions on the moon, which is essentially a vacuum, or Mars, which has an average atmospheric pressure of 0.006 atm (e.g., 0.6% of earth's). Pressure differential would be a major concern for any system that relies on a reactive liquid as there is an obvious concern that the liquid could spray out before it has an opportunity to polymerize.

Therefore, in order better simulate lunar or Martian conditions, high-velocity projectile ballistics testing was performed with a pressure differential between the front and back side of the panel; this method is compared with the one used previously, where there is no pressure gradient. Moreover, to investigate the influence of fillers on healing properties, glass fiber mat will be used a model filler and the self-healing behavior of both filled and non-filled formulations will be evaluated. It was hoped that the addition of the glass fiber would function as a scaffold and would assist in preventing the liquid monomer formulation from rapid ejection after ballistics puncture.

3.2 Experimental

3.2.1 Materials

Ethylene glycol dimercaptopropionate (EGDMP) was donated by Evans Chemetics and was distilled prior to use. Tributylborane (TBB) was purchased from Sigma-Aldrich was used as received. Trimethylolpropane triallyl ether (TMPTAE) was synthesized using the method describe in chapter 2. EGDMP and TMPTAE were thoroughly degassed prior to use by a freeze-pump-that process.[12] N-Nitrosophenylhydroxylamine aluminum salt, a radical inhibitor, was purchased from Wako Chemicals and used as received. Glass fiber mat, 0.25 mm thick with a mass of 3.7 grams/ft^2 (product 260-H), was purchased from Fibre Glast. The 1 mm poly(butadiene)-graft-poly(methyl acrylate-co-acrylonitrile)

(PBG – Barex 210 IG from Ineos) and partially neutralized poly(ethylene co- methacrylic acid) (EMAA – Surlyn 8940 from DuPont) panels were provided by the NASA Langley Research Center.

3.2.2 Assembly of Tri-layered Sample Panels

Utilized a method similar to the one described previously,[12] sample panels were assembled by sandwiching a 1 mm thick silicone rubber shim between the edges of a 1 mm thick sheets of PBG and EMAA. The cavity of the sample panel was either kept empty or filled with three sheets, totaling 0.75 mm, or glass fiber mat(see Scheme 25). The edges of this structure were sealed with a two-component epoxy adhesive, leaving a small hole for the injection of the reactive liquid resins. In an anaerobic chamber (less than 10 ppm O_2), the reactive monomer formulations, consisting of EGDMP and TMPTAE in a 1:1 thiol:ene stoichiometric ratio, 2 wt% tributylborane, and 0.1 wt% inhibitor, were injected to fill the empty space in the middle of the sample panels, after which the injection hole was sealed with additional epoxy adhesive.

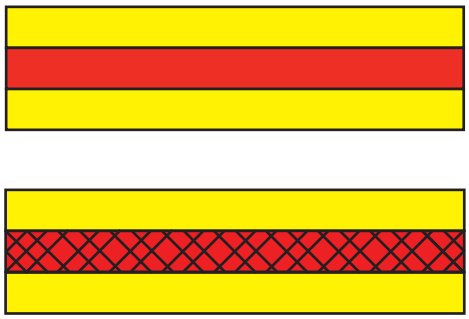

Scheme 25: Construction of tri-layered panels. Monomer formulations were sandwiched between two solid polymer support panels.

3.2.3 Ballistics Testing

Ballistics testing was performed in a ballistics testing facility located at the NASA Glenn Research Center. The tri-layered test panels were placed in a pressurizable aluminum sample holder where the panels form part of the front face of the pressure vessel; the PBG panel is the side that is facing outward, making it the side the will be initially puncture by the projectile. Once the sample is in place, the pressure vessel is sealed and the pressure, controllable by an attached air hose, was kept at 1 atm with the gas composition inside equivalent to air (e.g., 79% nitrogen and 21% oxygen). This pressurized sample holder sits within a much larger vacuum chamber that is connected to a 20 foot long steel pipe with a 2 inch inside diameter – this pipe serves as a very long gun barrel. The other end of this pipe can be connected to a metal pressure vessel that can hold very high pressure (approximately 26 atm). A polyester gasket is used to allow pressure to build in the vessel; this gasket has a wire attached to it that, after running current through it, will break and permit the projectile to be launched. All projectiles utilized in this series of experiments were 1/8 inch diameter ball bearings. As this diameter is significantly less than the inside diameter of the gun barrel, the projectile must be carried by a sabot. Here, polycarbonate sabots machined to a shaped designed by the Glenn Research Center were utilized – other sabot designs, notably those 3D printed from ABS plastic, would break apart during the shooting process. The sabot, with the ball-bearing placed within a small cavity on the front and held in place my a minimal amount of vacuum grease, is set inside the gun barrel immediately in front of the polyester gasket. Once the sabot-carrying projectile is placed in the gun barrel and the tri-layered sample is placed within the pressurized box, the entire system is sealed and the

pressure in the vacuum chamber is reduced to approximately 0.02 atm. Then, the pressure vessel used to launch the projectile is pressurized with nitrogen gas to a final pressure of 25.8 atm – this pressure greatly influences the projectile velocity. Once the desired pressure is attained, the polyester gasket is broken and the sabot and projectile are launched. To prevent the sabot from reaching the target, a sabot stopper, placed inside the vacuum chamber, redirects the sabot fragments away from the target; a small hole in the center of the stopper permits the projectile to fly through toward the target. As the release of pressure is the mechanism by which the projectile is launched, the pressure inside the vacuum chamber increases to approximately 0.1 atm after the projectile is fired. While this differential across the sample is far less than what a Martian habitat would experience, it is a significant change from the purely atmospheric conditions that were utilized in the previous chapter.

The projectile and sample are monitored with two high-speed video cameras, each capturing images at a rate of 200,000 per second. Once camera views the front of the test panel and is utilized to evaluate the self-healing behavior after impact, while another camera is placed perpendicular to the projectile flight path and is utilized to calculate projectile speed, here found to be approximately 900 m/s.

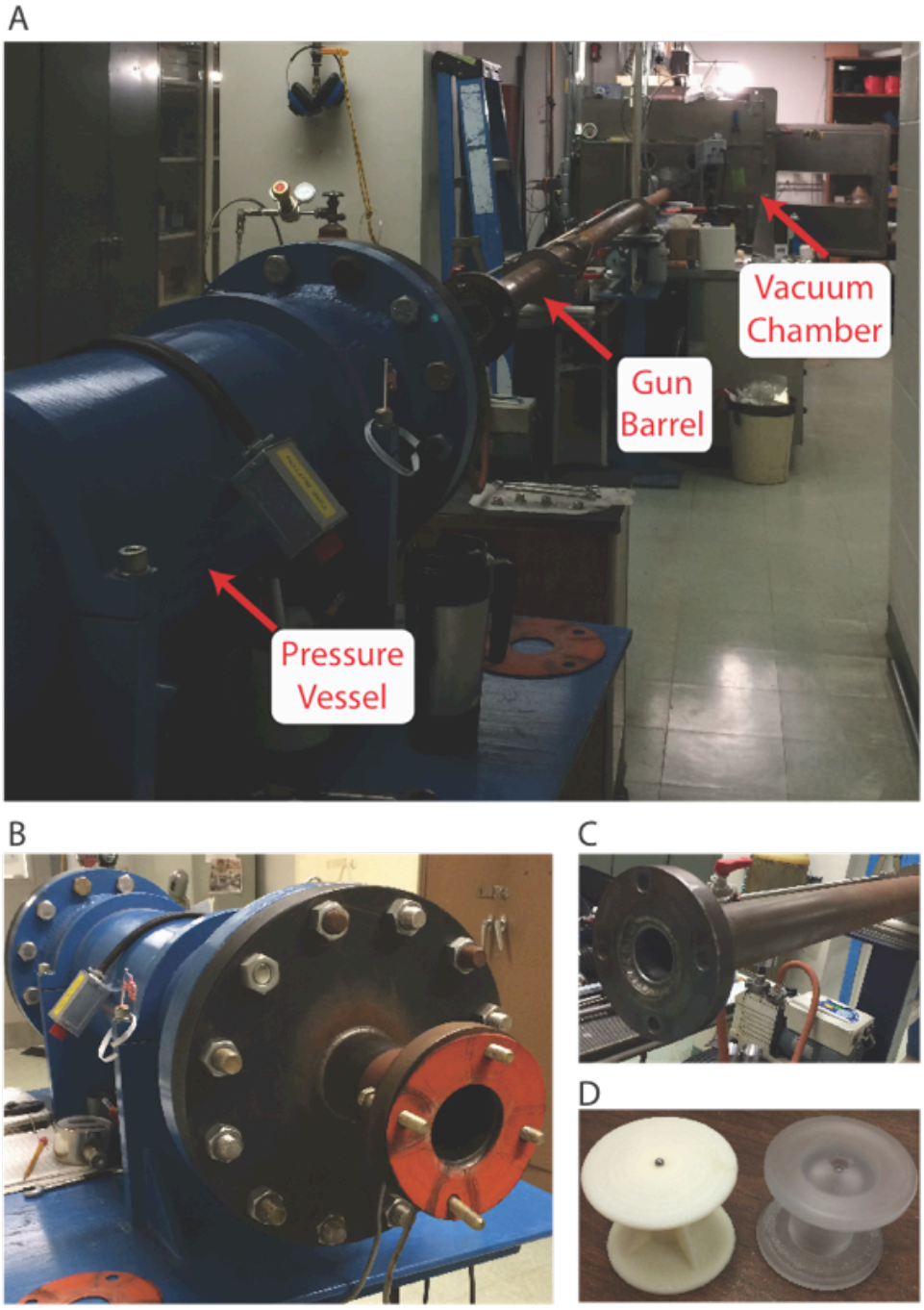

Figure 14: Ballistics test facilicity at the Glenn Research Center in Cleveland, OH. A) Outside view of pressure vessel, gun barrel, and vacumm chamber. Close-up view of the B) pressure vessel and B) gun barrel. D) The steel ball bearings are launched using a sabot. Shown are one made of 3D-printed acrylonitrile-butidiene-styrene (ABS) plastic (left) and machined polycarbonate (right)

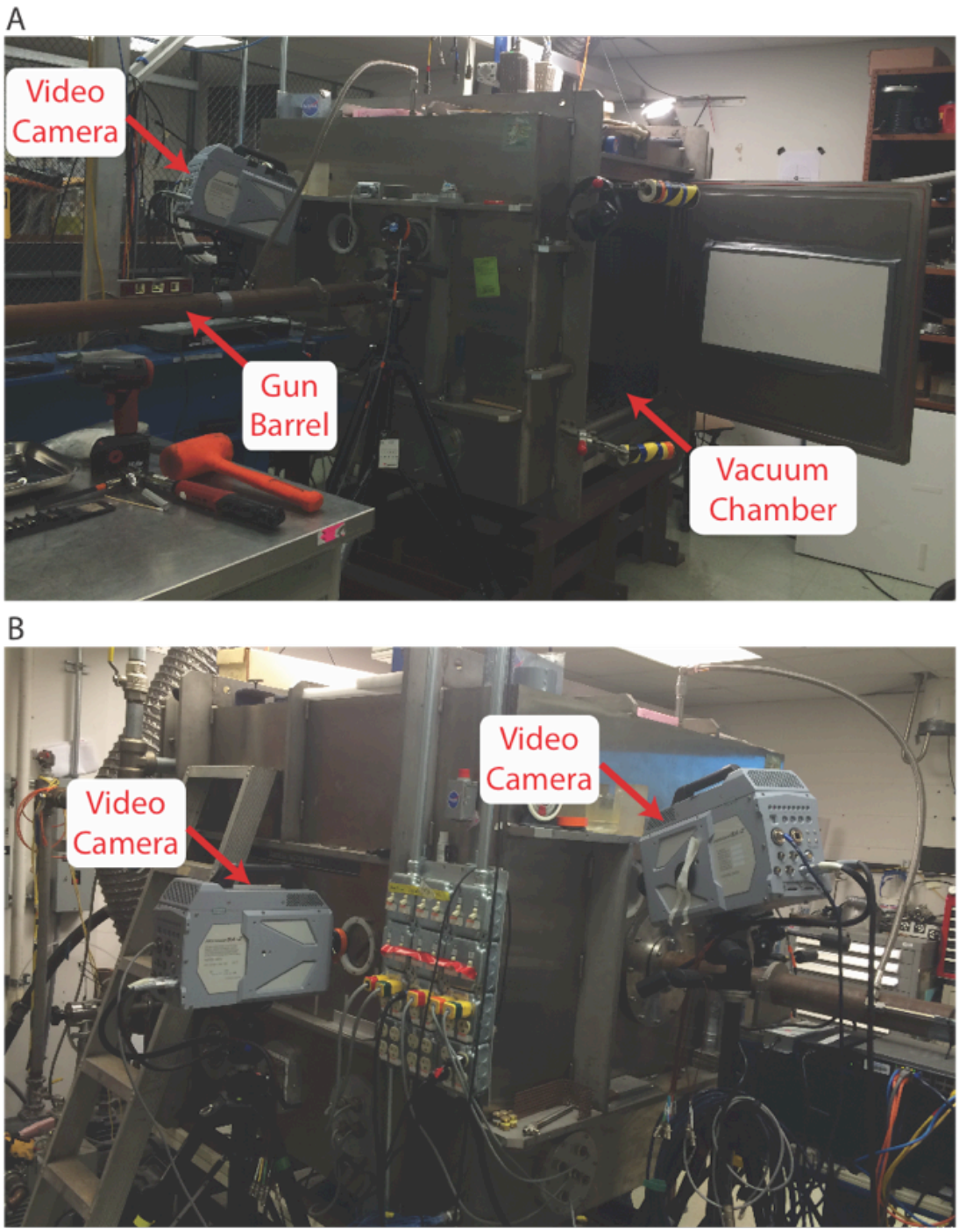

Figure 15: Outside view of the vacuum chamber utilized at the Glenn Research Center ballistics facility. A) Outside view of chamber showing the front side video camera. B) Alternative view of vacuum chamber showing both the front video camera, used to view projectile imopact, and the side camera used to calcualte projectile velocity.

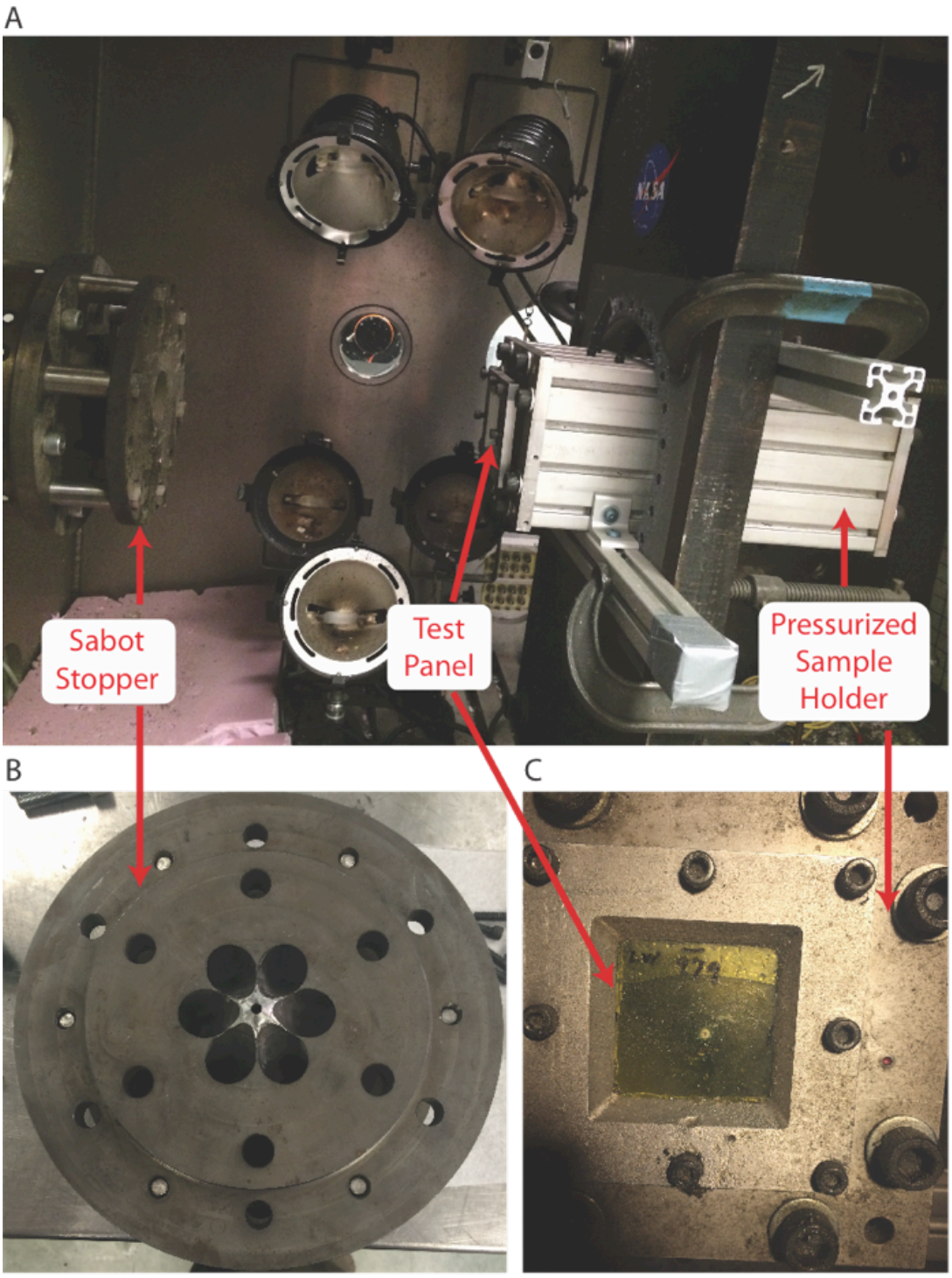

Figure 16: Inside view of the vacuum chamber utilized at the Glenn Research Center ballistics facility. A) The pressurized sample holder holder is fitted with the larger vacuum chamber, allowing for the sample panel to experience a pressure gradient. B) A "sabot stopper" is neccesary to redirect the plastic sabot away from the test panel while allowing the ball bearing projectile to reach its target. C) Close-up of test panel.

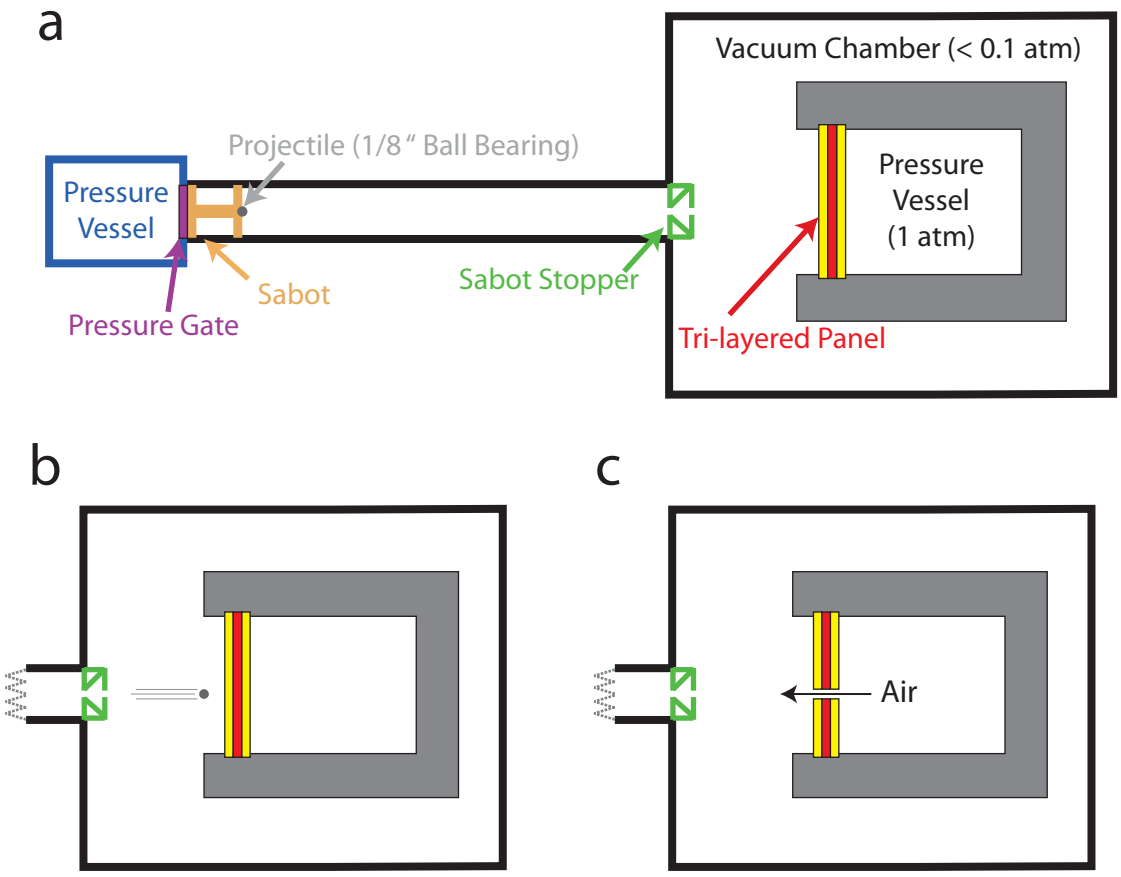

Scheme 26: Illustration of ballistics gun shown in Figure 14, Figure 15, and Figure 16. A) Ballistics gun prior to firing projectile. B) Projectile approaching target. C) After penetration, air rushes from inside the pressure vessel out toward the vacuum chamber.

3.2.4 Vacuum Test

To demonstrate the ability of the reactive liquid monomer formulations to mitigate loss of atmosphere after projectile puncture, a vacuum test (using an enhanced Pirani Pressure Gauge from Kurt J. Lesker Company) was performed. The test panels were allowed to sit undisturbed in the presence of air for over a month, allowing all reactive monomer formulations to polymerize. Then, for each tri-layered panel tested, the back-side (i.e., EMAA) panel was carefully removed, leaving the now solidified resin formulation attached to the front-side (i.e., PBG) panel. A vacuum was applied to the puncture site,

via a rubber hose, on the PBG panel and the vacuum attained was recorded. Then, the solidified resin formulation was carefully removed, with particular care taken when removing the solid resin from the puncture site; the vacuum hose was then reapplied to the puncture site and the vacuum attained was measured again.

3.3 Results and Discussion

In the previous chapter, the self-healing capabilities of several tributylborane containing formulations were evaluated via ballistics testing. While the methods employed proved invaluable at differentiating between non-healing and self-healing characteristics, it proved less useful at distinguishing between different self-healing formulations. For example, while all of the monomer formulations with TBB exhibit healing properties, it was difficult to asses how these formulations compared to each other as there was no clear difference in the high-speed video footage, thus making it difficult to evaluate how, say, changing the monomer functionality would have helped or hindered a formulations healing capability. This seems to be an inherent limitation of ballistics tests performed at atmospheric pressure. To further illustrate this limitation, using the same atmospheric pressure ballistics method, the self-healing properties of EGDMP/TMPTAE thiol-ene monomer formulations, with and without 2% TBB and containing glass fiber mat, were compared with the unfilled (i.e., no glass fiber mat) formulations, discussed in the previous chapter. The monomer formulation with glass fiber and no TBB displayed ejecta after ballistics penetration in a manner nearly identical to what was observed in the monomer formulation that contained neither TBB nor glass mat. This was entirely expected as the lack of TBB, or any other initiator, precludes any chance of the liquid monomer formulation from polymerizing; the presence of the glass fiber mat here doesn't

change this. On the other hand, the formulation with both 2% TBB and glass fiber mat did not display any ejecta after ballistics penetration, exactly as the 2% TBB without glass fiber performed;(Figure 17) thus, under atmospheric conditions, the 2% TBB monomer formulations with or without glass fiber will rapidly seal a high-velocity projectile-induced puncture at atmospheric conditions. Herein lies the problem: the addition of glass fiber mat has no apparent influence on the properties of the monomer formulation, something that seems counterintuitive and difficult to accept. Thus, a more stringent test method is needed to better differentiate between different formulations.

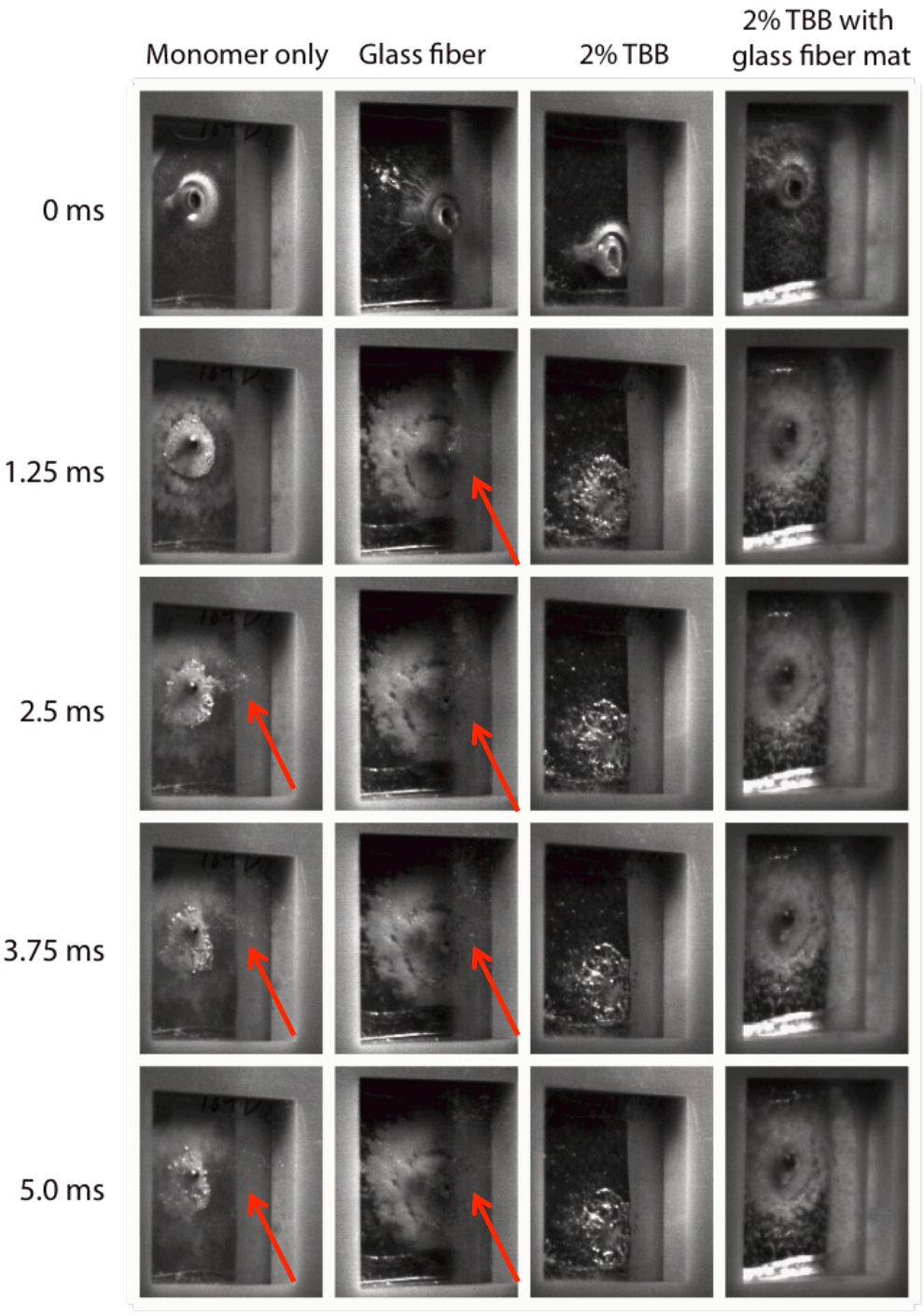

Figure 17: Still photos taken from high-speed videos during ballistics testing at atmospheric pressure. Formulations included, from left to right, monomer only, monomer + glass fiber, monomer + 2% TBB, monomer + 2% TBB + glass fiber. Red arrows assist in identifying liquid ejecta.

As noted above, the primary disadvantage of the ballistics test method is that both sides of the panel are under atmospheric pressure, conditions that do not model those found on the moon or Mars. In an effort to devise a ballistics test method that better matches lunar or Martian conditions, with the hope that it better discerns between different self-healing formulations, a pressurized sample holder was constructed; by placing this pressurized box, with the test panel forming part of the front face, within a larger vacuum chamber, the test panel experiences a pressure differential between the front and back faces. While the pressure differential here is not as high as it would on the moon or Mars, it is significantly greater that what has been attempted previously. Thus, when the test panel is punctured by a high velocity projectile, there will be a sudden rush of air from inside the pressured box out into the vacuum chamber.

Utilizing this new ballistics test method, thiol–ene monomer formulations with and without 2% TBB were evaluated. For the formulation without TBB, a plume of liquid was forcefully ejected through the entrance hole less than a millisecond after projectile impact (see Table 4);(see Figure 18) owing to the pressure differential between the front and back face, the effect here is much more dramatic that what was observed under strictly atmospheric conditions (Figure 17). Whereas before, when the ejecta plume was visible for only approximately 2 ms with both sides of the test panel at atmospheric pressure, under a pressure gradient, ejecta is observed for at least 20 ms; a result that is entirely expected as no polymerization will proceed in the absence of the TBB initiator, causing the monomer formulation to remain a low viscosity liquid that is unable to resist being violently ejected out toward the vacuum. In comparing the results

between the pressure gradient test versus the one at atmospheric pressure, the overall impression is that performing the pressure gradient ballistics test is much harsher than the one performed at the atmospheric pressure. This impression was further strengthened in examining the results for the test panel with 2% TBB added to the thiol–ene monomer formulation. When this test panel was punctured, a plume of liquid was observed less than one millisecond afterwards – results indistinguishable from those observed with the formulations that lacked TBB. Given the success of this formulation under atmospheric pressure,[12] this result was shocking and certainly offers further evidence that the pressure gradient ballistics test is very harsh. Unfortunately, the failure of this formulation under conditions that are nowhere as severe as those on the moon or Mars calls into serious question the viability of using a reaction liquid monomer formulation to seal a puncture-induced hole. After all, the formulation contained TBB and was certainly capable of solidifying rapidly after oxygen exposure (indeed, post-ballistics inspection of the sample showed that it had eventually polymerized); it simply did not solidify fast enough to seal the breach and behaved, during the first 20 ms, as if the TBB was not present. Clearly, in order for a reactive liquid monomer formulation to be of utility in a puncture-healing application, the reactive formulation must be retained near the puncture site until it has a chance to polymerize. Returning to the idea, discussed above, of incorporating glass fiber a filler in the formulation, it was hoped that the glass fiber would aid in retaining the reactive monomer formulation in the vicinity of the puncture site, providing a scaffold that the resin could cling to and giving it opportunity to polymerize. To evaluate the influence of glass fiber on the sealing properties of thiol–ene monomer formulations, test panels, with and without 2% TBB ,were evaluated utilizing the pressure differential

ballistics test. In the absence of TBB, the monomer formulation was rapidly ejected out toward the vacuum less than one millisecond after impact (see Table 4 and Figure 18) in a manner nearly indistinguishable from those without glass fiber; this was entirely expected as the lack of an initiator dictates that lack of any means for the monomer formulation to solidify. Far more interesting was the result when the monomer formulation contained both glass fiber and 2% TBB. For this formulation, there was no sign of ejecta until 6.68 ms after puncture, nearly an order of magnitude longer than all of the other samples evaluated with the pressure gradient ballistics test. (see Table 4 and Figure 18) This suppression of rapid monomer ejection, apparently effected by the glass fiber acting as a scaffold, appears to provide sufficient time for the monomer formulation to at least partially polymerize before it succumbs to the pressure differential and starts to be ejected outward. The ejecta for this formulation looks as if it is slowly being extruded through the entrance hole and is quite different in appearance than the others where the monomer formulation was violently sprayed outward; this difference in appearance provides further evidence that substantial polymerization takes place within 7 ms after ballistic penetration and subsequent oxygen exposure. While an ideal sample would show no ejecta, this formulation is obviously a vast improvement over all of the others evaluated with the pressure gradient ballistics test method; evidently, including both TBB and the glass fiber mat in the monomer formulation lead to a material with significantly-

improved puncture-healing properties.

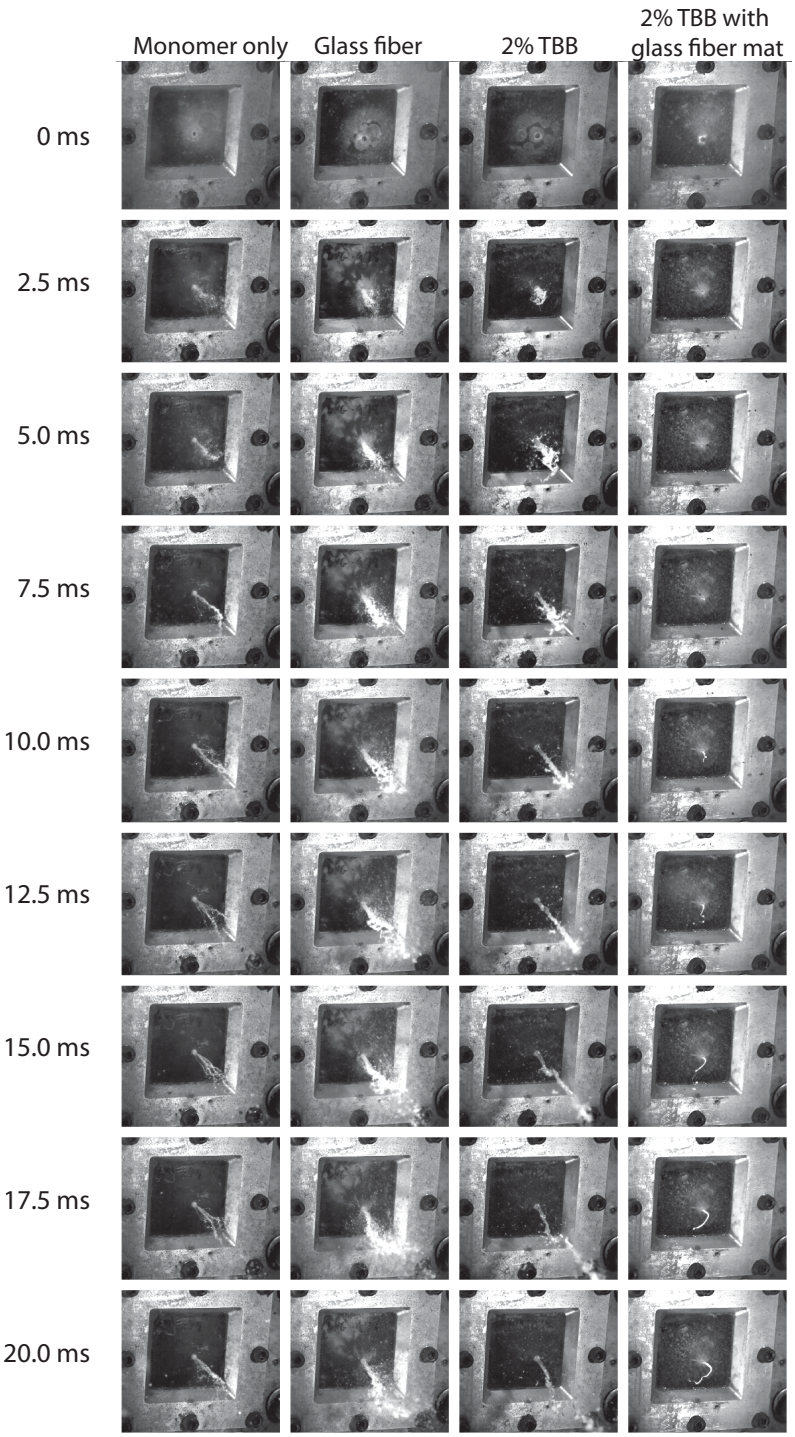

Figure 18: Still photos taken from high-speed videos during ballistics under a pressure gradient. Formulations included, from left to right, monomer only, monomer + glass fiber, monomer + 2% TBB, monomer + 2% TBB + glass fiber.

Table 4: Elapsed time after projectile impact for liquid ejecta to be visible.

	No tributylborane	2% tributylborane
No glass fiber	0.54 ms	0.78 ms
Contains glass fiber	0.76 ms	6.68 ms

To ascertain whether the thiol–ene/TBB/glass fiber resin sealed the puncture-induced hole, a post-ballistics vacuum test was performed. The panel was left to sit for over a month to allow the reactive monomer formulation to fully polymerize and, upon complete solidification of the resin, the back EMAA panel was removed. (see Figure 19 a and b for photos) After applying the vacuum hose to the puncture site (see Figure 20), the vacuum gauge read 4.0 torr, a value far greater than the 0.23 torr observed previously for a completely sealed sample,[12] confirming that the thiol–ene/TBB/glass fiber resin did not completely seal the puncture-induced entrance hole. Yet, despite the disappointment, this demonstration clearly shows the entrance hole was partially sealed; when the thiol–ene/TBB/glass fiber resin was carefully removed from the sample, clearly revealing a 2 mm entrance hole (see Figure 19c for photo), and the vacuum test applied to the sample, the vacuum gauge measured 270 torr, significantly greater than when the thiol–ene/TBB/glass fiber resin was present.

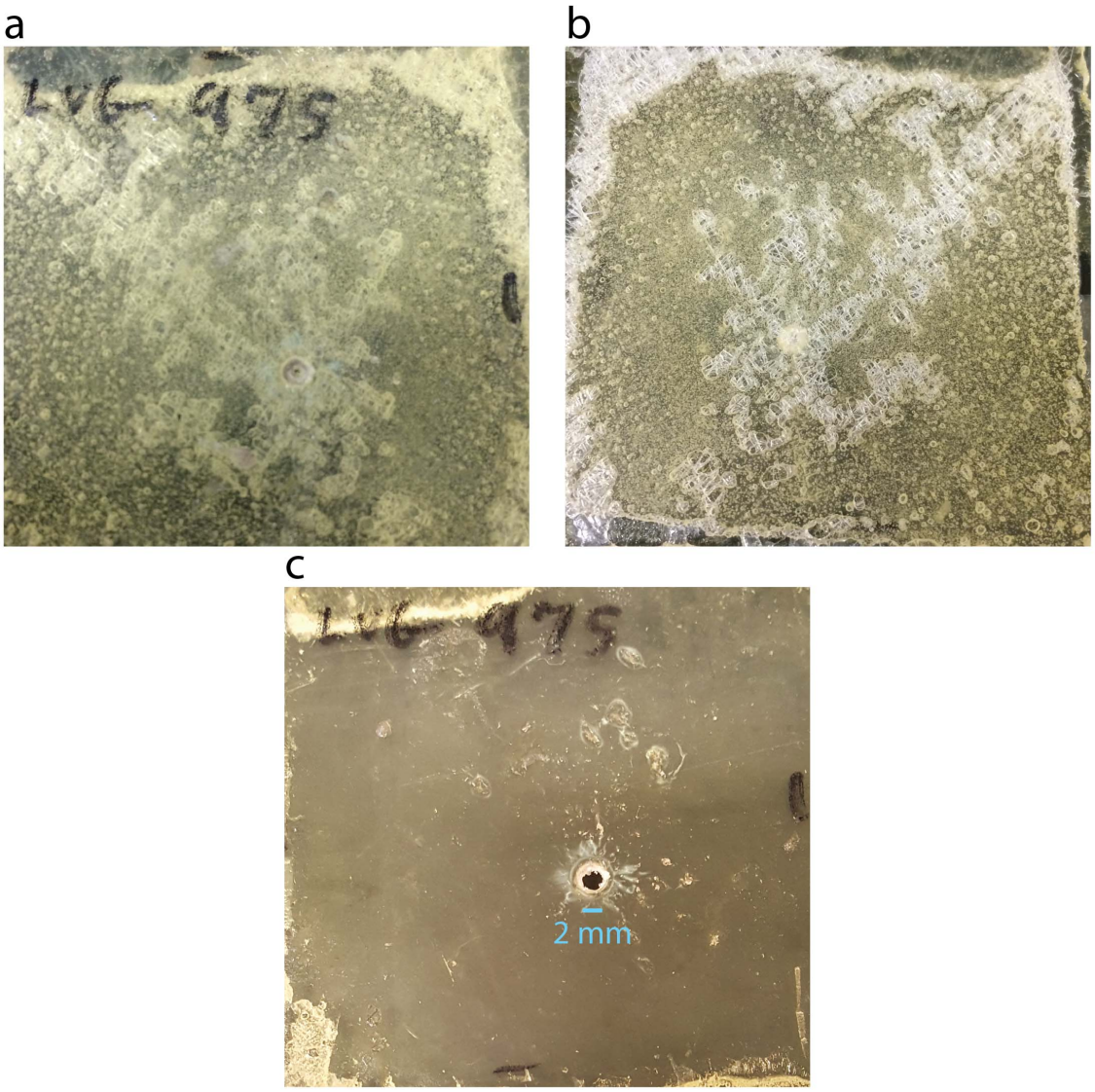

Figure 19: Post-ballistics photographs of test panel made from monomers, 2% TBB, and glassfiber mat. A) Front view. B) Rear view with back (EMAA) panel removed. C) Front view with cured resin removed from puncture site.

In order to gain additional insight into how the thiol–ene/TBB/glass fiber formulation behaves during ballistic puncture, photos were taken of the test panel. The front and rear photos (taken with the back EMAA panel removed) clearly show solid resin at the puncture site, something made even more obvious when these photos are compared with one where the thiol–ene/TBB/glass fiber resin was removed, allowing the

entrance hole, measuring 2 mm in diameter, to be easily observed. The photos convincingly demonstrate that it is the retention of a substantial quantity of solid polymer, with the glass fiber acting as a scaffold, that lead to the partially filling of the entrance hole. Conversely, these photos also show substantial quantities of air gaps present throughout the glass mat, particularly in the region centered on the puncture site, clarifying why the entrance hole did not completely seal. As shown in the images from the high speed video (Figure 18), a significant amount of material was extruded out through the entrance hole; while considerably less material was lost than in the other samples (i.e., those the lacked TBB or glass fiber), the amount absent was enough to permit for holes to form and prevent complete sealing of the puncture.

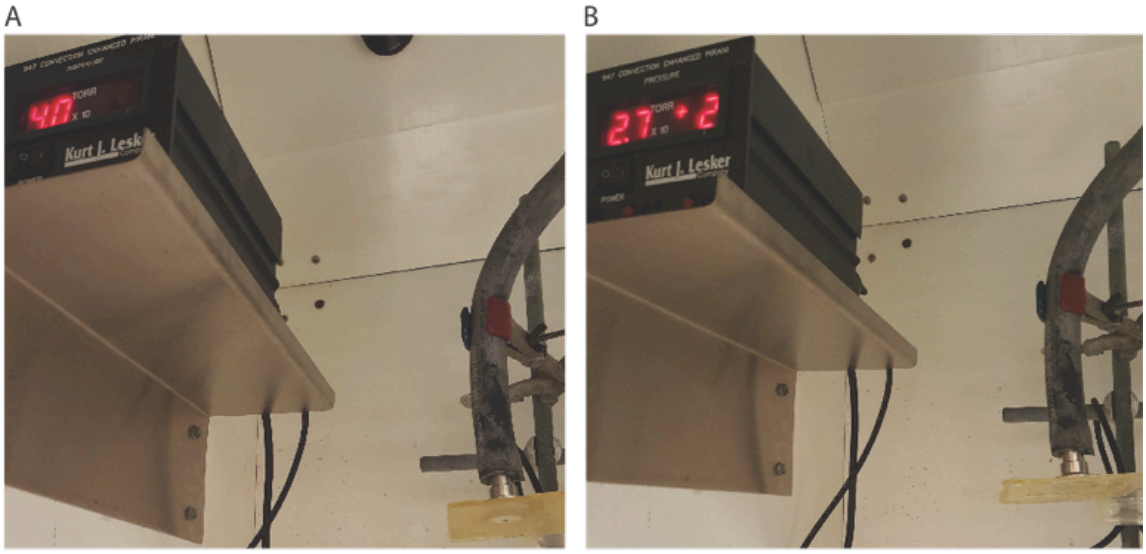

Figure 20: Vacuum applied to entrance-side puncture site of this test panel with the EMAA layer removed. A) With the polymerized resin and glass fiber in place. B) after removal of the polymerized resin and glass fiber.

3.4 Conclusion

A ballistics test method, utilizing projectiles with a velocity of 900 m/s, that applies a pressure differential between the front and back of a test panel has been demonstrated to be a much more stringent puncture-healing test than when both side are under atmospheric pressure. This new pressure gradient ballistics test method convincingly demonstrated the reactive monomer formulations containing both the TBB initiator and glass fiber performed significantly better than those without either; this is especially important as the previously-utilized atmospheric pressure ballistics test did not distinguish between reactive formulations (i.e., those with 2% TBB) that either contained or omitted glass fiber. While the thiol–ene/TBB/glass fiber formulation performed significantly better than those without either TBB or glass fiber, it only partially-sealed the puncture-induced hole owing to excessive loss of resin before it became sufficiently cross-linked to resist extrusion out toward the vacuum. Nonetheless, despite the lack of complete puncture sealing, the results here are highly encouraging and they suggest that, with further refinements to the reactive liquid monomer formulations, it is feasible to use oxygen-mediated polymerization as a self-healing mechanism.

3.5 References:

1. Fall, R. A., Puncture Reversal of Polyethylene Ionomers-Mechanistic Studies. **2001**.
2. Kalista, S. J., Self-healing of poly(ethylene-co-methacrylic acid) copolymers following projectile puncture. *Mech. Adv. Mater. Struc.* **2007,** *14* (5), 391-397.
3. Kalista, S. J.; Ward, T. C., Thermal characteristics of the self-healing response in poly (ethylene-co-methacrylic acid) copolymers. *J. R. Soc. Interface* **2007,** *4* (13), 405-411.
4. Varley, R. J.; van der Zwaag, S., Towards an understanding of thermally activated self-healing of an ionomer system during ballistic penetration. *Acta. Mater.* **2008,** *56* (19), 5737-5750.
5. Gordon, K.; Penner, R.; Bogert, P.; Yost, W. T.; Siochi, E., Puncture self-healing polymers for aerospace applications. *Abstr. Pap. Am. Chem. Soc.* **2011,** *242*.

6. Rahman, M. A.; Penco, M.; Peroni, I.; Ramorino, G.; Grande, A. M.; Di Landro, L., Self-Repairing Systems Based on Ionomers and Epoxidized Natural Rubber Blends. *ACS Appl. Mater. Interfaces* **2011,** *3* (12), 4865-4874.
7. Rahman, M. A.; Penco, M.; Peroni, I.; Ramorino, G.; Janszen, G.; Di Landro, L., Autonomous healing materials based on epoxidized natural rubber and ethylene methacrylic acid ionomers. *Smart Mater. Struct.* **2012,** *21* (3).
8. Haase, T.; Rohr, I.; Thoma, K., The self-healing of an ionomer at projectile velocities from quasi-static to hypervelocity impact. *RCMA* **2012,** *22* (1), 67-76.
9. Sundaresan, V. B.; Morgan, A.; Castellucci, M., Self-Healing of Ionomeric Polymers with Carbon Fibers from Medium-Velocity Impact and Resistive Heating. *Smart Mater. Res.* **2013,** *2013*, 12.
10. Brandon, E. J.; Vozoff, M.; Kolawa, E. A.; Studor, G. F.; Lyons, F.; Keller, M. W.; Beiermann, B.; White, S. R.; Sottos, N. R.; Curry, M. A.; Banks, D. L.; Brocato, R.; Zhou, L. S.; Jung, S. Y.; Jackson, T. N.; Champaigne, K., Structural health management technologies for inflatable/deployable structures: Integrating sensing and self-healing. *Acta Astronaut.* **2011,** *68* (7-8), 883-903.
11. Brown, P.; Jones, J.; Weryk, R.; Campbell-Brown, M. D., The velocity distribution of meteoroids at the Earth as measured by the Canadian meteor orbit radar (CMOR). *Earth Moon Planets* **2005,** *95* (1-4), 617-626.
12. Zavada, S. R.; McHardy, N. R.; Gordon, K. L.; Scott, T. F., Rapid, Puncture-Initiated Healing via Oxygen-Mediated Polymerization. *ACS Macro Lett.* **2015,** *4* (8), 819-824.

Chapter 4

Oxygen-Mediated Enzymatic Polymerization of Thiol–Ene Hydrogels

Abstract: Materials that solidify in response to an initiation stimulus are currently utilized in several biomedical and surgical applications; however, their clinical adoption would be more widespread with improved physical properties and biocompatibility. One chemistry that is particularly promising is based on the thiol–ene addition reaction, a radical-mediated step-growth polymerization that is resistant to oxygen inhibition and thus is an excellent candidate for materials that polymerize upon exposure to aerobic conditions. Here, thiol–ene-based hydrogels are polymerized by exposing aqueous solutions of multi-functional thiol and allyl ether PEG monomers, in combination with enzymatic radical initiating systems, to air. An initiating system based on glucose oxidase, glucose, and Fe^{2+} is initially investigated where, in the presence of glucose, the glucose oxidase reduces oxygen to hydrogen peroxide which is then further reduced by Fe^{2+} to yield hydroxyl radicals capable of initiating thiol–ene polymerization. While this system is shown to effectively initiate polymerization after exposure to oxygen, the polymerization rate does not monotonically increase with raised Fe^{2+} concentration owing to inhibitory reactions that retard polymerization at higher Fe^{2+} concentrations. Conversely, replacing the Fe^{2+} with horseradish peroxidase affords an initiating system is that is not subject to the iron-mediated inhibitory reactions and enables increased polymerization rates to be attained.

4.1 Introduction

Materials that are polymerizable in situ, such as composite dental restoratives,[1, 2] suture-less wound closures,[3, 4] and hemostatic sealants,[5-7] are currently used in a wide range of medical procedures. However, although several materials and approaches for tissue adhesives and sealants have emerged, substantial research attention is still required to fulfill the potential of polymeric materials that can be applied to a wound site in liquid form and solidify in situ, alleviating the need for sutures or bandages. The development of new biocompatible materials that polymerize rapidly upon application, demonstrate excellent adhesion to tissue, and are readily tailored to suit the requirements dictated by the wound site, is essential to fully realize this potential.

Many of the currently available systems are packaged as two liquid formulations that solidify via an in situ polymer network forming reaction upon combination. For example, the albumin/glutaraldehyde system, where glutaraldehyde serves as a difunctional cross-linker that reacts with the amine functionalities present in both albumin and the substrate tissue, has been successfully used to the seal tears in blood vessels.[5, 8] However, glutaraldehyde poses a host of safety concerns, including the potential for inducing nerve injury, mutagenicity, and tissue necrosis.[5] Fibrinogen/thrombin preparations similarly react in situ, mimicking the final stages of the blood clot-forming coagulation cascade,[9] to yield a cross-linked fibrin network. These fibrin-based materials are typically considered safer than albumin/glutaraldehyde formulations;[5] however, the resultant proteinaceous polymer network exhibits limited mechanical robustness, failing under moderate pressures.[5, 10, 11] Moreover, as both the albumin/glutaraldehyde and fibrinogen/thrombin systems are derived from animalian

sources, there exists a perceived risk of viral infection or allergic reaction to the patient.[5, 7] This potential risk is readily eliminated by utilizing formulations comprised of wholly synthetic materials such as poly(ethylene glycol) (PEG)-based hydrogels. Several reaction mechanisms have been employed to effect the cross-linking and gelation of aqueous telechelic PEG solutions including succinimide/amine additions[5] and catechol cross-linking upon addition of sodium periodate, a strong oxidant.[12] The primary deficiency of these binary-formulation systems is that they require mixing, typically performed within the delivery device itself, to induce polymerization;[5] consequently, inadequate mixing or improper mixing ratios prevents complete polymer network development, yielding incompletely polymerized regions throughout the material and adversely affecting its mechanical robustness and adhesion to the substrate tissue.

An alternative to systems that require mixing immediately prior to application are those that are packaged as a single formulation and that rely upon some external stimulus, such as light, elevated temperature, or exposure to an environmentally-borne chemical reactant, to initiate polymerization. For example, (meth)acrylate monomers formulated with a photoinitiator will readily polymerize, *via* a chain-growth mechanism, upon exposure to light.[13] While the use of light permits fine spatial and temporal reaction control, the necessary availability of an intense light source is undesirable for many medical procedures. Conversely, cyanoacrylate adhesives require no preparation or additional equipment to effect polymerization; rather, they polymerize immediately upon exposure to atmospheric water or weak nucleophiles such as hydroxyl and amine functional groups on skin, yielding a solid polymer.[4, 5] Owing to their rapid reaction kinetics, capacity for environmentally-triggered cure, and the high strength and excellent

tissue adhesion typically exhibited by the generated polymers,[4] cyanoacrylates have found widespread use as suture replacements for incision closure. Additionally, the application of cyanoacrylates to incision sites is far simpler and faster than suture placement, and subsequent clinician visits for suture removal is obviated by the hydrolytic degradability of poly(cyanoacrylates). Nevertheless, serious cytotoxicity concerns persist over the hydrolytic degradation products of these materials (e.g., formaldehyde),[4, 14, 15] limiting their clinical utilization exclusively to external applications. Furthermore, measures necessary to reduce chronic exposure to toxic cyanoacrylate vapor experienced by health professionals are burdensome.[16] Finally, cyanoacrylate resins are not amenable to chemical modification owing to the reactivity of the cyanoacrylate functional group; this lack of extensibility severely curtails the attainable property range which, as poly(cyanoacrylates) tend to be relatively brittle,[17] hinders their broader adoption.

Despite their limitations, cyanoacrylates illustrate the tremendous utility of employing an environmentally-borne initiation stimulus, rather than light or the co-reaction upon combination of two precursor formulations, to effect polymerization. Although water is a common stimulus to induce the polymerization of cyanoacrylates and other materials,[18, 19] oxygen poses as a convenient environmentally-borne polymerization initiation stimulus for radical-mediated polymerizations as it is both ubiquitous, being present at 21% of Earth's atmosphere, and highly reactive, being able to participate in redox reactions and generate free radicals. For example, oxygen has been used as a reactant in enzyme-mediated monosaccharide oxidations to ultimately yield radicals and initiate (meth)acrylate polymerizations of aqueous monomeric formulations.[20, 21] Thus,

the aqueous meth(acrylate) formulations were stable in the absence of oxygen but, upon exposure to air, reacted to generate polymeric materials and, for cross-linking systems, hydrogels. A limitation of this approach is the typically inhibitory influence oxygen has on radical-mediated chain-growth polymerizations, leading to incomplete cure and a high concentration of unreacted, leachable monomers. These enzyme-mediated polymerizations could thus be improved through the use of mechanisms that are resistant to oxygen inhibition such as the radical-mediated thiol–ene addition.[22]

Thiol–ene polymerizations proceed *via* alternating propagation and chain transfer events between thiols and electron-rich carbon-carbon double bonds (e.g., allyl ether or vinyl ether) (Scheme 19), leading to step-growth evolution of the molecular weight.[22] Unlike radical-mediated meth(acrylate) chain-growth polymerizations, the thiol–ene reaction mechanism is extraordinarily resistant to oxygen-inhibition,[22] owing to the facile abstractability of the thiol hydrogen, and thus is well-suited as the polymerization mechanism for an oxygen-mediated hydrogel formation. Furthermore, many thiol- and ene-functionalized monomers exist, offering versatility and fine control over the physical properties of the resultant polymer and potential degradation products. Additionally, the thiol–ene mechanism is tolerant to the presence of a wide range of functional groups that may be present on cell-binding epitopes or growth factors incorporated in the formulation. Here, we examine aqueous thiol–ene solutions formulated with oxidoreductase-based enzymatic radical initiation systems that remain stable under anaerobic conditions but polymerize rapidly upon exposure to atmospheric oxygen, combining the desirable features of thiol–ene chemistry with the convenience of an environmentally-borne initiation stimulus.

4.2 Experimental

4.2.1 Materials and Synthesis

D-Glucose (Fisher Scientific), iron(II) sulfate heptahydrate (Sigma-Aldrich), glucose oxidase from *Aspergillus niger* (GOx, 147.9 U/mg, Sigma-Aldrich), horseradish peroxidase (HRP, Type VI, 261 purpurogallin U/mg, Sigma-Aldrich), and acetylacetone (AA, Sigma-Aldrich) were used as received. Cupferron (*N*-nitroso-*N*-phenylhydroxylamine ammonium salt), used as a radical inhibitor to prevent premature polymerization, was obtained from Wako Chemicals. 2-(*N*-Morpholino)ethanesulfonic acid (MES) aqueous buffer (0.1 M MES, pH 4.5) was obtained from Teknova.

A model thiol–ene formulation, comprised of PEG-based trithiol and diallyl ether monomers, was used for all experiments. Ethoxylated trimethylolpropane tri(3-mercaptopropionate (ETTMP 1300, molecular weight (MW) ~1300 g/mol) was donated by Evans Chemetics and used without further purification. Poly(ethylene glycol) diallyl ether (PEGDAE) was synthesized using a modified method from the literature.[23] Briefly, dihydroxylated PEG (MW ~600 g/mol) was dissolved in toluene (~18 g PEG in 400 mL toluene) under nitrogen and excess sodium hydride was added slowly. After the gas evolution ceased, a large excess of allyl bromide was added slowly and the reaction mixture was stirred and heated to 70°C. After 24 hours, the mixture was filtered and the toluene and residual allyl bromide were removed under vacuum from the filtrate. Proton nuclear magnetic resonance (NMR) spectroscopy (Varian MR400, 400 MHz), with DMSO-d6 as solvent, was used to confirm the complete substitution of hydroxyl groups, characterized by the absence of a peak at 4.56 ppm.[24] The resulting product was a

slightly yellow liquid at room temperature. The monomers and buffer were subjected to at least six freeze-pump-thaw cycles to ensure rigorous deoxygenation prior to use.

4.2.2 Polymerization Kinetics

Under anaerobic conditions, the thiol- and ene-functionalized PEG monomers, in a 1:1 thiol:ene stoichiometric ratio, were dissolved in MES buffer to afford a final combined monomer concentration of 35 wt% (15.4 wt% PEGDAE, 19.6 wt% ETTMP) and stabilized by the addition of cupferron (3.2 mM) (Figure 21), to which stock solutions of the other formulation components (e.g., glucose, GOx, iron(II) sulfate heptahydrate, horseradish peroxidase, and acetylacetone) in MES buffer were added. The pH 4.5 for buffer was selected to ensure slightly acidic conditions for optimum GOx activity[25] and to minimize the thiolate concentration, owing to the dissociation of the thiol hydrogen (mercaptopropionate pK_a is approximately 10.4),[26] ensuring minimal disulfide or thiol oxidation by the generated hydrogen peroxide.[27] Glucose solutions were prepared 24 hours prior to use to ensure mutarotation equilibrium,[28] while enzyme solutions were used within 48 hours of dissolution. All stock solutions and thiol–ene formulations used were precipitate-free. For oxygen-mediated polymerization experiments, the thiol–ene formulations were removed from the anaerobic chamber, bubbled with air (21% oxygen) for 20 seconds, and immediately pipetted into a glass-bottomed cylindrical sample cell, affording 2.5 mm thick samples, and placed in a Thermo Scientific Nicolet 6700 FTIR spectrometer. The polymerization reaction commenced upon exposure to aerobic conditions, and functional group conversions were determined in real-time using FTIR spectroscopy[29] by monitoring the disappearance of the peak area centered at 6139 cm^{-1}, corresponding to the vinyl-CH stretch.[30] Spectra were collected at a rate of

approximately three every two seconds. Anaerobic control experiments were similarly performed using FTIR spectroscopy on samples that remained unexposed to oxygen. All experiments were performed in triplicate at ambient temperature and the average and standard error reported.

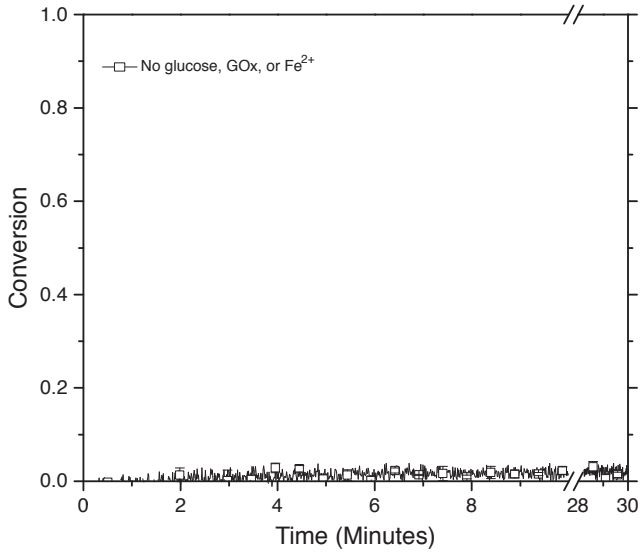

Figure 21: Stability of the thiol–ene solution in 0.1 M MES buffer. Allyl ether functional group conversion is shown for an aqueous thiol–ene solution in the absence of any components of the radical initiating systems and under aerobic conditions.

4.3 Results and discussion

4.3.1 Coupled Enzymatic-Fe(II)/Fe(III) Radical Initiation

Aqueous monomer solutions of ETTMP and PEGDAE in MES buffer were formulated with a three-component, enzymatic, radical initiating system, comprised of GOx, glucose, and $FeSO_4$, exposed to air (ca. 21% oxygen), and the polymerization reaction was monitored by FTIR spectroscopy for 30 minutes. In the presence of oxygen, GOx oxidizes glucose to generate gluconolactone and hydrogen peroxide which is subsequently reduced by Fe^{2+}, (i.e., the Fenton reaction) according to the reactions[21]

$$\text{Glucose} + O_2 \xrightarrow{\text{GOx}} \text{Gluconolactone} + H_2O_2 \quad (9)$$

$$H_2O_2 + Fe^{2+} \longrightarrow Fe^{3+} + OH^- + OH^{\bullet} \quad (10)$$

thus generating hydroxyl radicals capable of initiating the thiol–ene polymerization. As the radical-initiating system is composed of three components (excluding oxygen), studies were performed where the initial concentration of one component was varied while the initial concentrations of the other two were maintained. Previous work has shown that the Fe^{2+}-mediated production of hydroxyl radicals from H_2O_2 is significantly enhanced by the presence of physiological thiol-bearing compounds such as glutathione and cysteine,[31] suggesting a particular suitability for Fenton chemistry to effect rapid polymerization of thiol–ene materials owing to their ubiquitous thiol functional groups.

We first investigated the influence of Fe^{2+} concentration on the thiol–ene hydrogel polymerization by varying the initial concentration of Fe^{2+} from 0 to 720 μM while the initial concentrations of glucose and GOx were maintained at 56 mM and 14.8 kU/L, respectively (Figure 22). At low Fe^{2+} concentrations (≤ 72 μM), the maximum rate of polymerization and extent of reaction both increased as the Fe^{2+} concentration was raised. This initiating system relies on the Fe^{2+}-mediated Fenton reaction to generate hydroxyl radical initiating species from hydrogen peroxide afforded by the action of GOx on glucose in the presence of oxygen. The reaction depicted in Equation 10 suggests a simple relation between the Fe^{2+} concentration and the rate of hydroxyl radical generation; however, the several concurrent interactions between Fe^{2+}, Fe^{3+}, H_2O_2, and radical species convolute this process.

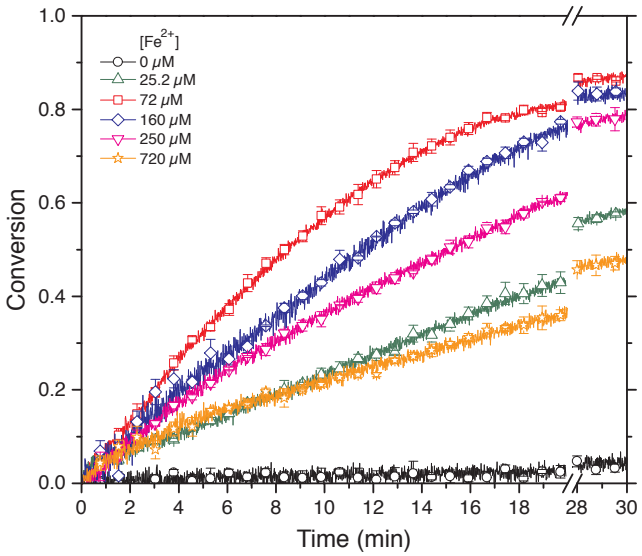

Figure 22: Influence of initial Fe^{2+} concentration. Allyl ether functional group conversions, monitored by FTIR spectroscopy, are shown for aqueous thiol–ene solutions formulated with glucose, GOx, and Fe^{2+} (56mM, 14.8 kU/L, and concentrations as shown in legend, respectively) upon exposure to air.

For example, several other reactions that lead to the generation of potential initiating radical species include[32, 33]

$$Fe^{3+} + H_2O_2 \longrightarrow Fe\text{-}OOH^{2+} + H^+ \tag{11}$$

$$Fe\text{-}OOH^{2+} + H_2O_2 \longrightarrow Fe(OH)(HO_2)^+ \tag{12}$$

$$Fe\text{-}OOH^{2+} \longrightarrow Fe^{2+} + HO_2^{\bullet} \tag{13}$$

$$Fe(OH)(HO_2)^+ \longrightarrow Fe^{2+} + HO_2^{\bullet} + OH^- \tag{14}$$

where the Fe^{3+} generated in Equation 10 is ultimately reduced back to Fe^{2+} which is thus catalytically decomposing H_2O_2. As seen in Figure 22, the extent of polymerization after 30 minutes monotonically decreases at initial Fe^{2+} concentrations in excess of 72 μM. Although this inhibitory effect of Fe^{2+} on radical polymerizations is not readily explained

by the reactions described in Equations 10–14, both Fe^{2+} and Fe^{3+} are known to participate in oxidative termination reactions with some radical species,[21, 32] such as

$$Fe^{2+} + OH^{\bullet} \longrightarrow Fe^{3+} + OH^{-} \quad (15)$$

$$Fe^{3+} + R^{\bullet} \longrightarrow Fe^{2+} + \text{products} \quad (16)$$

where R· is a propagating radical. Consequently, radicals are rapidly consumed in these competing reactions and are thus unavailable to participate in the hydrogel polymerization, leading to the observed Fe^{2+}-dependent polymerization retardation and ultimately limiting the maximum attainable polymerization rate and extent. The inhibitory effect of raised Fe^{2+} concentrations has previously been observed in the radical-mediated polymerization of an acrylate-based hydrogel that employed a GOx-glucose-Fe^{2+} radical-generating initiation system at similar Fe^{2+} concentrations.[21] The inhibition of radical polymerizations by Fe^{2+} and Fe^{3+} has been shown to be monomer dependent where, for example, the polymerization rate of methyl(methacrylate) is unaffected by Fe^{3+};[34] nevertheless, similar resistance to Fe^{2+}-dependent retardation is clearly not exhibited by the current thiol–ene formulation. Thus, while Fe^{2+} is necessary to induce polymerization, reaction rates do not scale with initial Fe^{2+} concentration. Notably, the polymerization proceeded under aerobic conditions even in the absence of added Fe^{2+}, albeit at an extremely slow rate. (Figure 22, 0 μM Fe^{2+}). As the generation of H_2O_2 does not require Fe^{2+} to proceed and it is stable in acidic media at ambient temperature, we ascribe the small amount of polymerization observed under aerobic conditions at 0 μM Fe^{2+} to the presence of trace amounts of iron impurities in the formulation precursors.

The influence of the initial glucose concentration on the polymerization rate, final conversion, and substrate saturation of GOx was examined by monitoring polymerizations of aqueous thiol–ene solutions formulated with initial Fe^{2+} and GOx concentrations of 72 μM and 14.8 kU/L, respectively, and initial concentrations of glucose varied from 0 to 170 mM upon exposure to oxygen (Figure 23). As expected, the polymerization rate and final conversion increase monotonically as the glucose concentration is raised at moderate glucose concentrations; however, at 28 mM and above, a zero-order dependence of glucose concentration on the polymerization rate is observed, demonstrating saturation of the GOx by its glucose substrate at these concentrations. At raised glucose concentrations, the allyl ether conversions approach 90% after 30 minutes of air exposure indicating the complete consumption of one of the reagents. The oxidation of glucose by GOx is initially accompanied by the reduction of flavine adenine dinucleotide (FAD) to $FADH_2$ which is subsequently reoxidized by O_2 to afford H_2O_2.[35] As both GOx and Fe^{2+} act catalytically to generate initiating species, the incomplete polymerization suggests complete consumption of either glucose or dissolved oxygen during the reaction. The consistent reaction extents after 30 minutes for glucose concentrations from 28 to 170 mM indicates that, rather than glucose being the limiting reagent, the dissolved oxygen initially introduced by bubbling the formulation with air is depleted by the oxidation of glucose faster than it can be replenished by diffusion from the atmosphere.

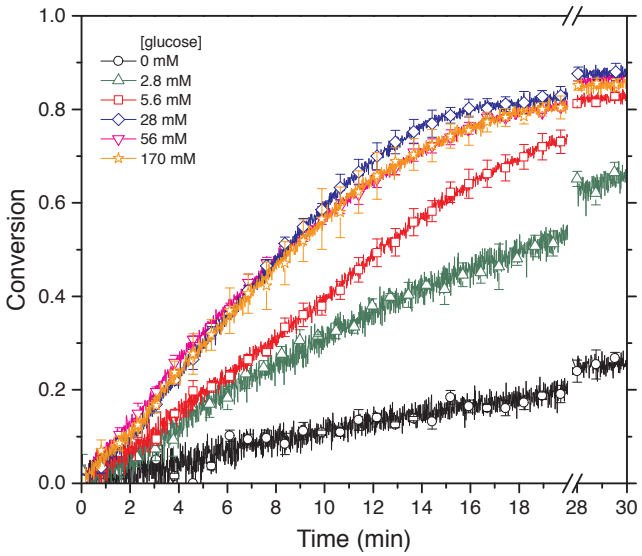

Figure 23: Influence of initial glucose concentration. Allyl ether functional group conversions are shown for aqueous thiol–ene solutions formulated with GOx, Fe^{2+}, and glucose (14.8 kU/L, 72 μM, and concentrations as shown in legend, respectively) upon exposure to air.

As the enzyme GOx is the most expensive of the formulation components in this coupled radical initiation scheme, we varied the GOx concentration to determine the minimum amount that would afford a reasonable polymerization rate and reaction extent. The concentration of GOx in the aqueous thiol–ene solutions was varied from 0 to 14.8 kU/L while maintaining initial glucose and Fe^{2+} concentrations at 56 mM and 72 μM, respectively (Figure 24), and both the reaction rate and extent increased as the GOx concentration was raised. An important parameter to consider for the clinical utilization of hydrogel sealants is the gelation time. Too short a gel time results in gelation prior to application at the wound site and hence prevents adequate adhesion and sealing; conversely, too long a gel time results in excessively delayed solidification of the sealing material. The theoretical gel point of an ideal step-growth polymerization, described by classical Flory-Stockmayer theory,[36] depends upon the average number of functional groups on each monomer and the stoichiometric ratio between functional groups. As the

model thiol–ene formulation, used throughout this study was comprised of trithiol and diallyl ether monomers in a 1:1 thiol:ene stoichiometric ratio, the theoretical gel point is calculated as approximately 70% conversion. Thus, the formulations containing 0 and 1.5 kU/L GOx did not gel over the course of 30 minute air exposure, while the 7.4 and 14.8 kU/L GOx formulations gelled after ~15 and ~13.5 minutes (excluding the initial air bubbling period and concomitant polymerization), respectively. Currently, these gel times are not clinically relevant; however, the gel point conversion can be conveniently decreased by increasing the monomer functionality. For example, replacing the PEG diallyl ether for a tetraallylated PEG in the current formulation would decrease the gel point conversion to ~41% corresponding to a gel time of a more useful ~6.5 minutes for the 14.8 kU/L GOx formulation.

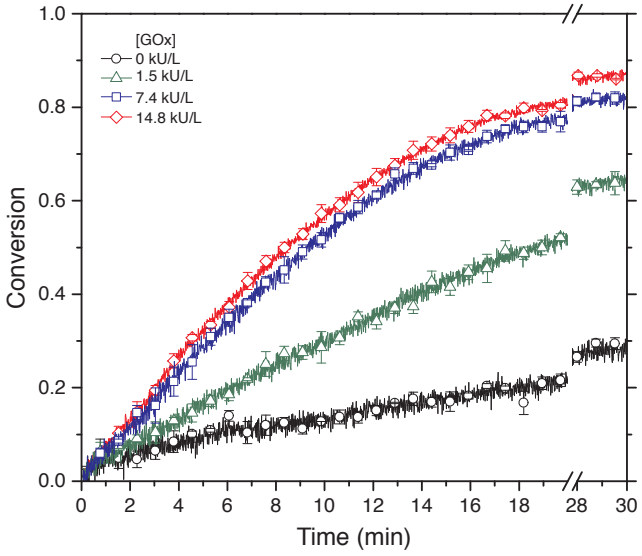

Figure 24: Influence of GOx concentration. Allyl ether functional group conversions are shown for aqueous thiol–ene solutions formulated with glucose, Fe2+, and GOx (56 mM, 72 μM, and concentrations as shown in legend, respectively) upon exposure to air.

Air exposure of a glucose-free, GOx- and Fe^{2+}-containing formulation (Figure 23, 0 mM glucose) and a GOx-free, glucose- and Fe^{2+}-containing formulation (Figure 24, 0

kU/L GOx) unexpectedly afforded slow polymerization; notably, the polymerization rates of these two formulations were, within the experimental error, identical and significantly faster than the Fe^{2+}-free, glucose- and GOx-containing formulation (Figure 1, 0 μM Fe^{2+}). Although an aqueous thiol–ene solution formulated with 14.8 kU/L GOx, 56 mM glucose, and 72 μM Fe^{2+} proved stable under anaerobic conditions (Figure 25), demonstrating the necessity for oxygen exposure to initiate the polymerization, an aqueous thiol–ene solution containing none of the initiating system components proved similarly stable under aerobic conditions (Figure 21). As GOx exhibits high substrate specificity,[25] enzymatic generation of H_2O_2 does not proceed in the absence of glucose. Moreover, there is no mechanism for glucose to generate initiating species by itself upon oxygen exposure at ambient temperature. Generation of radicals necessary for the observed polymerization is thus attributable to direct oxygen reduction by Fe^{2+} according to the reaction equations[37, 38]

$$O_2 + Fe^{2+} \longrightarrow O_2^{-\bullet} + Fe^{3+} \quad (17)$$

$$O_2^{-\bullet} + Fe^{3+} + 2H^+ \longrightarrow H_2O_2 + Fe^{3+} \quad (18)$$

where the generated H_2O_2 subsequently oxidizes Fe^{2+} to Fe^{3+} via the Fenton reaction (Equation 10) to yield hydroxyl radical initiating species. Notably, previously described acrylate systems polymerized by GOx-glucose-Fe^{2+} initiating systems did not demonstrate any evidence of polymerization in the absence of glucose.[20, 21] Given the strong inhibition of radical-mediated chain-growth acrylate polymerizations by oxygen, the low radical generation rate may not have been adequate to sufficiently deplete the

oxygen concentration to overcome this inhibition and allow the polymerization to proceed. In contrast, the radicals formed upon air exposure via this non-enzymatic mechanism are able to effect polymerization here, albeit at a low polymerization rate, owing to the resistance of the thiol–ene reaction to oxygen inhibition. Nevertheless, although the radicals afforded by this pathway do effect thiol–ene polymerization under aerobic conditions, all components of the combined GOx-glucose-Fe^{2+} system are necessary for useful polymerization rates.

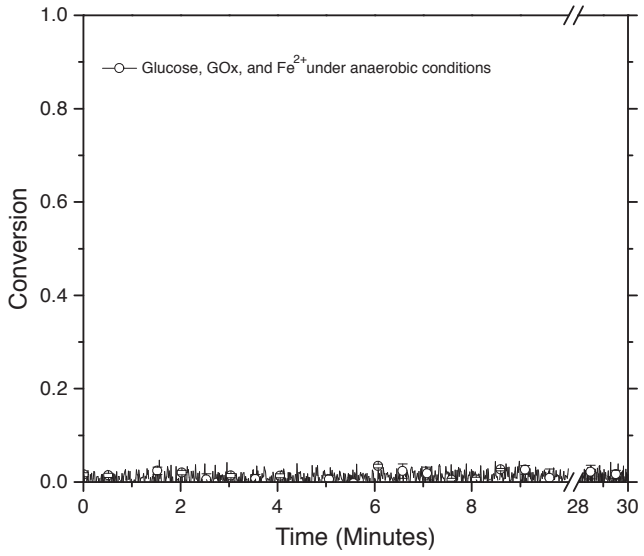

Figure 25: Stability of the thiol–ene solution formulated with the GOx-glucose-Fe^{2+} radical initiating system. Allyl ether functional group conversion is shown for an aqueous thiol–ene solution formulated with glucose, Fe^{2+}, and GOx (56 mM, 72 µM, and 14.8 kU/L, respectively) under anaerobic conditions.

The several redox reactions that lead to hydroxyl radical generation by the GOx-glucose-Fe^{2+} initiating system are summarized in Scheme 27. The introduction of oxygen leads to the generation of hydrogen peroxide both through the GOx-catalyzed oxidation of glucose and accompanying reduction of oxygen, or via a non-enzymatic route where oxygen is directly reduced by Fe^{2+}. The in situ generated hydrogen peroxide is further reduced by Fe^{2+} to yield hydroxyl radicals, a species capable of initiating the

thiol–ene polymerization, and Fe^{3+} which in turn can be recycled back to Fe^{2+}. This GOx-glucose-Fe^{2+} system is deficient as a radical initiating system for the fabrication of thiol–ene hydrogels primarily because raised Fe^{2+} concentrations significantly retard, rather than enhance, thiol–ene polymerization rates; indeed, the 720 μM Fe^{2+} system (Figure 22) did not gel even after exposure to aerobic conditions for thirty minutes. In clinical settings, it may be desirable to perform the polymerization at physiological pH values where the thiolate ion concentration is non-negligible. Under these conditions, the Fe^{3+} generated from Fe^{2+}-mediated H_2O_2 reduction would oxidize thiolate anions to thiyl radicals,[37, 38] potentially augmenting thiol–ene polymerization rates, and rapidly recovering the Fe^{2+} species which are then available to participate in further H_2O_2 decomposition events. Regardless, given the complexity of Fe^{2+}/Fe^{3+} redox chemistry, the development of an approach that enables radical generation from H_2O_2 decomposition, but avoids the utilization of Fe^{2+} and its associated inhibition of radical polymerizations, is attractive.

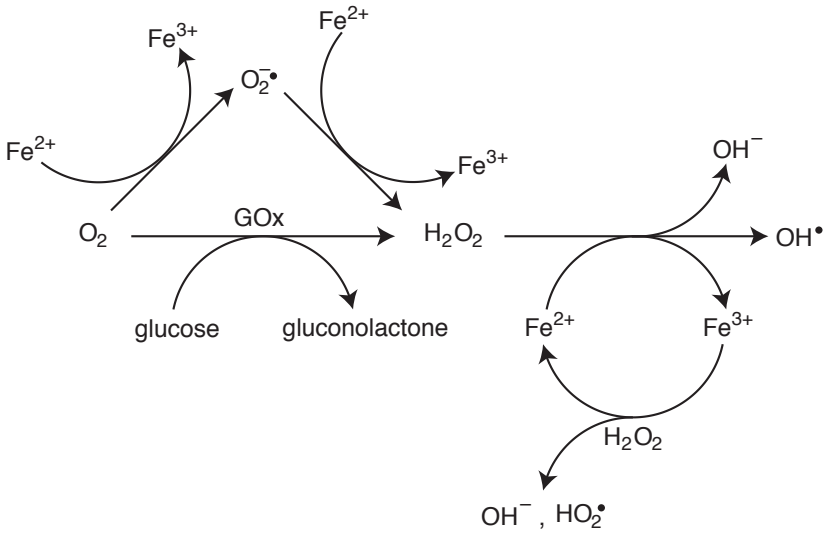

Scheme 27: The generation of hydroxyl radicals upon exposure of the GOx-glucose-Fe^{2+} system to aerobic conditions. The primary hydroxyl radical-generating

mechanism is the GOx-mediated reduction of oxygen to hydrogen peroxide that is further reduced to hydroxyl radicals by Fe^{2+}. Alternatively, the reduction of oxygen by Fe^{2+} yields superoxide radicals that are similarly reduced to hydrogen peroxide. The Fe^{3+} generated during these reactions is recycled back to Fe^{2+} via reaction with hydrogen peroxide.

4.3.2 Horseradish Peroxidase Radical Initiation

Horseradish peroxidase (HRP) is an oxidoreductase capable of generating radicals by catalyzing the action of a suitable oxidant, commonly hydrogen peroxide, on a reductant.[39] The utility of HRP for the initiation of polymerization reactions is well-documented and has been used to synthesize polymers through the oxidative polymerization of phenols[40] and the free-radical, chain-growth polymerization of acrylamides[41] and (meth)acrylates.[42] For example, poly(methyl methacrylate) (PMMA) was synthesized from a formulation of methyl methacrylate, HRP, hydrogen peroxide, and acetylacetone as a substrate for HRP-mediated oxidation.[42] The polymerization did not proceed in the absence of acetylacetone, indicating that the methacrylate monomer itself was a poor HRP substrate; however, in the presence of acetylacetone, oxidation by HRP generated radical species able to initiate the polymerization. As H_2O_2 was generated in our initial enzymatic polymerization approach by the action of GOx on glucose in the presence of oxygen, we investigated the potential for HRP in conjunction with H_2O_2 to generate radical initiation species to effect thiol–ene polymerization.

Aqueous solutions of our thiol and ene monomers in MES buffer were formulated with HRP and the influences of H_2O_2 and/or acetylacetone, a common reductant substrate utilized with HRP-mediated radical polymerizations, on the polymerization upon atmospheric exposure were examined (Figure 26). In the presence of H_2O_2, the polymerization proceeds rapidly, attributable to the generation of radicals by HRP-

mediated substrate oxidation. Notably, the presence of acetylacetone in the formulation did not influence the polymerization rate or extent. Low molecular weight thiols have previously been shown to act as HRP-mediated oxidation substrates,[43, 44] demonstrating not only that the thiol component of the polymerizable formulation is acting as the HRP substrate, but that it is saturating the enzyme. Although no HRP-mediated thiol–ene polymerization was observed under anaerobic, H_2O_2-free conditions (Figure 27), interestingly, the polymerization of a thiol–ene solution formulated with HRP did proceed slowly upon air exposure, even in the absence of added H_2O_2 (Figure 26, no AA or H_2O_2, and 0.1 M AA). Under this H_2O_2-free condition, the addition of acetylacetone again did not influence the reaction rate. HRP has previously been observed to use oxygen as a substrate to oxidize organic reductants, although at far lower efficiency than its utilization of H_2O_2.[44]

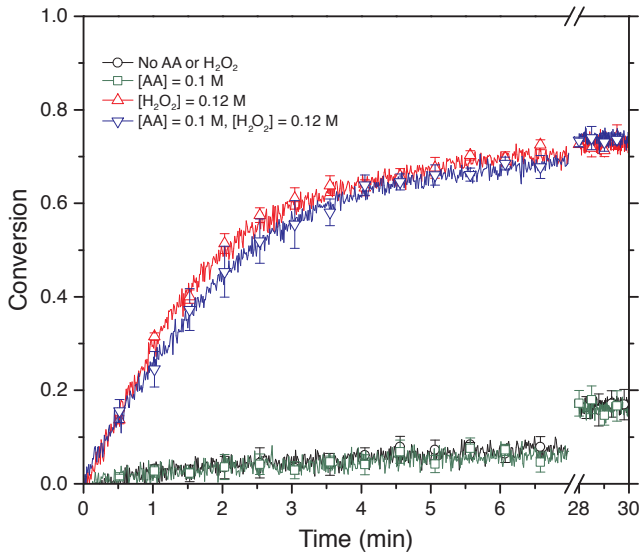

Figure 26: Influence of added oxidant and reductant. Allyl ether functional group conversions are shown for aqueous thiol–ene solutions formulated with HRP, H_2O_2, and acetylacetone (AA) (261 kU/L and concentrations as shown in legend, respectively) upon exposure to air.

Thus, we attribute the generation of adequate radicals to effect the exogenous H_2O_2-free thiol–ene polymerization observed in Figure 26 to this HRP-mediated aerobic oxidation of thiols.

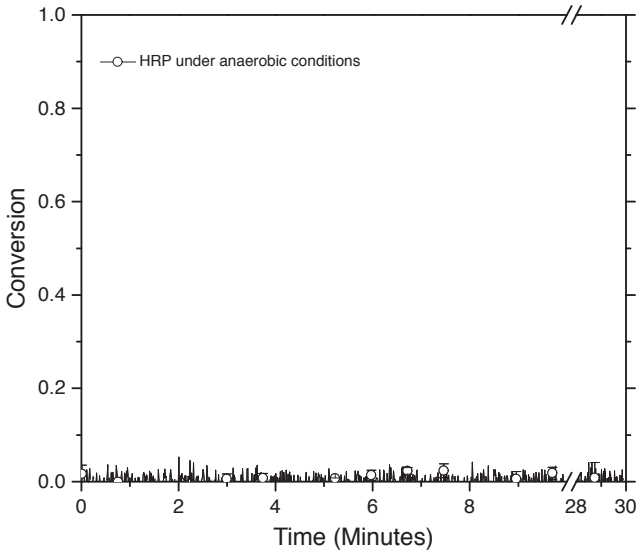

Figure 27: Stability of the thiol–ene solution formulated with HRP. Allyl ether functional group conversion is shown for an aqueous thiol–ene solution formulated with HRP (261 kU/L) under anaerobic conditions.

4.3.3 Coupled Bienzymatic GOx-HRP Radical Initiation

The H_2O_2 generation observed for the GOx-glucose formulations under aerobic conditions, evidenced by its oxidation of Fe^{2+} and concomitant radical generation (Figure 22), and the successful and rapid thiol–ene hydrogel polymerization by HRP and H_2O_2, even in the absence of an additional reductant such as AA (Figure 26), suggests that HRP may be a convenient, drop-in replacement for Fe^{2+} in a coupled, oxygen-mediated, thiol–ene radical initiation system. Here, the H_2O_2 generated by the GOx-glucose system upon exposure to oxygen would serve as an oxidant source for the action of HRP on the thiol functional groups to yield thiyl initiating radicals (Scheme 28). This coupled GOx-glucose-HRP initiating system would not require Fe^{2+} for radical generation and consequently would not suffer from the polymerization retardation resulting from high

Fe^{2+} concentrations. Such bienzymatic approaches are not without precedent. For example, Uyama *et al.* used the GOx-glucose system for the in situ generation of hydrogen peroxide to effect the oxidative polymerization of phenols by HRP,[45] circumventing potential HRP deactivation by high H_2O_2 concentrations.[39, 46] In contrast to our approach where polymerization proceeds upon exposure to atmospheric oxygen, Uyama *et al.* initiated polymerization by the addition of glucose.

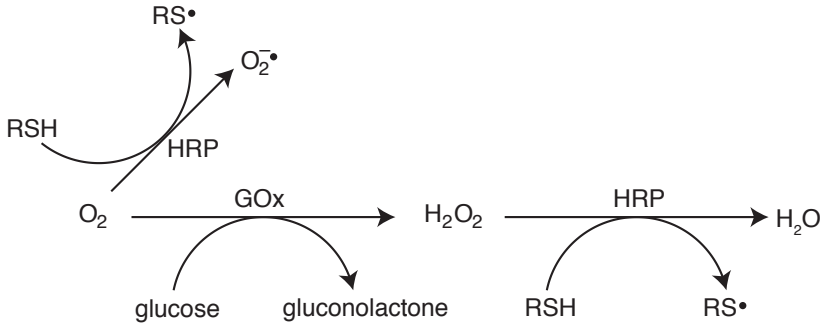

Scheme 28: The generation of radicals upon exposure of the GOx-HRP system to aerobic conditions. The radical species generated by this coupled bienzymatic system are capable of initiating thiol–ene polymerization. The primary radical generation mechanism proceeds via the GOx-mediated oxidation of glucose to yield H_2O_2, from which hydroxyl radicals are generated by the action of HRP on a substrate thiol. The direct, HRP-mediated oxidation of thiols by oxygen is a minor radical generation contributor.

We investigated the coupling of these two enzymatic reactions by examining the influence of the HRP concentration on the polymerization rate and final conversion of aqueous thiol–ene solutions formulated with initial glucose and GOx concentrations of 56 mM and 14.8 kU/L, respectively, and HRP concentrations varied from 26.1 to 261 kU/L upon exposure to oxygen (Figure 28). As expected, no polymerization was noted when the formulation was kept under anaerobic conditions; however, upon oxygen exposure, polymerization successfully proceeded at rates that monotonically increased with raised HRP concentration (Figure 28). Importantly, the polymerization rate at 261 kU/L HRP

exceeded that of the fastest GOx-glucose-Fe^{2+} system, reducing the gel time from ~13.5 minutes for the Fe^{2+}-based initiating system to ~8.5 minutes (again excluding the air bubbling period) when HRP was employed. Moreover, this gel time could be further reduced, as required for clinical utility, either by increasing the monomer functionality or by further raising the HRP concentration. Finally, the addition of acetylacetone again did not afford any significant polymerization rate or extent variation (Figure 29), demonstrating the HRP saturation by thiol and hence ineffective incorporation of additional reductant species.

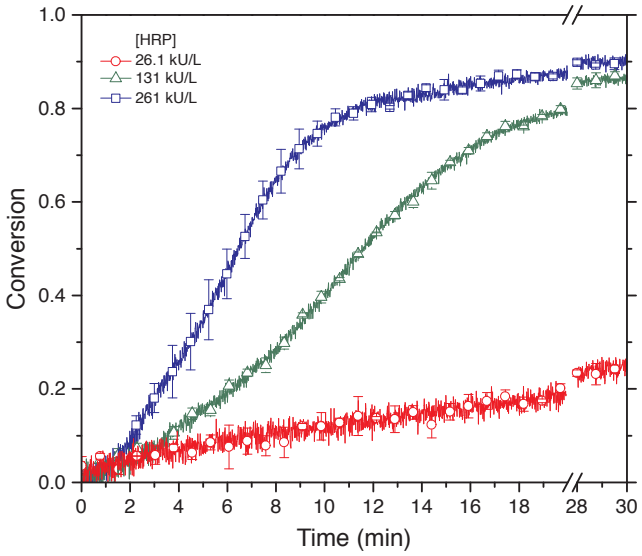

Figure 28: Influence of HRP concentration on a coupled GOx-HRP thiol–ene polymerization initiation. Allyl ether functional group conversions are shown for aqueous thiol–ene solutions formulated with glucose, GOx, and HRP (56 mM, 14.8 kU/L and concentrations as shown in legend, respectively) upon exposure to air.

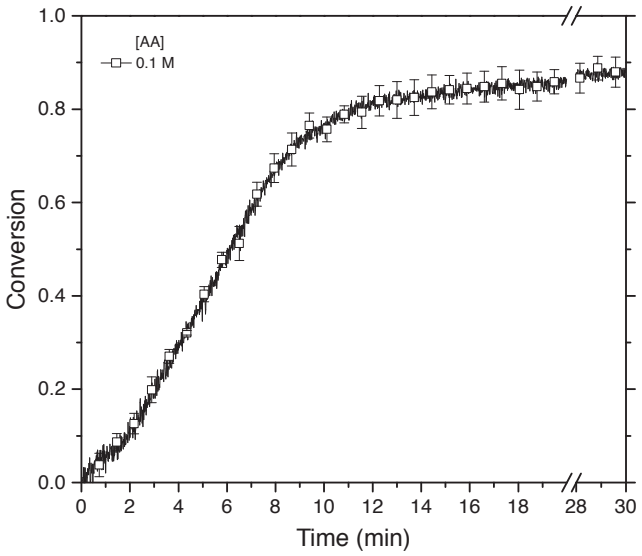

Figure 29: Influence of acetylacetone on a coupled GOx-HRP initiated thiol–ene polymerization. Allyl ether functional group conversion is shown for an aqueous thiol–ene solution formulated with glucose, GOx, HRP, and AA (56 mM, 14.8 kU/L, 261 kU/L and 0.1 M, respectively) upon exposure to air.

4.4 Conclusions

Aqueous solutions of multi-functional thiol and allyl ether monomers were polymerized into solid hydrogels through in situ enzymatic generation of radical initiating species. The first enzymatic system uses GOx, in the presence of glucose and oxygen, to generate hydrogen peroxide that, upon reduction by Fe^{2+}, forms hydroxyl radicals capable of initiating thiol–ene polymerization. In addition to this enzyme-mediated process, a non-enzymatic route involving the direct reduction of oxygen to hydroxyl ions by Fe^{2+} is also capable of initiating thiol–ene polymerization. While this second route is a minor contributor compared to the GOx-mediated mechanism, it is of interest as this process is seemingly unique to thiol–ene chemistry and is attributed to the resistance of the radical thiol–ene addition reaction to oxygen inhibition. However, although the ternary system of GOx, glucose, and Fe^{2+} proved capable of initiating polymerization of thiol–ene-based

formulations, the presence of Fe^{2+} limits polymerization rates through several reactions that consume radicals. Consequently, increasing the concentration of Fe^{2+} beyond 72 μM lead to decreased polymerization conversions where the monomer formulations did not gel even after thirty minutes air exposure. As an alternative to the utilization of Fe^{2+}, HRP was used as to catalyze the production of radicals from GOx-generated H_2O_2. Interestingly, the thiol–ene system did not require the incorporation of an additional reductant for polymerization to proceed, indicating that the thiol monomer is capable of being oxidized directly by HRP, using either oxygen or hydrogen peroxide as oxidant, to form initiating radical species. After successful demonstration of HRP to mediate thiol–ene polymerization, HRP was used in combination with GOx and glucose to afford an alternative three-component initiating system that only generates radicals upon oxygen exposure. The GOx-glucose-HRP system was not subject to the polymerization retardation caused by high Fe^{2+} concentrations and yielded polymerization rates that exceeded those of the GOx-glucose-Fe^{2+} system.

4.5 References:

1. Peutzfeldt, A., Resin composites in dentistry: The monomer systems. *Eur. J. Oral. Sci.* **1997,** *105* (2), 97-116.
2. Moszner, N.; Salz, U., New developments of polymeric dental composites. *Prog. Polym. Sci.* **2001,** *26* (4), 535-576.
3. Lauto, A.; Mawad, D.; Foster, L. J. R., Adhesive biomaterials for tissue reconstruction. *J. Chem. Technol. Biotechnol.* **2008,** *83* (4), 464-472.
4. Thennarasu, S.; Krishnamurti, N.; Shantha, K. L., Developments and applications of cyanoacrylate adhesives. *J. Adhes. Sci. Technol.* **1989,** *3* (4), 237-260.
5. Spotnitz, W. D.; Burks, S., Hemostats, sealants, and adhesives: Components of the surgical toolbox. *Transfusion* **2008,** *48* (7), 1502-16.
6. Spotnitz, W. D.; Burks, S., State-of-the-art review: Hemostats, sealants, and adhesives II: Update as well as how and when to use the components of the surgical toolbox. *Clin. Appl. Thromb. Hemost.* **2010,** *16* (5), 497-514.
7. Wheat, J. C.; Wolf, J. S., Jr., Advances in bioadhesives, tissue sealants, and hemostatic agents. *Urol. Clin. North Am.* **2009,** *36* (2), 265-75.

8. Bavaria, J. E.; Brinster, D. R.; Gorman, R. C.; Woo, Y. J.; Gleason, T.; Pochettino, A., Advances in the treatment of acute type A dissection: an integrated approach. *Ann. Thorac. Surg.* **2002,** *74* (5), S1848-52; discussion S1857-63.
9. Sierra, D. H., Fibrin sealant adhesive systems: A review of their chemistry, material properties and clinical applications. *J. Biomater. Appl.* **1993,** *7* (4), 309-52.
10. Silver, F. H.; Wang, M. C.; Pins, G. D., Preparation and Use of Fibrin Glue in Surgery. *Biomaterials* **1995,** *16* (12), 891-903.
11. Eriksen, J. R.; Bech, J. I.; Linnemann, D.; Rosenberg, J., Laparoscopic intraperitoneal mesh fixation with fibrin sealant (Tisseel) vs. titanium tacks: A randomised controlled experimental study in pigs. *Hernia* **2008,** *12* (5), 483-91.
12. Brubaker, C. E.; Kissler, H.; Wang, L. J.; Kaufman, D. B.; Messersmith, P. B., Biological performance of mussel-inspired adhesive in extrahepatic islet transplantation. *Biomaterials* **2010,** *31* (3), 420-7.
13. Choi, J. S.; Yoo, H. S., Pluronic/chitosan hydrogels containing epidermal growth factor with wound-adhesive and photo-crosslinkable properties. *J. Biomed. Mat Res. A* **2010,** *95* (2), 564-73.
14. Vote, B. J.; Elder, M. J., Cyanoacrylate glue for corneal perforations: A description of a surgical technique and a review of the literature. *Clin. Exp. Ophthalmol.* **2000,** *28* (6), 437-42.
15. Radosevich, M.; Goubran, H. A.; Burnouf, T., Fibrin sealant: Scientific rationale, production methods, properties, and current clinical use. *Vox Sang.* **1997,** *72* (3), 133-143.
16. Leggat, P. A.; Kedjarune, U.; Smith, D. R., Toxicity of cyanoacrylate adhesives and their occupational impacts for dental staff. *Ind. Health* **2004,** *42* (2), 207-11.
17. Chivers, R. A.; Wolowacz, R. G., The strength of adhesive-bonded tissue joints. *Int. J. Adhes. Adhes.* **1997,** *17* (2), 127-132.
18. Kowalewska, A., Photoacid catalyzed sol-gel process. *J. Mater. Chem.* **2005,** *15* (47), 4997-5006.
19. Ni, H.; Skaja, A. D.; Soucek, M. D., Acid-catalyzed moisture-curing polyurea/polysiloxane ceramer coatings. *Prog. Org. Coat.* **2000,** *40* (1-4), 175-184.
20. Iwata, H.; Hata, Y.; Matsuda, T.; Ikada, Y., Initiation of radical polymerization by glucose oxidase utilizing dissolved oxygen. *J. Polym. Sci. A Polym. Chem.* **1991,** *29* (8), 1217-1218.
21. Johnson, L. M.; Fairbanks, B. D.; Anseth, K. S.; Bowman, C. N., Enzyme-mediated redox initiation for hydrogel generation and cellular encapsulation. *Biomacromolecules* **2009,** *10* (11), 3114-21.
22. Hoyle, C. E.; Bowman, C. N., Thiol-Ene Click Chemistry. *Angew. Chem. Int. Ed.* **2010,** *49* (9), 1540-1573.
23. Scott, T. F.; Kloxin, C. J.; Draughon, R. B.; Bowman, C. N., Nonclassical dependence of polymerization rate on initiation rate observed in thiol-ene photopolymerizations. *Macromolecules* **2008,** *41* (9), 2987-2989.
24. Dust, J. M.; Fang, Z. H.; Harris, J. M., Proton Nmr Characterization of Poly(Ethylene Glycols) and Derivatives. *Macromolecules* **1990,** *23* (16), 3742-3746.
25. Bankar, S. B.; Bule, M. V.; Singhal, R. S.; Ananthanarayan, L., Glucose oxidase - An overview. *Biotechnol. Adv.* **2009,** *27* (4), 489-501.
26. Bernasconi, C. F.; Killion, R. B., Nucleophilic Additions to Olefins .23. High Intrinsic Rate-Constant and Large Imbalances in the Thiolate Ion Addition to Substituted Alpha-Nitrostilbenes. *J. Am. Chem. Soc.* **1988,** *110* (22), 7506-7512.
27. Winterbourn, C. C.; Metodiewa, D., Reactivity of biologically important thiol compounds with superoxide and hydrogen peroxide. *Free Radical Biol. Med.* **1999,** *27* (3-4), 322-328.
28. Le Barc'H, N.; Grossel, J. M.; Looten, P.; Mathlouthi, M., Kinetic study of the mutarotation of D-glucose in concentrated aqueous solution by gas-liquid chromatography. *Food Chem.* **2001,** *74* (1), 119-124.

29. Cramer, N. B.; Bowman, C. N., Kinetics of thiol-ene and thiol-acrylate photopolymerizations with real-time Fourier transform infrared. *J. Polym. Sci. A Polym. Chem.* **2001,** *39* (19), 3311-3319.
30. Cramer, N. B.; Couch, C. L.; Schreck, K. M.; Carioscia, J. A.; Boulden, J. E.; Stansbury, J. W.; Bowman, C. N., Investigation of thiol-ene and thiol-ene-methacrylate based resins as dental restorative materials. *Dent. Mater.* **2010,** *26* (1), 21-8.
31. Nappi, A. J.; Vass, E., Comparative studies of enhanced iron-mediated production of hydroxyl radical by glutathione, cysteine, ascorbic acid, and selected catechols. *Biochim. Biophys. Acta, Gen. Subj.* **1997,** *1336* (2), 295-302.
32. Siedlecka, E. M.; Wieckowska, A.; Stepnowski, P., Influence of inorganic ions on MTBE degradation by Fenton's reagent. *J. Hazard. Mater.* **2007,** *147* (1-2), 497-502.
33. Walling, C.; Goosen, A., Mechanism of Ferric Ion Catalyzed Decomposition of Hydrogen-Peroxide - Effect of Organic Substrates. *J. Am. Chem. Soc.* **1973,** *95* (9), 2987-2991.
34. Dainton, F. S.; Seaman, P. H., The Polymerization of Acrylonitrile in Aqueous Solution .1. The Reaction Catalyzed by Fenton Reagent at 25-Degrees-C. *J. Polym. Sci.* **1959,** *39* (135), 279-297.
35. Witt, S.; Wohlfahrt, G.; Schomburg, D.; Hecht, H. J.; Kalisz, H. M., Conserved arginine-516 of Penicillium amagasakiense glucose oxidase is essential for the efficient binding of beta-D-glucose. *Biochem. J.* **2000,** *347*, 553-559.
36. Macosko, C. W.; Miller, D. R., New Derivation of Average Molecular-Weights of Nonlinear Polymers. *Macromolecules* **1976,** *9* (2), 199-206.
37. Munday, R., Toxicity of Thiols and Disulfides - Involvement of Free-Radical Species. *Free Radical Biol. Med.* **1989,** *7* (6), 659-673.
38. Wadhwa, S.; Mumper, R. J., D-penicillamine and other low molecular weight thiols: Review of anticancer effects and related mechanisms. *Cancer Lett.* **2013,** *337* (1), 8-21.
39. Hollmann, F.; Arends, I. W. C. E., Enzyme Initiated Radical Polymerizations. *Polymers* **2012,** *4* (1), 759-793.
40. Dordick, J. S.; Marletta, M. A.; Klibanov, A. M., Polymerization of phenols catalyzed by peroxidase in nonaqueous media. *Biotechnol. Bioeng.* **1987,** *30* (1), 31-36.
41. Cai, Z. Q.; Wang, W. C.; Ruan, G.; Wen, X. F., Kinetic study of acrylamide radical polymerization initiated by the horseradish peroxidase-mediated system. *Int. J. Chem. Kinet.* **2012,** *44* (7), 475-481.
42. Kalra, B.; Gross, R. A., Horseradish peroxidase mediated free radical polymerization of methyl methacrylate. *Biomacromolecules* **2000,** *1* (3), 501-505.
43. Pichorner, H.; Couperus, A.; Korori, S. A. A.; Ebermann, R., Plant peroxidase has a thiol oxidase function. *Phytochemistry* **1992,** *31* (10), 3371-3376.
44. Burner, U.; Obinger, C., Transient-state and steady-state kinetics of the oxidation of aliphatic and aromatic thiols by horseradish peroxidase. *FEBS Lett.* **1997,** *411* (2-3), 269-274.
45. Uyama, H.; Kurioka, H.; Kobayashi, S., Novel bienzymatic catalysis system for oxidative polymerization of phenols. *Polym. J.* **1997,** *29* (2), 190-192.
46. Taboada-Puig, R.; Junghanns, C.; Demarche, P.; Moreira, M. T.; Feijoo, G.; Lema, J. M.; Agathos, S. N., Combined cross-linked enzyme aggregates from versatile peroxidase and glucose oxidase: Production, partial characterization and application for the elimination of endocrine disruptors. *Bioresour. Technol.* **2011,** *102* (11), 6593-6599.

Chapter 5

Fabrication of Chitosan-based Hydrogels via Oxygen-mediated Polymerization

Abstract: The in situ formation of hydrogels, assembled form a variety of synthetic and natural materials, is of increasingly vital importance for a variety of biomedical applications. One material that has shown great promise is chitosan, a polysaccharide obtained by the deacetylation of chitin, a natural polysaccharide obtained from crustacean shells. Chitosan is well-known for its biocompatibility, bioadhesion, and, owing to the presence of hydroxyl and amine groups, readily modifiable, allowing the facile introduction of additional functionality. Here, thiolated chitosan was synthesized from chitosan and 2-iminothiolane. Such a modification aids in improving the solubility as well as permitting the material to participate in thiol-based cross-linking reactions. Low-viscosity formulations of thiolated chitosan and poly(ethylene glycol) diallyl ether with an initiating system made of glucose, glucose oxidase, and either Fe^{2+} or horseradish peroxidase were found to rapidly afford hydrogels when exposed to the atmosphere. The progression of the gelation reactions were monitored with parallel plate rheometry and it was found that the gelation mechanism consisted of multiple chemical reactions, including thiol–ene polymerization, disulfide formation, and iron-chitosan interactions.

5.1 Introduction

As demonstrated in the previous chapter, hydrogels may be generated by exposing thiol–ene monomer formulations, containing an initiating system based on oxidoreductase enzymes, to atmospheric oxygen. Two three-component initiating system were explored, one with glucose, glucose oxidase (GOx) and Fe^{2+}, and the other where horseradish peroxidase (HRP) replaced Fe^{2+}. While this work successfully utilized a model monomer system of ethoxylated trimethylolpropane tri(3-mercaptopropionate) (ETTMP) and poly(ethylene glycol) diallyl ether (PEGDAE), the development of materials better suited for biomedical applications, including surgical adhesives and sealants, would be better served by utilizing more sophisticated precursors. One such material that has been extensively investigated for biomaterial applications is chitosan,[1-8] a polysaccharide made by the deacetylation of chitin, a natural polysaccharide obtained from crustacean shells. Interest in chitosan is driven by its excellent biocompatibility, bioadhesion, and, owing to the presence of hydroxyl and amine groups, facile modification.[1, 2] It is especially easy to introduce thiol functionality and the resulting thiolated chitosan (CS-SH) should readily participate in thiol–ene cross-linking reactions. Here, CS-SH was synthesized and, in buffered aqueous solution with PEGDAE, utilized to form hydrogels to rapidly form once exposed to atmospheric oxygen.

5.2 Experimental

5.2.1 Materials and Synthesis

Chitosan (product C2395, 5-20 mPaS, 0.5% in 0.5% acetic acid, 80.7% deacetylated) was purchased from TCI. D-Glucose was purchased from Fisher Scientific and was used as received. Iron(II) sulfate heptahydrate, glucose oxidase from *Aspergillus niger* (GOx,

147.9 U/mg), horseradish peroxidase (HRP, Type VI, 261 purpurogallin U/mg), and acetylacetone (AA) were purchased from Sigma-Aldrich. Cupferron (*N*-nitroso-*N*-phenylhydroxylamine ammonium salt), used as a radical inhibitor to prevent premature polymerization, was obtained from Wako Chemicals. 2-(*N*-Morpholino)ethanesulfonic acid (MES) aqueous buffer (0.1 M MES, pH 4.5) was obtained from Teknova. All materials were used as received.

Thiolated chitosan was synthesized by closely following previously published procedures.[1-3] Briefly, in a flask, 1 gram of chitosan was dissolved in 100 mL of a 1 vol% aqueous acetic acid solution and the pH was raised to 6.5 with 1 M NaOH solution. The flask was purged with nitrogen and 200 mg of Traut's reagent was added; the reaction mixture was then stirred and 24 hours at room temperature. Afterwards, the reaction mixture was dialyzed, using a membrane with a molecular weight cut-off of 3,500 g/mol, four times. The first time with a 5 mM HCl solution for 8 hours, the next two using a 5 mM HCl with 1% NaCl for 8 hours each, and finally with 5 mM HCl for 8 hours. The solution was then lyophilized for 3 days, affording a fibrous white material. The thiolated chitosan was stored under nitrogen at -20ºC to minimize disulphide formation. Thiol content was established by an Ellman's assay[9] performed in triplicate. 6 mg of CS-SH was dissolved in 2 mL phosphate buffer (0.1 M, pH = 8.), and 1 mL Ellman's solution (1 M 5,5'-dithiobis-(2-nitrobenzoic acid) in phosphate buffer). 1 mL of this solution was diluted with two mL of water and the absorbance at 412 nm was measured using an Agilent Technologies Cary 60 UV-Vis spectrophotometer. To calculate thiol concentration, an extinction coefficient of 14250 $M^{-1}cm^{-1}$ was utilized.

Synthesis of poly(ethylene glycol) diallyl ether (10 kg/mol)[10] and LAP[11, 12] were performed by previously described procedures.

All liquid materials were thoroughly degassed by subjecting them to at least six freeze-pump-thaw cycles to ensure complete removal of dissolved oxygen.

5.2.2 Rheometry

Solutions of the hydrogel precursors, either or CS-SH only, were dissolved in 0.1M pH 4.5 MES buffer. CS-SH solutions were mixed over night to ensure complete dissolution. To ensure mutarotation equilibrium,[13] glucose solutions were prepared 24 hours prior to use. GOx and HRP solutions were used within 48 hours of dissolution. Formulations with both CS-SH and PEGDAE were made with a strict 1:1 thiol-to-allyl ether ratio at 2.2 wt% (1.6 wt% CS-SH and 0.6 wt% PEGDAE), while formulations with only CS-SH were made at 1.6 wt; added to the precursor solutions were the initiating system components (i.e., glucose, GOx, $FeSO_4 \bullet 7H_2O$, or HRP) and 0.05 wt% cupferron as an inhibitor.[10]. All components were assembled under oxygen-free conditions in an anaerobic chamber and were tested within six hours, with the exception of $Fe_2(SO_4)_3 \bullet 5H_2O$, which was added immediately before it was tested. All formulations were bubbled with compressed air for 15 seconds, mixed for 15 seconds, and placed on the bottom plate of the rheometer. The top plate, 25 mm in diameter, was positioned to a 0.5 mm gap and measurements, taken every 8 seconds, were started two minutes after initial oxygen exposure using a 1% oscillatory strain at a frequency of 1 Hz. The same procedure was utilized for the photorheometry experiments, except 0.5% LAP, a photoinitiator, was added to all formulations and the rheological measurements were taken with a 20 mm quartz top plate. Once the formulations reached steady state for 10

minutes, the samples were exposed to 365 nm light at an intensity of 25 mW/cm^2 for 15 minutes. All rheometry experiments were performed in triplicate, with the average and standard error reported.

5.3 Results and Discussion

5.3.1 Justification for Utilizing Rheometry in Monitoring Gelation Reaction

Thiolated chitosan (CS-SH) was produced by reacting chitosan with 2-iminothiolane (i.e. Traut's reagent) (Scheme 29).[3] Using Ellman's assay,[9] absorption at 412 nm was 0.64±0.03; by utilizing an extinction coefficient of 14250 M^{-1} cm^{-1},[9] this absorbance corresponds to a thiol concentration of 67.6 μmol/g. While somewhat lower than previously reported values, Ponchel and coworkers reported a concentration of 213 μmol/g,[3] there are several advantages to having low functional group concentration, notably that the CS-SH is more likely to retain the useful properties of CS and that the demand for the allyl ether-functional monomer is low, ensuring that the percentage of CS-SH in the cross-linked polymer network remains quite high. Conversely, the low concentration of functional groups makes it difficult to monitor cross-linking reactions (i.e., the consumption of thiol and allyl ether groups to form thioethers) spectroscopically. Previous methods utilized IR spectroscopy to monitor the changes in the allyl ether peak at 6100 cm-1.[10] While the absorbance of this overtone peak is typically low, it has proven quite useful for monitoring thiol–ene polymerization reactions, particularly with low molecular weight model monomers previously utilized that allow for the formulation of concentrated aqueous solutions that are dense with functional groups.[10] For example, in the previous chapter, the aqueous solution monomer solution contained 15.4 wt% PEGDAE and 19.6 wt% ETTMP, corresponding to 445 mM allyl ether. Such a high

monomer concentration was necessary to provide an absorbance at 6100 cm-1 that could be adequately measured, though even at this concentration allyl ether absorbance was still relatively small and noisy. Unfortunately, when preparing aqueous solution of CS-SH, increasing solution concentration leads to excessively high viscosities and the resulting solution are quite difficult to work with. For the work described here, a CS-SH solution of 1.6 wt% was utilized as it was of sufficiently low viscosity to easily handle; this concentration yielded formulations with a thiol concentration of 1.1 mM. As all formulations here maintained a strict 1:1 thiol-to-ene ratio, adding an equivalent amount of PEGDAE results in a solution with 1.1 mM allyl ether groups, far lower than the model monomer formulation utilized in the previous chapter. Attempts to monitor the allyl ether peak at 6100 cm-1 failed as its intensity was so low it was buried in the noise. Moreover, the stronger absorbance of the allyl ether peak at 3100 cm-1 and the thiol peak at 2500 cm-1 lie within the region where water strongly absorbs, rendering these peak unusable as well.

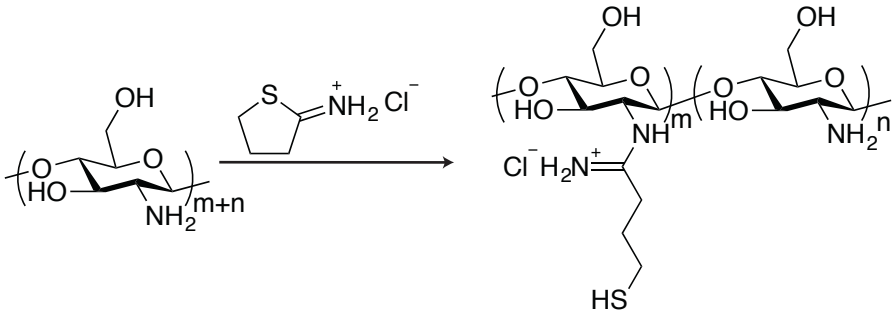

Scheme 29: Synthesis of thiolated chitosan from chitosan and 2-iminothiolane (i.e., Traut's reagent).

As IR spectroscopy proved ill-suited for monitoring the thiol–ene polymerization of aqueous CS-SH/PEGDAE formulations, parallel plate rheometry was utilized instead. Rather than monitoring the change in functional group concentrations, rheometry will

measure the change in shear storage modulus (G′) as the formulations transform, as a result of oxygen-mediated polymerization, from low viscosity liquid to cross-linked hydrogels. Admittedly, this method has a drawback: oxygen can only diffuse into the sample material from the sides, creating a gradient from the edges to the center for both oxygen and reaction extent. Nonetheless, as will be evident throughout this discussion, parallel plate rheometry proved quite useful in monitoring gelation.

5.3.2 Glucose/GOx/Fe^{2+} Initiating Systems

Using the work from the previous chapter as a model, CS-SH/PEGDAE aqueous formulations containing the glucose, GOx, Fe^{2+} initiating system were evaluated for their capacity to undergo gelation in response to exposure to the atmosphere. As the previously described work attained a maximum polymerization rate and extent using 56 mM glucose, 14.7 kU/L GOx, and72 μM, these concentrations were utilized with the CS-SH/PEGDAE formulations; after exposing the formulation to the atmosphere, G′ increases from approximately 0.1 Pa to over 1000 Pa in less than 25 minutes – a change of over 4 orders of magnitude (see Figure 30).

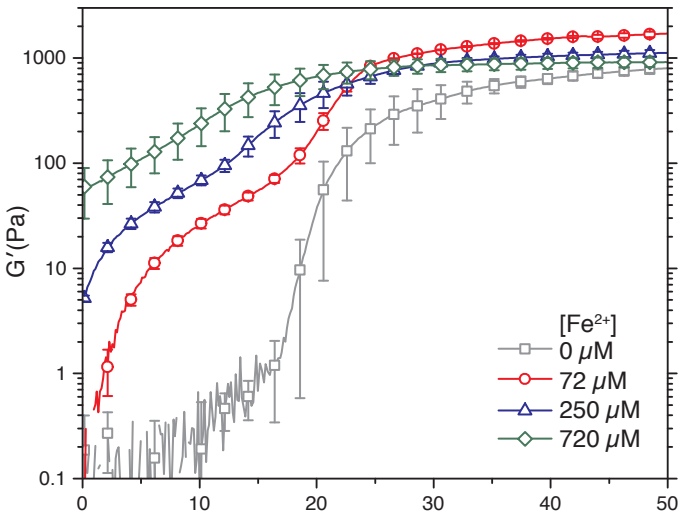

Figure 30: Influence of initial Fe^{2+} concentration on G'. Storage moduli are shown for aqueous CS-SH/PEGDAE solutions formulated with glucose, GOx, and Fe^{2+} (56mM, 14.8 kU/L, and concentrations as shown in legend, respectively) upon exposure to air.

With the glucose/GOx/Fe^{2+} initiating system, increasing the concentration of Fe^{2+} beyond 72 μM in the ETTMP/PEGDAE model monomer formulation lead to a decrease in reaction rates and extents owing to the influence of unwanted radical-destroying side reactions. However, with the CS-SH/PEGDAE formulation, reaction rates *increased* with Fe^{2+} concentration. In fact, at the 720 uM Fe^{2+}, the highest concentration attempted, the formulation was gelling as it was being pipetted on the bottom plate of the rheometer – approximately one minute after the formulation was first exposed to the atmosphere. While this result is certainly exciting as it convincingly demonstrates rapid hydrogel formation upon exposure to the atmosphere, it was entirely unexpected and requires further exploration. It appears that the presence of chitosan prevents one or more of the iron-mediated polymerization retarding reactions; one plausible explanation is that Fe^{2+} ions, included as part of the initiating system, or Fe^{3+} ions, formed in the Fenton reaction,

complex with the chitosan[14] in such a manner that hinders the capacity of the iron ions to undergo radical eliminating reactions.

Interestingly, not only was unexpected behavior observed at the highest Fe^{2+} concentration, but also in its absence. For CS-SH/PEGDAE formulations with glucose and GOx and no Fe^{2+}, gelation was observed after oxygen exposure, with G′ reaching nearly 1 kPa after 50 minutes. While gelation of this formulation was undoubtedly slower than those with Fe^{2+}, indeed there was an induction period where it took approximately 15 minutes for G′ to exceed 1 Pa, the fact that it gelled at all is remarkable; with the model ETTMP-TMPTAE monomer formulation, essentially no reaction was observed when Fe^{2+} was omitted.[10] Hydrogen peroxide, while it may be part of a radical-affording initiating system (e.g., along with Fe^{2+} or HRP),[10] would not be expected to initiate thiol–ene polymerization by itself. Thus, it is quite surprising to observe gelation without a clear means of generating the polymerization-initiating radicals. One tenable explanation is that gelation almost certainly involves the thiol groups in a redox reaction: in the presence of an oxidant, thiols will form disulfides.[15] In fact, this reaction has been intentionally utilized to form hydrogels. For example, the thiol groups naturally-present from cysteine residues in the protein albumin,[15] or those present on modified polysaccharides, including alginate,[16] hyaluronic acid,[17] and chitosan,[1, 4] can be readily oxidized to form disulfide cross-links. In a specific example, aqueous solutions of thiolated chitosan gelled after several hours when the temperature was increased to 37ºC, the pH increased to 7.4, and the solution was exposed to the atmosphere.[4] So while hydrogel-formation resulting from disulfide formation has been explored previously, the gelation times for the system described here seems somewhat faster.

The gelation mechanism of the CS-SH/PEGDAE formulations, based solely as on the results shown in Figure 30, has already been shown to differ significantly from the results obtained previously with the model ETTMP/PEGDAE monomer system. To gain further insight into the reactions responsible for gelation, a series of control experiments were performed where various components of the formulation were removed. The first of these series removed both glucose and GOx, and varied the concentration of Fe^{2+}. When Fe^{2+} was omitted, no gelation was observed and the G′ remained at 1 Pa or less over the entire 50 minute experiment; similar results were observed when 72 μM Fe^{2+} was added. Increasing the concentration of Fe^{2+} to 720 μM lead to the G′ increasing to approximately 3 Pa after 50 minutes, though still no gelation was observed. This minor increase in G′ is readily attributed to a reaction noted previously with the model ETTMP/PEGDAE monomer system: two equivalents of Fe^{2+} reduces oxygen to hydrogen peroxide, while a third is necessary for the radical generating Fenton reaction (Scheme 27). Despite this gentle increase in G′ at 720 μM Fe^{2+}, these result convincingly demonstrate that oxygen and Fe^{2+}, without the hydrogen peroxide-generating action of glucose and glucose oxidase, are insufficient in effecting any significant gelation reaction.

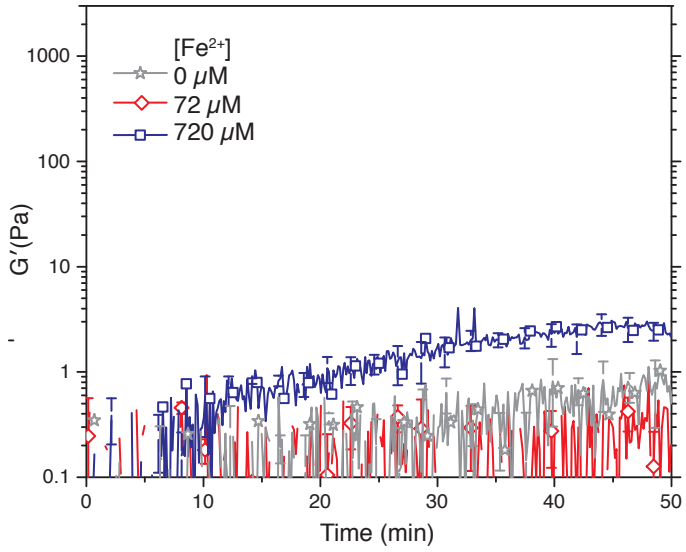

Figure 31: Influence of initial Fe^{2+} concentration on G' in the absence of glucose or GOx. Storage moduli are shown for aqueous solutions of CS-SH and PEGDAE formulated with varying amounts of Fe^{2+} (concentrations as shown in legend).

Far more interesting are the results obtained in a series where PEGDAE was omitted. Here, a glucose, GOx, Fe^{2+} initiating system was included in an aqueous formulation with CS-SH. As there is no allyl ether functionality present, no thiol–ene reaction is possible and, one would expect, no gelation would occur when this formulation was exposed to the atmosphere. Nonetheless, despite expectations, these formulations did gel upon exposure to atmospheric oxygen. Upon reflection, this should not have been a surprise: as noted above, water-soluble, thiol-containing precursors have readily been converted into hydrogels through the formation of disulfide linkages. [1, 4, 15-17] Indeed, here there may be several routes to disulfide formation. For all of the formulations, whether or not they contain Fe^{2+}, the hydrogen peroxide, formed by the GOx-catalyzed oxygen reduction, may be able to oxidize the thiols into disulfides; for those formulations that do contain Fe^{2+}, the thiyl radicals, formed by the abstraction of

thiol hydrogens from the Fenton reaction-generated hydroxyl radicals (Equation 10), may undergo radical-radical termination reactions that afford disulfides.[18]

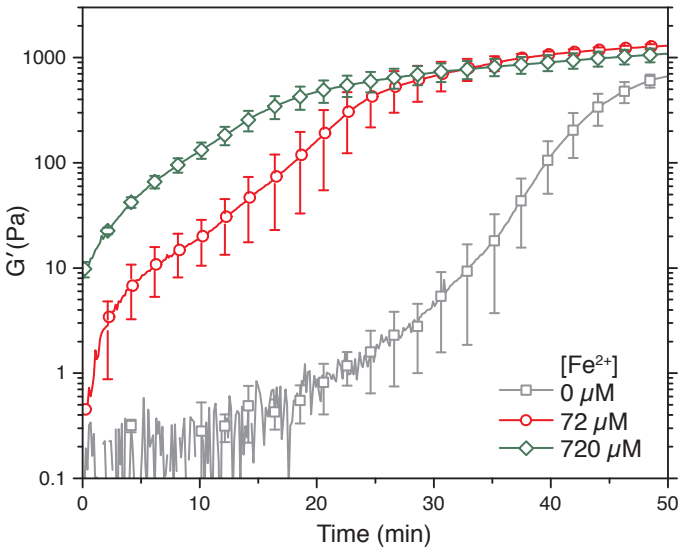

Figure 32: Influence of initial Fe^{2+} concentration on G' for formulations without PEGDAE. Storage moduli are shown for aqueous CS-SH solutions formulated with glucose, GOx, and Fe^{2+} (56mM, 14.8 kU/L, and concentrations as shown in legend, respectively) upon exposure to air.

In addition to the potential for both thioether and disulfide linkages to form, there is another plausible cross-linking reaction: the formation of ionic cross-links between iron ions and CS-SH. As noted above, Fe^{3+} ions are known to complex with chitosan[14] and this was brought forth as a plausible explanation for the lack of apparent iron-mediated inhibition reactions. An alternative explanation is that Fe^{3+} ions, generated through the Fenton reaction, ionically cross-link CS-SH, driving the increase in G′. To further explore the influence of Fe^{3+} ions, G′ of an aqueous solution of CS-SH with 720 μM Fe^{3+} was again monitored after exposure to the atmosphere – for comparison, a analogous formulation with Fe^{2+} ions was also examined. As the potential exists for Fe^{3+} ions to cross-link chitosan even in the absence of oxygen,[14] the Fe^{3+} was added

concomitant to oxygen exposure. For both Fe^{2+} and Fe^{3+}-based formulations, G′ only exhibited modest increases, reaching approximately 2 Pa, after 50 minutes and no gelation was observed– results that are quite similar to the 720 uM Fe^{2+} formulation, shown in Figure 31, that included PEGDAE as well as CS-SH. Thus, over the 50 minutes that were monitored via rheometry, the action of oxygen iron ions alone does not induce gelation. However, very different results were observed when glucose and GOx where added to a CS-SH solution with 720 μM Fe^{3+}. Here, G′ rises quickly and the reaction trajectory resembles the one observed with a glucose, GOx, and 720 μM Fe^{2+} initiating system (Figure 32), demonstrating that behavior with either Fe^{2+} or Fe^{3+}, in the presence of both glucose and GOx, is quite similar.

From this, there are several plausible explanations. One possibility is that Fe^{3+} ions may undergo Fenton reactions with H_2O_2,[19, 20] leading to the formation of radicals and Fe^{2+} ions that can, as seen previously, afford radicals (Equations 3–6). (These Fe^{3+} Fenton reactions were discussed in the previous chapter.) While this seems realistic, there may be an alternative explanation: interactions between iron ions and chitosan may be contributing to the observed rise in G′ after oxygen exposure. Chitosan, owing to the presence of multiple hydroxyl and amine groups, has been demonstrated to strongly coordinate with metal ions, including Fe^{3+},[14] and has been explored as means of removing Fe^{3+} aqueous solutions,[21] making it plausible that Fe^{3+} cross-links are at least partially responsible for the rise in G′ observed after oxygen exposure. Moreover, while ions have been used to cross-link anionic polysaccharides like alginates,[22] it is not obvious if Fe^{2+} is capable of doing so for chitosan. Thus it is likely that the increase in G′, observed with the glucose, GOx, Fe^{2+} initiating system (Figure 30), depends not only

on the formation of thioethers and disulfide linkages, but also upon the rapid formation of Fe^{3+},via the Fenton reaction, and its capacity for forming ionic cross-links. Clearly, this role of iron ions in this system is quite complex and warrants further investigation.

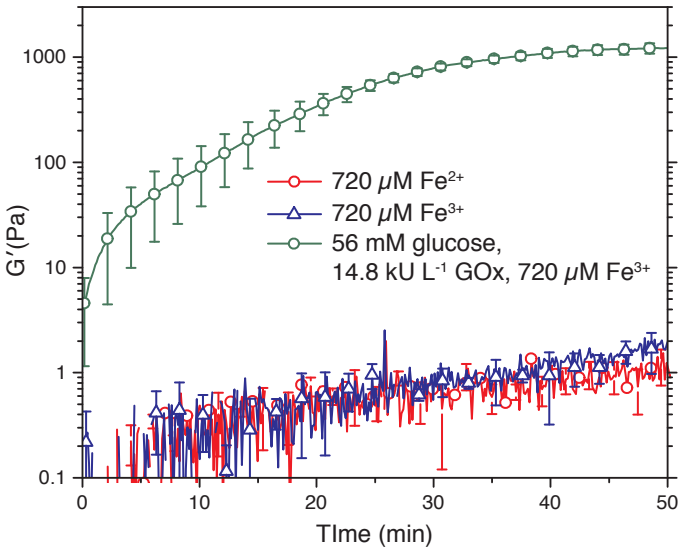

Figure 33: Influence of Fe^{3+} concentration on G' for formulations without PEGDAE. Storage moduli are shown for aqueous CS-SH solutions formulated with glucose, GOx, and Fe^{3+} or Fe^{2+} (concentrations as shown in legend) upon exposure to air.

5.3.3 Photo-mediated Breaking of Disulfide Linkages

In the above discussion, it is apparent that there are several reactions leading to an increase in G′ upon oxygen exposure, including disulfide formation. To confirm that disulfide formation is one of the cross-linking reactions contributing to oxygen-mediated gelation, photorheometry experiments were performed. Following work by Anseth and coworkers,[23] a lithium acyl phosphinate (LAP) water-soluble photoinitiator was added, at 0.5 wt%, to two formulations: one with CS-SH and PEGDAE with an initiating system of 56 mM glucose, 14.8 kU/L GOx, and 720 μM Fe^{2+} and the other with only CS-SH and 720 μM Fe^{2+}. The addition of the photoinitiator permitted the destruction of disulfide bonds (see Scheme 30a),[23] while leaving any thioethers unaffected,[24] upon light exposure

and photorheometry (see Scheme 30b) allowed for the real-time observation of the resultant change in G′. It was expected that the formulation with both CS-SH and PEGDAE would contain a significant quantity of thioether linkages, while the formulation with only CS-SH could only be cross-linked through disulfides; thus, when each of these formulations were exposed to UV light, it was expected that the G′ of CS-SH/PEGDAE formulation would stay close to its original value, while the G′ of the CS-SH-only formulation would decrease significantly.

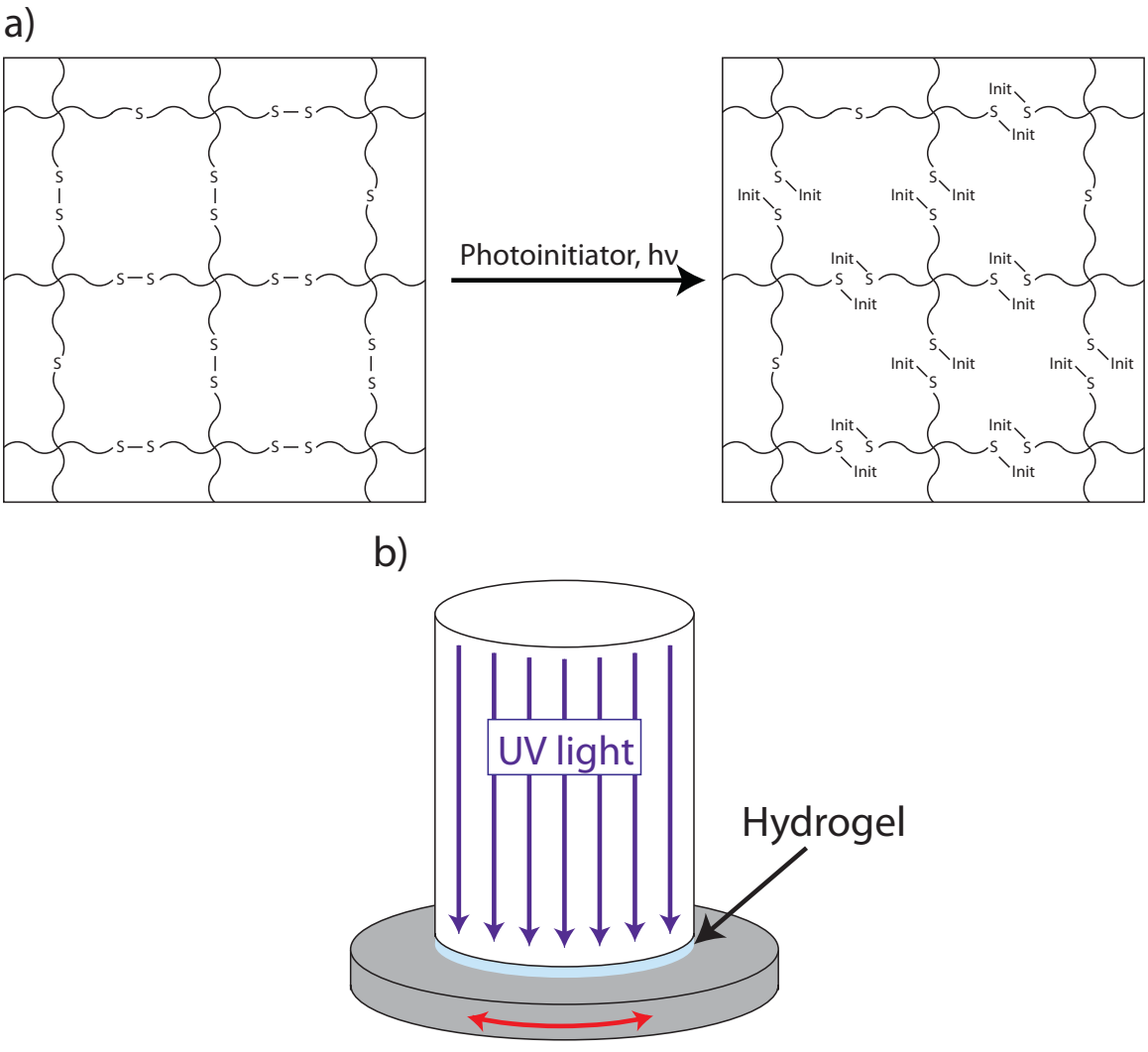

Scheme 30: Photo-induced destruction of disulfide bonds, monitored by photorheometry. A) A hypothetical network polymer cross-linked by both thioethers

and disulfides is exposed to ultraviolet light in the presence of a photoinitiator. Radicals form the photo-induced dissociation of the photoinitiator react with disulfides, resulting in the disulfides being broken and causing a decrease in cross-link density.[23] B) The resulting change in G' was monitored by photorheometry.

As before, each formulation was exposed to the atmosphere, placed on the rheometer, and allowed to gel. With G′ at steady state, the hydrogel was exposed to UV light and G′ was monitored for 15 minutes afterward (see Figure 34). Over 15 minute of UV light exposure, the G′ of the formulation with both CS-SH and PEGDAE decrease to 170 Pa, a far greater decrease than expected, while the CS-SH-only formulation saw the G′ drop to 90 Pa, less of a decrease than predicted. While the results in Figure 34 convincingly demonstrate the significant quantity of disulfides in both formulations, drawing any other real conclusions is troublesome owing to several experimental difficulties. One issue is that, in the presence of CS-SH, the LAP photoinitiator tended to stabilize the formation of foam and that is was not possible to remove all of the air bubbles while bubbling and mixing the formulations. Another issue is that, owing to the 20 mm diameter of the top rheometer plate, the solution at the center will receive less oxygen than the material at the edges, causing the center material to be less-fully cured than the edges. When material with any unreacted functionality is exposed to UV light, the radicals afforded from the photoinitiator will likely lead to the formation of cross-links, causing G′ to increase and counteracting the decrease caused by the destruction of disulfides. Therefore, all that can be safely concluded from the photorheometry experiments is that there are significant disulfide concentrations in both CS-SH/PEGDAE and CS-SH-only formulations.

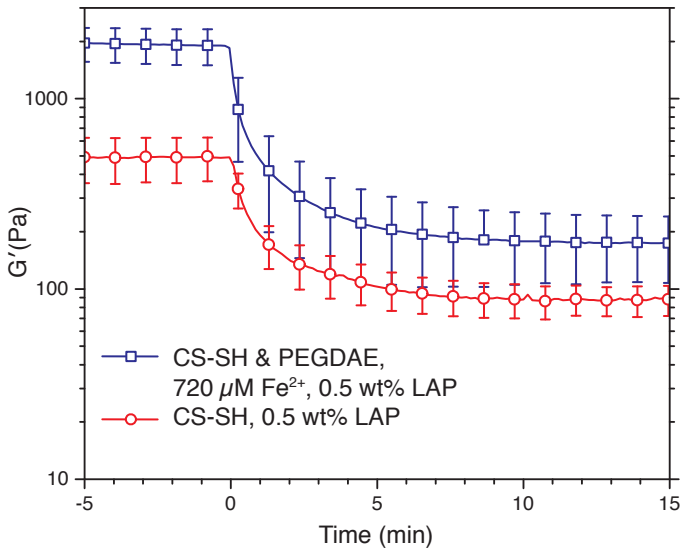

Figure 34: Monitoring decrease in G' as a result of photo-induced disulfide breaking* via photorheometry.** ***Two formulations with glucose and GOx (56mM, 14.8 kU/L, respectively) and additional components (listed in the legend) were allowed to gel and then exposed to 365 nm light with an intensity of 25 mW/cm^2. X-axis is the time after light exposure (i.e., light was turned on at t = 0 min).

5.3.4 Glucose/GOx/HRP Initiating Systems

As shown above (Figure 30, Figure 32, and Figure 33), iron ions contribute significantly to the cross-linking of CS-SH as does the formation of disulfide linkages, as seen in the photorheometry experiments (Figure 34). There is also evidence for the formation of thioether linkages formed via the radical-mediated thiol–ene reaction, though, unexpectedly, the evidence is somewhat more subtle than initially predicted. For example, the G′ of CS-SH/PEGDAE formulations with the glucose, GOX, Fe^{2+} initiating system (Figure 30) increases slightly more rapidly than the corresponding CS-SH-only formulations (Figure 32). In order to better demonstrate that the radical-mediated thiol–ene reaction, leading to the formation of thioether linkages, is also a major contributor to the cross-linked network, an alternative three-component initiating system was investigated, one that replaced the Fe^{2+} ions with HRP. This change eliminates the

possibility of iron-chitosan interactions contributing the gelation, leaving only thioether or disulfide linkages as potential cross-linking moieties.

As with the Fe^{2+}-based initiating system, gelation of CS-SH-based formulations after exposure to the atmosphere was monitored with parallel plate rheometry; four HRP-based formulations were attempted (Figure 34). As a control, an initiating system that contained only HRP and no glucose or GOx was evaluated; G′ only increased to approximately 1 Pa, even less than the analogous iron-only formulations (Figure 31 and Figure 33). While it is possible for HRP to act as a thiol oxidase, and was demonstrated to do so with the model ETTMP/PEGDAE monomer system of the previous chapter, such a route does not make a major contribution to gelation here. However, once glucose and GOx are included along with HRP, CS-SH/PEGDAE formulations exhibit rapid gelation, particularly at the highest concentration of HRP utilized (261 kU L^{-1}), with G′ exceeding 1 kPa; this formulation, as had the one discussed above with 720 μM Fe^{2+},(Figure 30) started gelling before the rheological measurements could be started – that is, it formed a hydrogel within a minute of oxygen exposure. A strong increase in G′ was also observed when the HRP concentration was decreased to 26.1 kU L^{-1}, with this formulation also exceeding 1 kPa. Interestingly, a short induction period, not seen in any of the analogous Fe^{2+}-based formulations, was observed in the 26.1 kU L^{-1} formulation. Induction periods have frequently been reported for HRP-based initiating system and, in a strategy that was utilized here, have been overcome simply by increasing initiating system concentrations.[25] The remaining HRP-based experiment utilized a formulation that included CS-SH, glucose, GOx, HRP and omitted PEGDAE. While G′ increased upon oxygen exposure, it never exceeded 200 Pa, far less than the formulations with

PEGDAE. Any increase in G′ with the PEGDAE-free formulations could only be caused by disulfide formation. Thus, for the formulation with PEGDAE, a major contributing factor to the increase in G′ has to be thioether linkages generated from the radical-mediated thiol–ene reaction.

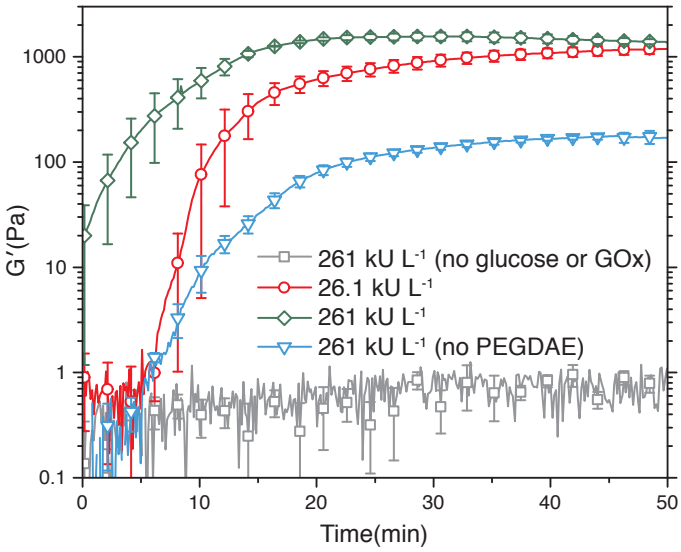

Figure 35: Influence of HRP concentration on G'. Storage moduli are shown for aqueous solutions of CS-SH and, except where noted, PEGDAE formulated with glucose, GOx, and HRP (56mM, 14.8 kU/L, and concentrations as shown in legend, respectively) upon exposure to air.

5.4 Conclusion

Here, aqueous formulations of thiolated chitosan and PEGDAE, with initiating systems composed of glucose, GOx, and either Fe^{2+} or HRP, were rapidly transformed into hydrogels simply by exposing the formulations to the atmosphere. The gelation mechanism is complex, with multiple reactions contributing to the observed increased in G′ after oxygen exposure. While the radical-mediated thiol–ene reaction, predicted to be the dominating gelation reaction, was certainly a major contributor, disulfide formation and iron-chitosan interactions were also responsible for the observed oxygen-mediated

hydrogel formation. Despite the complexity of this gelation process, the rapid reaction rates achieved here convincingly demonstrate that thiolated chitosan-based formulations should be investigated as biomedical adhesives and sealants.

5.5 References:

1. Bernkop-Schnurch, A.; Hornof, M.; Zoidl, T., Thiolated polymers-thiomers: synthesis and in vitro evaluation of chitosan-2-iminothiolane conjugates. *Int. J. Pharm.* **2003,** *260* (2), 229-237.
2. Bernkop-Schnurch, A.; Guggi, D.; Pinter, Y., Thiolated chitosans: development and in vitro evaluation of a mucoadhesive, permeation enhancing oral drug delivery system. *J. Contr. Rel.* **2004,** *94* (1), 177-186.
3. Bravo-Osuna, I.; Schmitz, T.; Bernkop-Schnurch, A.; Vauthier, C.; Ponchel, G., Elaboration and characterization of thiolated chitosan-coated acrylic nanoparticles. *Int. J. Pharm.* **2006,** *316* (1-2), 170-175.
4. Wu, Z. M.; Zhang, X. G.; Zheng, C.; Li, C. X.; Zhang, S. M.; Dong, R. N.; Yu, D. M., Disulfide-crosslinked chitosan hydrogel for cell viability and controlled protein release. *Eur. J. Pharm. Sci.* **2009,** *37* (3-4), 198-206.
5. Choi, J. S.; Yoo, H. S., Pluronic/chitosan hydrogels containing epidermal growth factor with wound-adhesive and photo-crosslinkable properties. *J. Biomed. Mat Res. A* **2010,** *95* (2), 564-73.
6. Francesko, A.; Tzanov, T., Chitin, chitosan and derivatives for wound healing and tissue engineering. *Adv. Biochem. Eng. Biotechnol.* **2011,** *125*, 1-27.
7. Ryu, J. H.; Lee, Y.; Kong, W. H.; Kim, T. G.; Park, T. G.; Lee, H., Catechol-functionalized chitosan/pluronic hydrogels for tissue adhesives and hemostatic materials. *Biomacromolecules* **2011,** *12* (7), 2653-9.
8. Dash, M.; Chiellini, F.; Ottenbrite, R. M.; Chiellini, E., Chitosan-A versatile semi-synthetic polymer in biomedical applications. *Prog. Polym. Sci.* **2011,** *36* (8), 981-1014.
9. Boyer, C.; Bulmus, V.; Davis, T. P., Efficient Usage of Thiocarbonates for Both the Production and the Biofunctionalization of Polymers. *Macromol. Rapid Commun.* **2009,** *30* (7), 493-497.
10. Zavada, S. R.; McHardy, N. R.; Scott, T. F., Oxygen-mediated enzymatic polymerization of thiol-ene hydrogels. *J. Mater. Chem. B* **2014,** *2* (17), 2598-2605.
11. Fairbanks, B. D.; Schwartz, M. P.; Bowman, C. N.; Anseth, K. S., Photoinitiated polymerization of PEG-diacrylate with lithium phenyl-2,4,6-trimethylbenzoylphosphinate: polymerization rate and cytocompatibility. *Biomaterials* **2009,** *30* (35), 6702-6707.
12. Majima, T.; Schnabel, W.; Weber, W., Phenyl-2,4,6-Trimethylbenzoylphosphinates as Water-Soluble Photoinitiators - Generation and Reactivity of O=P(C6h5)(O-) Radical-Anions. *Makromol. Chem.* **1991,** *192* (10), 2307-2315.
13. Le Barc'H, N.; Grossel, J. M.; Looten, P.; Mathlouthi, M., Kinetic study of the mutarotation of D-glucose in concentrated aqueous solution by gas-liquid chromatography. *Food Chem.* **2001,** *74* (1), 119-124.
14. Hernandez, R. B.; Franc, A. P.; Yola, O. R.; Lopez-Delgado, A.; Felcman, J.; Recio, M. A. L.; Merce, A. L. R., Coordination study of chitosan and Fe3+. *J. Mol. Struct.* **2008,** *877* (1-3), 89-99.
15. Sun, Y. L.; Huang, Y. B., Disulfide-crosslinked albumin hydrogels. *J. Mater. Chem. B* **2016,** *4* (16), 2768-2775.

16. Zhao, Y. Y.; Gao, S. Q.; Zhao, S.; Li, Y. M.; Cheng, L.; Li, J. J.; Yin, Y. J., Synthesis and characterization of disulfide-crosslinked alginate hydrogel scaffolds. *Mat. Sci. Eng. C Mater.* **2012,** *32* (8), 2153-2162.
17. Shu, X. Z.; Liu, Y. C.; Luo, Y.; Roberts, M. C.; Prestwich, G. D., Disulfide cross-linked hyaluronan hydrogels. *Biomacromolecules* **2002,** *3* (6), 1304-1311.
18. Hoyle, C. E.; Lowe, A. B.; Bowman, C. N., Thiol-click chemistry: a multifaceted toolbox for small molecule and polymer synthesis. *Chem. Soc. Rev.* **2010,** *39* (4), 1355-1387.
19. Walling, C.; Goosen, A., Mechanism of Ferric Ion Catalyzed Decomposition of Hydrogen-Peroxide - Effect of Organic Substrates. *J. Am. Chem. Soc.* **1973,** *95* (9), 2987-2991.
20. Siedlecka, E. M.; Wieckowska, A.; Stepnowski, P., Influence of inorganic ions on MTBE degradation by Fenton's reagent. *J. Hazard. Mater.* **2007,** *147* (1-2), 497-502.
21. Burke, A.; Yilmaz, E.; Hasirci, N.; Yilmaz, O., Iron(III) ion removal from solution through adsorption on chitosan. *J. Appl. Polym. Sci.* **2002,** *84* (6), 1185-1192.
22. Li, G. X.; Du, Y. M.; Tao, Y. Z.; Deng, H. B.; Luo, X. G.; Yang, J. H., Iron(II) cross-linked chitin-based gel beads: Preparation, magnetic property and adsorption of methyl orange. *Carbohyd. Polym.* **2010,** *82* (3), 706-713.
23. Fairbanks, B. D.; Singh, S. P.; Bowman, C. N.; Anseth, K. S., Photodegradable, Photoadaptable Hydrogels via Radical-Mediated Disulfide Fragmentation Reaction. *Macromolecules* **2011,** *44* (8), 2444-2450.
24. Valkevich, E. M.; Guenette, R. G.; Sanchez, N. A.; Chen, Y. C.; Ge, Y.; Strieter, E. R., Forging Isopeptide Bonds Using Thiol-Ene Chemistry: Site-Specific Coupling of Ubiquitin Molecules for Studying the Activity of Isopeptidases. *J. Am. Chem. Soc.* **2012,** *134* (16), 6916-6919.
25. Zavada, S. R.; Battsengel, T.; Scott, T. F., Radical-Mediated Enzymatic Polymerizations. *Int. J. Mol. Sci.* **2016,** *17* (2).

Chapter 6

Oxygen-mediated Polymerization Initiated by Oltipraz Derivative

Abstract: A pyrrolopyrazine-thione derived from oltipraz, a compound that has been investigated as a chemopreventive agent, affords radicals in the presence of thiols and oxygen via a redox cycle, an attribute that suggests its suitability as an initiator for oxygen-mediated polymerization. Here, we explore the utilization of this pyrrolopyrazine-thione, generated in situ from a precursor, as an initiator for the radical-mediated thiol–ene polymerization. While the pyrrolopyrazine-thione was shown to be capable of generating radicals in the presence of atmospheric oxygen and thiol groups, the reaction extents achievable were lower than desired owing to the presence of unwanted side reactions that would quench radical production and, subsequently, suppress polymerization. Moreover, we found that complex interactions between the pyrrolopyrazine-thione, its precursor, oxygen, and thiol groups determine whether or not the quenching reaction dominates over those favorable to polymerization.

6.1 Introduction

Numerous applications, including paints, coatings, and adhesives, rely on in situ polymerization, where a liquid monomer formulation is transformed, via a polymerization reaction, into a solid polymer in the location where the material is utilized. This transformation is effected by exposing the liquid monomer formulation to some initiation stimulus, most commonly light,[1] elevated temperature,[2] or a chemical reactant.[3] Often, the chemical stimulus, frequently labelled as a 'cross-linker', 'curing agent', or 'hardener', is packaged separately from the primary liquid monomer resin and the polymerization reaction only proceeds upon mixing of the reaction components. These two-component systems, examples of which include epoxy adhesives[4] and urethane coatings,[5] usually require precise mixing of the two reactants as deviating from the ideal ratio could lead to incomplete cross-linking, hindering the development of optimal properties. Alternatively, instead of storing the reactants in separate packages, the polymerization can rely upon a compound that is naturally and reliably present in the environment where the resultant polymer will be utilized. The development of suitable systems that respond to such environmentally-borne initiation stimuli could permit rapid advances in several emerging technologies, notably self-healing materials and surgical adhesives.

The list of environmentally-borne, chemical initiation stimuli primarily includes components of the atmosphere. Of these, nitrogen[6] and argon[7] can be readily dismissed owing to their low reactivity; carbon dioxide can similarly be discarded for being relatively unreactive[8] as well as its typically low atmospheric concentration. This leaves water[9-11] and oxygen,[12-14] both of which have been employed as polymerization initiation

stimuli. The utilization of atmospheric moisture is especially well known for initiating the polymerization of alkyl cyanoacrylates. In the presence of moisture or any weak nucleophile, alkyl cyanoacrylates undergo anionic polymerization, yielding poly(alkyl cyanoacrylates).[9] Of these, shorter chain (e.g., methyl and ethyl) alkyl cyanoacrylates are utilized for commonly-available consumer glues, while the longer alkyl chain (e.g., octyl) variants serve as surgical-grade adhesives owing to their hydrolysis resistance and thus improved biocompatibility.[15, 16] In addition to alkyl cyanoacrylates, moisture-cured isocyanate-based coatings[11] and silicone-based sealants[10] utilize atmospheric water to effect polymerization. Nevertheless, while moisture-cured adhesives and coatings certainly play an important role in many commercial products, there are inherent drawbacks that preclude their broader adoption in new applications. Notably, the reaction rates are strongly dependent upon the relative humidity, with polymerization nearly ceasing at very low concentrations of atmospheric moisture.[17, 18] Moreover, there are serious limitations as to the types of chemistries that can be utilized in a moisture-curing system: any system that reacts with water may also react with many weakly nucleophilic moieties, severely limiting the type of functional groups that can be present. Thus, in searching for a broadly applicable environmentally-borne initiation stimulus, we are left with atmospheric oxygen, a particularly promising candidate given its relatively high atmospheric concentration and its reactivity.

Oxygen has long served as the initiator for oil-based paints and coatings, where unsaturated fatty acids are cross-linked through sluggish oxygen-mediated reactions, catalysed by metal driers; oil-based paints typically do not fully cure until weeks or months after application.[19] A more generally useful free-radical polymerization

mechanism is one based on the radical-mediated chain-growth polymerization of vinyl monomers, notably acrylates and methacrylates,[20] whereby formulations of monomers and a latent initiating species polymerize rapidly by exposing the initiator to its radical-generating stimulus. Although oxygen is well-suited for generating polymerization-initiating radicals, owing to its capacity for participating in redox reactions,[21] radical-mediated chain-growth polymerizations are typically strongly inhibited by oxygen.[22]

The radical-mediated thiol–ene addition reaction, where a thiol and an electron-rich double bond form a thioether linkage, proceeds in the presence of radicals.[23, 24] In contrast to conventional radical-mediated chain-growth polymerizations, the ready hydrogen abstractability from the ubiquitous thiol functionalities in thiol–ene formulations affords a mechanism that is extraordinarily resistant to molecular oxygen at atmospheric concentrations. Notably, the utilization of oxygen to initiate thiol–ene polymerization has already been established. One such system utilized oxidoreductase enzymes as the basis for initiating systems capable of converting aqueous thiol–ene monomer formulations into hydrogels upon exposure to the atmosphere.[14] Another system employed alkylboranes, species capable of rapidly generating free radicals in the presence of oxygen.[25] While both of these systems have utility, there are limitations: enzymes may lack stability in non-aqueous systems, while the extreme reactivity of alkylboranes may also lead to long-term stability problems. Given these limitations, there remains a need to develop alternative oxygen-mediated polymerization approaches.

Interestingly, one such alternative approach arises from cancer research. 1,2-Dithiole-3-thiones, a class of compounds to which the cancer chemopreventive drug oltipraz belongs, have been shown to induce cellular production of chemoprotective

phase II detoxification enzymes.[26] The major metabolite of oltipraz is a pyrrolopyrazine-thione, which is produced in the presence of glutathione, an intracellular tripeptide thiol. This pyrrolopyrazine metabolite is relatively stable in the absence of oxygen; however, in the presence of further thiol and oxygen, thiyl and peroxy radicals are formed. Moreover, the metabolite can be conveniently liberated in situ via the action of thiol on 7-methyl-6,8-bis(methyldisulfanyl) pyrrolo[1,2-a]pyrazine (for brevity, referred to as the 'bis-disulfide' or 'bisDS'), a disulfide precursor (see Scheme 31a).[27] Thus, an approach utilizing such compounds appears particularly well-suited to the oxygen-mediated initiation of a thiol–ene polymerization. Whereas a thiol–ene resin formulated with a disulfide precursor in an inert atmosphere would form the pyrrolopyrazine-thione intermediate in situ, exposure to oxygen would subsequently generate radicals capable of initiating the polymerization. Here we investigate the suitability of bisDS as an oxygen-mediated initiator for thiol–ene polymerization.

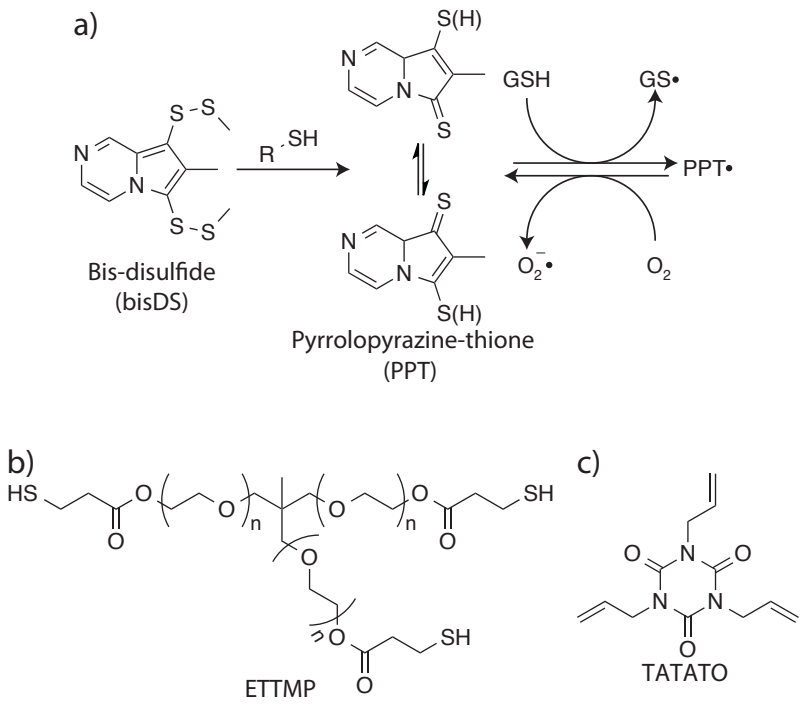

Scheme 31: Structures of the oxygen-mediated initiator and monomers used. a) The bis-disulfide (bisDS) derivative of oltipraz is converted to a PPT intermediate by reaction with a thiol. Subsequently, in the presence of both thiol and oxygen, the PPT participates in a radical-generating redox cycle.[28] b) Ethoxylated trimethylolpropane tri(3-mercaptopropionate) (ETTMP). c) 1,3,5-Triallyl-1,3,5-triazine-2,4,6(1H,3H,5H)-trione (TATATO).

6.2 Experimental

6.2.1 Materials and Synthesis

Ethoxylated trimethylolpropane tri(3-mercaptopropionate) (ETTMP, 1300 g/mol) was obtained from Evans Chemetics. Poly(ethylene glycol (PEG, 600 g/mol), dimethyl sulfoxide (DMSO), 1,3,5- triallyl-1,3,5-triazine-2,4,6(1H,3H,5H)-trione (TATATO), sodium thiomethoxide, methyl methane thiol sulfonate (MMTS), and 5,5-dimethyl-1-pyrroline *N*-oxide (DMPO) were obtained from Sigma-Aldrich. Oltipraz was obtained from LKT Laboratories. All materials were used as received. Thiol–ene resins were formulated from 83.6 wt% ETTMP (see Scheme 31b) and 16.4 wt% TATATO (see

Scheme 31c) such that the thiol to allyl stoichiometric ratio prior to polymerization was maintained at 1:1 for all experiments.

The synthesis of bisDS followed a previously published procedure.[27] Briefly, 1.22 g of oltipraz was dissolved in 200 mL of ethanol under nitrogen and heated to 44°C. To this solution, 1.89 g of sodium thiomethoxide was added while stirring. After 45 minutes, 3.5 mL of MMTS was added and stirred for 2 hours. The solvent was removed under vacuum and the resulting crude product was dissolved in 40 mL of chloroform and filtered. Upon sitting, the filtrate phase separated and the clear, oily layer was discarded. The solvent was again removed under vacuum and the resulting product placed in a freezer overnight, affording crystals. The crystals were washed with cold ethanol and recrystallized from hot ethanol. ^{1}H NMR (400 MHz, $CDCl_3$), δ: 2.48 (d, 6H), 2.57 (s, 3H), 7.83 (d, 1H), 8.24 (dd, 1H), 9.08 (d, 1H).

For experiments performed under anaerobic conditions, monomers and solvents were subjected to at least six freeze-pump-thaw cycles to ensure rigorous deoxygenation prior to use, and formulations were assembled and mixed in an anaerobic chamber. For the aerobic experiments, formulations were assembled under atmospheric conditions using air-saturated monomers.

6.2.2 UV-vis Spectroscopy

Ultraviolet-visible (UV-Vis) spectroscopy was performed using an Agilent Technologies Cary 60 UV-Vis spectrophotometer. Formulations were placed in a 1 mm pathlength quartz cuvette immediately after mixing, whereupon spectra from 300 to 700 nm were collected every 10 minutes for 5 hours.

6.2.3 EPR Spectrometry

Electron paramagnetic resonance (EPR) spectroscopy was performed using a Bruker EMX spectrometer. A TM_{110} cavity (ER 4103TM, Bruker), 100 kHz modulation frequency, and 1 G_{pp} modulation amplitude were used. Sample formulations were placed in a flat quartz cell and all experiments were performed at room temperature using DMPO as a spin trap. For experiments performed under initially anaerobic experiments, deoxygenated bisDS, ETTMP, and DMPO were dissolved in DMSO, 600 μL of which were injected into the flat quartz cell, and a spectrum was collected after two hours. Each formulation was then removed from the flat quartz cell, exposed to the atmosphere for three minutes, then reinjected back into the flat quartz cell, and a spectrum was collected after 15 minutes of oxygen exposure. For experiments performed under completely aerobic conditions, the air-saturated formulation components were combined and a spectrum was collected after 15 minutes.

6.2.4 IR Spectroscopy

For experiments performed under initially anaerobic experiments, an approximately 20 μm thick film of deoxygenated resin was spread on a glass slide in a sealed sample cell.[25] Infrared spectra of the resin formulations were monitored remotely and in transmission using a Nicolet 6700 FT-IR spectrometer equipped with a fiber optic coupling accessory via chalcogenide optical fiber patch cables fitted with silver reflective collimators (see Scheme 32a). Air was introduced into the sample chamber via ports on either side, and the reaction was monitored by observing the disappearance of the allyl ether (3100 cm^{-1}) and thiol (2570 cm^{-1}) absorbance peaks,[29] using the methyl peak at 4370 cm^{-1} as an

internal standard.[30, 31] Spectra were collected at a rate of two per second and 64 spectra were averaged for every reported data point.

For experiments performed under aerobic conditions, air-saturated resin samples were either injected between two glass microscope slides separated by 50 µm thick shims to prevent further atmospheric oxygen from diffusing into the sample (see Scheme 32b) or spread as an approximately 20 µm thick film exposed to the atmosphere on a glass slide (see Scheme 32c). Each sample was placed in a Nicolet 6700 FT-IR spectrometer equipped with a horizontal transmission accessory and spectra were collected from 6400 to 2000 cm^{-1} at a rate of two per second, and the reaction was again monitored as described above.

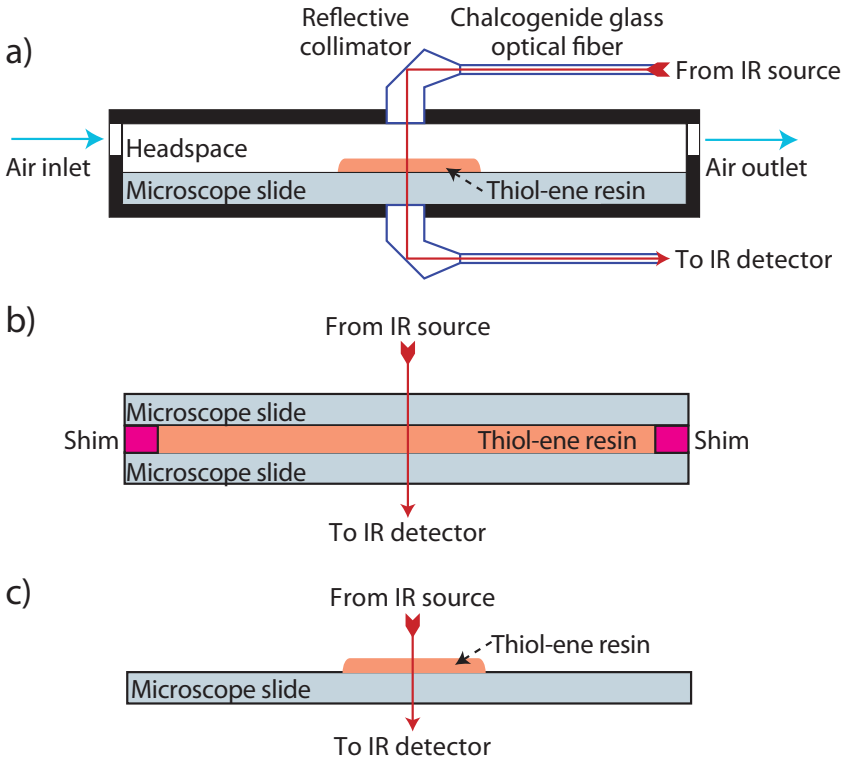

Scheme 32: Schematic diagrams of experimental configurations used to examine oxygen-mediated polymerization kinetics by FTIR spectroscopy. a) A sealed sample cell permits measurement of IR spectra under anaerobic conditions until air is introduced

into the cell via inlet and outlet ports. b) Sandwiching a resin formulation, mixed under oxygen-saturated conditions, between two glass slides throughout IR spectra collection prevents additional oxygen from diffusing into the sample during polymerization. c) A resin formulation, mixed under oxygen-saturated conditions, is exposed to the atmosphere throughout IR spectra collection, permitting oxygen to diffuse into the sample during polymerization.

6.2.5 Rheometry

Rheological measurements were performed using a TA Instruments ARES rheometer, configured with a 25 mm diameter parallel-plate fixture. Sample formulations were combined and mixed under aerobic conditions and, immediately after 0.300 mL were deposited on the lower plate and the upper fixture was lowered to a gap of 0.5 mm, data were collected at a rate of one point every 8 seconds using an oscillatory strain of 1% at a frequency of 1 Hz.

6.3 Results and Discussion

Prior to the polymerization reaction that is anticipated to proceed upon exposure of a thiol–ene resin formulated with bisDS to atmospheric oxygen, a pyrrolopyrazine-thione (PPT) reactive intermediate must be generated in situ from the reaction of bisDS with the thiol monomer. UV-Vis spectroscopy has previously been employed to monitor the PPT product formation from the reaction of bisDS with the monothiol glutathione;[27] generation of the PPT is readily observed as its thiocarbonyl moiety strongly absorbs at approximately 300 nm and in the 420-500 nm range owing to the π to π^* and the forbidden n to π^* transitions, respectively.[32] In their investigation of bisDS in an aqueous solution, Fishbein and coworkers found that the absorbance peak at 450 nm reached its maximum value within one minute and they concluded that the PPT is rapidly generated in near quantitative yield.[27] UV-Vis experiments were performed here to determine

whether the thiol functional groups affixed to the trithiol monomer ETTMP are similarly capable of generating the PPT in situ from bisDS. As the PPT participates in subsequent reactions in the presence of molecular oxygen, preliminary studies were performed under anaerobic conditions. Upon mixing of bisDS into a model thiol–ene resin composed of ETTMP and TATATO, an absorbance peak in the visible region of the spectrum (λ_{max} = 500 nm) was observed to increase over 2 hours for all concentrations of bisDS examined (see Figure 36a-c), indicating the generation of thiocarbonyl moieties and, hence, the PPT intermediate; as expected, the absorbance at λ_{max} increases linearly with raised bisDS concentration. Assuming complete conversion of bisDS into the PPT,[27] the molar absorptivity, ε, was found to be 5930 ± 180 M^{-1} cm^{-1}. In contrast, when thiol groups were omitted, there was no observable change in the UV-Vis spectrum of a bisDS-incorporating solution of TATATO and PEG over five hours and no absorbance observed at 500 nm (see Figure 36d), confirming that thiol functional groups must be present for reaction with bisDS to afford the PPT reactive intermediate.

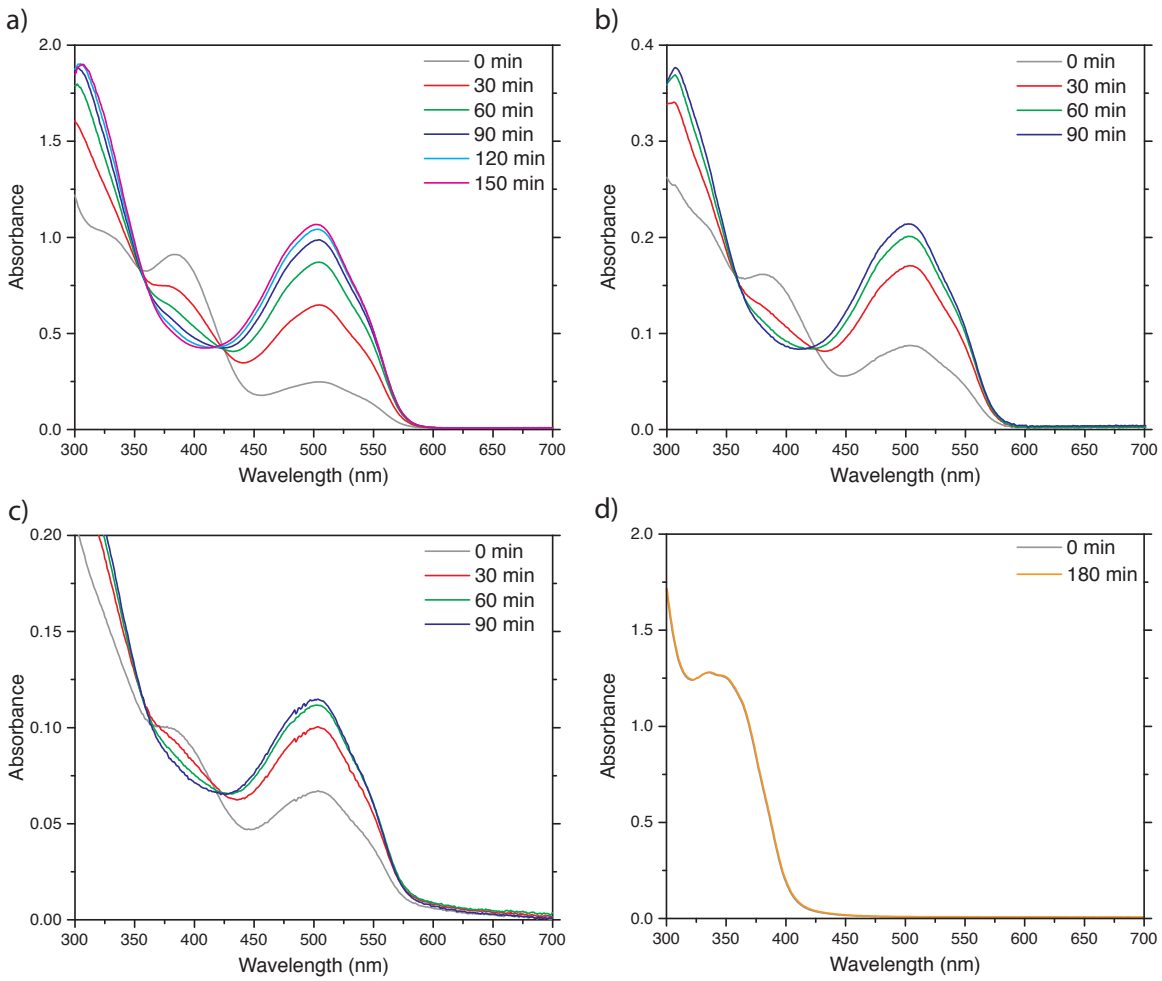

Figure 36: UV-Vis absorption spectra for bisDS-containing resin formulations mixed and maintained under anaerobic conditions. a) 0.05 wt% bisDS in ETTMP and TATATO; b) 0.01 wt% bisDS in ETTMP and TATATO; c) 0.005 wt% bisDS in ETTMP and TATATO; and d) 0.05 wt% in 83.6 wt% PEG (i.e., thiol-free) and 16.4 wt% TATATO.

Having established that the PPT intermediate is yielded by the reaction of bisDS and thiols, its oxygen-mediated radical generating characteristics were investigated using EPR spectroscopy by employing DMPO as a spin trap. In the absence of oxygen, no radicals were detected in a solution of 172 μM bisDS (equal to 0.005 wt%), 100 equivalents of thiol functional groups, and an excess of DMPO in DMSO; a ten-fold increase in the bisDS concentration yielded the same negative result (see Figure 37a), confirming that the reaction between bisDS and thiol to afford the PPT intermediate is

not radical-mediated. However, upon exposure of the thiol/bisDS solutions to the atmosphere, radical generation was clearly evident in their EPR spectra (see Figure 37b); an ETTMP formulation with 0.005 wt% bisDS, 100 equivalents of thiol groups, and excess DMPO exhibited a strong signal consistent with those previously reported where superoxide and thiyl radicals were identified.[28] Interestingly, when the bisDS concentration was increased from 0.005 wt% to 0.05 wt%, the resultant EPR signal intensity, and hence radical concentration, slightly decreased (Figure 37b). The decomposition rates of conventional radical initiators are typically first order with respect to the initiator concentration,[33] even for systems requiring a coinitiator,[34] such that the number of radicals generated scales with the initiator concentration; however, this expected behaviour is not observed in the current system. Rather, at sufficiently high initiator (i.e., either bisDS or thiol) concentrations, increasing the amount of initiator in the monomer formulation actually reduces the number of radicals generated. This phenomenon may be explained by the mechanism proposed by Fishbein and coworkers, where an undesired quenching reaction (Scheme 33),[28] favoured at high PPT concentrations, shuts down the radical-generating redox cycle. Nevertheless, despite this counterintuitive behaviour, radical generation does proceed upon exposure of the PPT intermediate to both oxygen and thiol, demonstrating similar behaviour for bisDS in both aqueous environments[28] and in bulk thiol–ene monomer formulations examined here. This in turn suggests that bisDS could function as an oxygen-mediated initiator for thiol–ene polymerizations, although the maximum attainable polymerization rate may be limited by the reduced radical generation at raised bisDS or thiol concentrations.

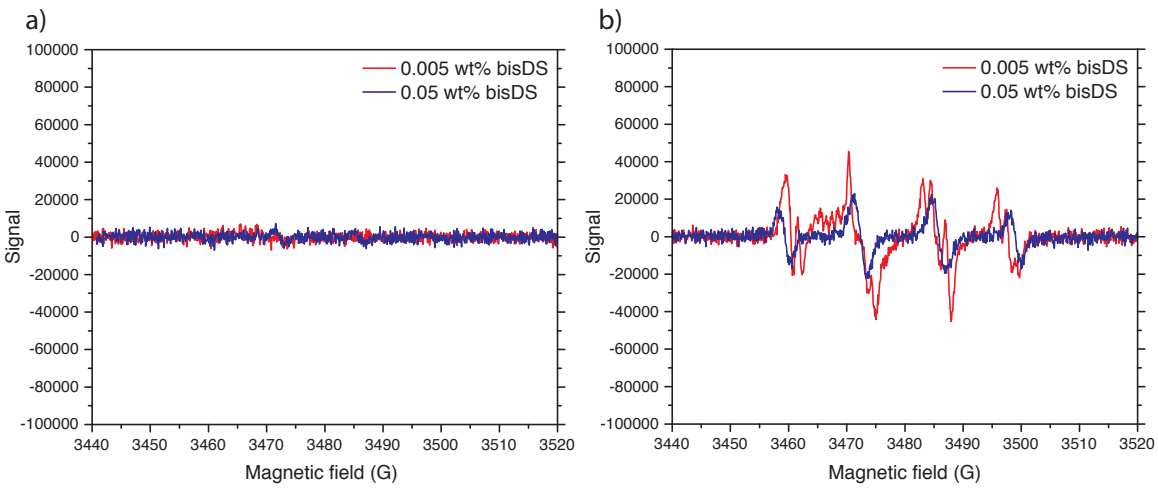

Figure 37: EPR spectra for solutions mixed under anaerobic conditions of bisDS, ETTMP, and DMPO in DMSO, a) maintained under anaerobic conditions and b) collected 15 minutes after exposure to the atmosphere.

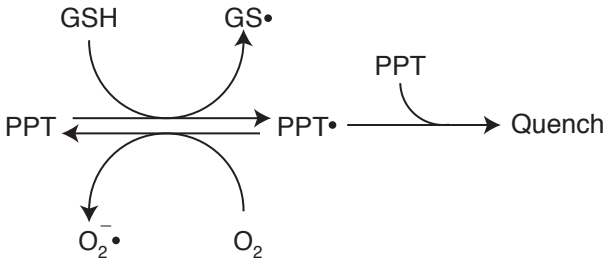

Scheme 33: In the presence of the excess PPT, the intermediate PPT• participates in a quenching reaction that prevents the radical-affording redox cycle as well as removing PPT.[28]

To evaluate this hypothesis, the polymerization of model thiol–ene resins, composed of ETTMP and TATATO and formulated with various concentrations of bisDS, was examined using FTIR spectroscopy to monitor the consumption of thiol and allyl functional groups during the reaction (Scheme 32a). In the absence of both oxygen and bisDS, the functional group conversion reached approximately 7% after five hours (see Figure 38), attributable to the often poor stability of thiol–ene formulations which have been observed to slowly react even in the absence of an initiator.[35] Although

incorporation of an appropriate inhibitor can improve stability,[36] inhibitors were not added to these formulations to avoid masking reactions caused by the bisDS. Notably, the formulations incorporating bisDS exhibited minimal functional group conversion in the absence of oxygen over five hours for all bisDS concentrations examined (Figure 38), indicating that bisDS does not generate polymerization-inducing radicals itself and supporting the results observed in the EPR experiments discussed above (Figure 37). Indeed, no inhibitor was needed in the formulations as the PPT generated in situ appears to induce an inhibitory effect.

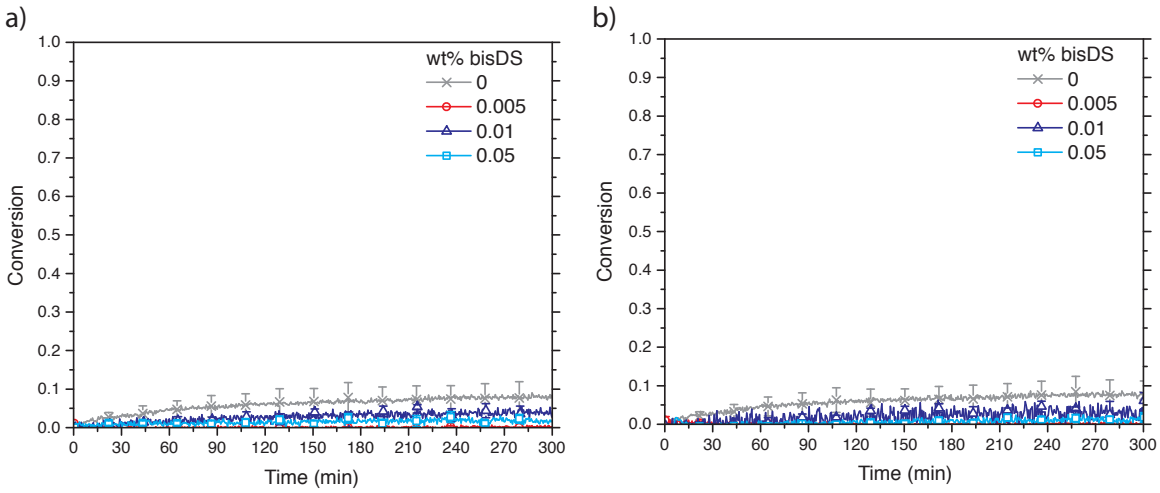

Figure 38: a) Thiol and b) allyl functional group conversions for bisDS-containing ETTMP/TATATO thiol–ene formulations mixed under anaerobic conditions. Experiments performed by maintaining anaerobic conditions.

Having established the minimal reaction progression under anaerobic conditions, these resin formulations were investigated for their behaviour upon exposure to atmospheric oxygen. As the UV-Vis experiments demonstrated that 2–3 hours were required to fully generate the PPT (see Figure 36), formulations were prepared under anaerobic conditions and left undisturbed for 3 hours prior to exposing them to atmospheric oxygen (see Figure 39). Upon exposure to the atmosphere, the observed

polymerization rates were low, with functional groups conversions for the resin incorporating 0.005 wt% bisDS, the fastest polymerizing formulation of those examined, reaching only 7% after 5 hours exposure. Notably, although radical generation was demonstrated in formulations containing bisDS and thiol functionalities upon exposure to atmospheric oxygen using EPR spectroscopy, this did not translate into significant, oxygen-mediated thiol–ene polymerization. Moreover, these polymerization kinetics results support those observed by EPR spectroscopy where increasing the bisDS concentration beyond a particular value affords a decreased radical concentration, behaviour that is consistent with the hypothesis discussed above of a radical quenching reaction (Scheme 33) that inhibits polymerization in the presence of excess PPT.

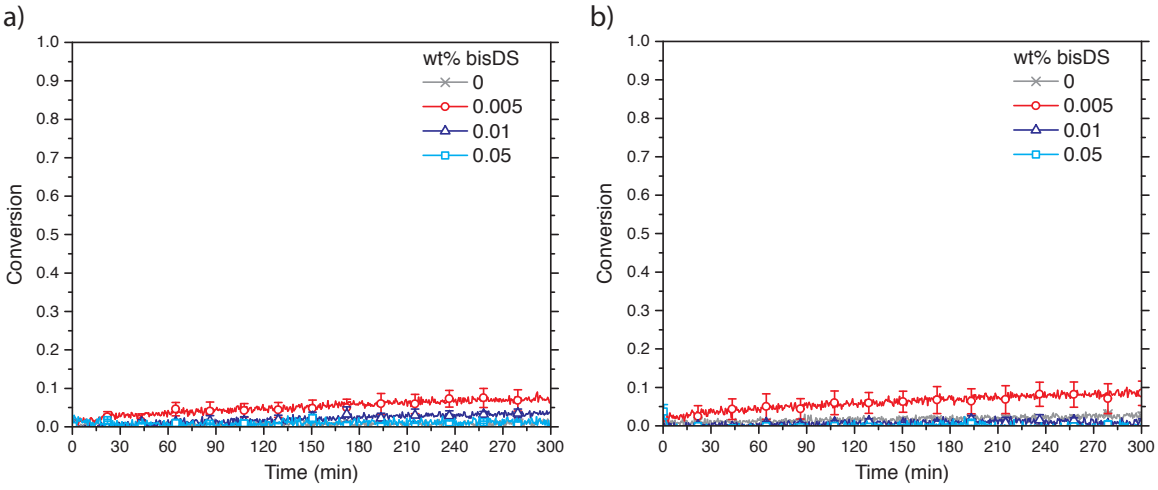

Figure 39: a) Thiol and b) allyl functional group conversions for bisDS-containing ETTMP/TATATO thiol–ene formulations mixed under anaerobic conditions. Experiments performed by exposing the samples to the atmosphere.

In contrast to conventional, radical-mediated chain growth polymerization reactions, oxygen does not wholly inhibit radical-mediated thiol–ene polymerizations; nevertheless, the presence of oxygen can retard polymerization rates even in thiol–ene systems. Thus, to prevent further oxygen from diffusing into the samples during

polymerization, a second set of polymerization kinetics experiments was performed where oxygen-saturated ETTMP/TATATO resins were formulated with bisDS under atmospheric conditions, immediately injected between two glass microscope slides, and the consumption of thiol and allyl functional groups was monitored by FTIR spectroscopy (see Scheme 32b). In contrast to the polymerization kinetics observed for resins under constant atmospheric exposure, here the formulation incorporating 0.005 wt% bisDS reached a reaction conversion of nearly 45% within 2 hours (see Figure 40). Unfortunately, as before, increasing the concentration of bisDS above 0.005 wt% deceased both the rate and extent of polymerization, a dramatic divergence from previously studied thiol–ene systems where the scaling of the polymerization rate with the initiation rate approaches unity;[29] indeed, the 0.05 wt% bisDS formulation exhibiting a reaction extent after five hours that was actually lower than the formulation with no bisDS. Nevertheless, similar behaviour, where an increase in the initiator concentration results in a suppressed reaction rate, has been observed previously in other initiator systems for both radical-mediated acrylate[37] and thiol–ene polymerization chemistries,[14] including those that employ iron-based Fenton chemistry or camphorquinone/tertiary amine photoinitiation systems at raised Fe^{2+} or amine concentrations, respectively.[34] For such systems, the reaction rates decrease at elevated Fe^{2+} or amine concentrations owing to the occurrence of unwanted inhibitory and termination reactions. Similarly, the behavior exhibited here may be attributable to the aforementioned quenching reaction that suppresses radical generation at high PPT concentrations, accounting for the difference in behavior between the experiments seen in Figure 39 and Figure 40. Under initially anaerobic conditions, bisDS is converted into the PPT intermediate over several

hours, such that the PPT concentration is high when atmospheric oxygen is introduced. Conversely, when the formulation is initially oxygen-saturated, the PPT generated by reaction of bisDS with thiol can immediately react with further thiol and oxygen to start the radical-generating redox cycle; thus, as the concentration of PPT is initially low such that the quenching reaction is minimized, initiating radicals are readily formed and the polymerization is able to proceed. The monomer conversion plateaus for formulations with both 0.005 and 0.01 wt% bisDS after approximately 2 hours reaction time suggest complete consumption of the dissolved oxygen such that radical-generating redox cycle ceases after that time.

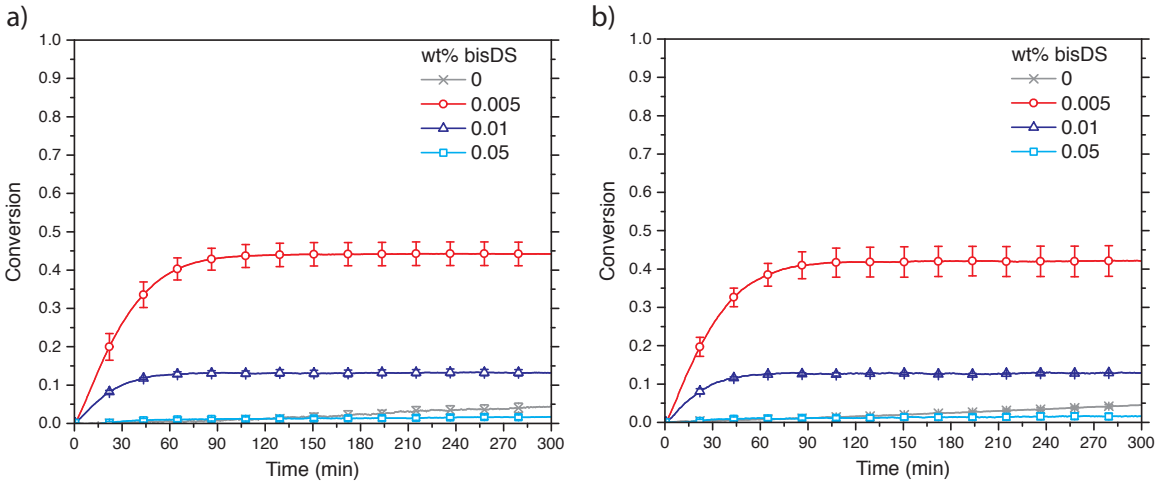

Figure 40: a) Thiol and b) allyl functional group conversions for bisDS-containing ETTMP/TATATO thiol–ene formulations mixed under oxygen-saturated conditions. Experiments performed by sandwiching samples between glass slides, preventing additional oxygen diffusion into each formulation.

Given the significant differences in polymerization kinetics between samples initially anaerobic but exposed to the atmosphere throughout their reaction and those initially oxygen-saturated but reacting within closed cells, additional UV-Vis and EPR experiments investigating the influence of oxygen on the PPT evolution were performed.

Initially, oxygen-saturated thiol–ene resins were formulated with bisDS at various concentrations and UV-Vis spectra were collected on the resultant solutions over time. The results of the UV-Vis experiments run under either oxygen-saturated or anaerobic conditions were superficially similar as the peaks at both 300 and 500 nm increased over time (see Figure 41); however, unlike the experiments performed under anaerobic conditions where the complete conversion of bisDS into the PPT intermediate took several hours (see Figure 36), the absorbance at λ_{max} did not plateau in the presence of oxygen even after 5 hours for any of the bisDS concentrations examined (Figure 41). Moreover, the observed λ_{max} absorbances did not scale linearly with the initial bisDS concentration; using the PPT molar absorptivity determined above, the conversion of bisDS to PPT after five hours for 0.005 wt%, 0.01 wt%, and 0.05 wt% bisDS were 29%, 65.1%, and 83.3%, respectively. Thus, when oxygen was initially present, the PPT generation was retarded and, at lower bisDS concentrations, the PPT concentration remained much lower than it did under anaerobic conditions, indicating that oxygen either inhibits the formation of the PPT from bisDS or it interacts with the PPT generated by the reaction between bisDS and thiol. To determine which of these mechanisms occurs, a formulation of 0.05 wt% bisDS in ETTMP and TATATO was initially assembled under anaerobic conditions and left undisturbed for three hours to wholly convert bisDS to the PPT (see Figure 42). Subsequently, this formulation was exposed to atmospheric oxygen for 8 hours, whereupon the absorbance at λ_{max} had dropped considerably (Figure 42), indicating that oxygen does indeed react with the generated PPT. Interestingly, after five hours under anaerobic conditions, the λ_{max} absorbance

partially recovered, indicating that the interactions between bisDS, PPT, thiol, and oxygen are in part reversible.

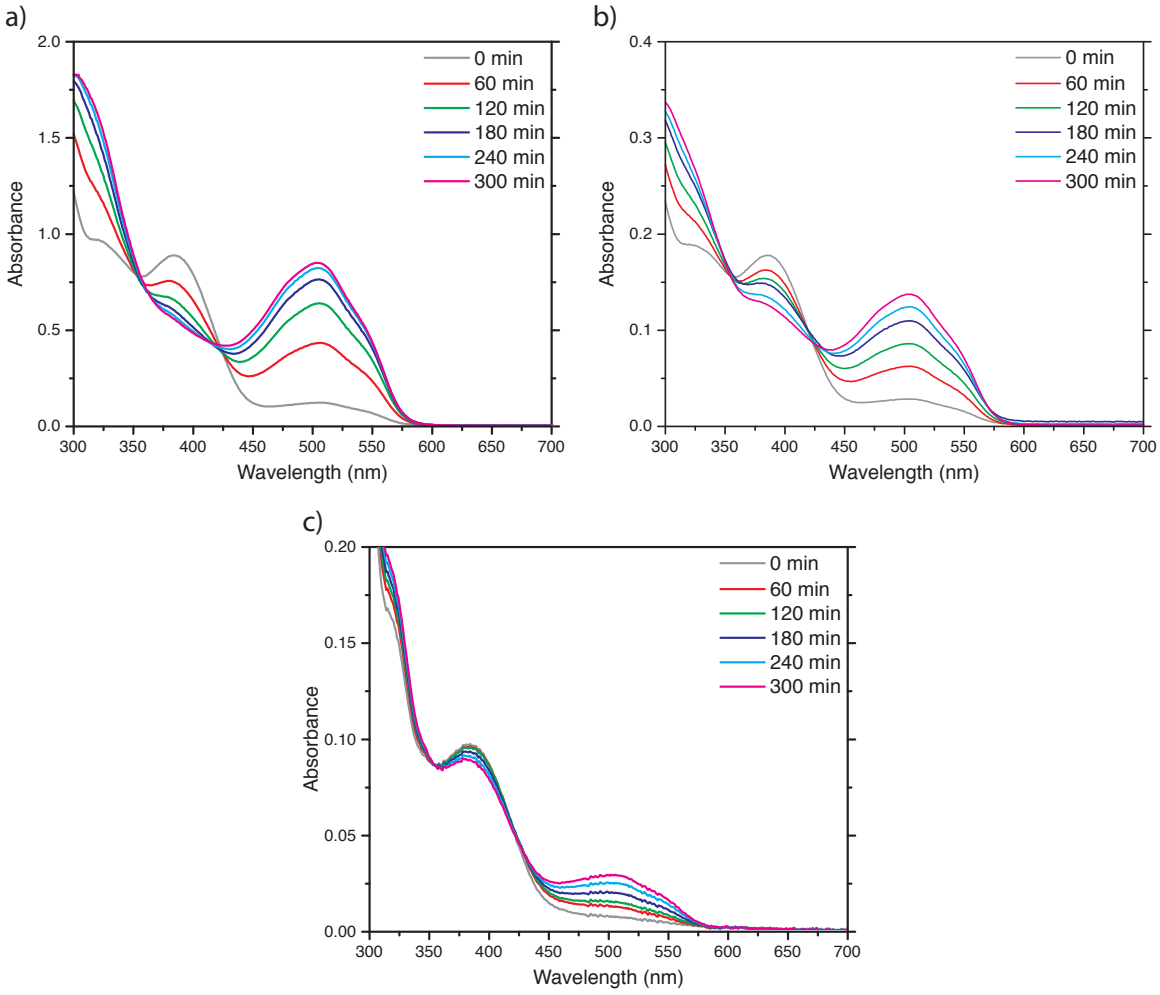

Figure 41: UV-Vis absorption spectra for bisDS-containing thiol–ene formulations mixed under oxygen-saturated conditions. a) 0.05 wt% bisDS in ETTMP and TATATO; b) 0.01 wt% bisDS in ETTMP and TATATO; and c) 0.005 wt% bisDS in ETTMP and TATATO.

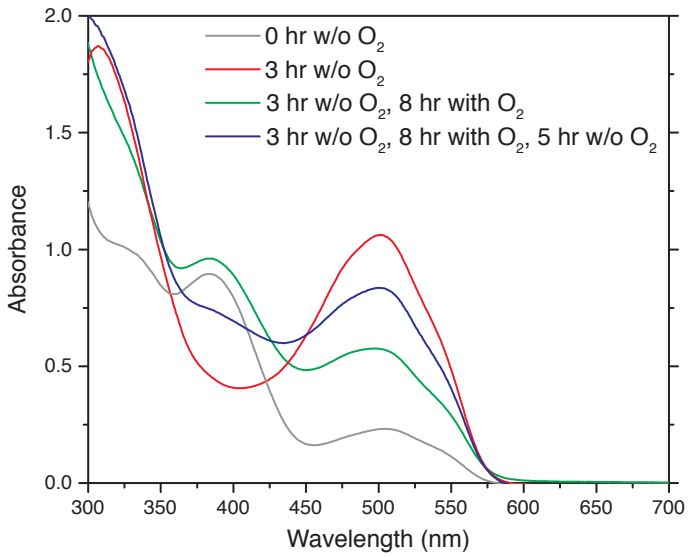

Figure 42: UV-Vis absorption spectra for a thiol–ene formulation of 0.05 wt% bisDS in ETTMP-TATATO immediately after mixing under anaerobic conditions, after 3 hours maintained under anaerobic conditions, after 8 hours of subsequent atmosphere exposure, and finally after 5 hours sealed in a cuvette to eliminate further oxygen diffusion.

Equivalent experiments examining the generation of radicals in oxygen-saturated solutions were performed using EPR spectroscopy. Here, a solution with 0.005 wt% bisDS and 100 equivalents of thiol exhibited a much stronger signal after reaction under initially aerobic conditions (see Figure 43) than when the experiment was performed under initially anaerobic conditions (Figure 37b). This again is likely a result of the significantly lower PPT concentration, as observed in the UV-Vis experiments (Figure 41), when oxygen is initially present and supports the hypothesis that formulations with low PPT concentrations are more capable of generating free radicals via the redox cycle (Scheme 33) as the polymerization-retarding influence of the quenching reaction dominates at higher PPT concentrations.

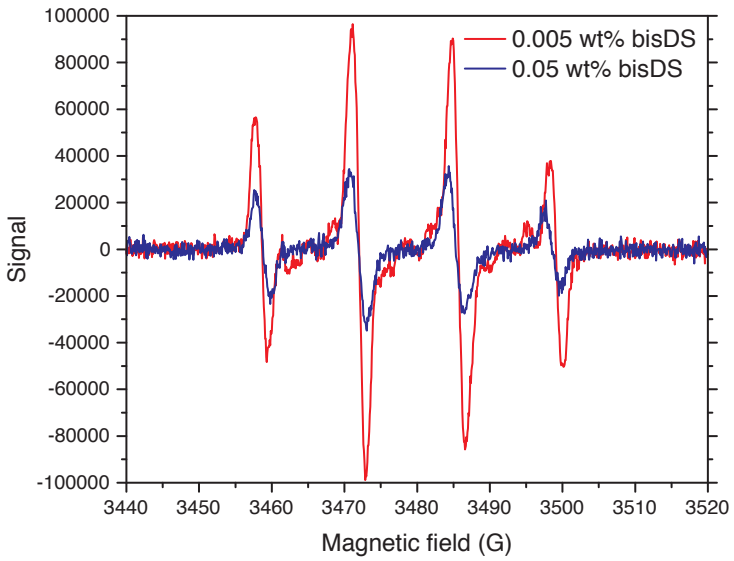

Figure 43: EPR spectra for solutions mixed under oxygen-saturated conditions of bisDS, ETTMP, and DMPO in DMSO, collected 15 minutes after mixing.

To further investigate the role of oxygen in the radical-generating behaviour of bisDS, additional polymerization kinetics experiments were performed under aerobic conditions (Scheme 32c): the resins, with bisDS concentrations ranging from 0 to 0.25 wt% were formulated in the presence of atmospheric oxygen and were continually exposed to the atmosphere throughout the reaction (see Figure 44a and b). At bisDS concentrations from 0 to 0.025 wt%, the polymerization rate and extent increased, as the bisDS concentration was raised and the maximum rate occurred at the start of the reaction. The monomer conversion after five hours reaction time for the resin formulated with 0.05 wt% bisDS was similar to that for the 0.025 wt% bisDS resin, although an induction period of approximately 20 minutes was apparent prior to the polymerization onset (see Figure 44c and d). Notably, of the experimental conditions examined, only the conditions used here effected appreciable monomer conversion with 0.05 wt% bisDS. This again suggests that the role of oxygen is complex, participating both in generating radicals from the PPT and thiol while simultaneously eliminating the PPT via some

quenching reaction. Whereas removing the PPT lessens the potential radical generation rate, it also reduces the occurrence of the polymerization-retarding quenching reaction. Thus, the constant influx of oxygen from the atmosphere destroyed excess PPT, suppressing the quenching reaction, while still retaining a sufficient PPT concentration to generate polymerization-initiating radicals. This hypothesis is further supported by the behavior at high bisDS concentrations where progressively longer induction times and decreased polymerization rates and extents were observed as bisDS concentrations were raised above 0.05 wt% (see Figure 44c and d); indeed, at a concentration of 0.25 wt% bisDS, the monomer conversion after five hours was only 5%, appreciably lower than all bisDS-containing formulations examined and indicating that the PPT concentration generated by this bisDS loading was too high to enable sufficient radical generation for significant polymerization.

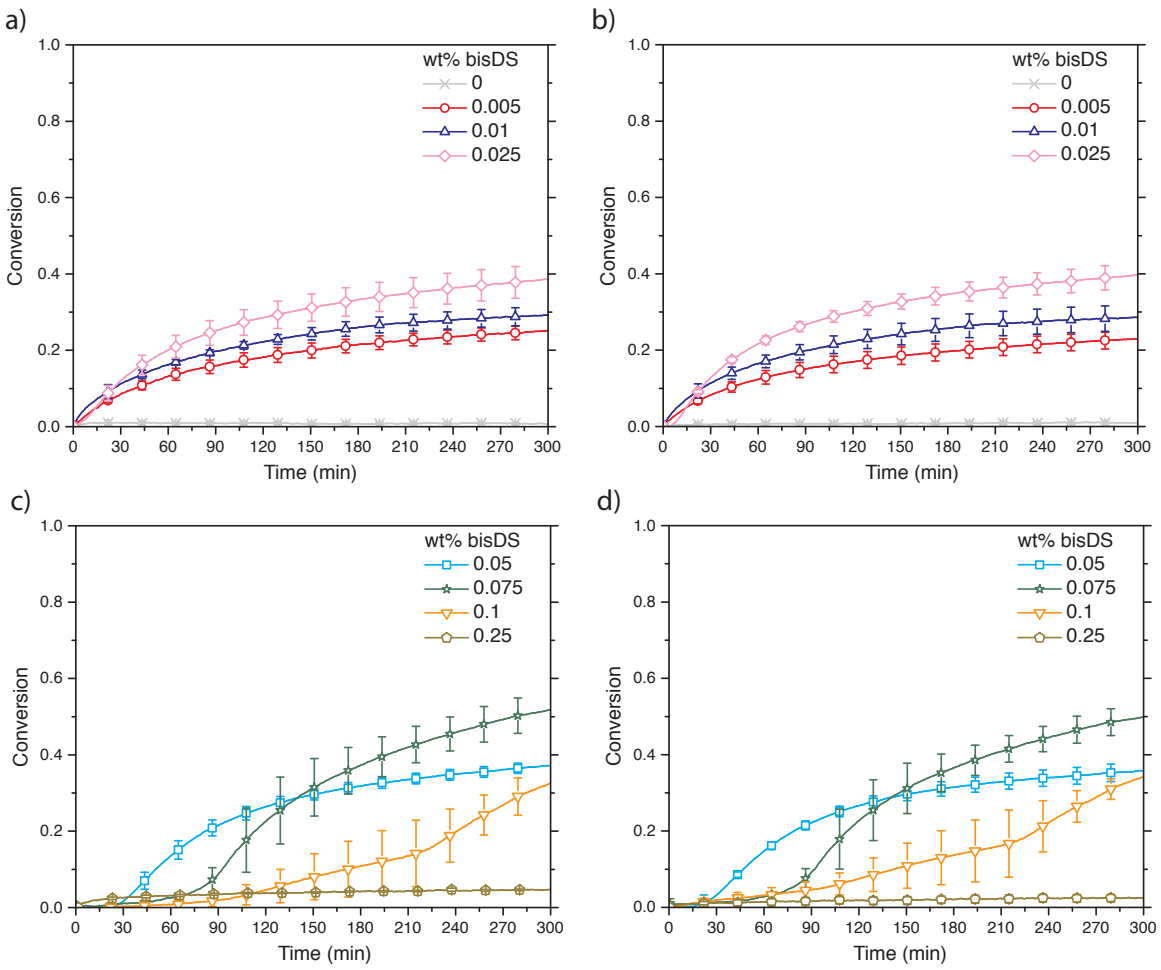

Figure 44: a&c) Thiol and b&d) allyl functional group conversions for bisDS-containing ETTMP/TATATO thiol–ene formulations mixed under oxygen-saturated conditions. Experiments performed by exposing the samples to the atmosphere. For clarity, bisDS-containing resin compositions separated into two ranges: a&b) 0 – 0.025 wt% bisDS; c&d) 0.05 – 0.25 wt% bisDS.

Finally, to confirm that the model, multifunctional thiol–ene resin in the presence of both bisDS and atmospheric oxygen results in the formation of cross-linked polymer, parallel plate rheometry was used to monitor oxygen-mediated polymerizations. The experimental conditions used here were similar to those used for the polymerization kinetics experiments performed using initially oxygen-saturated resins that were subsequently sealed throughout the polymerization reaction; however, whereas the formulations were made under aerobic conditions and most of the monomer/bisDS

formulation was sealed against the atmosphere by the rheometer plates, diffusion of oxygen from the atmosphere still occurred at the plate edges (see Figure 45). A control resin formulated without bisDS displayed essentially no change in either storage or loss modulus over five hours, indicating negligible polymerization over that period. When bisDS was included in the formulation at either 0.005 wt% or 0.05 wt%, a cross-over of the storage and loss moduli, indicative of gelation,[38] was observed. Whereas the cross-over point for the 0.005 wt% bisDS formulation was reached after 91 minutes, the cross-over for the 0.05 wt% formulation occurred significantly later at 158 minutes. Moreover, the 0.05 wt% formulation only achieved significant gelation in a ring around the edge, while the 0.005 wt% bisDS formulation exhibited solid polymer throughout the sample, results consistent with those observed in the polymerization kinetics experiments.

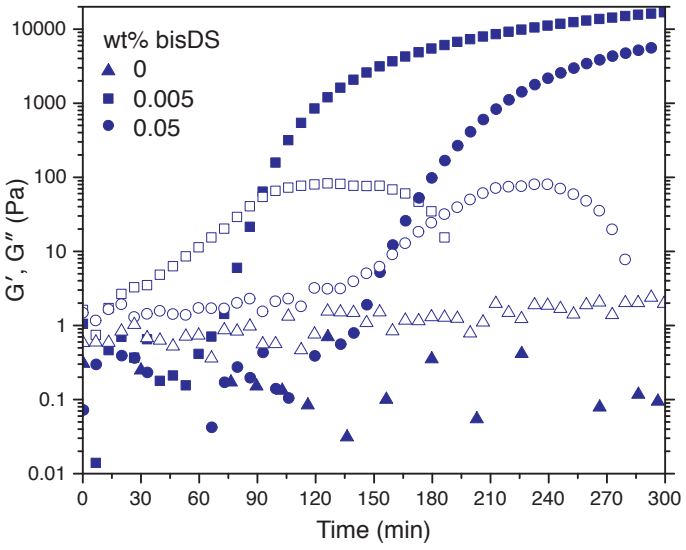

Figure 45: Storage (G', closed symbols) and loss (G", open symbols) moduli, measured by parallel plate rheometry, of bisDS-containing ETTMP/TATATO thiol–ene formulations mixed under oxygen-saturated conditions.

6.4 Conclusion

Incorporation of bisDS in model thiol–ene resin formulations has been shown to afford a PPT intermediate product, attributable to a reaction between bisDS and the thiol functional groups in the resin. Exposure of these bisDS-incorporating thiol–ene resins to atmospheric oxygen results in the generation of radicals via a redox cycle, in the presence of both thiol and molecular oxygen, permitting its utilization as an oxygen-mediated initiating system for thiol–ene polymerization. An unwanted side reaction dominates at elevated PPT concentrations that quenches the redox cycle, preventing radical formation and retarding polymerization. Although the influence of this quenching unfortunately limits the utility of bisDS as an oxygen-mediated initiator of thiol–ene polymerization, we anticipate that the development of approaches to suppress the quenching reaction will afford a rapid and efficient method of utilizing oxygen as an environmentally-borne polymerization initiation stimulus.

6.5 References

1. Cramer, N. B.; Bowman, C. N., Kinetics of thiol-ene and thiol-acrylate photopolymerizations with real-time Fourier transform infrared. *J. Polym. Sci. A Polym. Chem.* **2001,** *39* (19), 3311-3319.
2. Hill, L. W.; Lee, S. B., Effect of melamine-formaldehyde structure on cure response of thermoset coatings. *J. Coating. Technol.* **1999,** *71* (897), 127-133.
3. Cole, M. A.; Jankousky, K. C.; Bowman, C. N., Redox initiation of bulk thiol-ene polymerizations. *Polym. Chem.* **2013,** *4* (4), 1167-1175.
4. Deng, Y.; Martin, G. C., Diffusion and Diffusion-Controlled Kinetics during Epoxy-Amine Cure. *Macromolecules* **1994,** *27* (18), 5147-5153.
5. Chattopadhyay, D. K.; Raju, K. V. S. N., Structural engineering of polyurethane coatings for high performance applications. *Prog. Polym. Sci.* **2007,** *32* (3), 352-418.
6. Igarashi, R. Y.; Seefeldt, L. C., Nitrogen fixation: The mechanism of the Mo-dependent nitrogenase. *Crit. Rev. Biochem. Mol. Biol.* **2003,** *38* (4), 351-384.
7. Khriachtchev, L.; Rasanen, M.; Gerber, R. B., Noble-Gas Hydrides: New Chemistry at Low Temperatures. *Acc. Chem. Res.* **2009,** *42* (1), 183-191.
8. Cooper, A. I., Polymer synthesis and processing using supercritical carbon dioxide. *J. Mater. Chem.* **2000,** *10* (2), 207-234.
9. Thennarasu, S.; Krishnamurti, N.; Shantha, K. L., Developments and applications of cyanoacrylate adhesives. *J. Adhes. Sci. Technol.* **1989,** *3* (4), 237-260.

10. Comyn, J.; de Buyl, F.; Shephard, N. E.; Subramaniam, C., Kinetics of cure, crosslink density and adhesion of water-reactive alkoxysilicone sealants. *Int. J. Adhes. Adhes.* **2002,** *22* (5), 385-393.
11. Chattopadhyay, D. K.; Sreedhar, B.; Raju, K. V. S. N., The phase mixing studies on moisture cured polyurethane-ureas during cure. *Polymer* **2006,** *47* (11), 3814-3825.
12. Navarra, C.; Goodwin, C.; Burton, S.; Danieli, B.; Riva, S., Laccase-mediated oxidation of phenolic derivatives. *J. Mol. Catal. B: Enzym.* **2010,** *65* (1-4), 52-57.
13. Berron, B. J.; Johnson, L. M.; Ba, X.; McCall, J. D.; Alvey, N. J.; Anseth, K. S.; Bowman, C. N., Glucose oxidase-mediated polymerization as a platform for dual-mode signal amplification and biodetection. *Biotechnol. Bioeng.* **2011,** *108* (7), 1521-1528.
14. Zavada, S. R.; McHardy, N. R.; Scott, T. F., Oxygen-mediated enzymatic polymerization of thiol-ene hydrogels. *J. Mater. Chem. B* **2014,** *2* (17), 2598-2605.
15. Wachter, D.; Bruckel, A.; Stein, M.; Oertel, M. F.; Christophis, P.; Boker, D. K., 2-Octyl-cyanoacrylate for wound closure in cervical and lumbar spinal surgery. *Neurosurg. Rev.* **2010,** *33* (4), 483-9.
16. Singer, A. J.; Thode, H. C., Jr., A review of the literature on octylcyanoacrylate tissue adhesive. *Am. J. Surg.* **2004,** *187* (2), 238-48.
17. Lewis, L. A.; Smithwick, R. W.; Devault, G. L.; Bolinger, B.; Lewis, S. A., Processes involved in the development of latent fingerprints using the cyanoacrylate fuming method. *J. Forensic. Sci.* **2001,** *46* (2), 241-246.
18. Mankidy, P. J.; Ramakrishnan, R. B.; Foley, H. C., Facile catalytic growth of cyanoacrylate nanofibers. *Chem. Commun.* **2006,** (10), 1139-1141.
19. van Gorkum, R.; Bouwman, E., The oxidative drying of alkyd paint catalysed by metal complexes. *Coord. Chem. Rev.* **2005,** *249* (17-18), 1709-1728.
20. Colombani, D., Chain-growth control in free radical polymerization. *Prog. Polym. Sci.* **1997,** *22* (8), 1649-1720.
21. Wood, P. M., The Potential Diagram for Oxygen at Ph-7. *Biochem. J.* **1988,** *253* (1), 287-289.
22. O'Brien, A. K.; Bowman, C. N., Impact of oxygen on photopolymerization kinetics and polymer structure. *Macromolecules* **2006,** *39* (7), 2501-2506.
23. Hoyle, C. E.; Bowman, C. N., Thiol-Ene Click Chemistry. *Angew. Chem. Int. Ed.* **2010,** *49* (9), 1540-1573.
24. Hoyle, C. E.; Lowe, A. B.; Bowman, C. N., Thiol-click chemistry: a multifaceted toolbox for small molecule and polymer synthesis. *Chem. Soc. Rev.* **2010,** *39* (4), 1355-1387.
25. Zavada, S. R.; McHardy, N. R.; Gordon, K. L.; Scott, T. F., Rapid, Puncture-Initiated Healing via Oxygen-Mediated Polymerization. *ACS Macro Lett.* **2015,** *4* (8), 819-824.
26. Clapper, M. L., Chemopreventive activity of oltipraz. *Pharmacol. Ther.* **1998,** *78* (1), 17-27.
27. Navamal, M.; McGrath, C.; Stewart, J.; Blans, P.; Villamena, F.; Zweier, J.; Fishbein, J. C., Thiolytic chemistry of alternative precursors to the major metabolite of the cancer chemopreventive oltipraz. *J. Org. Chem.* **2002,** *67* (26), 9406-13.
28. Velayutham, M.; Villamena, F. A.; Navamal, M.; Fishbein, J. C.; Zweier, J. L., Glutathione-mediated formation of oxygen free radicals by the major metabolite of oltipraz. *Chem. Res. Toxicol.* **2005,** *18* (6), 970-5.
29. Scott, T. F.; Kloxin, C. J.; Draughon, R. B.; Bowman, C. N., Nonclassical dependence of polymerization rate on initiation rate observed in thiol-ene photopolymerizations. *Macromolecules* **2008,** *41* (9), 2987-2989.
30. Westad, F.; Schmidt, A.; Kermit, M., Incorporating chemical band-assignment in near infrared spectroscopy regression models. *J. Near Infrared Spectrosc.* **2008,** *16* (3), 265-273.

31. Hourant, P.; Baeten, V.; Morales, M. T.; Meurens, M.; Aparicio, R., Oil and fat classification by selected bands of near-infrared spectroscopy. *Appl. Spectrosc.* **2000,** *54* (8), 1168-1174.
32. Skrabania, K.; Miasnikova, A.; Bivigou-Koumba, A. M.; Zehm, D.; Laschewsky, A., Examining the UV-vis absorption of RAFT chain transfer agents and their use for polymer analysis. *Polym. Chem.* **2011,** *2* (9), 2074-2083.
33. Barrett, K. E. J., Determination of Rates of Thermal Decomposition of Polymerization Initiators with a Differential Scanning Calorimeter. *J. Appl. Polym. Sci.* **1967,** *11* (9), 1617-&.
34. Cook, W. D., Photopolymerization Kinetics of Dimethacrylates Using the Camphorquinone Amine Initiator System. *Polymer* **1992,** *33* (3), 600-609.
35. Szmant, H. H.; Mata, A. J.; Namis, A. J.; Panthananickal, A. M., The thiol-olefin co-oxidation (TOCO) Reaction—IV. *Tetrahedron* **1976,** *32* (22), 2665-2680.
36. Cook, W. D.; Chen, F.; Pattison, D. W.; Hopson, P.; Beaujon, M., Thermal polymerization of thiol-ene network-forming systems. *Polym. Int.* **2007,** *56* (12), 1572-1579.
37. Johnson, L. M.; Fairbanks, B. D.; Anseth, K. S.; Bowman, C. N., Enzyme-mediated redox initiation for hydrogel generation and cellular encapsulation. *Biomacromolecules* **2009,** *10* (11), 3114-21.
38. Winter, H. H.; Chambon, F., Analysis of Linear Viscoelasticity of a Crosslinking Polymer at the Gel Point. *J. Rheol.* **1986,** *30* (2), 367-382.

Chapter 7

Conclusion

7.1 Summary of Research

The viability of oxygen as an environmentally-borne initiation stimulus has been thoroughly established by the research presented here. As noted throughout this dissertation, the key to oxygen-mediated thiol–ene polymerization is to generate radicals in response to an influx of molecular oxygen. To achieve this, three systems were investigated, including alkylboranes, oxidoreductase enzymes, and thione chemistry, all of which proved capable of affording the radicals necessary to initiate thiol–ene polymerization upon exposure to atmospheric oxygen. As the development of these oxygen-mediated polymerization methods is driven by two emerging applications (i.e., self-healing materials for space exploration habitats and biomedical adhesives and sealants), the three oxygen-mediated initiating systems were evaluated for their suitability in these applications.

Trialkylboranes, in the presence of oxygen, produce radicals, notably alkyl and alkoxy radicals, that are capable of initiating polymerization. Here, trialkylboranes were successfully utilized in rapidly polymerizing thiol–ene monomer formulations after oxygen exposure. These reactive monomer formulations were then evaluated for their self-healing capabilities by sandwiching them between solid polymer plates. Ballistics testing, performed at atmospheric pressure, convincingly demonstrated that solid polymer

could form within seconds of atmospheric exposure after penetration and that this solid material could form a plug that would seal the puncture. While these results are extraordinarily encouraging, in order to develop a material suitable for use in a real space habitat, the ballistics testing needs to be performed under conditions much close to those on the moon or Mars. Thus, a much more stringent ballistics testing protocol was developed, one that applied a pressure gradient between the front and back faces of the test panel. Under these more realistic conditions, the unmodified thiol–ene-tributylborane formulation was unable to polymerize fast enough in order to seal the projectile-induced hole, thus confirming that the pressure gradient ballistics test is significant harsher than the one performed at atmospheric pressure. While the unmodified (i.e., monomer and initiator only with no filler) formulations failed, the addition of glass fiber as filler lead to significant improvements as sufficient resin was able to remain in the vicinity of the puncture in order to partially filled the hole. This is tremendously exciting as there are many further formula modifications, including increasing monomer functionality to decrease gel time or changing the rheological properties by the addition of other fillers or viscosity modifiers, that can easily be attempted in order to improve the healing properties and this is an especially ripe source of possibilities for future work. Of course, despite the successes with the alkylborane chemistry for self-healing applications, the extreme reactivity of the alkylborane chemistry likely renders it a poor choice for the biomedical applications that are also of interest.

In searching for oxygen-mediated radical-affording reactions that would be appropriate for biomedical applications, redox reactions catalyzed by oxidoreductase

enzymes seemed to be a likely candidate, particularly glucose oxidase as it is capable of reducing oxygen to hydrogen peroxide in the presence of glucose. The hydrogen peroxide can then, through a reaction with Fe^{2+} ions (i.e., the Fenton reaction), be converted into hydroxyl radicals, species capable of initiating polymerization. By utilizing this glucose/glucose oxidase/Fe^{2+} ternary initiating system, hydrogels were formed from aqueous solutions of model thiol–ene monomers approximately 13.5 minutes after atmospheric exposure. While this certainly meets the criteria of an oxygen-mediated polymerization, this is far too slow for a material meant to be explored as a surgical adhesive. Unfortunately, the gelation times with this system are inherently limited owing to undesirable side reactions that dominate in the presence of excess Fe^{2+}, present as part of the initiating system, and Fe^{3+} ions, formed as a byproduct in the Fenton reaction. One successful approach to decreasing gel times was to replace the Fe^{2+} with horseradish peroxidase, an oxidoreductase that reduces hydrogen peroxide while oxidizing a suitable substrate; fortuitously, the thiol groups present on the monomers function as a horseradish peroxidase substrate and are oxidized to thiyl radicals. By replacing Fe^{2+} with horseradish peroxide, gelation times were, with the same model aqueous thiol–ene monomer system, decreased to 8.5 minutes, a significant improvement, though still slower than desired. Further decreases in gelation times were attained during efforts to move beyond model monomer systems towards materials that may be more clinically useful. By using thiolated chitosan as the thiol source, hydrogels could be generated approximately a minute after oxygen exposure by using the glucose/glucose oxidase/Fe^{2+} initiating system. Gelation times became so short that it was difficult to monitor with rheometry; the most rapidly reacting formulations were gelling while the

samples were being loaded into the rheometer. Interestingly, the gelation mechanism, originally thought to be strictly a thiol–ene polymerization, seems to be far more complicated as both disulfide formation and chitosan-iron interactions also contribute. These unexpected side reactions are not necessarily a concern as they all seem to require the presence of oxygen. Having demonstrated the facile formation of chitosan-based hydrogels through oxygen-mediated processes, these materials may now be explored for a variety of medicals applications, including hemostats and surgical glues.

Despite the successes of both the alkylborane and oxidoreductase initiating systems, their limitations encourage the development of additional oxygen-mediated initiators. Ideally, an alternative initiating system should be stable (i.e., unreactive) in the absence of oxygen, unlike alkylboranes, and be suitable for use in a variety of monomer systems, unlike the enzyme-based system that are best suited for aqueous monomer solutions. Inspiration for such an initiating system that potentially met these requirements was found in the realm of cancer drug research. Specifically, the compound oltipraz has been investigated for chemopreventive character and was thought to function in vivo through a free radical mechanism; this mechanism involves a metabolite, a PPT. Previous research found that a bis-disulfide derivative of oltipraz could form the PPT in vitro by a reaction with thiols and that this in situ generated PPT affords radicals via a redox cycle in the presence of both oxygen and additional thiol; thus, it seemed feasible that, in the presence of thiol–ene monomer formulations, the bis-disulfide would generate the PPT and, only after exposure to oxygen, initiate thiol–ene polymerization. In the research described here, the radical-generating character of the PPT was confirmed, though its utilization as an oxygen-mediated initiator was not as simple and

straightforward as was hoped. Instead, there is a complex relation between initiator and oxygen concentrations: reaction rates decreased at higher initiator concentrations, though the manner by which oxygen was introduced into the system also had significant influence over reaction rates. This behavior is brought about by radical quenching reactions that dominate at higher PPT concentrations. Thus, when the bis-disulfide is added to degassed thiol–ene monomer formulations, the bis-disulfide is converted entirely into PPT; as its concentration is obviously quite high, very little polymerization is observed after oxygen exposure owing to the influence of these quenching reactions. On the other hand, when the bis-disulfide is added to thiol–ene monomer formulations that were not degassed, the PPT that is formed can immediately begin reacting with oxygen, affording initiating radicals under conditions where overall PPT concentration is low, limiting the influence of the radical quenching reactions, and resulting in fairly significant increases in polymerization extent. Further complicating matters are the different behaviors exhibited when these formulations, initially oxygen-saturated, are kept in either aerobic or anaerobic conditions. While the work here has provided some insight into the complex behavior of the bis-disulfide initiator, clearly this a rich area for future research. Nonetheless, as it currently stands, the bis-disulfide-based initiating system provides reaction rates that are too slow to be useful for either the self-healing or biomedical adhesive applications.

To briefly summarize the research presented within this dissertation, three oxygen-mediated initiating system were explored. In comparing the reaction rates attainable between each of the three, the trialkylboranes could readily form solid polymer in seconds, the oxidoreductase system within minutes, and the bis-disulfide-based system

within hours (or even days). Regarding the use of these systems in emerging applications, the trialkylborane-based system seems especially well-suited for self-healing applications requiring rapid sealing of a puncture, while the oxidoreductase system, with their ability to rapidly produce hydrogels within minutes of oxygen exposure, seems especially useful for biomedical applications. This research firmly establishes the utility of oxygen-mediated polymerization and strongly suggests that several areas of research that should be further investigated.

7.2 Future Work

While significant advances in the area of oxygen-mediated polymerization have been described throughout this dissertation, the research described here has also raised many questions that warrant further investigation. I am especially interested in seeing the further development of self-healing material capable of sealing a high-velocity projectile-induced puncture under conditions that model those found on the moon or Mars. Having established a testing protocol, in Chapter 3, that at least partially mimics lunar or Martian conditions, a multitude of formulations that expand on those discussed in Chapters 2 and 3 could readily be investigated; I would be particularly excited to explore the use of monomers with increased functionality as well as the addition of viscosity modifiers and fillers (e.g., particles, fibers, meshes, platelets) that change the rheological profile of the monomer formulations. I also think that a significant amount of work needs to be spent on establishing the best method for packaging the reactive liquid monomer formulations within the walls of the structure. Simply having a large, unbound liquid reservoir sandwiched between two solid plates (see Figure 46a) is not practical as the liquid offers no mechanical strength to the structure. Alternatively, the reactive liquid monomer could

be packaged within hexagonal structures (Figure 46b), hollow capsules (Figure 46c),[1] or a vascular network (Figure 46d),[2-4] and embedded within a solid, load-bearing material (in grey) or the reactive liquid monomer could saturate an open-celled foam (Figure 46e). Placing the liquid within a larger, load-bearing layer should allow the entire tri-layered structure to retain the necessary mechanical properties. Of course, a serious drawback of this approach, particularly with the capsules, is that the amount of reactive liquid present is much lower which almost certainly will limit the puncture sizes that could be successfully sealed. Conversely, by using a vascular network, reactive liquid monomer can be continuously flowed through the structure in a manner analogous to how blood flows through how our vascular system,[2-4] allowing a much larger quantity of the reactive liquid to be delivered to the projectile-induced "wound" and potentially permitting larger areas to be healed. Of course, a drawback to all methods that utilize a reactive liquid is they will have some measure of reduced mechanical strength and it will need to be established how much liquid can be included within a structure so that it retains the necessary strength. In thinking rather ambitiously to address this inherent limitation, one plausible approach is to completely replace the reactive liquid-containing layer with a solid self-immolative[5] material (Figure 46f). When this material is subjected to a strong mechanical force, like being puncture by a high-velocity projectile, it will under go self-immolation – a depolymerization reaction that will convert the solid material back into a liquid. Then, a second reaction, one that could possible be initiated through an oxygen-mediated process, would repolymerize the newly-formed liquid into a solid material that plug and seal the breech. Obviously, there is a rather complicated approach and one that will require significant research to implement.

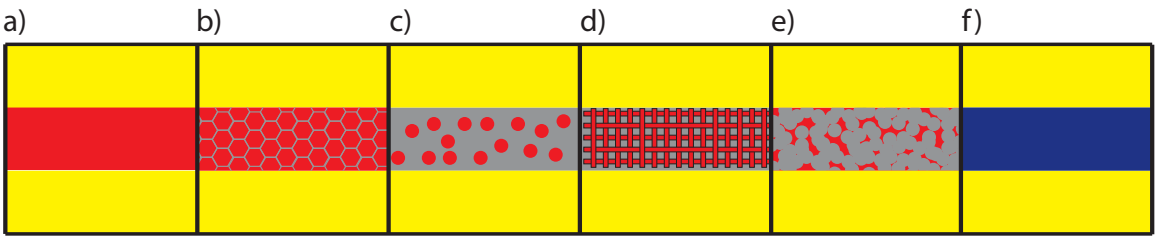

Figure 46: Tri-layered configurations for self-healing materials. In addition to the configuration utilized throughout this dissertation, a) with the liquid monomer layer (shown in red) sandwiched between two solid polymer support panels (in yellow), the monomer formulations could be packaged within a b) hexagonal structure, c) hollow capsules, d) a vascular network and embedded within a solid, load, bearing material or it could e) saturate an open-celled foam. More ambitiously, f) the liquid monomer layer could be replaced with a solid, load-bearing material that undergoes self-immolation, reverting it back into a liquid that is capable of subsequent polymerization that regenerates a solid polymer.

Of course, all of the proposed methods that utilize a reactive liquid will require significant research and product development as there are several practical issues that will need to be addressed. For example, any reactive liquid will need to remain a liquid throughout the length of the planned mission and thus must be stable for years if not decades. The trialkylborane initiator discussed in Chapter 2 and 3 is quite reactive and will begin to initiate polymerization even at very low oxygen concentrations. Attempts to develop an alternative initiator, the bis-disulfide discussed in Chapter 6 did not display polymerization times are rapid as those of observed in Chapter 2 with the alkylboranes; it may be that any initiator with sufficiently rapid reactivity may also have stability issues.

Another issue for any material that utilize a reactive liquid is that any realistic self-healing structure will need to survive multiple modes of damage besides complete puncture. For example, if a projectile only punctures the outer layers, reaching the reactive liquid layer but not penetrating deep enough to reach the interior, there would be no hole for that would allow oxygen would leak out and initiate polymerization; thus, the reactive monomer formulation remains liquid. This creates a serious problem as the

liquid is now exposed to vacuum or near vacuum conditions, permitting the monomer formulation to evaporate, removing the reactive liquid from where it is needed in the event of future impacts. One potential approach to mitigate this problems is to utilize ionic liquids as the monomers, as these materials can exhibit extremely low vapor pressure, allows them to resist evaporation into the vacuum of space. Acrylate-functional ionic liquid have already been development and it seems quite plausible that allyl and thiol functional ones could be developed as well.

There are also significant research opportunities for the hydrogel materials discussed in Chapters 4 and 5. While the gelation mechanism of the model thiol–ene monomer system was simply radical-mediated thiol–ene polymerization, gelation of the thiolated chitosan was much more complicated, with disulfide formation and iron-chitosan interactions also contributing to network formation. It would be useful to further isolate the contribution of each of the cross-linking reactions and to ascertain how each one contributes to the physicomechanical properties of the hydrogel. Despite the complexity of the gelation process, these systems have been shown to able to rapidly form hydrogels within a minute of atmosphere exposure, and thus could be suitable for use as surgical adhesive or hemostats. The next step would be to establish the biocompatibility of these materials through cell testing and immunocompatibility studies,[6] and to begin evaluating their mechanical properties and tissue adhesion.

It would also be useful to replace the thiolated chitosan with other thiomers, including other thiolated polysaccharides or thiol-rich proteins. One candidate material is mucin, a cysteine-rich glycoprotein with anti-viral properties that should behave as a high-thiol content polymer capable of participating in a thiol–ene polymerization

reaction.[7, 8] Indeed, mucins have already been used to form hydrogels by cross-linking with poly(ethylene glycol) diacrylate by a base-mediated Michael addition reaction.[9] As mucins are cheap, readily available, and have excellent biocompatibility, they may have significant utility in developing biomedical adhesives and sealants.

In looking for other opportunities to expand upon the research presented here, the richest source may very well be the thione-based initiators in Chapter 6. These materials, quite frankly, did not perform as well as was hoped; the reaction rates obtainable were much slower than what was achieved with alkylboranes or the oxidoreductase-based systems. Nonetheless, if the reaction rates could be increased to those approached what was attained for the alkylboranes or enzyme-based systems, they may overcome some of the stability and handling difficulties of the other initiating systems. Unfortunately, doing so is non-trivial and, given the effort it took to make the progress demonstrated in Chapter 6, there is no clear path forward. As the radical quenching reaction that limits achievable reaction rates seems to depend in part on the thiol concentration, it may be useful to try monomer systems that limit thiol concentration. With radical-mediated thiol–ene, that is difficult as the thiol and "ene" functional groups need to be in a 1:1 stoichiometric ratio. One potential option for breaking this stoichiometric requirement is to replace the thiol–ene monomer system with one based on the phosphane-ene reaction.[10, 11] This chemistry replaces the thiol, -SH, with phosphane moieties, $-PH_2$, and undergoes the same alternating propagation and chain transfer cycle as the thiol–ene reaction. By replacing some of the thiol monomer with an equivalent amount of phosphane, it may be possible to suppress the quenching reaction, allowing for more brisk polymerization rates.

They may also be opportunities for other thiones to be utilized as oxygen-mediated initiators, oltipraz (the parent compound for the bis-disulfide initiator), anethole dithiolethione, and 1,2-dithiole-3-thione (see Figure 47).[12] These compounds have been shown to generate superoxide radical anion in response to oxygen exposure and may be useful as oxygen-mediated initiators, either on there own or as part of an initiating system that could convert the thione-generated superoxide into, for example, hydrogen peroxide that, subsequently, could be converted to hydroxyl radicals via Fenton chemistry of peroxidase.

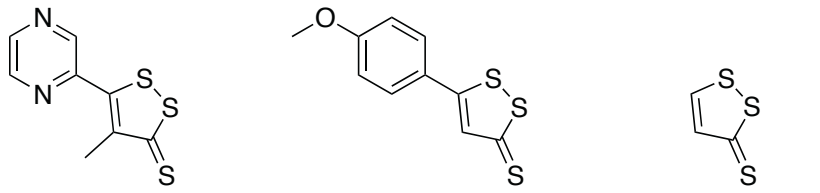

Figure 47: Other thione compounds capable of affording radicals in the presence of oxygen.

Finally, I am very interested in seeing the concept of environmentally-borne initiation stimuli be further developed, both with alternative oxygen-mediated chemistries that afford arbitrarily fast reaction rates while also addressing the stability issues of alkylboranes and enzymes as well as systems that utilize a stimulus other than oxygen. While the difficulty of using either nitrogen or carbon dioxide as stimuli was thoroughly discussed in Chapter 1, the idea of using either to initiate a polymerization reaction is rather seductive. In order for this to be feasible, particularly with nitrogen, significant advances would have to have been achieved. Presently, using either nitrogen or carbon

dioxide as a stimulus in the manner that oxygen was utilized here is not feasible, though it is something to consider for the future.

7.3 References

1. White, S. R.; Sottos, N. R.; Geubelle, P. H.; Moore, J. S.; Kessler, M. R.; Sriram, S. R.; Brown, E. N.; Viswanathan, S., Autonomic healing of polymer composites. *Nature* **2001,** *409* (6822), 794-797.
2. Hansen, C. J.; Wu, W.; Toohey, K. S.; Sottos, N. R.; White, S. R.; Lewis, J. A., Self-Healing Materials with Interpenetrating Microvascular Networks. *Adv. Mater.* **2009,** *21* (41), 4143-4147.
3. Hamilton, A. R.; Sottos, N. R.; White, S. R., Self-Healing of Internal Damage in Synthetic Vascular Materials. *Adv. Mater.* **2010,** *22* (45), 5159-+.
4. Toohey, K. S.; Sottos, N. R.; Lewis, J. A.; Moore, J. S.; White, S. R., Self-healing materials with microvascular networks. *Nat. Mater.* **2007,** *6* (8), 581-585.
5. Peterson, G. I.; Larsen, M. B.; Boydston, A. J., Controlled Depolymerization: Stimuli-Responsive Self-Immolative Polymers. *Macromolecules* **2012,** *45* (18), 7317-7328.
6. da Silva, R. A. B.; Leonardo, M. R.; da Silva, L. A. B.; Faccioli, L. H.; de Medeiros, A. I., Effect of a calcium hydroxide-based paste associated to chlorhexidine on RAW 264.7 macrophage cell line culture. *Oral. Surg. Ora.l Med.* **2008,** *106* (5), E44-E51.
7. Lieleg, O.; Lieleg, C.; Bloom, J.; Buck, C. B.; Ribbeck, K., Mucin Biopolymers As Broad-Spectrum Antiviral Agents. *Biomacromolecules* **2012,** *13* (6), 1724-1732.
8. Linden, S. K.; Sutton, P.; Karlsson, N. G.; Korolik, V.; McGuckin, M. A., Mucins in the mucosal barrier to infection. *Mucosal Immunol* **2008,** *1* (3), 183-97.
9. Davidovich-Pinhas, M.; Bianco-Peled, H., Novel mucoadhesive system based on sulfhydryl-acrylate interactions. *J Mater Sci Mater Med* **2010,** *21* (7), 2027-34.
10. Guterman, R.; Kenaree, A. R.; Gilroy, J. B.; Gillies, E. R.; Ragogna, P. J., Polymer Network Formation Using the Phosphane-ene Reaction: A Thiol-ene Analogue with Diverse Postpolymerization Chemistry. *Chem. Mater.* **2015,** *27* (4), 1412-1419.
11. Guterman, R.; Gillies, E. R.; Ragogna, P. J., Phosphane-ene chemistry: the reactivity of air-stable primary phosphines and their compatibility with the thiol-ene reaction. *Dalton Trans.* **2015,** *44* (35), 15664-15670.
12. Holland, R.; Navamal, M.; Velayutham, M.; Zweier, J. L.; Kensler, T. W.; Fishbein, J. C., Hydrogen Peroxide Is a Second Messenger in Phase 2 Enzyme Induction by Cancer Chemopreventive Dithiolethiones. *Chem. Res. Toxicol.* **2009,** *22* (8), 1427-1434.